

# UC Riverside

## UC Riverside Electronic Theses and Dissertations

### Title

Arsenic-Zinc Finger Protein Interaction and The Impact of Arsenic Exposure on Protein Quality Control

### Permalink

<https://escholarship.org/uc/item/0fq9j3kn>

### Author

Tam, Lok Ming

### Publication Date

2019

Peer reviewed|Thesis/dissertation

UNIVERSITY OF CALIFORNIA  
RIVERSIDE

Arsenic-Zinc Finger Protein Interaction and  
The Impact of Arsenic Exposure on Protein Quality Control

A Dissertation submitted in partial satisfaction  
of the requirements for the degree of

Doctor of Philosophy

in

Environmental Toxicology

by

Lok Ming Tam

December 2019

Dissertation Committee:

Dr. Yinsheng Wang, Chairperson

Dr. Wenwan Zhong

Dr. Ernest Martinez

Copyright by  
Lok Ming Tam  
2019

The Dissertation of Lok Ming Tam is approved:

---

---

---

Committee Chairperson

University of California, Riverside

## ACKNOWLEDGEMENTS

This dissertation was only possible due to the help of many people. First and foremost, my advisor, Dr. Yinsheng Wang, was invaluable in not only his guidance and resources for my Ph.D. study, but also providing me with the opportunities to grow and develop as a scientist. Without his time, patience, and effort in guiding me, this would not have been possible. In addition to the advice about this dissertation, he also provided me with financial support as well as networking and presentation opportunities through attendance of conferences every year. Besides, I would like to thank my committee members, Dr. Wenwan Zhong and Dr. Ernest Martinez for their support and advice. Their suggestions and discussion with my research in the past years are greatly appreciated and helpful. Additionally, I need to thank Dr. David Eastmond, my Ph.D. program advisor, for providing his useful advice of career and sharing his experience as a toxicologist. I am also grateful for the technical support from staff members in different core facilities at UC Riverside. Especially, I would like to send my gratitude to Dr. Ron New in Mass Spectrometry core facility as well as Dr. David Carter from Microscopy core facility for sharing their expertise on properly using MALDI-MS and confocal Inverted Zeiss 880 Airyscan UV PALM microscope, respectively. Also, I would like to thank Ms. Dawn Loyola for her useful advice and assistance in the administrative issues regarding to the graduate study.

There were many past and present lab members that are important for the accomplishment of this dissertation. My labmates Dr. Ji Jiang, Dr. Ming Huang, Dr. Weili Miao, Dr. Xiaoxia Dai, Dr. Chuanchun You, Dr. Shuo Liu, Dr. Hua Du, Dr. Xiaochuan Liu, Dr. Yuxiang Sun, Dr. Nathan Price, Dr. Xiaomei He, Dr. Kailin Yu, Jiabin Wu, Zi Wang, as well as other labmates, thank you for the training in lab techniques, help with critical thinking and advice. I need to thank Dr. Riva Dill and Dr. Kuan-Hui Chen from Dr. Ameae Walker's Lab for technical support during my early years of Ph.D. I also want to thank Dr. Emma Wilson and Dr. David Lo for their generosity of

sharing their flow cytometer as well as Marisol Arellano from Lo Lab, Edward Vizcarra from Wilson Lab for their technical assistance on the experiment of flow cytometry in Chapter 2. Furthermore, I would like to thank Dr. Meera Nair for her FlowJo software and her useful advice on the data analysis of flow cytometry experiment.

I would like to acknowledge funding sources which support this work of Ph.D. dissertation. Firstly, I would like to send my gratitude and thanks to Sir Edward Youde Memorial Fund Council from Hong Kong for Sir Edward Youde Memorial Overseas Fellowship, which provided me the major financial support and opportunity to pursue my Ph.D. study in UCR. Besides, this study was partly supported by the Dean's Distinguished Fellowship Award and the National Institutes of Health. Funding for attending numerous conferences was provided by the UCR Graduate Student Association Travel grants and T. Roy Fukuto Environmental Toxicology travel awards.

Finally, I would like to acknowledge those who helped me before in the past five years but are not listed here, for assisting my daily journey closer to achieving my Ph.D. degree.

## **COPYRIGHT ACKNOWLEDGEMENTS**

The text and figures of this dissertation in Chapter 3, in part or in full, are a reprint of the material as it appears in *Chemical Research in Toxicology*, Vol. 30, pages 1685-1693, 2017. The coauthor Dr. Yinsheng Wang directed and supervised the research that forms the basis of this chapter.

The text and figures of this dissertation in Chapter 4, in part or in full, are a reprint of the material as it appears in *Chemical Research in Toxicology*, Vol. 32, Issue 7, pages 1343-1350, 2019. The coauthor Dr. Yinsheng Wang directed and supervised the research that forms the basis of this chapter. The coauthor Ming Huang assisted with LC-MRM MS proteomic method development for proteomic data.

## **DEDICATION**

“Wisdom is not a product of schooling but of the lifelong attempt to acquire it.”

Albert Einstein (1879 – 1955)

This study is wholeheartedly dedicated to my beloved parents, who have always been my source of love, support and encouragement in my life.

To the lifelong love of my grandmothers and in the memorization of my uncle Sum Tam; to my friends for their countless supports, advice and encouragement; to teachers in Suen Mei speech training center for the firm foundation of my oral speaking to overcome communication barrier as a hard-of-hearing kid; to teachers who taught me in the past for their patience and guidance in schools; to my classmates who provided their knowledges; to numerous friendly nice people in my life journey. The reasons of what I become today.

To Science for the simple yet sophisticated ways that making our wonderful world work as our mind perceives, a beautiful miracle by God.

And lastly, I dedicated this work to the Almighty God, thank you for Your lifelong guidance, strength, power of mind, protection and wisdom.



## ABSTRACT OF THE DISSERTATION

### Arsenic-Zinc Finger Protein Interaction and The Impact of Arsenic Exposure on Protein Quality Control

by

Lok Ming Tam

Doctor of Philosophy, Graduate Program in Environmental Toxicology  
University of California, Riverside, December 2019  
Dr. Yinsheng Wang, Chairperson

Arsenic is an environmentally prevalent metalloid. Arsenic pollution through contaminated drinking water is a leading global public health problem that influences millions of people. Arsenic exposure has been demonstrated to elicit a variety of human diseases including tumorigenesis and neurodegenerative disorders. It is proposed that arsenic interferes with the post-translational modifications (PTMs) that primarily regulate pivotal quality control machineries of the genetic information flow, thereby leading to onset and/or progression of protein-misfolding disorders. Zinc finger (ZnF) proteins have diverse molecular functions, ranging from DNA/RNA binding to regulatory enzymes of protein PTMs, maintaining homeostasis. Arsenite was previously proposed to bind selectively to C<sub>3</sub>H- or C<sub>4</sub>-type ZnF by displacing Zn<sup>2+</sup> within their zinc coordination spheres, thus altering the functions of the ZnF proteins. The current dissertation aimed to characterize the arsenite-ZnF interaction of ribosome-associated protein quality control (RQC) initiator ZNF598 and epigenetic remodeler TIP60, and examine toxicity of arsenite on small GTPases.

Proteostasis is crucial in maintaining the homeostasis of protein synthesis and turnover, thereby preventing proteotoxic stress. RQC pathway is the frontline against proteotoxic stress in eukaryotes. Its initiation necessitates site-specific regulatory ubiquitinations of the ribosomal

protein subunits RPS10 and RPS20 for ribosome stalling of poly-(A) mRNA sequences, which are mediated by ZNF598 E3 ubiquitin ligase. In addition to ZNF598-mediated ribosomal ubiquitination in RQC, histone H4K16 acetylation is important in facilitating DNA repair through modulating chromatin accessibility of DNA damage sites for DNA repair enzymes. Proper regulation of TIP60 histone acetyltransferase is essential for de-compacting chromatin structure to facilitate DNA repair through H4K16Ac, lowering the likelihood of carcinogenesis. Here, arsenite binding to cysteine residues within ZNF598 and TIP60 was proposed to perturb their corresponding PTMs for dysregulating RQC (Chapter 2) and DNA repair (Chapter 3), respectively. Apart from ZnF proteins, a targeted quantitative proteomic method demonstrated that the expression levels of small GTPases were impacted by arsenite exposure in Chapter 4. Our results showed that the expression level of RhoB protein in cultured human cells was diminished upon arsenite exposure. Mechanism of As<sup>3+</sup>-induced down-regulation of RhoB protein was further elucidated by studying ubiquitin-proteasome system, whose function was impaired by arsenite, as reflected by enhanced proteasomal degradation of RhoB protein. These results show ZnF proteins involved in DNA repair and protein quality control are molecular targets for arsenite exposure, which disrupt proteostasis. Overall, these results will be useful for understanding arsenite-induced proteotoxic stress and inform studies on the mechanisms of toxicity of arsenite.

## TABLE OF CONTENTS

ACKNOWLEDGEMENTS.....	iv
COPYRIGHT ACKNOWLEDGEMENTS.....	vi
DEDICATION.....	vii
ABSTRACT OF THE DISSERTATION.....	viii
TABLE OF CONTENTS.....	x
LIST OF FIGURES.....	xiii
LIST OF TABLES.....	xix
Chapter 1	
Introduction.....	1
1. Arsenic (As).....	1
1.1. Arsenic Overview.....	2
1.2. Arsenic in the Environment.....	7
1.3. Toxicity of Arsenic to Humans.....	9
2. Zinc Finger Proteins (ZNFs).....	12
2.1. Diverse Functions of Zinc Finger Proteins.....	13
2.2. Zinc Finger Proteins and Human Diseases.....	13
2.3. Mode of Action of Arsenite on Zinc Finger Proteins.....	15
3. Mechanisms of As <sup>3+</sup> -elicited Disruption of DNA Repair and Protein Quality Control.....	15
3.1 Inhibition of DNA Repair.....	15
3.1.1. Excision Repair.....	18
3.1.1.1. BER.....	18
3.1.1.2. NER.....	19
3.1.2. DNA Ligation.....	21
3.1.3. Fanconi Anemia (FA)/BRCA Pathway for Interstrand DNA Crosslink and DNA-protein Crosslink Repair.....	22
3.1.4. DNA Double-strand Break Repair.....	23
3.1.5. Disruption of the DNA Damage Response Signaling.....	27
3.2. Disruption of Cell Cycle Checkpoints, Promotion of Cell Proliferation and Suppression of Apoptosis.....	29
3.3. Epigenetic Dysregulation Associated with Arsenic-induced Carcinogenesis.....	32

3.3.1.	Alterations of Histone PTMs .....	33
3.3.2.	DNA Methylation .....	36
3.4.	Perspectives of the Role of Zinc Finger Proteins in DNA Repair .....	39
3.5.	Proteotoxic Stress and Protein misfolding & Aggregation (Impaired protein quality control).....	40
3.5.1.	Arsenic and Proteotoxic Stress .....	40
3.5.2.	Ribosome-based Quality Control (RQC) as the Frontline of Proteostasis against Protein Misfolding.....	41
3.5.3.	Arsenic and RQC.....	43
3.6.	Disrupted Protein Degradation by Ubiquitin-Proteasomal System (UPS).....	45
3.6.1.	Dysregulation of Rho GTPases and Cancer .....	45
3.6.2.	UPS and Proteostasis .....	45
3.6.3.	The Effect of Arsenic on UPS and Rho GTPases in Cancer .....	46
4.	Scope of the dissertation .....	46
	References .....	49
Chapter 2		
	Arsenite Binds to ZNF598 to Perturb Regulatory Ubiquitination of Ribosomal Proteins and Induce Proteotoxic Stress .....	77
	Introduction .....	78
	Experimental Procedures.....	80
	Results.....	82
	Discussion .....	91
	References: .....	96
Chapter 3		
	Arsenite Binds to the Zinc Finger Motif of TIP60 Histone Acetyltransferase and Induces its Degradation via the 26S Proteasome .....	100
	Introduction .....	101
	Experimental Procedures.....	103
	Results.....	106
	Discussion .....	118
	References .....	123

Chapter 4	
Targeted Quantitative Proteomics Revealed Arsenite-induced Proteasomal Degradation of RhoB in Fibroblast Cells .....	126
Introduction .....	127
Experimental Procedures.....	128
Results.....	132
Discussion .....	145
References: .....	149
Chapter 5	
Conclusions and Future Directions .....	153
References: .....	159

## LIST OF FIGURES

- Figure 1.1.** The world map illustrating the prevalence of arsenic contamination in groundwater. The color scale of the map indicates the probability of inorganic arsenic (iAs) concentration being higher than 10 ug/L. Adopted from Amini, M. *et al.*<sup>4</sup> 2
- Figure 1.2.** Inorganic arsenic and its metabolism. In liver, absorbed As<sup>5+</sup> is reduced to As<sup>3+</sup> by GSH as an electron donor, and As<sup>3+</sup> undergoes sequential methylation and reduction with SAM and GSH as the donors of methyl group and electron, respectively, to generate MMA<sup>V</sup>, MMA<sup>III</sup>, DMA<sup>V</sup> and DMA<sup>III</sup> 4
- Figure 1.3.** As<sup>3+</sup> and iAs-elicited oxidative stress enhance carcinogenesis through impairing DNA repair pathway to induce mutations in DNA. As<sup>3+</sup> can induce the overproduction of ROS and RNS through mitochondria dysfunction, cellular antioxidant imbalance, and impairment of ROS-scavenging enzymes. Hence, iAs-elicited oxidative stress induces oxidative DNA damage, disturbs PTMs of DNA repair enzymes, and disrupts protein tyrosine phosphorylation, thereby enhancing DNA mutations to promote carcinogenesis 5
- Figure 1.4.** Multi-stage carcinogenesis model 17
- Figure 1.5.** Major events governing the disruption of DNA repair pathways by iAs and its trivalent metabolites. Arsenite and its metabolites increase positive growth signaling while inhibiting BER, NER, DSB repair, ICL repair, DDR signaling, cell cycle checkpoint regulation, apoptosis of damaged cells. These together diminish the capacity of DNA repair, thus impairing genetic integrity 18
- Figure 1.6.** Modes of action of inorganic arsenic and iAs-induced ROS/RNS in impairing the enzymatic activity of zinc finger proteins. iAs and ROS/RNS can target vicinal cysteines within the zinc coordination spheres of zinc finger proteins: i) As<sup>3+</sup> directly binds to these cysteines more strongly than Zn<sup>2+</sup>; ii) ROS oxidizes these cysteines to form a series of oxidized products, such as -SOH and -S-S-; iii) RNS, especially peroxynitrite, can S-nitrosylate these cysteines. In all these cases, Zn<sup>2+</sup> bound within zinc finger motifs is released by its displacement by As<sup>3+</sup>, which alters the conformation of zinc finger proteins and hence their enzymatic activities 26
- Figure 1.7.** Major events through which inorganic arsenite and its trivalent metabolites disrupt epigenetic integrity through inhibition of epigenetic regulators and chromatin remodelers. As<sup>3+</sup>, MMA<sup>III</sup> and DMA<sup>III</sup> can inhibit the enzymatic activities of epigenetic regulators (e.g. DNMTs, Tet and CTCF) and chromatin remodelers (e.g. hMOF, TIP60 and PARP1), which subsequently perturb DNA methylation and histone PTMs, respectively, thereby disrupting epigenetic integrity 32
- Figure 1.8.** Arsenite disrupts DNA methylation. Arsenite disrupts DNA methylation. Methylation events in gene promoters repress gene expression, whereas those in gene bodies activate gene expression. iAs metabolism induces SAM deficiency, which results in the global DNA hypomethylation. iAs exposure leads to decreased expressions of DNMT1, DNMT3A, DNMT3B, thus diminishing global DNA methylation. Additionally, iAs selectively inhibits CTCF binding to promoters of genes (e.g. DNMTs), leading to repression of tumor suppressors. Meanwhile, iAs inhibits Tet proteins, thus reducing the level of 5-hmC, which can be inhibited by the weakened occupancy of CTCF in the 38

promoters of Tet genes. Combined together, iAs can repress tumor suppressors and activate proto-oncogenes, thereby impairing DNA repair and genome integrity

**Figure 1.9.** Arsenite and iAs-induced oxidative stress enhance DNA damage through disrupting the functions of zinc finger proteins. Apart from iAs-induced oxidative stress,  $\text{As}^{3+}$  can inhibit the zinc finger-containing epigenetic regulators and DNA repair enzymes. Simultaneously, oxidative stress generates oxidative DNA damage. These together diminish DNA repair capacity in cells, which elevates DNA damage via disrupting zinc finger-modulated genetic and epigenetic integrity in DNA repair pathways, resulting in tumorigenesis 40

**Figure 1.10.** Overview of RQC and potential iAs targets 43

**Figure 1.11.** Arsenic induces proteotoxic stress through imbalance of protein synthesis and protein turnover 44

**Figure 1.12.** Hypothesis of iAs-induced enhancement of aging-related proteinopathies 48

**Figure 2.1.** Arsenite diminishes the levels of site-specific ubiquitination in ribosomal proteins RPS10 and RPS20. (A) The workflow of SILAC and LC-MS/MS for studying the effect of a 24-hr exposure of human skin fibroblast GM00637 cells to 5  $\mu\text{M}$   $\text{NaAsO}_2$  on the global ubiquitinated proteome. (B) Quantification of the ubiquitination levels of K138/K139 in RPS10 and K8 in RPS20 upon a 24-hr exposure to 5  $\mu\text{M}$   $\text{NaAsO}_2$ . The data represents the mean  $\pm$  S.D. of results obtained from 4 biological replicates. The  $p$  values were calculated using an unpaired two-tailed Student's  $t$ -test (\*,  $0.01 \leq p < 0.05$ ; \*\*,  $0.001 \leq p < 0.01$ ; \*\*\*,  $p < 0.001$ ) 84

**Figure 2.2.** LC-MS and MS/MS results showing the arsenite-induced decreases in the relative abundance of K- $\epsilon$ -GG-containing tryptic peptide, DTG(K8- $\epsilon$ -GG)TPVEPEVAIHR, derived from RPS20. (A) Positive-ion ESI-MS showing the  $[\text{M}+3\text{H}]^{3+}$  ions of the peptide obtained from forward and reverse SILAC experiments, where the  $m/z$  values for the monoisotopic peaks for the light and heavy-labeled peptide are 588.31 and 592.99, respectively. (B) MS/MS for the light and heavy-labeled peptide, where the inset showing a scheme summarizing the observed  $b$  and  $y$  ions 85

**Figure 2.3.** Arsenite binds to the ZNF598 protein in cells. (A) The chemical structure of the biotin-As probe. (B) Streptavidin agarose affinity pull-down assay showing the interaction between  $\text{As}^{3+}$  and ZNF598 in cells. The biotin-As probe was used to pull down ectopically expressed Flag-ZNF598 in HEK293T cells. The Flag-ZNF598 signal was detected using the anti-Flag antibody, and the input Flag-ZNF598 and actin were also monitored. (C, D) The interaction between the biotin-As probe and ZNF598 was substantially diminished upon pre-treatment of HEK293T cells with 10  $\mu\text{M}$   $\text{NaAsO}_2$  and PAPA0, but not with 10  $\mu\text{M}$   $\text{Zn}^{2+}$ . The Western blot images are shown in (C), and the quantification results are displayed in (D). The data represents the mean  $\pm$  S.D. of results obtained from 4 biological replicates. The  $p$  values were calculated using an unpaired two-tailed Student's  $t$ -test (\*,  $0.01 \leq p < 0.05$ ; \*\*,  $0.001 \leq p < 0.01$ ; \*\*\*,  $p < 0.001$ , 'n.s.' stands for no significant difference) 86

**Figure 2.4.**  $\text{As}^{3+}$ -bearing biarsenical dye ReAsH co-localizes with GFP-ZNF598, and  $\text{As}^{3+}$  competes with  $\text{Zn}^{2+}$  for binding to the tetracysteine motif within the RING finger domain of ZNF598. (A) Fluorescence microscopy results revealed the co-localization 88

between ReAsH and ectopically expressed GFP-ZNF598. The co-localization was significantly diminished in cells pre-treated with 10  $\mu$ M NaAsO<sub>2</sub> or PAPA0, but not Zn<sup>2+</sup>. (B) The chemical structure of ReAsH-EDT<sub>2</sub>. (C) Quantitative analysis of the frequencies of co-localization between ReAsH-EDT<sub>2</sub> and ZNF598. The data represents the mean  $\pm$  S.D. of results obtained from images of 30 different cells. The *p* values were calculated using an unpaired two-tailed Student's *t*-test (\*, 0.01  $\leq p <$  0.05; \*\*, 0.001  $\leq p <$  0.01; \*\*\*, *p* < 0.001, 'n.s.' represents no significant difference)

**Figure 2.5.** Arsenite inhibits the ribosomal stalling and augments the read-through of poly-A stalling sequences. (A) A schematic diagram showing the working principle of the dual fluorescence translation stall reporters. Plasmids expressing a reporter without a stall-inducing sequence or one containing 20 consecutive lysine codons (K<sup>AAA</sup>)<sub>20</sub> in the linker region were transfected into HEK293T cells. The diagram of the reporter cassette construct and expected protein products in the absence or presence of terminal stalling is modified from the work of Juskiewicz and Hedge.<sup>15</sup> (B) The resulting cellular GFP and ChFP levels are depicted in the scatter plot of individual cells. (C) Median ChFP:GFP ratio of 50,000 transfected HEK293T cells transiently expressing the reporter construct containing the indicated sequences. (D) Median ChFP:GFP ratio of 50,000 transfected cells transiently expressing the reporter plasmids containing either no stalling sequence or 20 consecutive lysine codons (K<sup>AAA</sup>)<sub>20</sub> in the linker region. In (C) and (D), the error bars represent S.E.M. for three separate transfections and flow cytometry measurements, and the *p* values were calculated using an unpaired two-tailed Student's *t*-test (\*, 0.01  $\leq p <$  0.05; \*\*, 0.001  $\leq p <$  0.01; \*\*\*, *p* < 0.001) 90

**Figure 2.6.** As<sup>3+</sup> induces ribosome stalling through inhibiting ZNF598. As<sup>3+</sup> binds to specific cysteine residues within zinc finger motif of ZNF598 E3 ubiquitin ligase, which subsequently inhibits its ubiquitination activity on specific lysine sites on RPS10 and RPS20, thereby diminishing the resolution of ribosome stalling 93

**Figure 3.1.** Arsenite treatment results in a dose-dependent decrease in TIP60, but not hMOF protein. Western blot images showing the effect of treatment with different doses of arsenite (0, 1, 2, and 5  $\mu$ M) on the protein level of HA-TIP60 (A) and hMOF (C). The quantification results of the relative level of TIP60 (B) and hMOF (D) proteins following exposure to different doses of NaAsO<sub>2</sub> (n=3). Error bars represent standard deviations. The *p* values were calculated using unpaired two-tailed student's *t*-test, and the asterisks designate significant differences between arsenite-treated samples and untreated control (\*, *p* < 0.05; \*\*, *p* < 0.01; \*\*\*, *p* < 0.001) 108

**Figure 3.2.** *In vitro* binding between arsenite and zinc finger peptide of TIP60. Shown is the MALDI-TOF MS results for monitoring the zinc finger peptide of TIP60 (A) and its interaction with As<sup>3+</sup> (B). The insets show the isotopic peaks of both apo-peptide of TIP60 and apo-peptide bound to arsenite 110

**Figure 3.3.** Streptavidin agarose affinity pull-down assay using biotin-As as a probe reveals the binding between As<sup>3+</sup> and the C3H-type zinc finger domain of TIP60. (A) The structure of the biotin-As probe. (B) Treatment of HEK293T cells expressing HA-TIP60 with 5  $\mu$ M biotin-As probe could pull down HA-TIP60 by using streptavidin agarose. (C). Pre-treatment of cells with 10  $\mu$ M ZnCl<sub>2</sub>, NaAsO<sub>2</sub>, or PAPA0 (i.e. *p*-aminophenylarsenoxide) for 2 hrs attenuates the binding between biotin-As and TIP60. (D) Relative protein level of TIP60 pulled down by streptavidin agarose using biotin-As 113



probe upon pretreatment with 10  $\mu\text{M}$   $\text{ZnCl}_2$  or  $\text{NaAsO}_2$  or PAPA0 when compared with untreated control (n=3). The  $p$  values were calculated using unpaired two-tailed student's  $t$ -test, and the asterisks designate significant differences between different pretreatments and control without pretreatment (\*,  $p < 0.05$ ; \*\*,  $p < 0.01$ ; \*\*\*,  $p < 0.001$ ). (E) Mutations of cysteine residues (Cys  $\rightarrow$  Ala) in the zinc finger motif of TIP60 weakened the pull-down of TIP60 with the biotin-As probe. (F) Relative levels of different forms of TIP60 protein pulled down by streptavidin agarose using the biotin-As probe. Specific Cys  $\rightarrow$  Ala mutations within the zinc finger domains of TIP60 led to compromised interaction between TIP60 and biotin-As (n=3). The  $p$  values were calculated using unpaired two-tailed student's  $t$ -test, and the asterisks designate significant differences between mutant forms of HA-TIP60 and the wild-type control (\*,  $p < 0.05$ ; \*\*,  $p < 0.01$ ; \*\*\*,  $p < 0.001$ ). Error bars in D and F indicate standard deviations

**Figure 3.4.** Exposure to arsenite induces proteasomal degradation of TIP60. (A) Co-treatment of HEK293T cells with 4  $\mu\text{M}$  MG132 together with different doses of  $\text{NaAsO}_2$  (0, 2, and 5  $\mu\text{M}$ ) could rescue the dose-dependent decrease of TIP60 protein induced by arsenite exposure. (B) Relative protein level of TIP60 upon treatment with different doses of  $\text{NaAsO}_2$  together with MG132 or DMSO control (n=3). The  $p$  values were calculated using unpaired two-tailed student's  $t$ -test, and the asterisks designate significant differences between the arsenite-treated samples and untreated control (\*,  $p < 0.05$ ; \*\*,  $p < 0.01$ ; \*\*\*,  $p < 0.001$ ). Error bars in panel B represent standard deviations 115

**Figure 3.5.** Arsenite exposure led to diminished H4K16Ac in both wild-type and *TIP60*<sup>-/-</sup> HEK293T cells, and a higher concentration of arsenite (i.e. 5  $\mu\text{M}$ ) gave rise to a more pronounced decrease in H4K16Ac level in wild-type cells than *TIP60*<sup>-/-</sup> cells. (A) Western blot image showing the effect of different concentrations (0, 2, and 5  $\mu\text{M}$ ) of  $\text{NaAsO}_2$  on the level of H4K16Ac in wild-type and *TIP60*<sup>-/-</sup> HEK293T cells. (B) Relative levels of H4K16Ac in wild-type and *TIP60* knock-out cells upon treatment with different concentrations of arsenite (n=4). Error bars represent standard deviations. The  $p$  values were calculated using unpaired two-tailed student's  $t$ -test, and the asterisks designate significant differences between arsenite-treated cells and untreated control as well as the significant difference upon the same arsenite treatment between wild-type and *TIP60*<sup>-/-</sup> cell lines (\*,  $p < 0.05$ ; \*\*,  $p < 0.01$ ; \*\*\*,  $p < 0.001$ ) 118

**Figure 3.6.** The proposed role of TIP60 in arsenic-induced carcinogenesis.  $\text{As}^{3+}$  interacts with cysteine residues in the zinc finger motifs of TIP60, promoting its degradation via the ubiquitin-proteasomal pathway. Diminished level of TIP60 protein results in lower level of H4K16Ac. This in turn generates a biochemically less accessible chromatin state, which may compromise DNA repair 121

**Figure 3.S1.** The effects of DTT on the interaction between  $\text{As}^{3+}$  and the zinc finger peptide of TIP60. Increasing concentration of DTT can affect the relative intensity of peak corresponding to  $\text{As}^{3+}$ -bound peptide (at  $m/z$  3219.5), as indicated in MALDI MS measurements when molar ratios of  $\text{As}^{3+}$ /DTT were 1:1 (A), 1:5 (B) and 1:25 (C) 111

**Figure 3.S2.** Arsenite does not induce dose-dependent decrease in protein level of any three zinc finger mutants of TIP60, i.e. C263A, C266A and C283A. Western blot images showing the effect of mutations in critical cysteine residues of the C3H-type zinc finger of TIP60, i.e. C263A (A), C266A (C) and C283A (E). The quantification results of the relative level of TIP60 mutant proteins C263A (B), C266A (D) and C283A (F) following 116

exposure to different concentrations of NaAsO<sub>2</sub> (n=3). Error bars represent standard deviations. The p values were calculated using unpaired two-tailed Student's t-test, and the asterisks designate significant differences between arsenite-treated samples and untreated control (\*, p < 0.05; \*\*, p < 0.01; \*\*\*, p < 0.001)

**Figure 3.S3.** Arsenite does not attenuate the histone acetyltransferase (HAT) activity of TIP60. (A) HAT assay indicating the effect of treatment of cells with 5 μM of NaAsO<sub>2</sub> on HAT activity of TIP60, as shown by the acetylation of H4K16 residue, with the untreated control. (B) Relative HAT activity of TIP60 with or without 5 μM of NaAsO<sub>2</sub>. The data represents the mean and standard deviation of results from three independent experiments 117

**Figure 4.1. A targeted proteomic strategy for high-throughput quantitative profiling of small GTPases upon arsenite exposure in IMR90 human lung fibroblast cells.** (A) A schematic illustration of the targeted quantitative proteomic workflow, relying on forward SILAC labeling, SDS-PAGE fractionation, and scheduled LC-MRM analysis; (B) Venn diagrams displaying the overlap between quantified small GTPases in the forward and reverse SILAC experiments obtained from the MRM and DDA analyses, respectively, and the comparison between the performances of the two methods; (C) Correlation between the Log<sub>2</sub>-transformed SILAC ratios (Log<sub>2</sub>R) obtained from one forward and one reverse SILAC labeling experiments with a relatively high linear correlation coefficient ( $R^2 = 0.8243$ ); (D) A bar chart showing significantly up- and down-regulated (> 1.5-fold) small GTPases quantified from two LC-MRM experiments 134

**Figure 4.2. LC-MRM and Western blot analyses revealed consistently lower levels of expression of RhoB upon a 12 h exposure to 5 μM NaAsO<sub>2</sub> in IMR90 cells.** (A) Extracted MRM traces for three transitions ( $y_9$ ,  $y_8$ , and  $y_7$ ) monitored for the [M+2H]<sup>2+</sup> ion ( $m/z$  537.78) of a tryptic peptide from RhoB, i.e. LVVVGDGACCGK (underlined 'C' designates carbamidomethylated Cys), with blue and red traces representing MRM transitions for the light- and heavy-isotope labeled forms of the peptide, respectively; (B) Western blot analysis confirmed the diminished expression of both endogenous and ectopically-expressed RhoB in IMR90 cells upon exposure to 5 μM of NaAsO<sub>2</sub> for 24 h. Shown are the quantification results for the relative levels of RhoB protein following exposure to 5 μM of NaAsO<sub>2</sub> obtained from Western blot analysis. Error bars represent standard deviations (n = 3). The p values were calculated using unpaired two-tailed student's t-test, and the asterisks designate significant differences between arsenite-treated samples and untreated control (\*,  $0.01 \leq p < 0.05$ ; \*\*,  $0.001 \leq p < 0.01$ ; \*\*\*,  $p < 0.001$ ) 142

**Figure 4.3. Arsenite treatment results in a dose-dependent decrease in both endogenous and ectopically expressed RhoB proteins.** (A) Western blot images showing the effect of 24 h treatment with different doses of arsenite (0, 1, 2, and 5 μM) on expression level of endogenous RhoB protein in IMR90 cells and ectopically-expressed RhoB protein in HeLa, HEK293T and GM00637 cells. (B) The quantification results of the relative levels of endogenous and ectopically-expressed RhoB protein in the four cell lines as shown in (A) following exposure to different doses of NaAsO<sub>2</sub>. Error bars represent standard deviations (n = 3). The p values were calculated using unpaired two-tailed student's t-test, and the asterisks designate significant differences between arsenite-treated samples and untreated control (\*,  $0.01 \leq p < 0.05$ ; \*\*,  $0.001 \leq p < 0.01$ ; \*\*\*,  $p < 0.001$ ) 144

**Figure 4.4. Exposure to arsenite induces proteasomal degradation of RhoB.** (A) Co-treatment of HEK293T cells with 4  $\mu$ M MG132 together with different doses of NaAsO<sub>2</sub> (0, 2, and 5  $\mu$ M) for 24 h could abolish the dose-dependent decrease of RhoB protein induced by arsenite exposure. (B) Relative protein level of HA-RhoB upon treatment with different doses of NaAsO<sub>2</sub> together with MG132 or DMSO control (n = 3). The *p* values were calculated using unpaired two-tailed student's *t*-test, and the asterisks designate significant differences between the arsenite-treated samples and untreated control (\*, 0.01  $\leq p < 0.05$ ; \*\*, 0.001  $\leq p < 0.01$ ; \*\*\*,  $p < 0.001$ ). n.s. represents no significant difference between arsenite-treated samples and untreated control

**Figure 4.5.** Arsenite exposure diminishes the protein expression level of RhoB through enhancing its proteasomal degradation.

**Figure 4.S1. LC-MRM and Western blots revealed no appreciable change in levels of expression of Rab31 and Rab32 upon a 12 h exposure to 5  $\mu$ M NaAsO<sub>2</sub> in IMR90 cells.** (A) Extracted MRM traces for three transitions ( $y_6$ ,  $y_4$ , and  $y_3$ ) monitored for the [M+2H]<sup>2+</sup> ( $m/z$  501.25) of a unique tryptic peptide from RAB31, i.e. QDSFYTLK, and for three transitions ( $y_7$ ,  $y_6$ , and  $y_4$ ) monitored for the [M+2H]<sup>2+</sup> ( $m/z$  572.78) ion of a unique tryptic peptide from RAB32, i.e. DNINIEEAAR, with blue and red traces denoting MRM transitions for the light- and heavy-isotope labeled peptides respectively. (B) Western blot analysis confirmed the lack of change in the expression of endogenous Rab31 and Rab32 proteins upon a 24 h exposure to 5  $\mu$ M of NaAsO<sub>2</sub> in IMR90 lung fibroblast cells. (C) The quantification results of the relative expression of endogenous Rab31 and Rab32 proteins following exposure to 5  $\mu$ M NaAsO<sub>2</sub> (n=3). Error bars represent standard deviations. The *p* values were calculated using unpaired two-tailed student's *t*-test, and the asterisks designate significant differences between arsenite-treated samples and untreated control (\*, 0.01  $\leq p < 0.05$ ; \*\*, 0.001  $\leq p < 0.01$ ; \*\*\*,  $p < 0.001$ ). n.s. represents no significant difference between arsenite-treated samples and untreated control

**Figure 5.1.** Summary of the conclusions from Chapters 2-4.

## LIST OF TABLES

### Chapter 4

<b>Table 4.S1:</b> Quantification data of LC-MRM analysis results	135
---	-----

# Chapter 1

## Introduction

The central dogma of molecular biology is that genetic information flows from DNA through mRNA via transcription and then from mRNA to protein via translation.<sup>1,2</sup> At first glimpse, it may seem simple, but post-translational modifications (PTM) make this flow complicated yet interesting. PTM is a general enzymatic and covalent modification of proteins after their syntheses, where PTM can control the extent of the flow of genetic information from DNA to protein expression through addition or removal of biochemical modifications on amino acids of a protein. Protein is the functional unit of genetic information in human bodies, and PTMs of proteins are known to regulate their expression levels and protein-protein interactions. In a plethora of cellular processes, a crosstalk of PTM network ensures the tight regulation through cellular communications via these modifications on proteins.

However, PTMs on proteins are vulnerable to environmental exposure, especially carcinogenic metals and metalloids. In this chapter, I will first discuss about arsenic, a metalloid prevalent in the environment, and its environmental fate, transport and toxicity. Next, I will describe zinc finger proteins, as well as arsenic-induced toxicity elicited by the disruption of zinc finger proteins and its association with human diseases, which is the primary focus of my Ph.D. work.

### 1. Arsenic (As)

Arsenic (As) is a widely distributed metalloid, both naturally occurring and anthropogenically in the environment. Being 20<sup>th</sup> most abundant element on the Earth's crust, arsenic exists in both inorganic and organic forms as well as arsine gas.<sup>3</sup> Arsenic has several oxidation states and can be present in its elemental form (As, 0), or as arsenite (As<sup>3+</sup>, +3), arsenate (As<sup>5+</sup>, +5) or organoAs

[such as methylated arsenic species dimethylarsinate (DMA) and monomethylarsonate (MMA)], or arsine gas ( $\text{As}^3-$ , -3).<sup>3</sup> Present naturally in minerals with other metal elements, As can be released into surface waters via weathering and Earth movement and uptake by living organisms can negatively impact them. Arsenic pollution events have been documented around the world including the USA, influencing more than 200 million people in over 70 countries (Fig. 1.1). Therefore, it is important to understand how arsenic exposure exerts its toxicity to living organisms via protein quality control, though a large body of knowledge is available concerning the toxicity of arsenic.

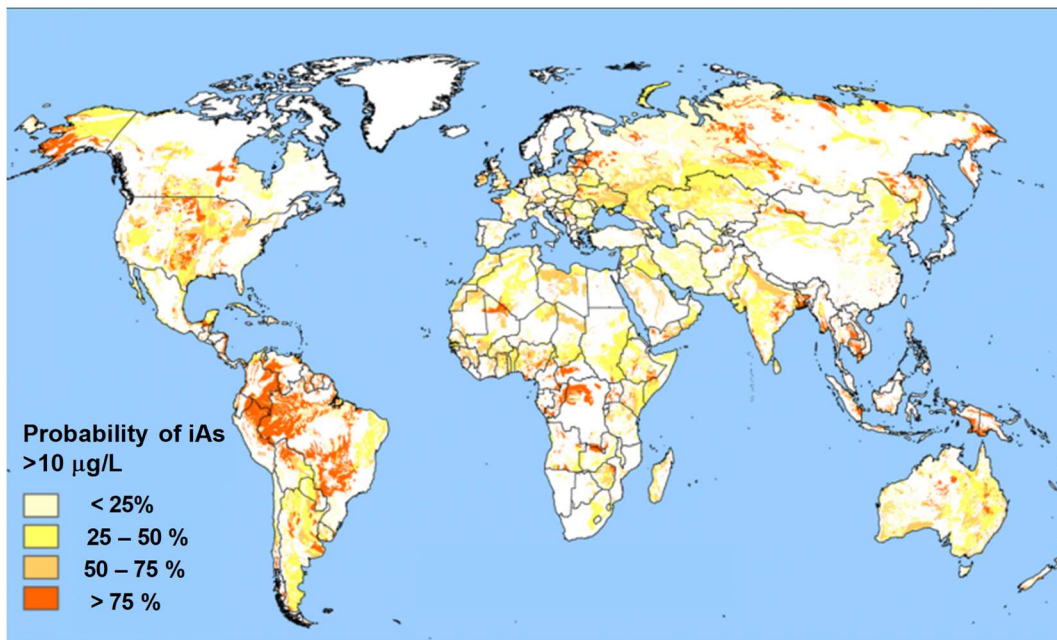


**Figure 1.1.** The world map illustrating the prevalence of arsenic contamination in groundwater. The color scale of the map indicates the probability of inorganic arsenic (iAs) concentration being higher than 10 ug/L. Adopted from Amini, M. *et al.*<sup>4</sup>

## 1.1. Arsenic Overview

### *Physiological Roles*

Arsenic is not considered as an essential micronutrient, but numerous lines of evidence suggest that arsenic plays a physiological role in methionine metabolism. Arsenic is thought to be involved

in maintaining the metabolic pool of *S*-adenosyl-L-methionine (SAM), which is indispensable for a diversity of pivotal processes including DNA methylation and the metabolism of arginine, as supported by arsenic-deprived studies in rats.<sup>5</sup> Animal studies have suggested that arsenic deficiency would result in heightened mortality, declining fertility, higher spontaneous abortion rate, lower birth weight in offspring as well as damage to red blood cells.<sup>6</sup> However, due to the limited knowledge associated with beneficial functions of arsenic, its other potential physiological roles remain to be investigated in the future.

### *Metabolism*

Toxicity of inorganic arsenic ( $\text{As}^{3+}$  and  $\text{As}^{5+}$ ) in humans largely depends on their metabolism after arsenic exposure and absorption. Approximately 90% of ingested inorganic arsenic ( $\text{As}^{3+}$  or  $\text{As}^{5+}$ ) is absorbed by the gastrointestinal tract.<sup>7</sup> Inorganic  $\text{As}^{5+}$  subsequently undergoes a sequential process, i.e. glutathione (GSH)-mediated two-electron reduction to  $\text{As}^{3+}$ , and oxidative methylation of  $\text{As}^{3+}$  by arsenic methyltransferase (As3MT) to pentavalent organic arsenic intermediates (e.g.  $\text{MMA}^{\text{V}}$  and  $\text{DMA}^{\text{V}}$ ) in the liver (Fig. 1.2).<sup>8,9</sup>  $\text{DMA}^{\text{V}}$  was previously shown to be a teratogen, a nephrotoxin, a tumor promoter, and a complete carcinogen in mammals.<sup>10-13</sup> In this biotransformation process, inorganic arsenic (iAs) can also be biomethylated to yield trivalent arsenical intermediates such as  $\text{MMA}^{\text{III}}$  and  $\text{DMA}^{\text{III}}$ , which exhibit higher potency in being cytotoxic/genotoxic agents and enzyme inhibitors over inorganic arsenite ( $\text{iAs}^{3+}$ ).<sup>8</sup> Therefore, it is important to consider both inorganic arsenic and their trivalent methylated arsenic species when discussing arsenic toxicity.<sup>14-16</sup>

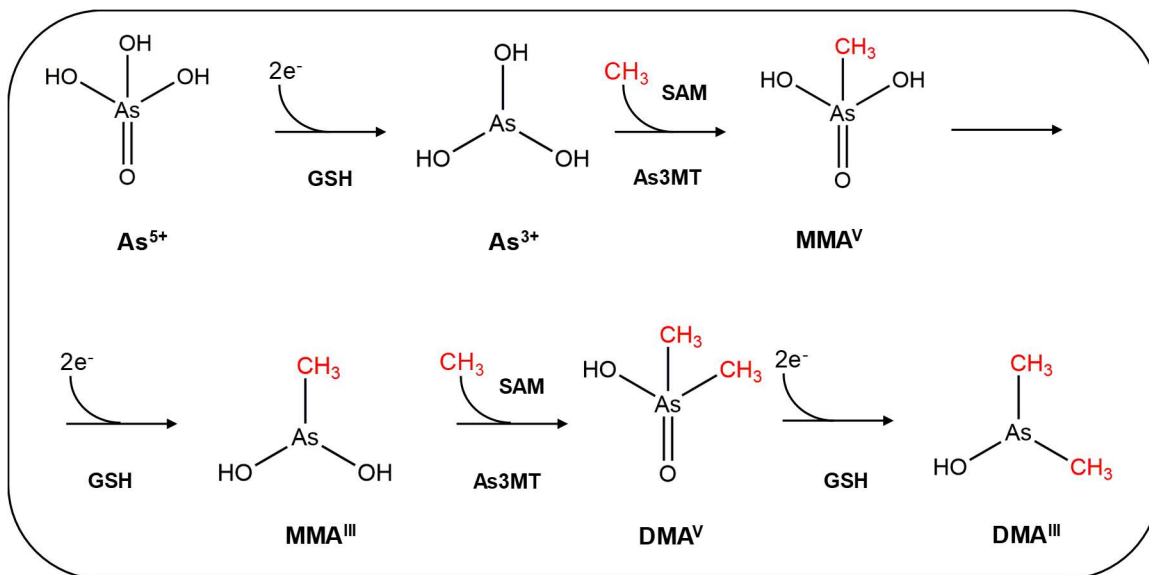


**Figure 1.2.** Inorganic arsenic and its metabolism. In liver, absorbed  $\text{As}^{5+}$  is reduced to  $\text{As}^{3+}$  by GSH as an electron donor, and  $\text{As}^{3+}$  undergoes sequential methylation and reduction with SAM and GSH as the donors of methyl group and electron, respectively, to generate  $\text{MMA}^{\text{V}}$ ,  $\text{MMA}^{\text{III}}$ ,  $\text{DMA}^{\text{V}}$  and  $\text{DMA}^{\text{III}}$ .

### *Arsenic Exposure and Oxidative Stress*

Given the weak mutagenicity of iAs and high genotoxicity of methylated trivalent arsenic metabolites,<sup>8</sup> arsenic-induced oxidative stress has been widely studied and is likely a major contributor to arsenic-induced carcinogenesis (Fig. 1.3.). Throughout the remainder of this dissertation we will discuss inorganic and methylated trivalent arsenic species as a group, which together have been shown to induce ROS generation and oxidative stress in mammalian cells.<sup>17–19</sup> Major arsenic-induced ROS include superoxide anion ( $\text{O}_2^{\cdot-}$ ), hydroxyl radical ( $\cdot\text{OH}$ ), singlet oxygen ( $^1\text{O}_2$ ), hydrogen peroxide ( $\text{H}_2\text{O}_2$ ), and peroxy radicals ( $\text{ROO}^{\cdot}$ ).<sup>20</sup>



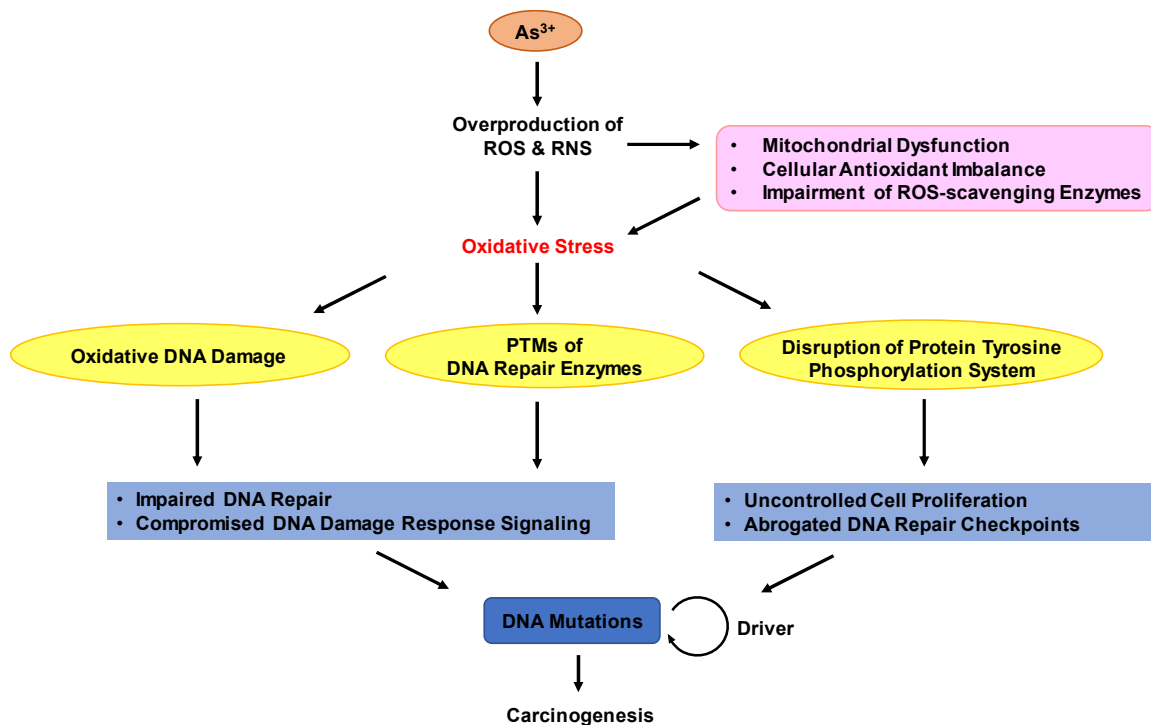


**Figure 1.3.** As<sup>3+</sup> and iAs-elicited oxidative stress enhance carcinogenesis through impairing DNA repair pathway to induce mutations in DNA. As<sup>3+</sup> can induce the overproduction of ROS and RNS through mitochondria dysfunction, cellular antioxidant imbalance and impairment of ROS-scavenging enzymes. Hence, iAs-elicited oxidative stress induces oxidative DNA damage, disturbs PTMs of DNA repair enzymes and disrupts protein tyrosine phosphorylation, thereby enhancing DNA mutations to promote carcinogenesis.

Apart from direct generation of ROS from arsenic and its metabolites, arsenic exposure can result in antioxidant imbalance, mitochondrial dysfunction, and impairment of ROS-scavenging enzymes, which together result in arsenic-induced oxidative stress, as discussed previously.<sup>21</sup> Due to its involvement as an electron donor in arsenic metabolism,<sup>8,9</sup> the intracellular pool of glutathione (GSH) is heavily depleted upon chronic arsenic exposure and becomes unavailable for scavenging ROS as a cellular defense against oxidative stress. In addition, arsenic-mediated disruption of the mitochondrial electron transport chain further exacerbates oxidative stress, because the mitochondrion constitutes a major source of intracellular ROS, especially the superoxide anion generated from complexes I and III, and RNS (e.g. peroxynitrite).<sup>22-24</sup> Apart from mitochondrial

dysfunction, arsenic-induced oxidative stress also emanates from impaired activities of ROS-scavenging enzymes, such as superoxide dismutase (SOD), catalase (CAT), glutathione peroxidase (GPx), glutathione *S*-transferase (GST), and glutathione reductase (GR).<sup>21,25</sup> Therefore, it is reasonable to conclude that arsenic-induced carcinogenesis is attributed, in part, to arsenic-associated oxidative stress, which results in genotoxicity and disruption of vital cellular processes where ROS act as secondary messengers.<sup>25-28</sup>

Arsenic-induced oxidative stress may result in carcinogenesis through the genotoxicity of ROS and RNS. Along this line, increasing lines of evidence demonstrated that iAs and its biomethylated metabolites damage DNA indirectly through induction of free radicals, which generate DNA adducts, DNA strand breaks, cross-links and chromosomal aberrations.<sup>19,29-32</sup> For instance, hydroxyl radicals generated from arsenite exposure are believed to react with all four canonical nucleobases in DNA to form DNA lesions, such as 8-oxo-7,8-dihydroguanine, 5-hydroxycytosine and 5-hydroxyuracil.<sup>33</sup> ROS/RNS can induce nucleobase substitutions, insertions, deletions, and rearrangements.<sup>33</sup> In addition, arsenite-induced ROS and RNS are believed to induce cross-links between DNA and proteins or other molecules in cells (e.g. lipids).<sup>34</sup> Moreover, *in vitro* studies with cultured human cells indicated that arsenite-induced oxidative stress causes persistent telomere attrition, DNA strand breaks, chromosomal aberrations and sister chromatid exchanges.<sup>27,35-37</sup>

Aside from oxidative DNA damage, arsenite-induced ROS function as secondary messengers to interfere with signal transduction pathways and transcription factor regulation, such as disruption of tyrosine phosphorylation system by mitogen-activated protein kinases (MAPKs) and transcription factor families (e.g. NF- $\kappa$ B and AP-1), enhancing the carcinogenic potential of arsenite.<sup>19,21</sup> Last but not the least, ROS/RNS generated by arsenite can directly inhibit important thiol-containing proteins involved in DNA repair and DNA damage response (DDR). For example,

inhibition of poly(ADP-ribose) polymerase-1 (PARP1) by peroxyxynitrite through *S*-nitrosylation of its zinc finger cysteines was shown to impair DNA repair capacity.<sup>38,39</sup>

## **1.2. Arsenic in the Environment**

### *Sources and Speciation*

Arsenic is present naturally in the Earth's crust, particularly in its sulfide form in complex minerals containing silver, lead, copper, nickel, antimony, cobalt and iron.<sup>3</sup> Arsenopyrite is the most common among over 200 arsenic-containing mineral species.<sup>3</sup> Arsenic can be mobilized by a variety of natural and anthropogenic activities. Natural occurrences, such as volcanic eruptions and weathering of rocks and soils, are secondary to arsenic release in comparison to anthropogenic activities.<sup>3</sup> Mining, smelting of non-ferrous metals, burning of fossil fuels and agricultural irrigation of contaminated ground water are the primary causes of arsenic release into the environment, with the historical use of arsenic-containing pesticides releasing a significant amount of arsenic in contaminated agricultural soil.<sup>3</sup> Global natural emissions of arsenic and arsenic compounds have been estimated to be approximately 8,000 metric tons per year while anthropogenic emissions are about three times more.<sup>40</sup>

Aquatic arsenic is the most significant source of arsenic contamination, mainly in groundwater due to its solubility in water.<sup>41</sup> Groundwater is the main source for drinking water, rendering human susceptible to arsenic exposure. Inorganic arsenite ( $\text{As}^{3+}$ ) and arsenate ( $\text{As}^{5+}$ ) are the predominant forms in water<sup>42</sup>, and they also contain the highest potency in toxicity to living organisms through oral ingestion of contaminated drinking water. Contaminated drinking water is the major source of arsenic exposure in humans, becoming one of the most pivotal global public health issues to be encountered.

### *Environmental Fate and Transport of Arsenic*

The fate and transport of arsenic into aquatic systems depends largely on the arsenic source and the receiving waters. Arsenic form in the environment largely depends on the pH and redox potential, with  $\text{As}^{3+}$  and  $\text{As}^{5+}$  being the dominant forms under anaerobic reducing and aerobic oxidizing circumstances at normal pH ranges respectively.<sup>43</sup> In addition to direct dissolution of inorganic arsenic from minerals to groundwater, naturally occurring arsenic from minerals and anthropogenic source of arsenic is mobilized, via volcanic eruption and burning of fossil fuel respectively to the atmosphere, where rain leads to lixiviation and mobilization of arsenic aerosol particulates to the hydrosphere, especially surface water.<sup>44</sup> Arsenic in the hydrosphere infiltrates into the geosphere, where biogeochemical redox processes strongly influence its environmental fate and mobility.<sup>45</sup> Since iron is the most abundant transition metal on the Earth's surface, it plays a critical role in environmental biogeochemical transformation of arsenic, which is either abiotic or biotic.<sup>45</sup> In abiotic redox cycling of arsenic, semiquinones and hydroquinones generated by microbial reduction of humic substances oxidize  $\text{As}^{3+}$  and reduce  $\text{As}^{5+}$  respectively, while reactive  $\text{Fe}^{2+}/\text{Fe}^{3+}$  mineral phase can be generated by microbial production of  $\text{Fe}^{2+}$  and can mediate redox cycling of arsenic. In biotic ones,  $\text{Fe}^{3+}$  mineral formation, where  $\text{Fe}^{2+}$  is microbially oxidized by bacteria, can sequester arsenic by sorption or co-precipitation of  $\text{As}^{3+}/\text{As}^{5+}$  to these  $\text{Fe}^{3+}$  minerals. Additionally, microbially catalyzed arsenic redox transformations, particularly reduction of  $\text{As}^{5+}$  to  $\text{As}^{3+}$ , contributes to arsenic mobilization.<sup>45</sup> To this end, the mobility of arsenic in the geosphere into groundwater is solely controlled by a sophisticated balance between the biogeochemical redox reactions of  $\text{Fe}^{3+}$  and  $\text{Fe}^{2+}$ .<sup>45</sup> Arsenite and arsenate constitute the predominant forms of arsenic in the hydrosphere, including the groundwater reserve for drinking among human populations. Therefore, given that arsenic has high water solubility and is highly mobilized by microbial catalyzed redox transformations in the geosphere, aquatic arsenic pool in the hydrosphere acts as a

sink collecting and concentrating environmental iAs, such as iAs-containing aerosol in the atmosphere and pesticide residues in the geosphere, constituting the notorious arsenic pollution in groundwater reserves in close intimacy with minerals deep on the Earth's surface.<sup>41,43</sup> In this vein, inorganic arsenic leaches into groundwater or being bioaccumulated in agricultural products (e.g. rice) through irrigation of contaminated water or through contaminated soils.

### **1.3. Toxicity of Arsenic to Humans**

Arsenic is known to be highly toxic to all life forms.<sup>42</sup> According to the long-standing golden rule of toxicology 'toxicity depends on the dose', the toxicity of arsenic in humans mainly relies on its dose in human bodies, which could be determined by the duration of exposure time, the level of arsenic in contact, the frequency of arsenic exposure and the route of exposure to arsenic. In humans, arsenic from drinking water or diet is mainly absorbed from small intestine while only a minority of arsenic exposure occurs through skin contact and inhalation.<sup>6</sup>

Arsenic toxicity is roughly classified into acute and chronic toxicities, depending on whether the length of exposure time is short- or long-term. The majority of acute arsenic poisoning events are caused by accidental ingestion of arsenic-containing pesticides and occasionally by suicide attempts.<sup>6</sup> The lethal dose of inorganic arsenic in a human adult is predicted to be within a range of 1 to 3 mg/kg.<sup>9</sup> The prominent clinical features of severe acute arsenic toxicity observed in humans have been reported to include but not limited to nausea, vomiting, colicky abdominal pain, diarrhea, anuria, convulsions, acute psychosis, peripheral neuropathy, encephalopathy, cardiomyopathy, seizure, coma and sometime death.<sup>6,9</sup> However, urinary arsenic concentration is currently used as an indicator of recent acute arsenic poisoning, usually within 2 days.<sup>6</sup>

Aside from acute arsenic exposure, chronic arsenic exposure reported in humans is primarily caused by long-term ingestion of contaminated drinking water and agricultural products (e.g. rice)

especially among the populations living in geothermal areas, typically in months to years. During the long exposure time-window, most of the absorbed arsenic usually accumulates in liver, kidneys, heart and lungs, with a minority amount in the muscles, nervous system, gastrointestinal tract and spleen.<sup>6</sup> Typically, prolonged arsenic exposure can lead to a series of diseases in multiple body systems, ranging from skin lesions and diabetes mellitus to malignancy and peripheral neuropathy, as well as cognitive impairment and memory loss.<sup>6,9</sup>

Among different kinds of arsenic exposure, chronic low-level arsenic exposure is more environmental relevant. This explains the exposure setting of a majority of worldwide arsenic mass poisoning events, especially those in India and Bangladesh, resulting in the major global public health issue deserving our attention.

#### *Tumorigenesis and Neurotoxicity*

Arsenic is classified as Group I human carcinogen by International Agency for Research on Cancer (IARC, 2012) and the US Environmental Protection Agency (EPA, 1988).<sup>3,46</sup> People under the chronic arsenic exposure are susceptible to various cancers mainly through inhalation of airborne inorganic arsenic in particulate matters and ingestion of contaminated drinking water.<sup>40,47</sup> People are most likely to develop lung cancers after inhaling to airborne arsenic whereas those exposed to arsenic through oral ingestion of contaminated drinking water usually develop skin cancers.<sup>3</sup> Apart from lung and skin cancers, arsenic is also known to induce liver, prostate, bladder and kidney cancers in humans.<sup>3</sup> Over last few decades, numerous epidemiological and animal studies have demonstrated the strong association between arsenic exposure and tumor progression in skin, lung, bladder, kidney and liver.<sup>3,47</sup> Since arsenic is somehow a universal toxicant, there are a number of proposed mechanisms underlying the arsenic-elicited carcinogenesis, which include but not limited to genotoxicity, altered DNA repair, dysregulated cell proliferation, DNA methylated oxidative stress and promoted tumor development.<sup>9</sup>

Aside from carcinogenesis, inorganic arsenic has been reported to induce encephalopathy and neurodegenerative disorders such as Alzheimer's disease and Parkinson's disease. Inorganic arsenite is known to be neurotoxic as it can increase beta-amyloid (A $\beta$ ) peptides, causing amyloid plaques characteristic of Alzheimer's disease.<sup>48</sup> A number of cellular, animal and epidemiological studies have indicated that chronic arsenic exposure is closely related to higher incidence of declined neurocognitive function and memory loss.<sup>15,48-50</sup> The mechanisms underlying arsenic-induced neurotoxicity are very complicated and have been proposed to include but not limited to mitochondrial dysfunction, dysregulated A $\beta$  homeostasis, increased protein misfolding and aggregation as well as malfunctioning protein homeostasis.<sup>15,50-52</sup>

#### *Potential Mechanisms of Arsenic Toxicity*

Most of the inorganic arsenic toxicity are caused by the specific modes of action of pentavalent arsenate and trivalent arsenite species. Pentavalent arsenate and trivalent arsenite have two distinct chemical properties and structures, resulting in different modes of action as described below.

##### ➤ Mode of action of pentavalent arsenate

Owing to similar structure and properties with phosphate, arsenate is able to substitute phosphate in numerous biochemical reactions, inactivating approximately 200 enzymes involved in cellular energy pathways.<sup>6,9</sup> In this vein, arsenate can react with glucose to generate glucose-6-arsenate, resembling glucose-6-phosphate which can inhibit hexokinase akin to glucose-6-phosphate.<sup>9</sup> Similarly, arsenate can substitute phosphate in the sodium pump and the anion exchange transport system of the human red blood cells as well as its replacement of phosphate during the formation of the anhydride 1-arsenato-3-phospho-D-glycerate instead of 1,3-biphospho-D-glycerate in one enzymatic step of the glycolytic pathway via one mechanism named arsenolysis.<sup>9</sup> Thereby, arsenate could inhibit the generation of ATP through competition with

phosphate in phosphate-dependent biochemical processes as well as disturbance of cellular membrane potential.

➤ Mode of action of trivalent arsenite

Thiols or vicinal sulfhydryl groups within enzymes or receptors play an important role in their activities.<sup>9</sup> Trivalent arsenite can readily bind to these critical thiol groups inside a variety of enzymes involved in pivotal biochemical events, such as PARP1, estrogen receptor and zinc finger proteins, to alter cellular homeostasis and lead to toxicity.<sup>9,53</sup> For instance, trivalent arsenite might bind to the lipoic acid moiety, thereby inhibiting pyruvate dehydrogenase (PDH) which requires the dithiol lipoic acid as the cofactor for its enzymatic activity. In this way, inhibition of PDH by arsenite binding could interfere with the citric acid cycle and lead to depletion of ATP.<sup>9</sup> Likewise, arsenite binds selectively with zinc finger proteins containing C<sub>3</sub>H- or C<sub>4</sub>-type zinc finger motifs such as promyelocytic leukemia protein (PML) which enhances its proteasomal degradation via SUMOylation and ubiquitination.<sup>54,55</sup>

## 2. Zinc Finger Proteins (ZNFs)

Zinc finger proteins are a group of proteins harboring the structural motif characterized by its coordination with one or more Zn<sup>2+</sup> ions to stabilize the folding. Zinc finger was identified by Dr. Klug in the study of transcription factor TFIIIA from *Xenopus oocytes* in 1985.<sup>56</sup> Since then, this 'classical' TFIIIA-type C<sub>2</sub>H<sub>2</sub> zinc finger motif has been demonstrated to be common in humans. It is suggested that over 15000 zinc finger domains are predicted to exist in approximately 1000 different proteins whereas more than 20 additional classes of structurally distinct modules of zinc finger proteins have been recognized, e.g. RING finger, FYVE-type zinc finger and PHD-type zinc finger.<sup>57</sup>



## **2.1. Diverse Functions of Zinc Finger Proteins**

Zinc is an indispensable micronutrient for all forms of life.<sup>58</sup> Zinc mainly plays the structural and catalytic roles in proteins because of its redox inertness, relatively strong binding affinity than most of the essential metal ions, Lewis acid strength and fast ligand exchange.<sup>58,59</sup> It is estimated that approximately 10% of the human genome encodes zinc finger proteins, constituting about 3,000 zinc proteins in humans.<sup>58</sup> These zinc finger proteins are roughly categorized into 6 different classes of enzymes, namely oxidoreductases, transferases, hydrolases, lyases, isomerases and ligases.<sup>58</sup> Additionally, zinc finger proteins have a multitude of structures, resulting in diverse functions in cells. They include recognition of DNA, RNA packaging, transcriptional activation, regulation of apoptosis, protein folding and assembly, as well as lipid binding, mediating protein-RNA and protein-protein interactions.<sup>59,60</sup> Additionally, based on their ability to regulate gene expression, zinc finger proteins play a wide variety of physiological roles, accomplishing the tissue homeostasis through regulating cell proliferation, differentiation and apoptosis.<sup>61</sup> Therefore, according to the importance of zinc proteome in eukaryota domain of life, environmental disturbance on the enzymatic activities involved by zinc finger motifs can be critical to understand how cellular processes are disrupted through interference of zinc finger protein functions.

## **2.2. Zinc Finger Proteins and Human Diseases**

Zinc finger proteins play pivotal roles in regulating a wide variety of cell signaling pathways involved in important cellular processes; therefore, alterations of proper functions of ZNFs give rise to the development of several human diseases such as cancer, neurodegenerative disorders and type 2 diabetes.

Some of ZNFs can act as tumor suppressors or oncogenes, participating in the onset and progression of tumorigenesis, based on the three major reasons as followed.<sup>61</sup> i) ZNFs can be

molecular players involved in most of the primary signaling pathways underlying cancer progression from the onset of carcinogenesis to metastasis formation; ii) ZNFs can favor cancer progression by their transcription factor function; iii) ZNFs can regulate cancer cell migration and invasion by their roles as the recruiters of chromatin modifiers or as structural proteins.<sup>61</sup> Also, some of the DNA repair enzymes harbor zinc fingers, such as hMOF, XPA and PARP1. Loss-of-function mutations of these DNA repair zinc finger proteins can result in exacerbated DNA repair capacities, leading to higher genomic instability and hence higher incidence of carcinogenesis.<sup>62–65</sup>

Aside from cancer, some ZNFs play pivotal roles in maintaining the proper functioning of nervous system, thereby malfunctioning of these proteins can elicit the pathogenesis of neurological diseases.<sup>61</sup> Parkin, an E3 ubiquitin ligase with a RING finger motif, is a paradigm of critical ZNFs involved in neurodegenerative disorders especially Parkinson's disease (PD) by losing its E3 ubiquitin ligase activity on ZNF746 in this case.<sup>61</sup>

ZNFs might also be involved in the progression of metabolic diseases, particularly type 2 diabetes which can be caused by insulin insensitivity in adipose tissue or default insulin secretion in pancreatic  $\beta$ -cells. For examples, ZFP407 plays a regulatory role on insulin-stimulated glucose uptake through modulating the mRNA level of glucose transporter 4 (GLUT4) in peripheral tissues including adipose tissue,<sup>66</sup> while GLIS3, a C<sub>2</sub>H<sub>2</sub>-type Kruppel-like zinc finger protein highly expressed in human pancreatic  $\beta$ -cells, is involved in neonatal diabetes and congenital hypothyroidism (NDH).<sup>61</sup>

Taken together, ZNFs are critical players that participate in regulating a wide variety of important cellular processes, ranging from cell proliferation to transcriptional regulation and protein homeostasis, rendering them being molecular targets of environmental toxicants including arsenic for the pathogenesis of a range of human diseases.

### **2.3. Mode of Action of Arsenite on Zinc Finger Proteins**

Over the past decade,  $\text{As}^{3+}$  binding to zinc finger motifs of proteins has been proposed as the mode of action of arsenic on zinc finger proteins.<sup>39,67</sup> In each zinc finger protein,  $\text{Zn}^{2+}$  is coordinated by critical cysteine residues within the zinc finger motifs of the protein, where the zinc coordination sphere is important for the structure recognizing DNA, RNA and protein as well as constituting the active site of enzymatic activity.<sup>68</sup> However, under most circumstances,  $\text{As}^{3+}$  has higher binding affinity toward the sulfhydryl group of cysteine residues coordinating  $\text{Zn}^{2+}$ , resulting in the displacement of  $\text{Zn}^{2+}$  from the zinc finger motifs. To this end, the zinc coordination sphere is greatly disrupted by  $\text{As}^{3+}$  binding to cysteine residues, leading to its subsequent conformational change of the zinc finger motif. This can explain how  $\text{As}^{3+}$  binding could perturb the molecular and cellular functions of zinc finger proteins. Additionally, a variety of researches have demonstrated that  $\text{As}^{3+}$  very likely binds to alter the conformation and enzymatic activity of zinc finger proteins.<sup>55,69,70</sup> Therefore,  $\text{As}^{3+}$  binding on zinc finger motifs sets the biochemical basis of my PhD research.

### **3. Mechanisms of $\text{As}^{3+}$ -elicited Disruption of DNA Repair and Protein Quality Control**

Most human cancers and neurodegenerative disorders are mainly attributed to impaired DNA repair capacity and/or dysregulation of protein homeostasis resulting from protein misfolding and aggregation. Exposure to arsenic has been demonstrated to impair DNA repair and also induce protein misfolding and aggregation. In this dissertation, the molecular mechanisms of arsenic-induced tumorigenesis and protein misfolding-associated diseases are discussed with a focus on impaired DNA repair and proteotoxic stress as below.

#### **3.1 Inhibition of DNA Repair**

Carcinogenesis has been believed to be a multi-step process, namely initiation, promotion and malignant progression (Fig. 1.4.).<sup>71</sup> Cancer arises by accumulation of DNA mutations in cells,

which could be elicited by impaired DNA repair capacity. In general, environmental chemicals such as metals and polycyclic aromatic hydrocarbons (PAHs) are usually bioactivated to act as electrophilic species or oxidizing agents which can attack DNA (i.e. nucleotide bases) chemically or directly, causing DNA damages through generating DNA adducts.<sup>71</sup> Hence, DNA damage sensor proteins such as ATR detect DNA damage sites, hence triggering the DNA damage response pathway. Meanwhile, DNA repair enzymes such as XPA, poly(ADP-ribose) polymerase-1 and hMOF mediate their catalytic functions in order to repair DNA damage before DNA replication in cell cycles.<sup>61,64,65,72</sup> In order to provide sufficient time for DNA repair machinery to proceed, cell cycle checkpoint proteins function as gatekeeper to transiently pause the cell cycle at DNA damage checkpoints at the G1/M or G2/M boundaries. However, under the circumstance that the DNA damage including oxidative DNA adducts cannot be removed before DNA replication, error-prone translesion synthesis (TLS) DNA polymerases would substitute three major high-fidelity DNA polymerases (i.e. pol  $\epsilon$ , pol  $\delta$  and pol  $\alpha$ ) to help proceed the DNA replication by bypassing these bulky or distorted DNA damages, thereby introducing DNA mutations into the newly synthesized DNA strands.<sup>71</sup> Depending on the location of the mutation in chromosomes (gene loci), several major consequences could happen: i) proto-oncogenes could be activated by driver mutation to initiate the tumorigenesis, ii) tumor suppressor genes could be turned off to favor tumor progression, and iii) mutator mutation would trigger the chain reactions of introducing more DNA mutations (e.g. malfunctioning the checkpoint gatekeeper proteins or the members of the DNA repair machinery). To this end, defaults in any of the abovementioned steps could interfere with the DNA repair machinery, leading to DNA mutations and tumorigenesis.

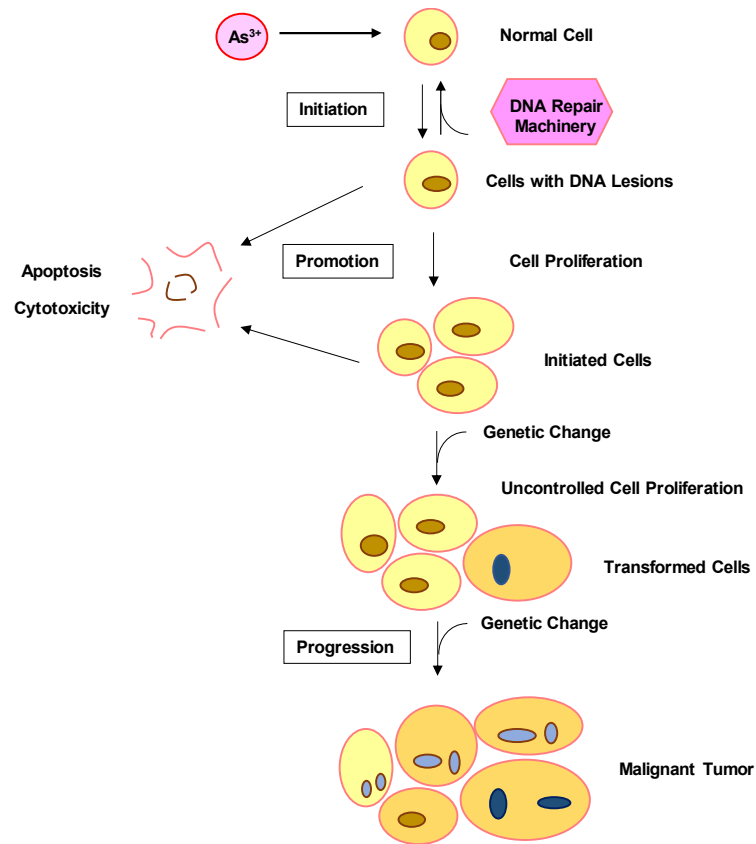


**Figure 1.4.** Multi-stage carcinogenesis model.

Arsenite alone is a weak mutagenic agent, but it is known to enhance the mutagenicity of other carcinogens. For instance, arsenite has been reported to enhance the mutagenicity or clastogenicity of X-rays, UV, methyl methanesulfonate (MMS) and diepoxybutane in mammalian cells.<sup>73-75</sup> The arsenic's role in augmenting the mutagenicity of other carcinogens perhaps can be attributed to its influence on inhibiting the repair of DNA lesions induced by other carcinogens. Here we review the previous work regarding the perturbation of various cellular DNA repair and DDR pathways after exposure to iAs (Fig. 1.5).

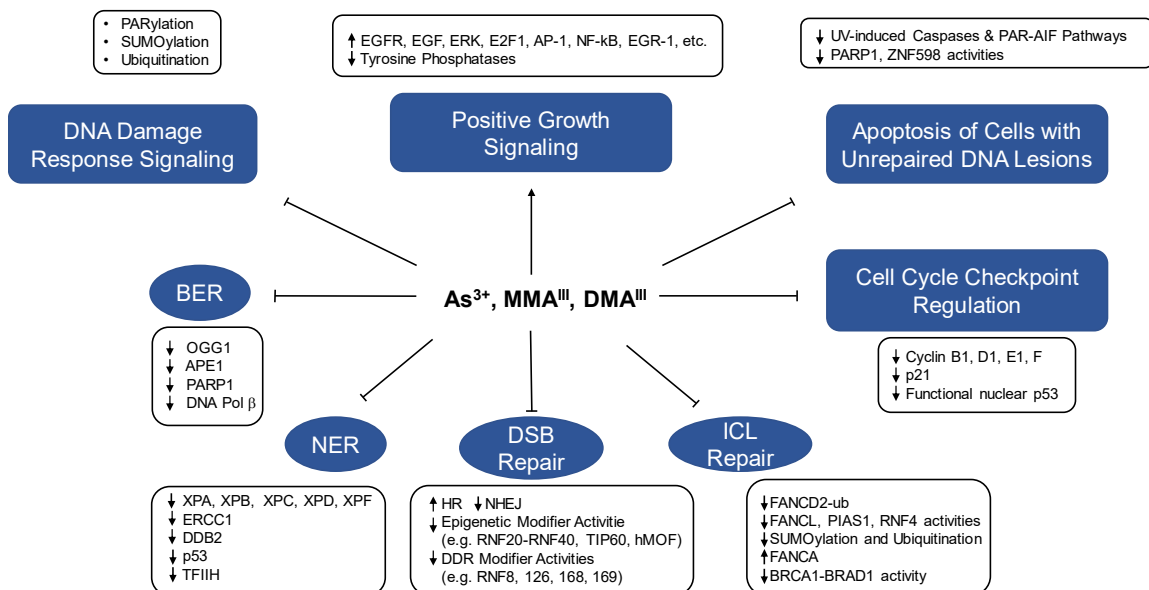


**Figure 1.5.** Major events governing the disruption of DNA repair pathways by iAs and its trivalent metabolites. Arsenite and its metabolites increase positive growth signaling while inhibiting BER, NER, DSB repair, ICL repair, DDR signaling, cell cycle checkpoint regulation, apoptosis of damaged cells. These together diminish the capacity of DNA repair, thus impairing genetic integrity.

### 3.1.1. Excision Repair

A number of studies revealed that arsenite can target several key molecular players in base excision repair (BER) and nucleotide excision repair (NER) pathways through perturbation of the expression levels of DNA repair genes and catalytic activities of DNA repair proteins.

#### 3.1.1.1. BER

BER is a crucial DNA repair pathway mainly responsible for the removal of oxidatively generated and alkylated nucleobase lesions, apurinic/aprimidinic (AP) sites and strand breaks.<sup>76</sup> For instance, 8-oxoG is one of the most abundant oxidatively generated DNA lesions.<sup>77-79</sup> 8-Oxoguanine DNA glycosylase-1 (OGG1) is the main glycosylase responsible for the excision of 8-oxoG from DNA in mammals.<sup>79-81</sup> A previous study revealed a dose-dependent decline in mRNA

level and enzymatic activity of OGG1 in A549 human lung epithelial cells after exposure to micromolar concentrations of arsenite and its metabolites.<sup>82</sup>

Aside from OGG1, AP endonuclease 1 (APE1), the major endonuclease responsible for the excision of apurinic/aprimidinic (AP) sites in eukaryotic cells, was shown to be diminished at the mRNA and protein levels after exposure to 0 – 10  $\mu\text{M}$   $\text{As}^{3+}$ .<sup>83</sup> Additionally, DNA polymerase  $\beta$ , an important enzyme for DNA repair synthesis during BER,<sup>84</sup> exhibited decreased expression at both the mRNA and protein levels after exposure to  $\text{As}^{3+}$  at concentrations that are  $\geq 5 \mu\text{M}$ .<sup>83</sup> Moreover, Osmond *et al.*<sup>85</sup> observed a dose-dependent decrease in mRNA levels of APE1, DNA ligase I (LIG1), OGG1, PARP1 and DNA polymerase  $\beta$  (DNA Pol $\beta$ ) in 24-week old mice sub-chronically (2 weeks) exposed to arsenite-contaminated drinking water, further suggesting that arsenic impairs the BER pathway.

### **3.1.1.2. NER**

NER is a critical and versatile DNA repair pathway for the removal of bulky DNA adducts and helix-distorting lesions induced by environmental carcinogens (e.g. UV-induced dimeric DNA photoproducts and adducts generated from metabolites of polycyclic aromatic hydrocarbons).<sup>86</sup>

Arsenic mainly interferes with NER by disrupting the gene expression levels and activities of crucial NER players, where the arsenic-induced disruption of NER was supported by a number of prior studies. In one study involving a US population, exposure to arsenic in drinking water was found to be correlated with reductions in mRNA levels of *ERCC1*, *XPB* and *XPF* genes in lymphocytes,<sup>87</sup> and the mRNA and protein expression levels of *ERCC1* were also shown to be diminished upon arsenic exposure in a follow-up study.<sup>88</sup> Additionally, a dose-dependent decline in mRNA levels of *ERCC1* gene was observed in human cardiomyocytes following a 72-hr exposure to arsenite.<sup>89</sup>

An earlier large-scale microarray analysis revealed that the mRNA expression levels of a number of DNA repair genes, encompassing *XPC*, *DDB2* and *TP53*, were significantly down-regulated in human epidermal keratinocytes after exposure to submicromolar concentrations of arsenite.<sup>90</sup> Another microarray study showed that the mRNA expression levels of *XPD*, *PCNA*, *APE1*, *RFC*, *XPC* and DNA ligase I were reduced by at least 1.5-fold after a 4-hr exposure to 5  $\mu$ M arsenite.<sup>91</sup> Moreover, treatment of human skin fibroblast cells with arsenite and MMA<sup>III</sup> lowered, in a dose-dependent manner, the mRNA levels of *XPC* and *DDB2*, as well as the protein level of *XPC*.<sup>92</sup> Furthermore, treatment of IMR-90 human lung fibroblasts with arsenite reduced the protein level of *XPC*, partially through proteasomal degradation, as well as reducing the mRNA levels of several NER genes, including *XPA*, *XPC* and *DDB2*.<sup>93</sup> A recent Bru-seq study showed that a 1-hr acute exposure to 5  $\mu$ M arsenite led to diminished transcription of *RAD23B* and *DDB2* genes.<sup>94</sup> Impairment of NER by arsenic was also observed for DNA lesions induced by cisplatin, an effective chemotherapeutic drug for treating human cancers through the generation of Pt-d(GpG) intrastrand cross-link lesions in DNA.<sup>95</sup> In particular, exposure to arsenite prevented the induction of *XPC* after treatment of mice with cisplatin.<sup>96</sup>

Interestingly, arsenic exposure has been shown not to affect the protein level of *XPA*,<sup>93</sup> which is essential in NER for recognizing damaged DNA and subsequent recruitment of other NER components, especially *RPA70* and *TFIIH*.<sup>97,98</sup> The *XPA* protein contains a Cys<sub>4</sub> (C<sub>4</sub>)-type zinc finger that is involved in binding damaged DNA and *RPA70*. A single amino acid substitution mutation experiment for these cysteines demonstrated a reduction in the binding capability of *XPA* for damaged DNA and *RPA70*.<sup>97</sup> Biochemical studies also indicated that mutations in any of the four zinc-coordinating cysteines result in an unfolded protein.<sup>99</sup> Arsenite has been demonstrated to interact with zinc finger proteins by substituting for the zinc ion,<sup>100,101</sup> and several zinc finger



proteins involved in DNA repair, e.g. XPA and poly(ADP-ribose) polymerase 1 (PARP1), have been shown to be direct molecular targets for binding with  $iAs^{3+}$  and  $MMA^{III}$ .<sup>63,102–104</sup>

Lastly, arsenite exposure has been proposed to interfere with and inhibit NER activity through NO-mediated nitrosylation of DNA repair enzymes.<sup>38,39,105,106</sup> All the above studies together support that arsenite and its trivalent metabolites may perturb NER by acting on central NER players at both transcript and protein levels.

### **3.1.2. DNA Ligation**

DNA ligases assume important roles in various DNA metabolic processes including DNA replication, repair and recombination, and arsenite has been shown to inhibit DNA ligation process. It was reported that the levels of mRNA, protein and enzymatic activities of DNA ligase I and DNA ligase III are significantly diminished in mammalian cells after exposure to  $iAs^{3+}$  and  $MMA^{III}$ .<sup>83,107</sup> It was also shown that arsenite inhibits DNA ligation by interacting with the vicinal cysteines in DNA ligase III, thereby retarding DNA break rejoining in MMS-treated hamster cells.<sup>108</sup> In addition, XRCC1 plays an indispensable role in recruiting and stabilizing ligase III $\alpha$  in the DNA ligation step of excision repair by acting as a scaffolding protein,<sup>109–112</sup> where down-regulation of the XRCC1 protein by  $iAs$  exposure also contributes to the impairment of the DNA ligation step of the excision repair pathways.<sup>113</sup> Because the inhibition of DNA ligation by arsenic exposure prevents the completion of DNA repair, it may lead to accumulation of damaged intermediates including single- and double-strand breaks, ultimately contributing to genome instability.

### **3.1.3. Fanconi Anemia (FA)/BRCA Pathway for Interstrand DNA Crosslink and DNA-protein Crosslink Repair**

DNA interstrand cross-links (ICLs) can arise from endogenous metabolism or from exposure to therapeutic cross-linking agents such as mitomycin C (MMC).<sup>114</sup> ICLs are extremely cytotoxic because covalent linkage of the two strands of DNA blocks essential DNA metabolic processes including replication and transcription.<sup>114</sup> FA/BRCA pathway, which encompasses three stages of DNA repair processes – nucleolytic incision, translesion synthesis (TLS) and homologous recombination (HR) – is indispensable for the repair of DNA ICLs.<sup>114,115</sup> As<sup>3+</sup> was shown to disrupt the FA/BRCA pathway-mediated repair of DNA ICLs.<sup>116</sup>

In the FA/BRCA pathway, monoubiquitination of FANCD2 is essential for the recruitment of SLX4/FANCP – an endonuclease protein complex required for unhooking the DNA cross-link and for the downstream TLS and HR steps of the ICL repair pathway – to DNA damage sites.<sup>114,117</sup> Monoubiquitination of FANCD2, catalyzed by the E3 ubiquitin ligase FANCL,<sup>118,119</sup> is also necessary for the relocalization of the Fanconi-associated nuclease 1 into nuclear DNA repair foci for recovery of stalled replication forks during ICL repair.<sup>120</sup> Recently, arsenite was shown to inhibit the repair of DNA ICLs induced by MMC through diminishing monoubiquitination and compromising the access of FANCD2 to DNA damage sites in chromatin in cultured human cells.<sup>121</sup> This occurs through inhibition of the E3 ubiquitin ligase activity of FANCL via direct binding of arsenite to its RING finger domain.<sup>121</sup> Apart from FANCL, arsenite may also bind to RING finger-containing SUMO E3 ligases PIAS1 and RNF4, which may inhibit the SUMOylation, polyubiquitination and degradation of FANCA, thereby impairing the function of FANCA in the FA/BRCA pathway.<sup>122</sup>

Unhooking of an ICL by XPF-ERCC1 is necessary for the stable localization of FANCD2 onto chromatin and its subsequent HR-mediated repair of DNA DSBs, as manifested by the failure to

repair ICL-induced DSBs in XPF-ERCC1-deficient human cells.<sup>123-125</sup> Decreases in the mRNA levels of XPF and ERCC1,<sup>87</sup> and in the protein level of ERCC1,<sup>88</sup> among individuals exposed to arsenite in drinking water suggest that arsenite may impair ICL repair through suppressing mRNA and protein expression and disrupting the proper function of the XPF-ERCC1 complex.

BRCA1 has been proposed to be crucial for homologous recombination-independent repair of DNA ICLs by promoting the recruitment of FANCD2 to DNA damage sites.<sup>126,127</sup> In particular, BRCA1 was shown to antagonize the inhibitory effect of the Ku70-Ku80 heterodimer on FANCD2 foci formation,<sup>126</sup> and promote unloading of the CMG helicase from stalled replication forks during ICL repair.<sup>128</sup> Additionally, BRCA1 is believed to amplify the FA/BRCA pathway by regulating FANCD2 localization through interaction with other proteins.<sup>129</sup> It has been hypothesized that BRCA1 is involved in homology-based DNA repair during DNA damage response against tumor progression via its E3 ubiquitin ligase activity; the RING domain of the ligase is indispensable for its interaction with BRCA1-associated RING domain (BARD1) protein, forming a heterodimeric complex to modulate the enzymatic activity and stability of BRCA1.<sup>128,130</sup> Exposure to arsenite was recently found to diminish the recruitment of BRCA1 to DNA DSB sites,<sup>69</sup> suggesting that arsenite might also interfere with ICL repair through binding and inhibiting the E3 ubiquitin ligase activity of the BRCA1-BARD1 complex.

#### **3.1.4. DNA Double-strand Break Repair**

Double strand breaks (DSBs) are among the most deleterious types of DNA lesions, which can lead to mutations, loss of heterozygosity, and chromosomal rearrangement; if not properly repaired, they can lead to cell death and cancer.<sup>131,132</sup> In mammalian cells, DSB repair proceeds through two different pathways, namely, HR and non-homologous end-joining (NHEJ).<sup>133</sup> Exposure to arsenic was shown to induce DSBs, and ultimately lead to chromosomal aberrations and sister chromatid exchanges.<sup>134,135</sup> Exposure to arsenic was also found to inhibit DNA DSB repair and influence the

DNA DSB repair pathway choice by favoring error-prone NHEJ repair while inhibiting the error-free HR pathway, leading to mis-repair of DSBs and genome instability.<sup>136</sup>

Since DSB repair occurs on DNA substrates that are localized in chromatin, the efficiency in DSB repair depends largely on how accessible the site of damage is, which is largely determined by the compactness of the local chromatin.<sup>137</sup> Generation of open chromatin involves the actions of multi-subunit chromatin-remodeling complexes and post-translational modifications of core histone proteins. In the latter regard, acetylation of lysine 16 in histone H4 (H4K16Ac) and mono-ubiquitination of lysine 120 in histone H2B (H2BK120ub) represent those histone epigenetic marks that promote the formation of biochemically accessible chromatin at or near DNA DSB sites.<sup>69,138,139</sup> Recently, it was reported that arsenite inhibits H4K16Ac by binding to the zinc finger motif of two MYST family histone acetyltransferases TIP60 and hMOF,<sup>140,141</sup> and arsenite was also shown to inhibit H2BK120ub catalyzed by RNF20-RNF40 histone E3 ubiquitin ligase in a similar fashion, thereby diminishing the recruitment of BRCA1 and RAD51 to DSB sites for repair.<sup>69</sup> Therefore, arsenite could disrupt DSB repair by inhibiting histone epigenetic modifications, which leads to compact chromatin structures unfavorable for DNA DSB repair.

In addition to chromatin reorganization, a myriad of zinc finger proteins are involved in post-translational modifications (PTMs) of proteins that regulate DDR and transcription of DNA repair genes. For instance, the RING finger E3 ubiquitin ligases RNF8 and RNF168 are essential for driving DDR to DSBs through ubiquitination of H2A/H2AX surrounding DNA DSB sites.<sup>142</sup> Furthermore, RNF168 couples PALB2-containing protein complex to DSB-induced H2A ubiquitination via PALB2-interacting domain, thereby promoting DSB repair.<sup>143</sup> In addition, DNA DSB repair pathway choice is also modulated by deubiquitinating enzymes (DUBs) and other E3 ubiquitin ligases (e.g. RNF169 and RNF126).<sup>144-147</sup> In this vein, being a negative regulator of the ubiquitin-dependent DDR signaling, RNF169 directly recognizes RNF168-mediated ubiquitination

near DNA DSB sites, and competes with other ligases for nonproteolytic ubiquitination at DSB sites to limit the deposition of 53BP1 and RAP80, thereby fine-tuning the DSB repair pathway choice.<sup>145,146,148</sup> Moreover, after being recruited to DSB sites in a RNF8-dependent manner, RNF126 directly interacts with and ubiquitinates RNF168 to negatively regulate the RNF168-mediated H2AX ubiquitination and favor the HR-mediated repair of DSBs.<sup>147</sup>

Within seconds after DSB induction, poly(ADP-ribose) polymerases, including PARP1, sense, recognize and bind to DSBs to catalyze global protein poly(ADP-ribosyl)ation (PARylation).<sup>149–151</sup> Global PARylation around DSB sites serves as a docking platform for rapid recruitment of various DNA repair factors, including MRE11, NBS1, BARD1, CHFR, and RNF146.<sup>150,152</sup> Meanwhile, PARP1 can PARylate different proteins globally, including BRCA1, DNA-dependent protein kinase catalytic subunits (DNA-PKcs) and core histones, to promote DNA DSB repair.<sup>152–154</sup> In addition, arsenite was shown to interfere with DNA damage-elicited global PARylation in human cells, by inhibiting PARP1 activity through displacement of zinc ions from its zinc finger motifs.<sup>54,63,155,156</sup>

PARP1 perhaps can be viewed as a typical paradigm among DNA repair proteins, many of which contain redox-sensitive cysteine residues within zinc finger domains.<sup>21,157,158</sup> Given that arsenic exposure can stimulate the generation of ROS/RNS,<sup>19,38,159</sup> arsenite-induced oxidative stress can result in modification of thiol groups on the cysteine residues in zinc finger motifs of these DNA repair proteins, leading to the loss of their enzymatic function.<sup>103,106,160,161</sup> This has been demonstrated for PARP1, which could be inhibited by peroxynitrite-mediated *S*-nitrosation of its zinc finger cysteine(s).<sup>38,39,63</sup> Global PARylation, a PTM predominantly mediated by PARP1 and critical for immediate initiation of DDR to maintain genomic stability, was shown to be markedly inhibited upon an 18-hr exposure to 0.01  $\mu\text{M}$  arsenite.<sup>162</sup> Therefore, in addition to direct  $\text{As}^{3+}$

binding, arsenic-induced oxidative stress also contributes, in part, to diminished DNA repair arising from arsenic exposure (Fig. 1.6).<sup>105,163</sup>

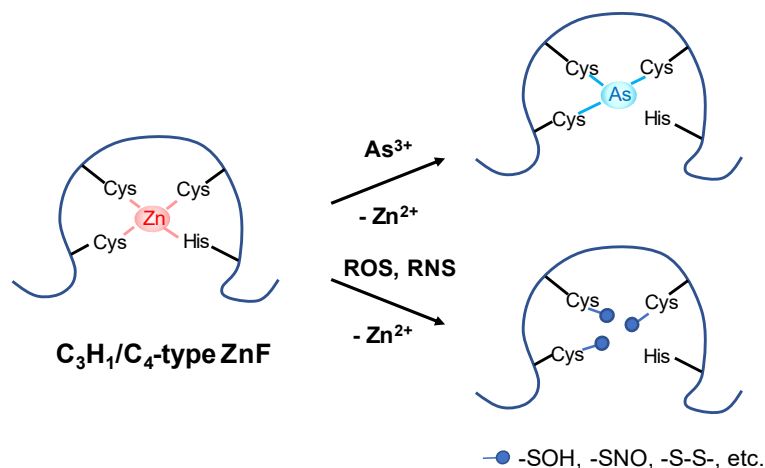


**Figure 1.6.** Modes of action of inorganic arsenic and iAs-induced ROS/RNS in impairing the enzymatic activity of zinc finger proteins. iAs and ROS/RNS can target vicinal cysteines within the zinc coordination spheres of zinc finger proteins: i) As<sup>3+</sup> directly binds to these cysteines more strongly than Zn<sup>2+</sup>; ii) ROS oxidizes these cysteines to form a series of oxidized products, such as -SOH and -S-S-; iii) RNS, especially peroxyntirite, can *S*-nitrosylate these cysteines. In all these cases, Zn<sup>2+</sup> bound within zinc finger motifs is released by its displacement by As<sup>3+</sup>, which alters the conformation of zinc finger proteins and hence their enzymatic activities.

Recently, CTCF, a versatile 11-zinc finger transcription regulator with well-established roles in three-dimensional genome organization and transcriptional regulation, was found to facilitate DNA DSB repair by enhancing HR.<sup>164,165</sup> Arsenite was shown to inhibit CTCF binding at the proximal, weak CTCF binding sites located in the promoters of *TET1* and *TET2* genes while enhancing its binding at the stronger distal binding sites.<sup>166</sup> CTCF is recruited to DSB sites through its zinc finger domains independently of PARylation.<sup>164</sup> Therefore, substitution of zinc ions within those 11 zinc finger domains of CTCF by iAs<sup>3+</sup> can block its DNA binding capability and might explain the arsenic-associated inhibition of CTCF binding to weak CTCF binding sites in promoters of *TET* genes. Additionally, a recent study demonstrated that CTCF binds to both MRE11 and CtIP

through its zinc finger domains, which enables robust CtIP recruitment for 5' end DNA resection, thereby promoting HR while suppressing NHEJ pathway of DNA DSB repair.<sup>167</sup> Hence, the binding of iAs<sup>3+</sup> with CTCF might explain, in part, how arsenite disrupts the outcome of this DSB repair pathway.

### **3.1.5. Disruption of the DNA Damage Response Signaling**

Arsenite exposure has been shown to impair DDR signaling, especially through dysregulation of protein PARylation, ubiquitination and SUMOylation,<sup>168,169</sup> as reviewed recently.<sup>94</sup> DDR is a tightly regulated temporal- and spatial-sensitive chromatin-associated process important for sensing DNA damage, recruiting DNA repair machinery to damage sites, and intertwining DNA repair with other DNA-transacting processes.<sup>170</sup> For example, ATM-dependent H2AX phosphorylation, PARP1-mediated PARylation, and TIP60-catalyzed histone acetylation are among the earliest events in DNA damage response; they are activated by DNA damage, and involve early and rapid detection of DNA lesions and chromatin decompaction, thereby creating better accessibility for DNA repair machinery to DNA damage sites.<sup>170</sup> The reversible ubiquitination and SUMOylation of DDR proteins are crucial for effective DSB repair and signaling in DDR,<sup>171</sup> where zinc finger-containing ubiquitin ligases and SUMO-conjugating enzymes can be disrupted by arsenic exposure, with examples of RAD18, MORC2, RNF4 and RNF111 being briefly discussed below.<sup>94</sup>

During replication stress, the E3 ubiquitin ligase RAD18 induces monoubiquitination of PCNA, which is in turn recognized and bound by Spartan for its subsequent recruitment of Pol  $\eta$  (i.e. a TLS polymerase important for bypassing UV-induced DNA lesions).<sup>172-174</sup> The monoubiquitinated PCNA also promotes efficient monoubiquitination and chromatin localization

of FANCD2,<sup>175,176</sup> and this ubiquitination is indispensable for recruiting SNM1A to DNA repair complexes assembled at MMC- and UV-induced DNA lesions to promote ICL repair.<sup>177</sup>

PARylation is also important in DDR. In order to achieve DNA damage-induced PARylation and PAR-dependent recruitment of DNA repair proteins to DNA damage sites, PARP1 recruits chromatin remodeling enzyme MORC2 to DNA damage sites and catalyzes PARylation on its CW-type zinc finger domain, activating its ATPase and chromatin remodeling activities. Meanwhile, PARylated MORC2 stabilizes PARP1 through enhancing the NAT10-mediated acetylation of lysine 949 in PARP1, which is no longer ubiquitinated and becomes degraded by E3 ubiquitin ligase CHFR.<sup>152,178</sup> This illustrates that the crosstalk between different DNA repair enzymes is important for the dynamics of PARylation in DDR.

SUMOylation and ubiquitination are also necessary for robust DDR. To favor DDR with coordinated SUMOylation and ubiquitination, the SUMO E3 ligases PIAS1 and PIAS4 are recruited to DSB sites and lead to accumulation of SUMO1/2/3 at DSB sites, which leads to the recruitment of RNF4 to DNA damage sites.<sup>179,180</sup> RNF4 subsequently ubiquitinates and facilitates the degradation of polySUMOylated MDC1 and RPA, thus promoting efficient DSB repair.<sup>168,181-</sup>

184

Similar to RNF4, RNF111 promotes non-proteolytic ubiquitination of SUMOylated XPC which is in turn recruited to UV-damaged DNA.<sup>185</sup> Given the extensive involvement of zinc finger-containing ubiquitin and SUMO E3 ligases in DDR signaling (e.g. RAD18, RNF4), arsenite exposure may hamper ubiquitination and/or SUMOylation through direct binding or inducing oxidative modifications of cysteine residues in their zinc finger motifs, thereby disrupting DDR.



### **3.2. Disruption of Cell Cycle Checkpoints, Promotion of Cell Proliferation and Suppression of Apoptosis**

In arsenic-induced carcinogenesis, iAs has been shown to interfere with cell cycle regulation and abrogate the G2/M checkpoint, promote cell proliferation and suppress apoptosis, which indirectly suppress DNA repair by not allowing enough time for the repair and allow cells with DNA damage to propagate.<sup>186-188</sup>

Cell cycle checkpoints, including DNA damage checkpoints at the G1/S and G2/M boundaries as well as in the S phase, tightly regulate cell cycle progression by accurately assessing mitogenic signals and properly repairing DNA damage, while avoiding further propagation of damaged genomes through promoting apoptosis of the severely damaged cells.<sup>189-192</sup> This tight regulation is executed by checkpoint proteins, which comprise cyclins, cell cycle-dependent kinases and phosphatases.<sup>190,191</sup>

A recent study demonstrated that a 48-hr exposure of acute promyelocytic leukemia (APL) cells to 2  $\mu\text{M}$   $\text{iAs}^{3+}$  increased the mRNA expression of several cell cycle-associated genes, including *CCND1* (encodes for cyclin D1 protein), *CCNE1* (cyclin E1 protein) and *GADD45A*, while reduced those of *CCNF* (cyclin F) and *CDKN1A* (p21), resulting in a transition of cell populations from G1/S phases to G2/M phases and arrest cell cycle progression. This result suggests that acute exposure to  $\text{iAs}^{3+}$  disturbs cell cycle checkpoints, leading to uncontrolled cell cycle progression and proliferation of APL cells.<sup>188</sup> Notably, the DNA damage checkpoint at the G1/S boundary was bypassed by  $\text{iAs}^{3+}$ -mediated alterations in gene expression of checkpoint proteins, especially cyclin D1.<sup>193-195</sup>

Another recent study demonstrated that a 1-month exposure of human BEAS-2B cells and keratinocytes to 0.5  $\mu\text{M}$  arsenite delayed the transition from mitosis by compromising mitotic

checkpoint through the attenuation of anaphase promoting complex-mediated cyclin B1 degradation.<sup>187</sup> In this vein, long-term arsenite exposure up-regulates Polo-like kinase 1 via acting on Akt in the PI3K/Akt pathway, thereby potentiating mitotic catastrophe and genetic instability.<sup>187,196</sup>

Arsenite-elicited up-regulation of p53 protein expression and abrogation of p53-dependent increase in p21 expression together unleash the checkpoint restraints at the G1/S and G2/M boundaries as well as in the S phase.<sup>194,197,198</sup> Both chronic low-dose (e.g. 14 days, 0.1  $\mu\text{M}$ ) or acute noncytotoxic-level (e.g. 24-hr, 1  $\mu\text{M}$ ) of arsenite exposure as well as acute low-level (e.g. 24 hr, 1  $\mu\text{M}$ ) of MMA<sup>III</sup> exposure were found to induce p53 protein expression in normal human fibroblast cells.<sup>92,194,197</sup> In addition, arsenite-elicited up-regulation of Hdm2 and the ensuing ubiquitination of p53 promote nuclear export of p53, thereby disrupting its ability to transcriptionally activate its target genes, including p21 and NER genes.<sup>199–201</sup> These may give rise to unimpeded cell cycle progression and accrual of mutations from unrepaired DNA lesions.<sup>198,201</sup>

Arsenite has been reported to promote the proliferation of human cells.<sup>19,90,202–207</sup> Arsenite is thought to achieve this through enhancing pathways for cell growth, proliferation and survival (e.g. Erk, EGFR, MAPK pathways), while inhibiting pathways involved in cell death (e.g. JNK signaling) via modulation of a myriad of transcription factors (e.g. AP-1 and NF- $\kappa\text{B}$ ).<sup>207</sup> Exposure to 5  $\mu\text{M}$  arsenite was found to increase the proliferation of SH-SY5Y human neuroblastoma cells via activation of ERK in VEGF signaling, which might favor tumor progression.<sup>204</sup> Arsenite-induced cell proliferation was shown to arise from elevated levels of epidermal growth factor receptor (EGFR) ligand, heparin-binding EGF, and its subsequent activation of EGFR phosphorylation that induces pERK and cyclin D1 expression in human cells.<sup>208</sup> Arsenite-elicited ERK signaling is required for arsenic-induced transactivation of NF- $\kappa\text{B}$ ,<sup>209</sup> which might be

mediated by arsenic-stimulated oxidative stress.<sup>210-212</sup> Additionally, low-dose arsenite treatment has been documented to activate ERK, transcription factors E2F1 and Activating Protein 1 (AP-1), and enhance the DNA binding activities of AP-1 and NF- $\kappa$ B, as well as elevate the expression of a number of positive cell growth-related genes including *c-fos*, *c-jun*, *c-myc* and *EGR-1*.<sup>205,210,213-217</sup>

The major cell growth and ROS-mediated pathways are regulated by protein tyrosine phosphorylation, which itself is controlled by tyrosine kinases and protein tyrosine phosphatases. Therefore, arsenite exposure is believed to inactivate protein tyrosine phosphatases by ROS/RNS-induced modifications of redox-sensitive cysteines at their active sites, thereby augmenting the total cellular tyrosine phosphorylation in a dose-dependent manner.<sup>21,218-223</sup> Combined, arsenite and arsenite-induced ROS/RNS are believed to maintain a phosphorylated state of EGFR, and activate ERK, transcription factor AP-1 complex and its downstream target genes *c-jun*, *c-fos* and *c-myc*, thereby increasing cyclin D1 expression.<sup>210,224</sup> Together with arsenite-activated E2F transcription factors and their modulation of cyclin E levels, arsenite exposure elicits prolonged activation of cell growth signaling and leads to uncontrolled cell proliferation.<sup>214,224-226</sup>

Chronic exposure to arsenic has been shown to increase cell survival and elevate levels of DNA damage in cultured human cells.<sup>32</sup> PARP1 inhibition by low concentrations of arsenic has been proposed to enhance the survival of cells with unrepaired DNA lesions, which might include a population of “initiated carcinogenic cells” that represents the first step of the multi-stage carcinogenesis process.<sup>227</sup> Chronic arsenic exposure was also shown to decrease p53 at the posttranslational level via arsenic-induced PARylation as well as the mRNA expression level of Bax.<sup>32</sup> This demonstrates that arsenite-elicited inhibition of apoptotic mediators impairs XPC-mediated global-genome NER, resulting in mutation accrual and neoplastic transformation in DNA damage-containing cells.<sup>32</sup>

Together, arsenite-induced positive cell growth signaling and suppression of apoptosis confer insufficient time for efficient DNA repair before replication of damaged DNA and/or allow cells with damaged DNA to propagate, which may give rise to mutations and genome instability.

### 3.3. Epigenetic Dysregulation Associated with Arsenic-induced Carcinogenesis

Arsenic-elicited carcinogenesis is believed to stem, in part, from its disruption of epigenetic signaling by alterations of histone PTMs and DNA methylation patterns (Fig. 1.7.). Histone PTMs and DNA methylation tightly regulates the chromatin dynamics to modulate the inheritable expression patterns of different genes.<sup>228</sup> Therefore, arsenic can induce carcinogenesis by epigenetic silencing of tumor suppressor genes or activation of oncogenes. Here, we review the current evidence about the role of arsenic exposure in modulating the epigenetic pathway of gene regulation.

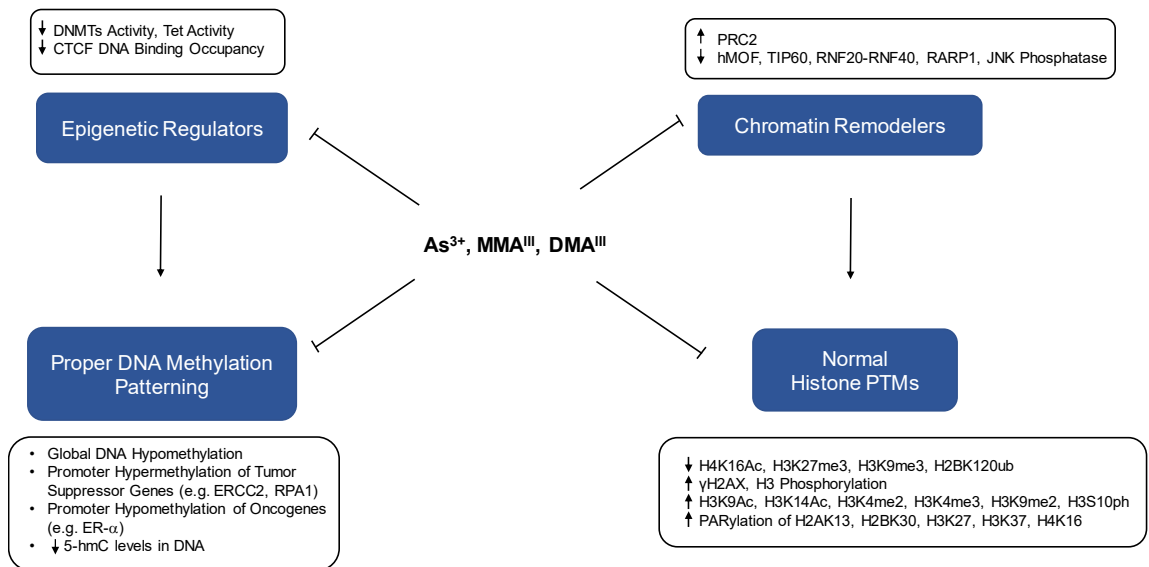


**Figure 1.7.** Major events through which inorganic arsenite and its trivalent metabolites disrupt epigenetic integrity through inhibition of epigenetic regulators and chromatin remodelers. As<sup>3+</sup>, MMA<sup>III</sup> and DMA<sup>III</sup> can inhibit the enzymatic activities of epigenetic regulators (e.g. DNMTs, Tet and CTCF) and chromatin remodelers (e.g. hMOF, TIP60 and PARP1), which subsequently perturb DNA methylation and histone PTMs, respectively, thereby disrupting epigenetic integrity.

### 3.3.1. Alterations of Histone PTMs

In the nucleus, DNA is packaged into chromatin, where the nucleosome core consists of stretches of DNA (~147 bp) wrapping around a histone octamer consisting of two copies each of core histones H2A, H2B, H3 and H4.<sup>229</sup> Hence, nucleosomes form linear 11 nm beads-on-a-string structures that further compact into 30 nm fibers and other higher-order chromatin states.<sup>230</sup> The N-terminal histone tails extending from nucleosomes are subjected to a range of PTMs, including methylation, acetylation, phosphorylation, ubiquitination, SUMOylation, ADP ribosylation, deimination and proline isomerization,<sup>231</sup> which in turn modify the chromatin compaction and recruitment of non-histone proteins, including gene regulatory factors and DNA repair enzymes, to chromatin. The formation of open, relaxed chromatin conformation is required for DNA repair machinery to gain access to the spatially confined region surrounding DNA damage sites, as described in the “access-repair-restore” model.<sup>232,233</sup>

Inorganic arsenic and its metabolites have been demonstrated to disrupt histone PTMs, including but not limited to H2AX phosphorylation, H2AX ubiquitination, H2B ubiquitination, H3 methylation and H4K16 acetylation,<sup>69,140,141,234,235</sup> which were reviewed elsewhere.<sup>228,236,237</sup> Here, we focus on the effect of arsenic exposure on those histone PTMs that are closely associated with DNA repair and genomic stability.

A number of previous *in vitro* studies have demonstrated that arsenic exposure elicits alterations in a variety of global histone PTMs, which include loss of H4K16Ac, H3K27me3 and ubiquitination of H2B, as well as gain of H3K4me2, H3K4me3, H3K9me2, H3K9Ac, H3K14Ac, phosphorylation of H3S10 and H2AX ( $\gamma$ H2AX).<sup>138,238–243</sup> For example, the PBMC from the participants of the folic acid and creatine supplementation trial (FACT) study exposed to 50-500  $\mu$ g/L arsenite in drinking water exhibited a decrease in H3K9me3 and H3K9ac, and a gain in

H3K9me2.<sup>238,241</sup> In addition, A549 human lung carcinoma cells displayed a global loss of H3K4me1 and a global gain of H3K4me2 and H3K4me3 following a 24-hr exposure to 1  $\mu$ M arsenite, where H3K4me3 remained elevated and even at one week after arsenite withdrawal.<sup>240</sup> In another study, a 24-hr exposure of A549 cells to arsenite led to elevated levels of gene-silencing marks, H3K9me2 and H3K27me3, while also augmenting the global level of the gene-activating H3K4me3 mark.<sup>239</sup>

In contrast to transcriptional activators, increased H3K9me2 levels mediated by increased mRNA and protein levels of histone methyltransferase G9a correlates with transcriptional repression,<sup>239,244</sup> which has been shown to be involved in the silencing of tumor suppressor genes in cultured cancer cells.<sup>245,246</sup> H3K27me3 is frequently accompanied with inactive promoters and gene silencing, and it labels chromatin by polycomb repressive complex 1 (PRC1) via H2AK119 ubiquitination in order to facilitate chromatin compaction.<sup>247</sup> Exposure of human cells to 0.5  $\mu$ M of arsenic trioxide (ATO) significantly induces the expression of components PRC2 protein complex, consisting of SUZ12, EZH2 and BMI1, resulting in elevated H3K27me3 levels and the corresponding suppression of mRNA and protein expression of tumor suppressors p16<sup>INK4a</sup> and p14<sup>ARF</sup>.<sup>248</sup> Arsenite-induced H3K27me3 in chromatin silences tumor suppressor genes, such as *HOXB7* and *CDKN2A*, which are involved in DNA repair.<sup>249–251</sup> Therefore, histone H3 PTMs are among the targets of arsenic exposure and aid in its disruption of DNA repair.

Histone H2BK120ub and histone H4K16Ac also play a significant role in the generation of relaxed chromatin environment that is conducive for the access of DNA repair enzymes. Histone H2BK120ub is crucial for decompacting the 30 nm chromatin fiber<sup>252</sup>, while H4K16Ac also decondenses chromatin,<sup>253</sup> thereby facilitating DSB repair by increasing the accessibility of chromatin to DNA repair machinery.<sup>254–256</sup> H2BK120ub is mediated by the E3 ubiquitin ligase

comprised of the RNF20-RNF40 heterodimer,<sup>254</sup> whereas H4K16Ac is modulated by both hMOF and TIP60 MYST-family of histone acetyltransferases.<sup>257</sup> In UROtsa human bladder epithelial cells, global H4K16Ac levels were reduced in a dose- and time-dependent manner upon exposure to As<sup>3+</sup> and MMA<sup>III</sup>.<sup>138</sup> Arsenite exposure was also documented to diminish H2BK120ub and H4K16Ac by inhibiting the above-mentioned zinc finger-containing proteins.<sup>69,140,141</sup> Moreover, the PARylation of lysine residues of the core histone tails mediated by PARP1, including H2AK13, H2BK30, H3K27, H3K37, and H4K16, can result in a rapid decondensation of chromatin around DNA damage sites and facilitate DNA repair.<sup>153,154,258</sup> Therefore, arsenic exposure could result in a compact chromatin structure by interfering with these histone-modifying enzymes and by diminishing the chromatin-decompacting histone PTMs, limiting the chromatin access of DNA repair proteins.

Finally, phosphorylation of H2AX, which is mediated by ATM and DNA-PKcs after DNA damage,<sup>259</sup> contributes to the initiation of DNA damage response.<sup>235,260</sup> Phosphorylation of H2AX at different sites triggers distinct downstream cellular processes, such as the stimulation of XPD-dependent apoptosis by Tyr142 phosphorylation in H2AX, thereby enhancing DDR.<sup>261</sup> Recently, it was reported that a 24-hr exposure to 4  $\mu$ M ATO significantly stimulated levels of phosphorylated H2AX in mouse embryonic fibroblasts (MEFs), possibly via inhibition of *de novo* dTMP biosynthesis through inducing SUMOylation, ubiquitination and subsequent degradation of MTHFD1.<sup>234</sup> Since iAs has been documented to elicit ATR and DNA-PKcs *in vivo* and *in vitro*,<sup>262-264</sup> this increase in  $\gamma$ H2AX levels is thought to originate from the activation of ATR and DNA-PKcs, and might also be modulated by TOPK.<sup>265</sup>

Studies have suggested that arsenic-induced phosphorylation of histone H3 might be responsible for the up-regulation of caspase 10, a proto-apoptotic factor,<sup>243</sup> and the proto-oncogenes

*c-fos* and *c-jun*,<sup>266</sup> which can lead to transformation of human fibroblast cells and the induction of tumors in animals.<sup>267</sup> Additionally, since arsenite could induce *c-fos* and *c-jun* via activation of JNKs and p38/MAPK2 kinases, and promote H3S10 phosphorylation via JNK kinase.<sup>242,268</sup> Therefore, the impact of the arsenic-induced H3 phosphorylation on DNA repair may be regulated by JNK/MAPK pathway, which was recently linked to DNA damage response.<sup>269</sup>

### 3.3.2. DNA Methylation

DNA methylation is another epigenetic mechanism that regulates the expression of DNA repair genes. Depending on the type of regulatory elements where the methylation occurs, the effect of DNA methylation on gene expression varies. Under normal circumstances, DNA methylation events in the promoter and gene body are associated with gene repression and activation, respectively.<sup>270</sup> Alterations in DNA methylation are known to play a role in carcinogenesis partly through inactivation of tumor suppressors and/or activation of oncogenes.<sup>271</sup>

Several potential mechanisms have been proposed to account for the arsenite-induced alterations in DNA methylation, including SAM deficiency, diminished expression of DNMT genes, inhibition of Tet proteins, and selective suppression of CTCF binding (Fig. 1.8.). As noted above, biotransformation of inorganic arsenic depletes SAM, which is also utilized in DNA methylation catalyzed by DNA cytosine-5-methyltransferases (DNMTs).<sup>272</sup> In addition, arsenic exposure was found to repress, in a dose-dependent manner, the mRNA expression and activity of DNA methyltransferases DNMT1, DNMT3A and DNMT3B, thereby resulting in the loss of global DNA methylation.<sup>272-274</sup> Interestingly, arsenic exposure was also shown to reduce CTCF expression and inhibit CTCF binding to DNA, which diminishes the occupancy of CTCF in the promoters of DNMT1, DNMT3A, and DNMT3B genes; this may explain the observation of arsenite-induced diminished expressions of DNMTs.<sup>275</sup> Moreover, arsenic was thought to selectively inhibit CTCF



binding to different genes involved in DNA repair machinery, leading to transcriptional repression of tumor suppressors and activation of proto-oncogenes.<sup>166,275</sup>

Arsenic exposure has been documented to lead to SAM depletion and result in global DNA hypomethylation,<sup>195,276–278</sup> which is a hallmark of various human cancers.<sup>279–281</sup> It was reported that chronic exposure of cultured rat liver cells to a low dose (0.5  $\mu$ M) of arsenite resulted in global DNA hypomethylation.<sup>278</sup> DNA hypomethylation was also observed in leukocytes of human populations who were exposed to arsenic and developed skin cancers.<sup>282</sup> Chronic exposure of mice to 45 ppm arsenite for 48 weeks induced hepatic global DNA hypomethylation as well as promoter hypomethylation of the *ESR1* gene, which encodes for estrogen receptor  $\alpha$ .<sup>195</sup> Promoter hypomethylation is believed to stimulate the expression of *ESR1* gene, which in turn can induce cell cycle-dependent DSBs and contribute to initiation of breast cancer.<sup>283,284</sup> Arsenic-induced promoter hypomethylation of the *ESR1* gene is consistent with the observation of frequent mutations of DDR and DNA repair proteins observed in estrogen-dependent breast cancers, suggesting that ER signaling converges to inhibit effective DNA repair and apoptosis in favor of proliferation.<sup>195,284</sup>

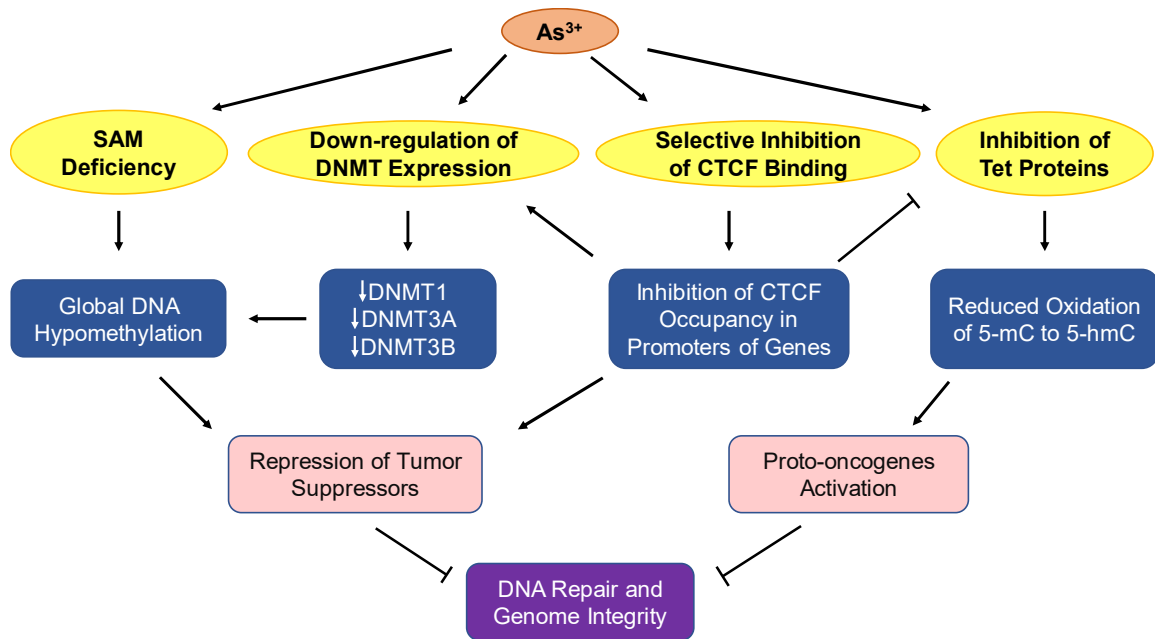


**Figure. 1.8.** Arsenite disrupts DNA methylation. Methylation events in gene promoters repress gene expression, whereas those in gene bodies activate gene expression. iAs metabolism induces SAM deficiency, which results in the global DNA hypomethylation. iAs exposure leads to decreased expressions of DNMT1, DNMT3A, DNMT3B, thus diminishing global DNA methylation. Additionally, iAs selectively inhibits CTCF binding to promoters of genes (e.g. DNMTs), leading to repression of tumor suppressors. Meanwhile, iAs inhibits Tet proteins, thus reducing the level of 5-hmC, which can be inhibited by the weakened occupancy of CTCF in the promoters of Tet genes. Combined together, iAs can repress tumor suppressors and activate proto-oncogenes, thereby impairing DNA repair and genome integrity.

Although arsenic exposure causes global DNA hypomethylation, it also leads to promoter hypermethylation and repression of specific tumor suppressor genes. For instance, the DNA repair gene *MLH1* displays significant promoter hypermethylation in whole blood obtained from humans chronically exposed to arsenic.<sup>285</sup> Additionally, significant promoter hypermethylation of NER genes (*ERCC2*, *RPA1*, *POLD3*, *POLE2*) were observed in human hepatocytes exposed to 0.2  $\mu\text{M}$  ATO for 3 months.<sup>286</sup> Recently, hypermethylation of NER genes *ERCC1* and *ERCC2*, and suppression of their expression in human cells were correlated with chronic arsenic exposure, suggesting that chronic arsenic exposure can alter methylation patterns of NER genes.<sup>287</sup>

5-mC in DNA can be oxidized by the ten-eleven translocation (Tet) family enzymes to 5-hydroxymethylcytosine (5-hmC), which may convey regulatory epigenetic functions by binding to specific regulatory proteins and mediate active gene transcription.<sup>70,288–290</sup> In addition, diminished levels of 5-hmC in DNA is a hallmark of human cancers.<sup>288</sup> Tet enzymes were found to prevent DNA damage-induced chromosomal mis-segregation, indicating that 5-hmC is pivotal in promoting DNA repair and maintenance of genome integrity.<sup>291,292</sup> Arsenite exposure was shown to bind directly with the zinc finger motifs of Tet proteins and inhibit the Tet-mediated oxidation of 5-mC to 5-hmC.<sup>70</sup> On the other hand, global and site-specific hyper-hydroxymethylation of cytosine in arsenite-transformed BEAS-2B cells was shown to be correlated with the elevated expression of Tet enzymes, which is attributed to arsenic-elicited selective inhibition of CTCF binding on the proximal, weaker CTCF binding sites of their promoters.<sup>166</sup>

Combined together, chromatin compaction around damaged DNA and disturbed methylation pattern in DNA upon arsenite exposure perturb the sophisticated epigenetic network of DNA repair machinery, which may compromise genome stability and result in arsenic-elicited carcinogenesis.

### **3.4. Perspectives of the Role of Zinc Finger Proteins in DNA Repair**

Distinct modes of action for arsenic-induced impairment of DNA repair and epigenetic pathways are extensively discussed. The findings cited in this review suggest that zinc finger proteins, which constitute approximately 10% of the human genome and play significant roles in DNA repair as well as in epigenetic regulation, constitute important molecular targets for arsenic binding (Fig. 1.9).<sup>58</sup> Since iAs exposure induces oxidative stress which generates ROS/RNS, the redox-active nucleophilic sulfhydryl group on cysteine residues located within the zinc finger motifs of these proteins are also important targets for ROS/RNS attack. The modifications induced by these reactive species, especially *S*-nitrosylation, disturb the native Zn<sup>2+</sup> coordination sphere of the zinc finger proteins and alter their structure and functions.<sup>38,39,293–297</sup>

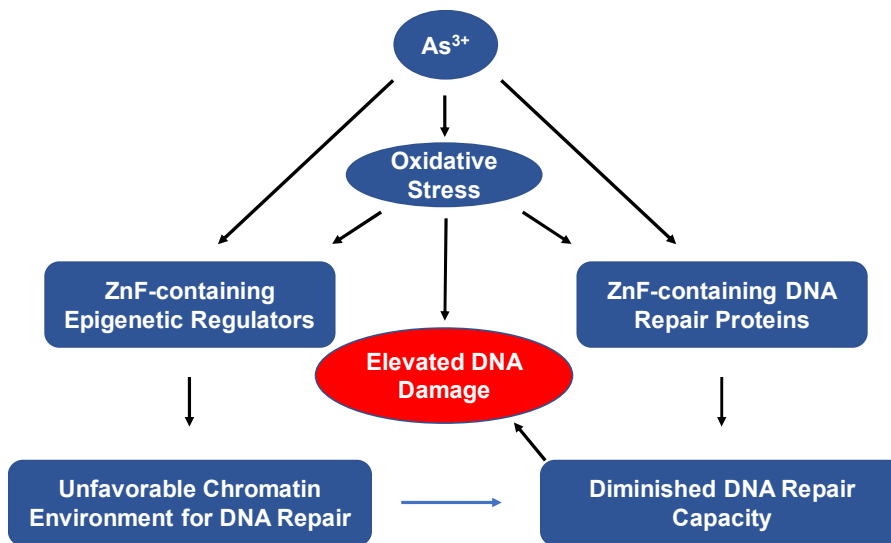


**Figure. 1.9.** Arsenite and iAs-induced oxidative stress enhance DNA damage through disrupting the functions of zinc finger proteins. Apart from iAs-induced oxidative stress,  $As^{3+}$  can inhibit the zinc finger-containing epigenetic regulators and DNA repair enzymes. Simultaneously, oxidative stress generates oxidative DNA damage. These together diminish DNA repair capacity in cells, which elevates DNA damage via disrupting zinc finger-modulated genetic and epigenetic integrity in DNA repair pathways, resulting in tumorigenesis.

Taken together, direct  $iAs^{3+}$  binding, in combination with oxidation and nitrosylation of cysteine sulfhydryl groups of zinc finger motifs of proteins involved in DNA repair and epigenetic regulation of gene expression, constitute important molecular mechanisms underlying the modes of action for the exacerbated DNA repair capacity and epigenetic instability in arsenic-induced carcinogenesis.

### **3.5. Proteotoxic Stress and Protein misfolding & Aggregation (Impaired protein quality control)**

#### **3.5.1. Arsenic and Proteotoxic Stress**

Protein misfolding and aggregation account for almost 50% of all human diseases, including cancers and neurodegenerative disorders. Recently, accumulating lines of evidence suggest that iAs may influence the aggregation propensity of disease-causing disordered proteins and promote

neurodegenerative diseases.<sup>52,298–304</sup> For instances, one epidemiological study in Texas correlated chronic low-dose iAs exposure with higher incidence of neurodegenerative diseases among human populations exposed to iAs-contaminated drinking water,<sup>48,304</sup> while a recent cell-based study demonstrated that iAs induces accumulation of  $\alpha$ -synuclein, the etiology of Parkinson's disease.<sup>15</sup> Combined together, iAs-induced protein misfolding is believed to elicit a myriad of proteinopathies, possibly due to the failure of proteostasis.<sup>305–308</sup>

### **3.5.2. Ribosome-based Quality Control (RQC) as the Frontline of Proteostasis against Protein Misfolding**

From a biophysical perspective, the processes of protein folding, unfolding, aggregation, and amyloid formation are dynamic. In cells, each individual protein is continuously shifting between the native folded state and the non-native unfolded state via breathing process.<sup>309</sup> In this process, the folding of a nascent polypeptide often does not occur spontaneously, instead it necessitates the involvement of molecular chaperones and foldases.<sup>310,311</sup> By folding, the hydrophobic collapse buries most of the aggregation-prone hydrophobic surfaces deeply inside the native protein structure. Therefore, proteins undergoing folding are much more susceptible to iAs binding than proteins that have already reached their native state.<sup>312–314</sup>

During translation of a nascent polypeptide chain, the vectoral nature of *de novo* protein synthesis at ribosome introduces the temporal and spatial translation restraints on protein folding, especially for longer and/or multidomain proteins.<sup>306,315–318</sup> Given that protein translation is relatively slow (i.e. with an average of 2-min) when compared with the millisecond time-scale of *in vitro* protein folding,<sup>319</sup> this allows the formation of partially folded structures in the extensive protein folding process before protein synthesis is completed.<sup>315</sup> Before the nascent polypeptides are completely synthesized from the ribosome, the aggregation-prone and structural-sensitive sites (e.g. cysteine-rich or hydrophobic) are susceptible to iAs binding.<sup>320,321</sup> On the basis that stronger As<sup>3+</sup>-cysteine

interaction can better stabilize the misfolded intermediate conformations and resist the refolding by chaperones relative to the noncovalent hydrophobic interactions stabilizing the native conformations.<sup>322</sup>

In cells, every single step of protein synthesis is tightly regulated and monitored carefully for potential translation error.<sup>323</sup> Most cellular resources for protein translation are devoted to maintaining quality control at ribosomes to guarantee the folding stability of nascent polypeptides before, during and after protein synthesis.<sup>324,325</sup> It is evolutionarily and energetically beneficial for the cell to predict, detect and remove any potential errors at the earliest time points and locations from which potentially erroneous nascent polypeptides originate.<sup>326</sup> As a result, nature has evolved a specialized protein quality control (PQC) pathway at ribosomes to sense and eliminate any erroneous polypeptides.<sup>326,327</sup>

In RQC, there are four distinct and successive stages: i) sensing the aberrant codon usage in mRNA sequences and ribosome collisions events with the assistance of detector proteins and stalling the ribosomes; ii) splitting of a stalled ribosome into subunits; iii) assembling RQC for ubiquitination of nascent polypeptide chains; and iv) extraction and degradation of the ubiquitinated nascent polypeptide chains, based on the recent discoveries of RQC<sup>326,328–330</sup> and are reviewed recently (Fig. 1.10.).<sup>331</sup>

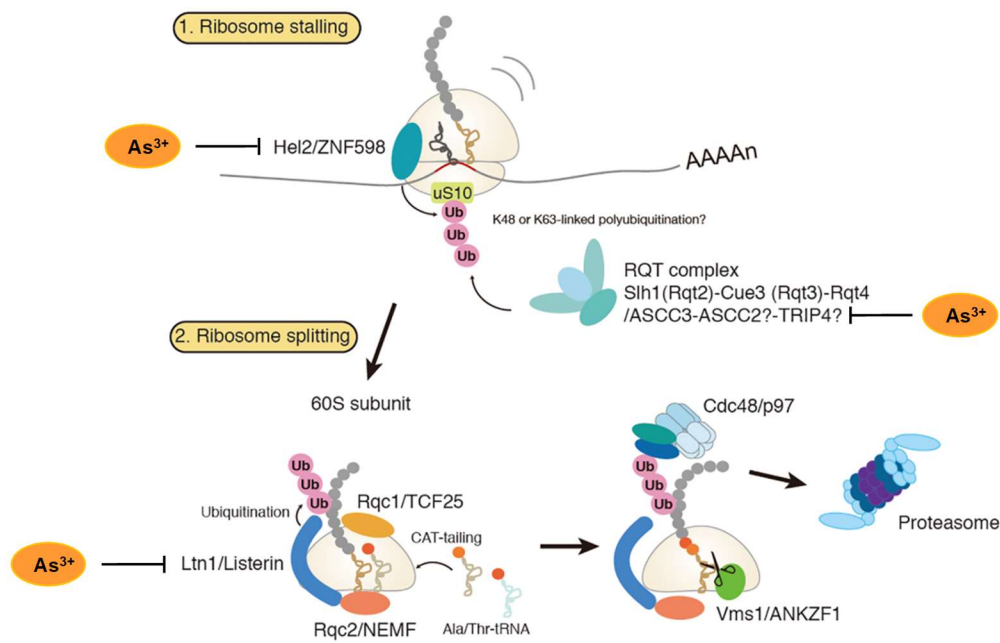


**Figure 1.10.** Overview of RQC and potential iAs targets. Modified from Ikeuchi, K. *et al.*<sup>331</sup>

### 3.5.3. Arsenic and RQC

The failure of RQC machinery leads to disastrous consequences of inducing protein aggregation and proteotoxic stress,<sup>308</sup> which is supported by genetic screening studies.<sup>332–334</sup> Environmental exposure to iAs has been well documented to interfere with global protein PTMs,<sup>55,236,238,335</sup> especially protein ubiquitination by zinc finger-containing E3 ubiquitin ligases.<sup>69,101,121,336</sup> Since  $As^{3+}$  has been proposed to bind to and oxidize the redox-active thiol groups of cysteine residues within the zinc finger motifs of proteins, where the arsenite-cysteine interaction can displace the  $Zn^{2+}$  ions, thereby resulting in the altered conformation of ZnF and its subsequent inhibition of the enzymatic activity of the proteins.<sup>39,67,70,140,335</sup> In this vein, we reason that arsenite might also disrupt other critical RING-finger E3 ubiquitin ligases or ZnF-containing proteins involved in RQC, especially ZNF598, listerin, TRIP4, and Not4, which are known to detect the collided ribosomes and initiate RQC, target the stalled nascent polypeptide chains for

ubiquitination, act as transcription coactivator in RQT complex, and mediate nonstop mRNA degradation and translation inhibition, respectively.<sup>331,337,338</sup> Likewise, elevated production of ROS and RNS arising from arsenic exposure may also oxidize or nitrosylate the thiolates from the cysteines within the ZnF of these RQC protein enzymes, thereby perturbing their functions.<sup>38,39,293–297</sup> Therefore, arsenic compromises the frontline defense of PQC, RQC, against aberrant translation products. To this end, arsenic overburdens the proteostasis network by overloading the synthesis of default proteins which cannot be overcome by its degradation capacity, thereby conferring proteotoxic stress (Fig. 1.11.).

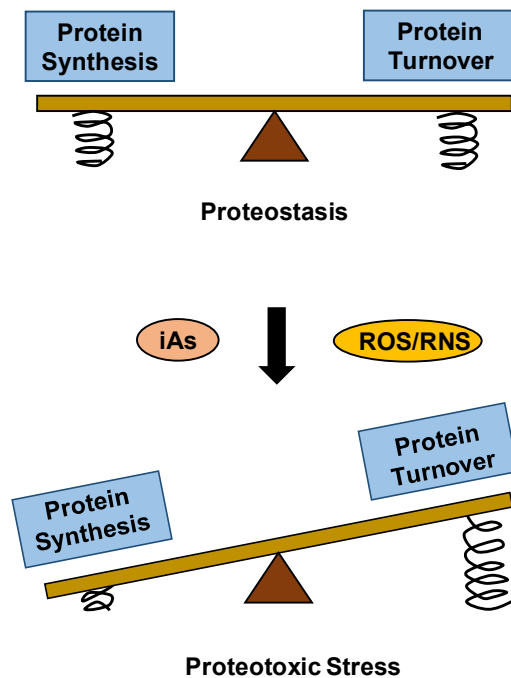


**Figure 1.11.** Arsenic induces proteotoxic stress through imbalance of protein synthesis and protein turnover.



### **3.6. Disrupted Protein Degradation by Ubiquitin-Proteasomal System (UPS)**

#### **3.6.1. Dysregulation of Rho GTPases and Cancer**

Small GTP binding proteins of the Ras superfamily (Ras, Rho, Rab, Arf, and Ran), which are also called small GTPases, function as key regulators of intracellular trafficking and central cellular processes, such as cell differentiation and proliferation.<sup>339</sup> Therefore, small GTPases are particularly important in maintenance of a plethora of signaling transduction pathways. Among small GTPases, the highly conserved Rho family of GTPases especially contribute to organization of the actin and microtubule cytoskeletons, cell cycle progression, cell polarity and cell migration.<sup>340</sup> Dysregulation of Rho GTPases leads to different hallmarks of cancers, which include oncogenic transformation, survival of damaged cells and metastasis.<sup>341</sup> In particular, RhoB has been demonstrated as a tumor suppressor which its loss facilitates cell migration and invasion in human lung.<sup>342-344</sup>

#### **3.6.2. UPS and Proteostasis**

Maintenance of protein homeostasis is very important in keeping normal physiology and proper cellular homeostasis, which is necessary to prevent carcinogenesis.<sup>345</sup> Protein folding is a dynamic process that is continuously balanced by synthesis and degradation of cellular proteins, allowing the proper functioning of proteins by folding into correct three-dimensional structures.<sup>345</sup> Proteostasis is particularly important against a plethora of age-associated human diseases, where aging leads to diminished capacity of protein turnover.<sup>315,346</sup> Ubiquitin Proteasome System (UPS), an important arm of the proteostasis network responsible for protein degradation, is comprised of a plethora of ubiquitin E3 ligases, 26S proteasome and segregase p97.<sup>315,347,348</sup> UPS is particularly important in cell cycle regulation by mediating the precise spatial and temporal proteolysis of key cell cycle proteins.<sup>348,349</sup> Therefore, dysregulation of various components of UPS would compromise proteostasis, leading to the onset of carcinogenesis.<sup>350</sup>

### **3.6.3. The Effect of Arsenic on UPS and Rho GTPases in Cancer**

Environmental exposure to carcinogenic metals such as arsenic can disrupt UPS,<sup>351</sup> and this exposure to arsenic is also shown to elicit a variety of human cancers, which include liver, lung, skin and bladder cancers.<sup>47,352,353</sup> Additionally, inorganic arsenic was recently shown to compromise E3 ubiquitin ligases, proteasome and p97 functions in UPS,<sup>55,69,101,354</sup> which are tightly regulated transcriptionally and post-transcriptionally under the normal circumstances.<sup>355</sup> Given that Rho GTPase signaling is tightly coordinated with the involvement of a series of regulatory proteins (e.g. guanine-nucleotide exchange factors, GTPase-activating proteins and guanine-nucleotide dissociation inhibitors), post-translational modifications including ubiquitination and SUMOylation are particularly essential for regulatory crosstalk between different signaling pathways including Rho GTPases, thus tightly controlling the key cellular processes.<sup>340,356</sup> Therefore, it is necessary and important to understand how exposure to arsenic can influence the expression of small GTPases and their corresponding impairment in cellular processes (e.g. cell migration and invasion), in order to better enact the strategies of molecular intervention against arsenic-induced carcinogenesis. This sets the foundation of my proteomic study of small GTPases upon arsenic exposure in chapter 4.

## **4. Scope of the dissertation**

In life, every single step in the central dogma of molecular biology is error-prone. In order to minimize the stochastic DNA replication infidelity and translation errors, the evolutionary pressure has shaped the DNA repair and proteostasis machineries to ensure the accurate and efficient information flow. Sophisticated temporal and spatial cellular responses to ever-changing cellular environmental stressors (e.g. oxidative stress and metal exposures) necessitate a highly regulated and harmonic network involving a plethora of metabolic signaling pathways to make everything

coordinated and responsive to stress. To achieve thorough coordination among signal transduction cascades, the evolutionary pressure sculpts an additional layer of regulation on DNAs, mRNAs and proteins, the post-translational modifications (PTMs). Importantly, any slight perturbation or default in modulating the PTMs of regulatory proteins, especially those in DNA repair and proteostasis, gives rise to a myriad of human diseases, including cancer and protein misfolding-associated diseases, through impaired capacities to correct for any infidelity in the information flow steps and turnover of aberrant translation products to achieve cellular homeostasis (Fig. 1.12.).

The project described herein was designed to further elucidate mechanisms of carcinogenesis and proteotoxicity of arsenic exposure through  $\text{As}^{3+}$  binding to zinc finger proteins. Arsenic contamination has been a global public health concern throughout the world, including the USA, and the characterization of arsenic toxicity on protein quality control is crucial for comprehensively understanding how arsenic causes proteostatic stress as well as its associated diseases. Based on the body of knowledge on mechanisms of  $\text{As}^{3+}$  binding on zinc finger proteins, RQC and DNA repair, as well as the effect of arsenic on ubiquitin-proteasome system (UPS), the following hypotheses were tested:

- i.  $\text{As}^{3+}$  will interact with critical vicinal cysteine residues within the zinc binding motif of histone acetyltransferase TIP60 and E3 ubiquitin ligase ZNF598 *in vitro* and in cultured human cells
- ii.  $\text{As}^{3+}$ -cysteine interaction will displace the  $\text{Zn}^{2+}$  coordinated by the zinc finger motif of TIP60 and ZNF598 through competition of binding to cysteines in cultured human cells
- iii.  $\text{As}^{3+}$  will interfere with the enzymatic activity of TIP60 and ZNF598 through disruption of their zinc coordination sphere as reflected by PTMs of their substrate proteins in cultured human cells

- iv.  $As^{3+}$  will alter the stability of TIP60, ZNF598 and RhoB GTPase proteins in a dose-dependent manner in cultured human cells
- v. The  $As^{3+}$ -induced disruption of PTMs regulated by TIP60 and ZNF598 will dysregulate vital DNA repair and RQC processes in cultured human cells
- vi. The  $As^{3+}$ -induced perturbation of UPS will dysregulate the turnover of RhoB protein via proteasomal degradation
- vii.  $As^{3+}$  treatment will diminish the fidelity of genetic information flow and proteostasis through dysregulating zinc finger-containing enzymes and small GTPases

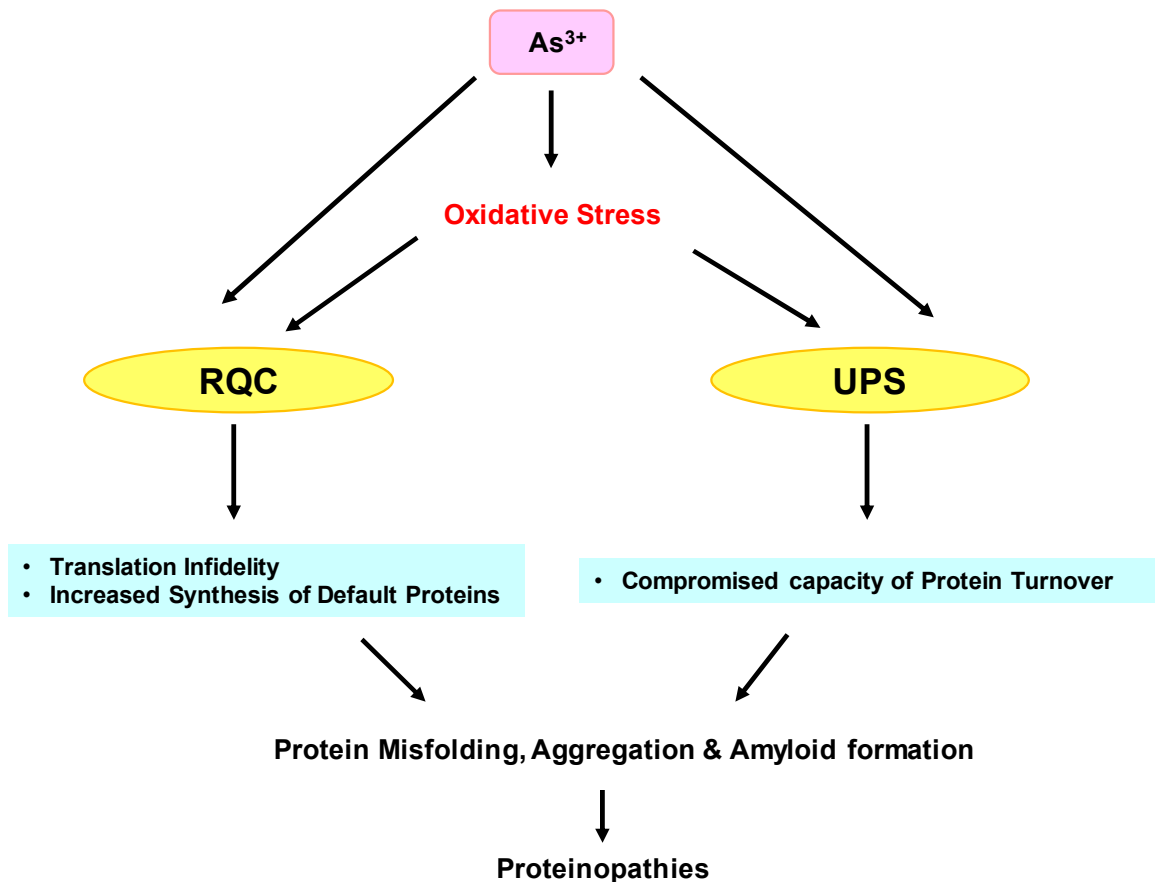


**Figure 1.12.** Hypothesis of iAs-induced enhancement of aging-related proteinopathies.

## References

1. Crick, F. Central dogma of molecular biology. *Nature* 1970;227:561-563.
2. Cobb, M. 60 years ago, Francis Crick changed the logic of biology. *PLoS Biol.* 2017;15:1-8.
3. International Agency for Research on Cancer (IARC). *Arsenic, Metals, Fibres, and Dusts*. Vol 100 C. the International Agency for Research on Cancer; 2012. <https://www.iarc.fr/>.
4. Amini, M., Mueller, K., Abbaspour, K.C., et al. Statistical modeling of global geogenic fluoride contamination in groundwaters. *Environ. Sci. Technol.* 2008;42:3662-3668.
5. Uthus, E.O. Evidence for Arsenic Essentiality. *Environ. Geochem. Health* 1992;14:55-58.
6. Ratnaik, R.N. Acute and chronic arsenic toxicity. *Postgrad. Med. J.* 2003;79:391-396.
7. Vahter, M., and Norin, H. Metabolism of <sup>74</sup>As-labeled trivalent and pentavalent inorganic arsenic in mice. *Environ. Res.* 1980;21:446-457.
8. Drobna, Z., Styblo, M., and Thomas, D.J. An Overview of Arsenic Metabolism and Toxicity. *Curr. Protoc. Toxicol.* 2009;42:1-9.
9. Hughes, M.F. Arsenic toxicity and potential mechanisms of action. *Toxicol. Lett.* 2002;133:1-16.
10. Rogers, E.H., Chernoff, N., and Kavlock, R.J. The teratogenic potential of cacodylic acid in the rat and mouse. *Drug Chem. Toxicol.* 1981;4:49-61.
11. Murai, T., Iwata, H., Otoshi, T., Endo, G., Horiguchi, S., and Fukushima, S. Renal lesions induced in F344/DuCrj rats by 4-weeks oral administration of dimethylarsinic acid. *Toxicol. Lett.* 1993;66:53-61.
12. Yamamoto, S., Matsuda, T., Murai, T., et al. Cancer Induction by an Organic Arsenic Compound, Dimethylarsinic Acid (Cacodylic Acid), in F344/DuCrj Rats after Pretreatment with Five Carcinogens. *Cancer Res.* 1995;55:1271-1276.
13. Wei, M., Wanibuchi, H., Morimura, K., et al. Carcinogenicity of dimethylarsinic acid in male F344 rats and genetic alterations in induced urinary bladder tumors. *Carcinogenesis* 2002;23:1387-1397.
14. Trouba KJ, Wauson EM, Vorce RL. Sodium arsenite-induced dysregulation of proteins involved in proliferative signaling. *Toxicol. Appl. Pharmacol.* 2000;164:161-170.
15. Cholanians, A.B., Phan, A.V., Ditzel, E.J., Camenisch, T.D., Lau, S.S., and Monks, T.J. Arsenic induces accumulation of  $\alpha$ -synuclein: Implications for synucleinopathies and neurodegeneration. *Toxicol. Sci.* 2016;153:271-281.

16. Liu, S., Guo, X., Wu, B., Yu, H., Zhang, X., and Li, M. Arsenic induces diabetic effects through beta-cell dysfunction and increased gluconeogenesis in mice. *Sci. Rep.* 2014;4:1-10.
17. Yamanaka, K., Hoshino, M., Okamoto, M., Sawamura, R., Hasegawa, A., and Okada, S. Induction of DNA Damage by Dimethylarsine, A Metabolite of Inorganic Arsenics, is for the Major Part Likely Due to Its Peroxyl Radical. *Biochem. Biophys. Res. Commun.* 1990;168:58-64.
18. Liu, S.X., Athar, M., Lippai, I., Waldren, C., and Hei, T.K. Induction of oxyradicals by arsenic: Implication for mechanism of genotoxicity. *Proc. Natl. Acad. Sci. U S A.* 2001;98:1643-1648.
19. Ruiz-Ramos, R., Lopez-Carrillo, L., Rios-Perez, A.D., De Vizcaya-Ruiz, A., and Cebrian, M.E. Sodium arsenite induces ROS generation, DNA oxidative damage, HO-1 and c-Myc proteins, NF- $\kappa$ B activation and cell proliferation in human breast cancer MCF-7 cells. *Mutat. Res. - Genet. Toxicol. Environ. Mutagen* 2009;674:109-115.
20. De Vizcaya-Ruiz, A., Barbier, O., Ruiz-Ramos, R., and Cebrian, M.E. Biomarkers of oxidative stress and damage in human populations exposed to arsenic. *Mutat. Res. - Genet. Toxicol. Environ. Mutagen* 2009;674:85-92.
21. Flora, S.J.S. Arsenic-induced oxidative stress and its reversibility. *Free Radic. Biol. Med.* 2011;51:257-281.
22. Muller, F.L., Liu, Y., and Van Remmen, H. Complex III releases superoxide to both sides of the inner mitochondrial membrane. *J Biol Chem.* 2004;279:49064-49073.
23. Liu, S.X., Davidson, M.M., Tang, X., et al. Mitochondrial damage mediates genotoxicity of arsenic in mammalian cells. *Cancer Res.* 2005;65:3236-3242.
24. Gadelha, F.R., Thomson, L., Fagian, M.M., Costa, A.D.T., Radi, R., and Vercesi, A.E. Ca<sup>2+</sup>-independent permeabilization of the inner mitochondrial membrane by peroxynitrite is mediated by membrane protein thiol cross-linking and lipid peroxidation. *Arch. Biochem. Biophys.* 1997;345:243-250.
25. Nordenson, I., and Beckman, L. Is the genotoxic effect of arsenic mediated by oxygen free radicals? *Hum. Hered.* 1991;41:71-73.
26. Valko, M., Izakovic, M., Mazur, M., Rhodes, C.J., and Telser, J. Role of oxygen radicals in DNA damage and cancer incidence. *Mol. Cell. Biochem.* 2004;266:37-56.
27. Liu, L., Trimarchi, J.R., Navarro, P., Blasco, M.A., and Keefe, D.L. Oxidative stress contributes to arsenic-induced telomere attrition, chromosome instability, and apoptosis. *J. Biol. Chem.* 2003;278:31998-32004.
28. Kitchin, K.T., and Ahmad, S. Oxidative stress as a possible mode of action for arsenic carcinogenesis. *Toxicol. Lett.* 2003;137:3-13.

29. Hei, T.K., Liu, S.U.X., and Waldren, C. Mutagenicity of arsenic in mammalian cells: Role of reactive oxygen species. *Proc. Natl. Acad. Sci. U S A.* 1998;95:8103-8107.
30. Shi, H., Shi, X., and Liu, K.J. Oxidative mechanism of arsenic toxicity and carcinogenesis. *Mol. Cell. Biochem.* 2004;255:67-78.
31. Kligerman, A.D., Doerr, C.L., Tennant, A.H., et al. Methylated Trivalent Arsenicals as Candidate Ultimate Genotoxic Forms of Arsenic: Induction of Chromosomal Mutations but Not Gene Mutations. *Environ. Mol. Mutagen* 2003;42:192-205.
32. Singh, K.P., Kumari, R., Treas, J., and Dumond, J.W. Chronic exposure to arsenic causes increased cell survival, DNA damage, and increased expression of mitochondrial transcription factor A (mtTFA) in human prostate epithelial cells. *Chem. Res. Toxicol.* 2011;24:340-349.
33. Huang, C., Ke, Q., Costa, M., and Shi, X. Molecular mechanisms of arsenic carcinogenesis. *Mol. Cell. Biochem.* 2004;255:57-66.
34. Bau, D.T., Wang, T.S., Chung, C.H., Wang, A.S.S., and Jan, K.Y. Oxidative DNA adducts and DNA-protein cross-links are the major DNA lesions induced by arsenite. *Environ. Health Perspect.* 2002;110:753-756.
35. Helleday, T., Nilsson, R., and Jenssen, D. Arsenic[III] and heavy metal ions induce intrachromosomal homologous recombination in the hprt gene of V79 Chinese hamster cells. *Environ Mol Mutagen.* 2000;35:114-122.
36. Coluzzi, E., Colamartino, M., Cozzi, R., et al. Oxidative stress induces persistent telomeric DNA damage responsible for nuclear morphology change in mammalian cells. *PLoS One.* 2014;9:e110963.
37. Klein, C.B., Leszczynska, J., Hickey, C., and Rossman, T.G. Further evidence against a direct genotoxic mode of action for arsenic-induced cancer. *Toxicol. Appl. Pharmacol.* 2007;222:289-297.
38. Zhou, X., Ding, X., Shen, J., Yang, D., Hudson, L.G., and Liu, K.J. Peroxynitrite contributes to arsenic-induced PARP-1 inhibition through ROS/RNS generation. *Toxicol. Appl. Pharmacol.* 2019;378:114602.
39. Zhou, X., Cooper, K.L., Huestis, J., et al. S-nitrosation on zinc finger motif of PARP-1 as a mechanism of DNA repair inhibition by arsenite. *Oncotarget* 2016;7:80482-80492.
40. WHO. WHO Air Quality Guidelines for Europe. Chapter 6.1 Arsenic. 2000;(4):1-14.
41. Chung, J.Y., Yu, S. D., and Hong, Y.S. Environmental source of arsenic exposure. *J. Prev. Med. Public Heal.* 2014;47:253-257.

42. Nicomel, N.R., Leus, K., Folens, K., Van Der Voort, P., and Du Laing, G. Technologies for arsenic removal from water: Current status and future perspectives. *Int. J. Environ. Res. Public Health*. 2015;13:1-24.
43. Jang, Y.C., Somanna, Y., and Kim, H. Source, distribution, toxicity and remediation of arsenic in the environment – A review. *Int. J. Appl. Environ. Sci.* 2016;11:973-6077.
44. Wurl, J., Lamadrid, M.I., Mendez-Rodriguez, L., and Vargas, B.A. Arsenic concentration in the surface water of a former mining area: The la junta creek, baja california sur, Mexico. *Int. J. Environ. Res. Public Health*. 2018;15:437.
45. Borch, T., Kretzschmar, R., Skappler, A., et al. Biogeochemical redox processes and their impact on contaminant dynamics. *Environ. Sci. Technol.* 2010;44:15-23.
46. US Environmental Protection Agency. *Special Report on Ingested Inorganic Arsenic: Skin Cancer; Nutritional Essentiality*; 1988. EPA/625/3-87/-13.
47. Rossman, T.G. Mechanism of arsenic carcinogenesis: An integrated approach. *Mutat. Res. - Fundam. Mol. Mech. Mutagen* 2003;533:37-65.
48. Chin-Chan, M., Navarro-Yepes, J., and Quintanilla-Vega, B. Environmental pollutants as risk factors for neurodegenerative disorders: Alzheimer and Parkinson diseases. *Front. Cell. Neurosci.* 2015;9:1-22.
49. Chen, P., Miah, M.R., and Aschner, M. Metals and Neurodegeneration. *F1000 Res.* 2016;5:366.
50. Niño, S.A., Morales-Martínez, A., Chi-Ahumada, E., et al. Arsenic Exposure Contributes to the Bioenergetic Damage in an Alzheimer's Disease Model. *ACS Chem. Neurosci.* 2019;10:323-336.
51. Tamás, M., Sharma, S., Ibstedt, S., Jacobson, T., and Christen, P. Heavy Metals and Metalloids As a Cause for Protein Misfolding and Aggregation. *Biomolecules* 2014;4:252-267.
52. Jacobson, T., Navarrete, C., Sharma, S.K., et al. Arsenite interferes with protein folding and triggers formation of protein aggregates in yeast. *J. Cell Sci.* 2012;125:5073-5083.
53. Kitchin, K.T, and Wallace, K. The role of protein binding of trivalent arsenicals in arsenic carcinogenesis and toxicity. *J. Inorg. Biochem.* 2008;102:532-539.
54. Zhou, X., Sun, X., Cooper, K.L., Wang, F., Liu, K.J., and Hudson, L.G. Arsenite interacts selectively with zinc finger proteins containing C3H1 or C4 motifs. *J. Biol. Chem.* 2011;286:22855-22863.



55. Zhang, X. W., Yan, X. J., Zhou, Z. R., Yang, F. F., Wu, Z. Y., Sun, H. B., Liang, W. X., Song, A. X., Lallemand-Breitenbach, V., Jeanne, M., Zhang, Q. Y., Yang, H. Y., Huang, Q. H., Zhou, G. B., Tong, J. H., Zhang, Y., Wu, J. H., Hu, H. Y., de Thé, H., Chen, S. J., and Chen, Z. (2010) Arsenic trioxide controls the fate of the PML-RARalpha oncoprotein by directly binding PML. *Science* 328, 240–243.
56. Miller, J., Mclachlan, A.D., and Klug, A. Repetitive zinc-binding domains in the protein transcription factor. *EMBO J.* 1985;4:1609-1614.
57. Gamsjaeger, R., Liew, C.K., Loughlin, F.E., Crossley, M., and Mackay, J.P. Sticky fingers: zinc-fingers as protein-recognition motifs. *Trends Biochem. Sci.* 2007;32:63-70.
58. Element, K. Zinc Biochemistry: From a Single Zinc Enzyme to a key element of life. *Adv. Nutr.* 2013;4:82-91.
59. Andreini, C., Bertini, I., and Cavallaro, G. Minimal functional sites allow a classification of zinc sites in proteins. *PLoS One* 2011;6:e26325.
60. Laity, J.H., Lee, B.M., and Wright, P.E. Zinc finger proteins: new insights into structural and functional diversity. *Curr. Opin. Struct. Biol.* 2001;11:39-46.
61. Cassandri, M., Smirnov, A., Novelli, F., et al. Zinc-finger proteins in health and disease. *Cell Death Discov.* 2017;3:17071.
62. Bassi, C., Li, Y.T., Khu, K., et al. The acetyltransferase Tip60 contributes to mammary tumorigenesis by modulating DNA repair. *Cell Death Differ.* 2016;23:1198-1208.
63. Ding, W., Liu, W., Cooper, K.L., et al. Inhibition of poly(ADP-ribose) Polymerase-1 by Arsenite interferes with repair of oxidative DNA damage. *J. Biol. Chem.* 2009;284:6809-6817.
64. Li, X., Corsa, C.A.S., Pan, P.W., et al. MOF and H4 K16 Acetylation Play Important Roles in DNA Damage Repair by Modulating Recruitment of DNA Damage Repair Protein Mdc1. *Mol. Cell. Biol.* 2010;30:5335-5347.
65. Zhi, Y., Ji, H., Pan, J., et al. Downregulated XPA promotes carcinogenesis of bladder cancer via impairment of DNA repair. *Tumor Biol.* 2017;39:1-9.
66. Buchner, D.A., Charrier, A., Srinivasan, E., et al. Zinc finger protein 407 (ZFP407) regulates insulin-stimulated glucose uptake and glucose transporter 4 (Glut4) mRNA. *J. Biol. Chem.* 2015;290:6376-6386.
67. Shen, S., Li, X., Cullen, W.R., Weinfeld, M., and Le, X.C. Arsenic Binding to Proteins. *Chem. Rev.* 2013;113:1-48.
68. Hartwig, A. Zinc finger proteins as potential targets for toxic metal ions: differential effects on structure and function. *Antioxid. Redox Signal.* 2001;3:625-634.

69. Zhang, F., Paramasivam, M., Cai, Q., et al. Arsenite Binds to the RING Finger Domains of RNF20-RNF40 Histone E3 Ubiquitin Ligase and Inhibits DNA Double-Strand Break Repair. *J. Am. Chem. Soc.* 2014;136:12884-12887.
70. Liu, S., Jiang, J., Li, L., Amato, N.J., Wang, Z., and Wang, Y. Arsenite Targets the Zinc Finger Domains of Tet Proteins and Inhibits Tet-Mediated Oxidation of 5-Methylcytosine. *Environ. Sci. Technol.* 2015;49:11923-11931.
71. Basu, A.K. DNA damage, mutagenesis and cancer. *Int. J. Mol. Sci.* 2018;19:970.
72. Sharma, G.G., So, S., Gupta, A., et al. MOF and Histone H4 Acetylation at Lysine 16 Are Critical for DNA Damage Response and Double-Strand Break Repair. *Mol. Cell. Biol.* 2010;30:3582-3595.
73. Jha, A.N., Noditi, M., Nilsson, R., and Natarajan, A.T. Genotoxic effects of sodium arsenite on human cells. *Mutat. Res. - Fundam. Mol. Mech. Mutagen* 1992;284:215-221.
74. Lee-Chen, S.F., Gurr, J.R., Lin, I.B., and Jan, K.Y. Arsenite enhances DNA double-strand breaks and cell killing of methyl methanesulfonate-treated cells by inhibiting the excision of alkali-labile sites. *Mutat. Res. Repair* 1993;294:21-28.
75. Wiencke, J.K., and Yager, J.W. Specificity of arsenite in potentiating cytogenetic damage induced by the DNA crosslinking agent diepoxybutane. *Environ. Mol. Mutagen* 1992;19:195-200.
76. Hang, B. Base excision repair. *DNA Repair, Genet. Instab. Cancer* 2007:23-64.
77. Cooke, M.S., Evans, M.D., Dizdaroglu, M., and Lunec, J. Oxidative DNA damage: mechanisms, mutation, and disease. *FASEB J.* 2003;17:1195-1214.
78. Ziech, D., Franco, R., Georgakilas, A.G., et al. The role of reactive oxygen species and oxidative stress in environmental carcinogenesis and biomarker development. *Chem. Biol. Interact.* 2010;188:334-339.
79. Grollman, A.P., and Moriya, M. Mutagenesis by 8-oxoguanine: an enemy within. *Trends Genet.* 1993;9:246-249.
80. Shockley, A.H., Doo, D.W., Rodriguez, G.P., and Crouse, G.F. Oxidative damage and mutagenesis in *Saccharomyces cerevisiae*: Genetic studies of pathways affecting replication fidelity of 8-oxoguanine. *Genetics* 2013;195:359-367.
81. Ba, X., Boldogh, I. 8-Oxoguanine DNA glycosylase 1: Beyond repair of the oxidatively modified base lesions. *Redox Biol.* 2018;14:669-678.
82. Ebert, F., Weiss, A., Bültemeyer, M., Hamann, I., Hartwig, A., and Schwerdtle, T. Arsenicals affect base excision repair by several mechanisms. *Mutat. Res. - Fundam. Mol. Mech. Mutagen* 2011;715:32-41.

83. Sykora, P., and Snow, E.T. Modulation of DNA polymerase beta-dependent base excision repair in cultured human cells after low dose exposure to arsenite. *Toxicol. Appl. Pharmacol.* 2008;228:385-394.
84. Idriss, H.T., Al-Assar, O., and Wilson, S.H. DNA polymerase  $\beta$ . *Int. J. Biochem. Cell. Biol.* 2002;34:321-324.
85. Osmond, M.J., Kunz, B.A., and Snow, E.T. Age and exposure to arsenic alter base excision repair transcript levels in mice. *Mutagenesis* 2010;25:517-522.
86. Scha, O.D. Nucleotide Excision Repair in Eukaryotes. *Cold Spring Harb. Perspect. Biol.* 2013;5:a012609.
87. Andrew, A.S., Karagas, M.R., and Hamilton, J.W. Decreased DNA repair gene expression among individuals exposed to arsenic in United States drinking water. *Int. J. Cancer* 2003;104:263-268.
88. Andrew, A.S., Burgess, J.L., Meza, M.M., et al. Arsenic exposure is associated with decreased DNA repair in vitro and in individuals exposed to drinking water arsenic. *Environ. Health Perspect.* 2006;114:1193-1198.
89. Mo, J., Xia, Y., Wade, T.J., DeMarini, D.M., Davidson, M., and Mumford, J. Altered gene expression by low-dose arsenic exposure in humans and cultured cardiomyocytes: Assessment by real-time PCR arrays. *Int. J. Environ. Res. Public Health* 2011;8:2090-2108.
90. Hamadeh, H.K., Trouba, K.J., Amin, R.P., Afshari, C.A., and Germolec, D. Coordination of altered DNA repair and damage pathways in arsenite-exposed keratinocytes. *Toxicol. Sci.* 2002;69:306-316.
91. Andrew, A.S., Warren, A.J., Barchowsky, A., Temple, K.A., Klei, L., Soucy, N.V., O'Hara, K.A., and Hamilton, J.W. Genomic and Proteomic Profiling of Responses to Toxic Metals in Human Lung Cells. *Environ. Health Perspect.* 2003;111:825-838.
92. Nollen, M., Ebert, F., Moser, J., Mullenders, L.H.F., Hartwig, A., and Schwerdtle, T. Impact of arsenic on nucleotide excision repair: XPC function, protein level, and gene expression. *Mol. Nutr. Food Res.* 2009;53:572-582.
93. Holcomb, N., Goswami, M., Han, S.G., Scott, T., D'Orazio, J., Orren, D.K., Gairola, C.G., and Mellon, I. Inorganic arsenic inhibits the nucleotide excision repair pathway and reduces the expression of XPC. *DNA Repair* 2017;52:70-80.
94. Muenyi, C.S., Ljungman, M., and States, J.C. Arsenic disruption of DNA damage responses—potential role in carcinogenesis and chemotherapy. *Biomolecules* 2015;5:2184-2193.

95. Yimit, A., Adebali, O., Sancar, A., and Jiang, Y. Differential damage and repair of DNA-adducts induced by anti-cancer drug cisplatin across mouse organs. *Nat. Commun.* 2019;10:309.
96. Muenyi, C.S., States, V.A., Masters, J.H., Fan, T.W., Helm, C.W., and States, J.C. Sodium arsenite and hyperthermia modulate cisplatin-DNA damage responses and enhance platinum accumulation in murine metastatic ovarian cancer xenograft after hyperthermic intraperitoneal chemotherapy (HIPEC). *J. Ovarian Res.* 2011;4:9.
97. Saijo, M., Takedachi, A., and Tanaka, K. Nucleotide excision repair by mutant xeroderma pigmentosum group A (XPA) proteins with deficiency in interaction with RPA. *J. Biol. Chem.* 2011;286:5476-5483.
98. Sugitani, N., Sivley, R.M., Perry, K.E., Capra, J.A., and Chazin, W.J. XPA: A key scaffold for human nucleotide excision repair. *DNA Repair* 2016;44:123-135.
99. Morita, E.H., Ohkubo, T., Kuraoka, I., Shirakawa, M., Tanaka, K., and Morikawa, K. Implications of the zinc-finger motif found in the DNA-binding domain of the human XPA protein. *Genes to Cells.* 1996;1:437-442.
100. Quintal, S.M., Depaula, Q.A., and Farrell, N.P. Zinc finger proteins as templates for metal ion exchange and ligand reactivity. Chemical and biological consequences. *Metallomics* 2011;3:121-139.
101. Jiang, J., Tam, L.M., Wang, P., and Wang, Y. Arsenite Targets the RING Finger Domain of Rbx1 E3 Ubiquitin Ligase to Inhibit Proteasome-Mediated Degradation of Nrf2. *Chem. Res. Toxicol.* 2018;31:380-387.
102. Asmuss, M. Differential effects of toxic metal compounds on the activities of Fpg and XPA, two zinc finger proteins involved in DNA repair. *Carcinogenesis* 2000;21:2097-2104.
103. Hartwig, A., Blessing, H., Schwerdtle, T., and Walter, I. Modulation of DNA repair processes by arsenic and selenium compounds. *Toxicology* 2003;193:161-167.
104. Qin, X.J., Hudson, L.G., Liu, W., Timmins, G.S., and Liu, K.J. Low concentration of arsenite exacerbates UVR-induced DNA strand breaks by inhibiting PARP-1 activity. *Toxicol. Appl. Pharmacol.* 2008;232:41-50.
105. Bau, D.T., Gurr, J.R., and Jan, K.Y. Nitric oxide is involved in arsenite inhibition of pyrimidine dimer excision. *Carcinogenesis* 2001;22:709-716.
106. Davis, K.L., Martin, E., Turko, I.V., and Murad, F. Novel Effects of Nitric Oxide. *Annu. Rev. Pharmacol. Toxicol.* 2001;41:203-236.
107. Snow, E.T., Hu, Y., Klein, C.B., McCluskey, K.L., Schuliga, M., and Sykora, P. Regulation of redox and DNA repair genes by arsenic: low dose protection against oxidative stress? *Arsenic Exposure and Health Effects V.* ; 2003:305-319.

108. Lynn, S., Lai, H.T., Gurr, J.R., and Jan, K.Y. Arsenite retards DNA break rejoining by inhibiting DNA ligation. *Mutagenesis* 1997;12:353-358.
109. Ellenberger, T., and Tomkinson, A.E. Eukaryotic DNA Ligases: Structural and Functional Insights. *Annu. Rev. Biochem.* 2008;77:313-338.
110. Cappelli, E., Taylor, R., Cevasco, M., Abbondandolo, A., Caldecott, K., and Frosina, G. Involvement of XRCC1 and DNA ligase III gene products in DNA base excision repair. *J. Biol. Chem.* 1997;272:23970-23975.
111. Cannan, W.J., Rashid, I., Tomkinson, A.E., Wallace, S.S., and Pederson, D.S. The human ligase III $\alpha$ -XRCC1 protein complex performs DNA nick repair after transient unwrapping of nucleosomal DNA. *J. Biol. Chem.* 2017;292:5227-5238.
112. Caldecott, K.W., McKeown, C.K., Tucker, J.D., Ljungquist, S., and Thompson, L.H. An interaction between the mammalian DNA repair protein XRCC1 and DNA ligase III. *Mol. Cell. Biol.* 1994;14:68-76.
113. Li, J-H., and Rossman, T.G. Inhibition of DNA ligase activity by arsenite: A possible mechanism of its comutagenesis. *Mol. Toxicol.* 1989;2:1-9.
114. Kim, H., and D'Andrea, A.D. Regulation of DNA cross-link repair by the Fanconi anemia/BRCA pathway. *Genes Dev.* 2012;26:1393-1408.
115. Wang, W. Emergence of a DNA-damage response network consisting of Fanconi anaemia and BRCA proteins. *Nat. Rev. Genet.* 2007;8:735-748.
116. Peremartí, J., Ramos, F., Marcos, R., and Hernández, A. Arsenic exposure disrupts the normal function of the FA/BRCA repair pathway. *Toxicol. Sci.* 2014;142:93-104.
117. Yamamoto, K.N., Kobayashi, S., Tsuda, M., Kurumizaka, H., Takata, M., Kono, K., Jiricny, J., Takeda, S., and Hirota, K. Involvement of SLX4 in interstrand cross-link repair is regulated by the Fanconi anemia pathway. *Proc. Natl. Acad. Sci. U S A* 2011;108:6492-6496.
118. Alpi, A.F., Pace, P.E., Babu, M.M., and Patel, K.J. Mechanistic Insight into Site-Restricted Monoubiquitination of FANCD2 by Ube2t, FANCL, and FANCI. *Mol. Cell* 2008;32:767-777.
119. Meetei, A.R., De Winter, J.P., Medhurst, A.L., Wallisch, M., Waisfisz, Q., van de Vrugt, H.J., Oostra, A.B., Yan, Z., Ling, C., Bishop, C.E., Hoatlin, M.E., Joenje, H., and Wang, W. A novel ubiquitin ligase is deficient in Fanconi anemia. *Nat. Genet.* 2003;35:165-170.
120. Chaudhury, I., Stroik, D.R., and Sobek, A. FANCD2-Controlled Chromatin Access of the Fanconi-Associated Nuclease FAN1 Is Crucial for the Recovery of Stalled Replication Forks. *Mol. Cell. Biol.* 2014;34:3939-3954.

121. Jiang, J., Bellani, M., Li, L., Wang, P., Seidman, M.M., and Wang, Y. Arsenite Binds to the RING Finger Domain of FANCL E3 Ubiquitin Ligase and Inhibits DNA Interstrand Crosslink Repair. *ACS Chem. Biol.* 2017;12:1858-1866.
122. Xie, J., Kim, H., Moreau, L.A., Puhalla, S., Garber, J., Abo, M.A., Takeda, S., and D'Andrea, A.D. RNF4-mediated polyubiquitination regulates the Fanconi anemia/BRCA pathway. *J. Clin. Invest.* 2015;125:1523-1532.
123. Bhagwat, N., Olsen, A.L., Wang, A.T., Hanada, K., Stuckert, P., Kanaar, R., D'Andrea, A., Niedernhofer, L.J., and McHugh, P.J. XPF-ERCC1 Participates in the Fanconi Anemia Pathway of Cross-Link Repair. *Mol. Cell. Biol.* 2009;29:6427-6437.
124. Rahn, J.J., Adair, G.M., and Nairn, R.S. Multiple roles of ERCC1-XPF in Mammalian Interstrand Crosslink Repair. *Environ. Mol. Mutagen.* 2010;51:567-581.
125. Niedernhofer, L.J., Odijk, H., Budzowska, M., van Drunen, E., Maas, A., Theil, A.F., de Wit, J., Jaspers, N.G.J., Beverloo, H.B., Hoeijmakers, J.H.J., and Kanaar, R. The Structure-Specific Endonuclease Ercc1-Xpf Is Required To Resolve DNA Interstrand Cross-Link-Induced Double-Strand Breaks. *Mol. Cell. Biol.* 2004;24:5776-5787.
126. Long, D.T., and Walter, J.C. A Novel Function for BRCA1 in Crosslink Repair? *Mol. Cell* 2012;46:111-112.
127. Bunting, S.F., Callén, E., Kozak, M.L., Kim, J.M., Wong, N., Lopez-Contreras, A.J., Ludwig, T., Baer, R., Faryabi, R.B., Malhowski, A., Chen, H-T., Fernandez-Capetillo, O., D'Andrea, A., and Nussenzweig, A. BRCA1 Functions Independently of Homologous Recombination in DNA Interstrand Crosslink Repair. *Mol. Cell* 2012;46:125-135.
128. Long, D.T., Joukov, V., Budzowska, M., and Walter, J.C. BRCA1 promotes unloading of the CMG helicase from a stalled DNA replication fork. *Mol. Cell* 2014;56:174-185.
129. D'Andrea, A.D. BRCA1: A Missing Link in the Fanconi Anemia/BRCA Pathway. *Cancer Discov.* 2013;3:376-378.
130. Rosen, E.M. BRCA1 in the DNA damage response and at telomeres. *Front. Genet.* 2013;4:1-14.
131. Hoeijmakers, J.H.J. Genome maintenance mechanisms for preventing cancer. *Nature* 2001;411:366-374.
132. Lindahl, T., and Wood, R.D. Quality control by DNA repair. *Science* 1999;286:1897-1905.
133. Symington, L.S., and Gautier, J. Double-Strand Break End Resection and Repair Pathway Choice. *Annu. Rev. Genet.* 2011;45:247-271.
134. Dong, J.T., and Luo, X.M. Arsenic-induced DNA-strand breaks associated with DNA-protein crosslinks in human fetal lung fibroblasts. *Mutat. Res. Lett.* 1993;302:97-102.

135. Jiménez-Villarreal, J., Rivas-Armendariz, D.I., Pineda-Belmontes, C.P., Betancourt-Martinez, N.D., Macias-Corral, M.A., Guerra-Alanis, A.J., Nino-Castaneda, M.S. and Moran-Martinez, J. Detection of damage on single- or double-stranded DNA in a population exposed to arsenic in drinking water. *Genet. Mol. Res.* 2017;16.
136. Morales, M.E., Derbes, R.S., Ade, C.M., Ortego, J.C., Stark, J., Deininger, P.L., and Roy-Engel, A.M. Heavy Metal Exposure Influences Double Strand Break DNA Repair Outcomes. *PLoS One* 2016;11:e0151367.
137. Price, B.D., and D'Andrea, A.D. Chromatin remodeling at DNA double-strand breaks. *Cell* 2013;152:1344-1354.
138. J Jo, W.J., Ren, X., Chu, F., Aleshin, M., Wintz, H., Burlingame, A., Smith, M.T., Vulpe, C.D., and Zhang, L. Acetylated H4K16 by MYST1 Protects UROtsa Cells from the Carcinogen Arsenic and is Decreased Following Chronic Arsenic Exposure. *Toxicol. Appl. Pharmacol.* 2009;241:294-302.
139. Chu, F., Ren, X., Chasse, A., Hickman, T., Zhang, L., Yuh, J., Smith, M.T., and Burlingame, A.L. Quantitative mass spectrometry reveals the epigenome as a target of arsenic. *Chem. Biol. Interact.* 2011;192:113-117.
140. Tam, L.M., Jiang, J., Wang, P., Li, L., Miao, W., Dong, X., and Wang, Y. Arsenite binds to the zinc finger motif of TIP60 histone acetyltransferase and induces its degradation via the 26S proteasome. *Chem. Res. Toxicol.* 2017;30:1685-1693.
141. Liu, D., Wu, D., Zhao, L., Yang, Y., Ding, J., Dong, L., Hu, L., Wang, F., Zhao, X., Cai, Y., and Jin, J. Arsenic trioxide reduces global histone H4 acetylation at lysine 16 through direct binding to histone acetyltransferase hMOF in human cells. *PLoS One* 2015;10:1-16.
142. Mattioli, F., Vissers, J.H.A., Van Dijk, W.J., Ikpa, P., Citterio, E., Vermeulen, W., Marteijn, J.A., and Sixma, T.K. RNF168 ubiquitinates K13-15 on H2A/H2AX to drive DNA damage signaling. *Cell* 2012;150:1182-1195.
143. Luijsterburg, M.S., Typas, D., Caron, M.C., Wiegant, W.W., van den Heuvel, D., Boonen, R.A., Couturier, A.M., Mullenders, L.H., Masson, J-Y., and van Attikum, H. A PALB2-interacting domain in RNF168 couples homologous recombination to DNA break-induced chromatin ubiquitylation. *Elife* 2017;6:1-26.
144. Nakada, S. Opposing roles of RNF8/RNF168 and deubiquitinating enzymes in ubiquitination-dependent DNA double-strand break response signaling and DNA-repair pathway choice. *J. Radiat. Res.* 2016;57:i33-i40.
145. Chen, J., Feng, W., Jiang, J., Deng, Y., and Huen, M.S.Y. Ring finger protein RNF169 antagonizes the ubiquitin-dependent signaling cascade at sites of DNA damage. *J. Biol. Chem.* 2012;287:27715-27722.

146. Poulsen, M., Lukas, C., Lukas, J., Bekker-Jensen, S., and Mailand, N. Human RNF169 is a negative regulator of the ubiquitin-dependent response to DNA double-strand breaks. *J. Cell. Biol.* 2012;197:189-199.
147. Zhang, L., Wang, Z., Shi, R., Zhu, X., Zhou, J., Peng, B., and Xu, X. RNF126 Quenches RNF168 Function in the DNA Damage Response. *Genomics, Proteomics Bioinforma.* 2018;16:428-438.
148. An, L., Dong, C., Li, J., Chen, J., Yuan, J., Huang, J., Chan, K.M., Yu, C., and Huen, M.S.Y. RNF169 limits 53BP1 deposition at DSBs to stimulate single-strand annealing repair. *Proc. Natl. Acad. Sci. U S A* 2018;115:E8286-E8295.
149. Wei, H., and Yu, X. Functions of PARylation in DNA Damage Repair Pathways. *Genomics, Proteomics Bioinforma.* 2016;14:131-139.
150. Liu, C., Vyas, A., Kassab, M.A., Singh, A.K., and Yu, X. The role of poly ADP-ribosylation in the first wave of DNA damage response. *Nucleic Acids Res.* 2017;45:8129-8141.
151. Beck, C., Robert, I., Reina-San-Martin, B., Schreiber, V., and Dantzer, F. Poly(ADP-ribose) polymerases in double-strand break repair: Focus on PARP1, PARP2 and PARP3. *Exp. Cell. Res.* 2014;329:18-25.
152. Chaudhuri, A.R., and Nussenzweig, A. The multifaceted roles of PARP1 in DNA repair and chromatin remodelling. *Nat. Rev. Mol. Cell. Biol.* 2017;18:610-621.
153. Poirier, G.G., de Murcia, G., Jongstra-Bilen, J., Niedergang, C., and Mandel, P. Poly (ADP-ribosyl)ation of polynucleosomes causes relaxation of chromatin structure. *Proc. Natl. Acad. Sci. U S A* 1982;79:3423-3427.
154. Messner, S., Altmeyer, M., Zhao, H., Pozivil, A., Roschitzki, B., Gehrig, P., Rutishauser, D., Huang, D., Cafilisch, A., and Hottiger, M.O. PARP1 ADP-ribosylates lysine residues of the core histone tails. *Nucleic Acids Res.* 2010;38:6350-6362.
155. Qin, X.J., Liu, W., Li, Y.N., Sun, X., Hai, C.X., Hudson, L.G., and Liu, K.J. Poly(ADP-ribose) polymerase-1 inhibition by arsenite promotes the survival of cells with unrepaired DNA lesions induced by UV exposure. *Toxicol. Sci.* 2012;127:120-129.
156. Ding, X., Zhou, X., Cooper, K.L., Huestis, J., Hudson, L.G., and Liu, K.J. Differential sensitivities of cellular XPA and PARP-1 to arsenite inhibition and zinc rescue. *Toxicol. Appl. Pharmacol.* 2017;331:108-115.
157. Brandes, N., Schmitt, S., and Jakob, U. Thiol-based redox switches in eukaryotic proteins. *Antioxidants Redox Signal.* 2009;11:997-1014.
158. Vilas, C.K., Emery, L.E., Denchi, E.L., and Miller, K.M. Caught with One's Zinc Fingers in the Genome Integrity Cookie Jar. *Trends Genet.* 2018;34:313-325.



159. Shi, H., Hudson, L.G., and Liu, K.J. Oxidative stress and apoptosis in metal ion-induced carcinogenesis. *Free Radic. Biol. Med.* 2004;37:582-593.
160. Witkiewicz-Kucharczyk, A., and Bal, W. Damage of zinc fingers in DNA repair proteins, a novel molecular mechanism in carcinogenesis. *Toxicol. Lett.* 2006;162:29-42.
161. Phoa, N., and Epe, B. Influence of nitric oxide on the generation and repair of oxidative DNA damage in mammalian cells. *Carcinogenesis* 2002;23:469-475.
162. Hartwig, A., Pelzer, A., Asmuss, M., and Burkle, A. Very Low Concentrations of Arsenite Suppress Poly(ADP-Ribosylation) in Mammalian Cells. *Int. J. Cancer* 2003;104:1-6.
163. Jaiswal, M., LaRusso, N.F., Shapiro, R.A., Billiar, T.R., and Gores, G.J. Nitric oxide-mediated inhibition of DNA repair potentiates oxidative DNA damage in cholangiocytes. *Gastroenterology* 2001;120:190-199.
164. Hilmi, K., Jangal, M., Marques, M., Zhao, T., Saad, A., Zhang, C., Luo, V.M., Syme, A., Rejon, C., Yu, Z., Krum, A., Fabian, M.R., Richard, S., Alaoui-Jamali, M., Orthwein, A., McCaffrey, L., and Witcher, M. CTCF facilitates DNA double-strand break repair by enhancing homologous recombination repair. *Sci. Adv.* 2017;3:e1601898.
165. Lang, F., Li, X., Zheng, W., Li, Z., Lu, D., Chen, G., Gong, D., Yang, L., Fu, J., Shi, P., and Zhou, J. CTCF prevents genomic instability by promoting homologous recombination-directed DNA. *Proc. Natl. Acad. Sci.* 2017;114:10912-10917.
166. Rea, M., Gripshover, T., and Fondufe-mittendorf, Y. Selective inhibition of CTCF binding by iAs directs TET-mediated reprogramming of 5-hydroxymethylation patterns in iAs-transformed cells. *Toxicol. Appl. Pharmacol.* 2018;338:124-133.
167. Hwang, S.Y., Kang, M.A., Baik, C.J., Lee, Y., Hang, N.T., Kim, B.G., Han, J.S., Jeong, J.H., Park, D., Myung, K., and Lee, J.S. CTCF cooperates with CtIP to drive homologous recombination repair of double-strand breaks. *Nucleic Acids Res.* 2019:1-20.
168. Galanty, Y., Belotserkovskaya, R., Coates, J., and Jackson, S.P. RNF4, a SUMO-targeted ubiquitin E3 ligase, promotes DNA double-strand break repair. *Genes Dev.* 2012;26:1179-1195.
169. Pinder, J.B., Attwood, K.M., and Dellaire, G. Reading, writing, and repair: The role of ubiquitin and the ubiquitin-like proteins in DNA damage signaling and repair. *Front. Genet.* 2013;4:1-14.
170. Giglia-Mari, G., Zotter, A., and Vermeulen, W. DNA damage response. *Cold Spring Harb. Perspect. Biol.* 2011;3:1-19.
171. Jackson, S.P., and Durocher, D. Regulation of DNA Damage Responses by Ubiquitin and SUMO. *Mol. Cell* 2013;49:795-807.

172. Centore, R.C., Yazinski, S.A., Tse, A., and Zou, L. Spartan/C1orf124, a Reader of PCNA Ubiquitylation and a Regulator of UV-Induced DNA Damage Response. *Mol. Cell* 2012;46:625-635.
173. Ting, L., Jun, H., and Junjie, C. RAD18 lives a double life: Its implication in DNA double-strand break repair. *DNA Repair (Amst)* 2010;9:1241-1248.
174. Vaziri, C., Tateishi, S., Mutter-Rottmayer, E., and Gao, Y. Roles of RAD18 in DNA Replication and Postreplication Repair. *Genome Stability: From Virus to Human Application* 2016;257-273.
175. Ceccaldi, R., Sarangi, P., and D'Andrea, A.D. The Fanconi anaemia pathway: New players and new functions. *Nat. Rev. Mol. Cell. Biol.* 2016;17:337-349.
176. Williams, S.A., Longerich, S., Sung, P., Vaziri, C., and Kupfer, G.M. The E3 ubiquitin ligase RAD18 regulates ubiquitylation and chromatin loading of FANCD2 and FANCI. *Blood* 2011;117:5078-5087.
177. Yang, K., Moldovan, G.L., and D'Andrea, A.D. RAD18-dependent recruitment of SNM1A to DNA repair complexes by a ubiquitin-binding zinc finger. *J. Biol. Chem.* 2010;285:19085-19091.
178. Zhang, L., and Li, D-Q. MORC2 regulates DNA damage response through a PARP1-dependent pathway. *Nucleic Acids Res.* 2019;47:8502-8520.
179. Galanty, Y., Belotserkovskaya, R., Coates, J., Polo, S., Miller, K.M., and Jackson, S.P. Mammalian SUMO E3-ligases PIAS1 and PIAS4 promote responses to DNA double-strand breaks. *Nature* 2009;462:935-939.
180. Hendriks, I.A., and Vertegaal, A.C.O. Sumo in the DNA damage response. *Oncotarget* 2015;6:15734-15735.
181. Luo, K., Zhang, H., Wang, L., Yuan, J., and Lou, Z. Sumoylation of MDC1 is important for proper DNA damage response. *EMBO J.* 2012;31:3008-3019.
182. Chung, I., and Zhao, X. Dna break-induced sumoylation is enabled by collaboration between a sumo ligase and the ssdnabinding complex rpa. *Genes Dev.* 2015;29:1593-1598.
183. Dou, H., Huang, C., Singh, M., Carpenter, P.B., and Yeh, E.T.H. Regulation of DNA Repair through DeSUMOylation and SUMOylation of Replication Protein A Complex. *Mol. Cell* 2010;39:333-345.
184. Dhingra, N., Wei, L., and Zhao, X. Replication protein A (RPA) sumoylation positively influences the DNA damage checkpoint response in yeast. *J. Biol. Chem.* 2019;294:2690-2699.

185. Poulsen, S.L., Hansen, R.K., Wagner, S.A., van Cuijk, L., van Belle, G.J., Streicher, W., Wikstrom, M., Choudhary, C., Houtsmuller, A.B., Marteijn, J.A., Bekker-Jensen, S., and Mailand, N. RNF111/Arkadia is a SUMO-targeted ubiquitin ligase that facilitates the DNA damage response. *J. Cell. Biol.* 2013;201:787-807.
186. Luo, Q., Li, Y., Deng, J., and Zhang, Z. PARP-1 inhibitor sensitizes arsenic trioxide in hepatocellular carcinoma cells via abrogation of G2/M checkpoint and suppression of DNA damage repair. *Chem. Biol. Interact.* 2015;226:12-22.
187. Ganapathy, S., Liu, J., Xiong, R., Yu, T., Makriyannis, A., and Chen, C. Chronic low dose arsenic exposure preferentially perturbs mitotic phase of the cell cycle. *Genes and Cancer.* 2019;10:39-51.
188. Hassani, S., Khaleghian, A., Ahmadian, S., Alizadeh, S., Alimoghaddam, K., Ghavamzadeh, A., and Ghaffari, S.H. Redistribution of cell cycle by arsenic trioxide is associated with demethylation and expression changes of cell cycle related genes in acute promyelocytic leukemia cell line (NB4). *Ann. Hematol.* 2018;97:83-93.
189. Zhou, B.S., and Elledge, S.J. The DNA damage response: putting checkpoints in Perspective. *Nature* 2000;408:433-439.
190. Nyberg, K.A., Michelson, R.J., Putnam, C.W., and Weinert, T.A. Toward Maintaining the Genome: DNA Damage and Replication Checkpoints. *Annu. Rev. Genet.* 2002;36:617-656.
191. Barnum, K.J., and O'Connell, M.J. Cell Cycle Regulation by Checkpoints. *Methods Mol. Biol.* 2014; 1170:29-40.
192. Shaltiel, I.A., Krenning, L., Bruinsma, W., and Medema, R.H. The same, only different - DNA damage checkpoints and their reversal throughout the cell cycle. *J. Cell. Sci.* 2015;128:607-620.
193. Beezhold, K., Klei, L.R., and Barchowsky, A. Regulation of cyclin D1 by arsenic and microRNA inhibits adipogenesis. *Toxicol. Lett.* 2017;265:147-155.
194. Vogt, B.L., and Rossman, T.G. Effects of arsenite on p53, p21 and cyclin D expression in normal human fibroblasts - A possible mechanism for arsenite's comutagenicity. *Mutat. Res. - Fundam. Mol. Mech. Mutagen* 2001;478:159-168.
195. Chen, H., Li, S.F., Liu, J., Diwan, B.A., Barrett, J.C., and Waalkes, M.P. Chronic inorganic arsenic exposure induces hepatic global and individual gene hypomethylation: Implications for arsenic hepatocarcinogenesis. *Carcinogenesis* 2004;25:1779-1786.
196. Chen, Y.J., Lai, K.C., Kuo, H.H., Chow, L.P., Yih, L.H., and Lee, T.C. HSP70 colocalizes with PLK1 at the centrosome and disturbs spindle dynamics in cells arrested in mitosis by arsenic trioxide. *Arch. Toxicol.* 2014;88:1711-1723.

197. Salazar, A.M., Ostrosky-Wegman, P., Menéndez, D., Miranda, E., García-Carrancá, A., and Rojas, E. Induction of p53 protein expression by sodium arsenite. *Mutat. Res. - Fundam. Mol. Mech. Mutagen.* 1997;381:259-265.
198. Karimian, A., Ahmadi, Y., and Yousefi, B. Multiple functions of p21 in cell cycle, apoptosis and transcriptional regulation after DNA damage. *DNA Repair (Amst)* 2016;42:63-71.
199. Huang, Y., Zhang, J., Mchenry, K.T., Kim, M.M., Zeng, W., Lopez-Pajares, V., Dibble, C.C., Mizgerd, J.P., and Yuan, Z.M. Induction of Cytoplasmic Accumulation of p53: A Mechanism for Low Levels of Arsenic Exposure to Predispose Cells for Malignant Transformation. *Cancer Res.* 2008;68:9131-9136.
200. Tang, F., Liu, G., He, Z., Ma, W-Y., Bode, A.M., and Dong, Z. Arsenite Inhibits p53 Phosphorylation, DNA Binding Activity, and p53 Target Gene p21 Expression in Mouse Epidermal JB6 Cells. *Mol. Carcinog.* 2006;45:861-870.
201. Shen, S., Wang, C., Weinfeld, M., and Le, X.C. Inhibition of nucleotide excision repair by arsenic. *Chinese Sci. Bull.* 2013;58:214-221.
202. Germolec, D.R., Yoshida, T., Gaido, K., Wilmer, J.L., Simeonova, P.P., Kayama, F., Burleson, F., Dong, W., Lange, R.W., and Luster, M.I. Arsenic induces overexpression of growth factors in human keratinocytes. *Toxicol. Appl. Pharmacol.* 1996;141:308-318.
203. Simeonova, P.P., and Luster, M.I. Mechanisms of arsenic carcinogenicity: genetic or epigenetic mechanisms? *J. Env. Pathol. Toxicol. Oncol.* 2000;19:281-286.
204. Watcharasit, P., Visitnonthachai, D., Suntararuks, S., Thiantanawat, A., and Satayavivad, J. Low arsenite concentrations induce cell proliferation via activation of VEGF signaling in human neuroblastoma SH-SY5Y cells. *Environ. Toxicol. Pharmacol.* 2012;33:53-59.
205. Simeonova, P.P., Wang, S., Toriuma, W., Kommineni, V., Matheson, J., Unimye, N., Kayama, F., Harki, D., Ding, M., Vallyathan, V., and Luster, M.I. Arsenic mediates cell proliferation and gene expression in the bladder epithelium association with activating protein-1 transactivation. *Cancer Res.* 2000;60:3445-3453.
206. Jeon, B.G., Kumar, B.M., Kang, E.J., Maeng, G.H., Lee, Y.M., Hah, Y.S., Ock, S.A., Kwack, D.O., Park, B.W., and Rho, G.J. Differential cytotoxic effects of sodium meta-arsenite on human cancer cells, dental papilla stem cells and somatic cells correlate with telomeric properties and gene expression. *Anticancer Res.* 2011;31:4315-4328.
207. Dreval, K., Tryndyak, V., Kindrat, I., Twaddle, N.C., Orisakwe, O.E., Mudalige, T.K., Beland, F.A., Doerge, D.R. and Pogribny, I.P. Cellular and molecular effects of prolonged low-level sodium arsenite exposure on human hepatic HepaRG cells. *Toxicol. Sci.* 2018;162:676-687.
208. Andrew, A.S., Mason, R.A., Memoli, V., and Duell, E.J. Arsenic activates EGFR pathway signaling in the lung. *Toxicol. Sci.* 2009;109:350-357.

209. Huang, C., Li, J., Ding, M., Wang, L., Shi, X., Castranova, V., Vallyathan, V., Gong, J., and Costa, M. Arsenic-induced NF $\kappa$ B transactivation through Erks-and JNKs-dependent pathways in mouse epidermal JB6 cells. *Mol. Cell. Biochem.* 2001;222:29-34.
210. Chowdhury, R., Chatterjee, R., Giri, A.K., Mandal, C., and Chaudhuri, K. Arsenic-induced cell proliferation is associated with enhanced ROS generation, Erk signaling and CyclinA expression. *Toxicol. Lett.* 2010;198:263-271.
211. Gupta, A., Rosenberger, S.F., and Bowden, G.T. Increased ROS levels contribute to elevated transcription factor and MAP kinase activities in malignantly progressed mouse keratinocyte cell lines. *Carcinogenesis* 1999;20:2063-2073.
212. Morgan, M.J., and Liu, Z.G. Crosstalk of reactive oxygen species and NF- $\kappa$ B signaling. *Cell. Res.* 2011;21:103-115.
213. Liu, Y., Guyton, K.Z., Gorospe, M., Xu, Q., Lee, J.C., and Holbrook, N.J. Differential activation of ERK, JNK/SAPK and P38/CSBP/RK map kinase family members during the cellular response to arsenite. *Free Radic. Biol. Med.* 1996;21:771-781.
214. Kao, Y.T., Wu, C.H., Wu, S.Y., Lan, S.H., Liu, H.S, and Tseng, Y.S. Arsenic treatment increase Aurora-A overexpression through E2F1 activation in bladder cells. *BMC Cancer* 2017;17:1-10.
215. Wijeweera, J.B., Gandolfi, A.J., Parrish, A., and Lantz, R.C. Sodium arsenite enhances AP-1 and NF $\kappa$ B DNA binding and induces stress protein expression in precision-cut rat lung slices. *Toxicol. Sci.* 2001;61:283-294.
216. Lau, A.T.Y., Li, M., Xie, R., He, Q.Y., and Chiu, J.F. Opposed arsenite-induced signaling pathways cell proliferation or apoptosis in cultured lung cells. *Carcinogenesis* 2004;25:21-28.
217. Chen, H., Liu, J., Zhao, C.Q., Diwan, B.A., Merrick, B.A., and Waalkes, M.P. Association of c-myc overexpression and hyperproliferation with arsenite-induced malignant transformation. *Toxicol. Appl. Pharmacol.* 2001;175:260-268.
218. Natarajan, V., Scribner, W.M., Al-Hassani, M., and Vepa, S. Reactive oxygen species signaling through regulation of protein tyrosine phosphorylation in endothelial cells. *Environ. Health Perspect.* 1998;106:1205-1212.
219. Hamann, I., and Klotz, L.O. Arsenite-induced stress signaling: Modulation of the phosphoinositide 3'-kinase/Akt/FoxO signaling cascade. *Redox Biol.* 2013;1:104-109.
220. Rodríguez-Gabriel, M.A., and Russell, P. Distinct signaling pathways respond to arsenite and reactive oxygen species in *Schizosaccharomyces pombe*. *Eukaryot. Cell* 2005;4:1396-1402.

221. Souza, K., Maddock, D.A., Zhang, Q., Chen, J., Chiu, C., Mehta, S., Wan, Y. Arsenite activation of PI3K/AKT cell survival pathway is mediated by p38 in cultured human keratinocytes. *Mol. Med.* 2001;7:767-772.
222. Wetzler, M., Brady, M.T., Tracy, E., Li, Z.R., Donohue, K.A., O'Loughlin, K.L., Cheng, Y., Mortazavi, A., McDonald, A.A., Kunapuli, P., Wallace, P.K., Baer, M.R., Cowell, J.K., and Baumann, H. Arsenic Trioxide Affects Signal Transducer and Activator of Transcription Proteins through Alteration of Protein Tyrosine Kinase Phosphorylation. *Clin. Cancer Res.* 2006;12:6817-6825.
223. Hunter, T. The phosphorylation of proteins on tyrosine: Its role in cell growth and disease. *Philos. Trans. R. Soc. B. Biol. Sci.* 1998;353:583-605.
224. Wee, P., and Wang, Z. Epidermal growth factor receptor cell proliferation signaling pathways. *Cancers (Basel)* 2017;9:1-45.
225. Müller, H., and Helin, K. The E2F transcription factors: Key regulators of cell proliferation. *Biochim. Biophys. Acta. - Rev. Cancer* 2000;1470:M1.
226. Ren, B., Cam, H., Takahashi, Y., Volkert, T., Terragni, J., Young, R.A., and Dynlacht, B.D. E2F integrates cell cycle progression with DNA repair, replication, and G 2 /M checkpoints. *Genes Dev.* 2002;16:245-256.
227. Weston, A., and Harris, C.C. Multistage Carcinogenesis. In: Kufe, D.W., Pollock, R.E., Weichselbaum, R.R., eds. *Holland-Frei Cancer Medicine*. 6th editio. Hamilton (ON): BC Decker; 2003. <https://www.ncbi.nlm.nih.gov/books/NBK13982/>.
228. Eckstein, M., Eleazer, R., Rea, M., and Fondufe-Mittendorf, Y. Epigenomic reprogramming in inorganic arsenic-mediated gene expression patterns during carcinogenesis. *Rev. Environ. Health* 2017;32:93-103.
229. Luger, K., Mäder, A.W., Richmond, R.K., Sargent, D.F., and Richmond, T.J. Crystal structure of the nucleosome core particle at 2.8 Å resolution. *Nature* 1997;389:251-260.
230. McGinty, R.K., and Tan, S. Nucleosome structure and function. *Chem. Rev.* 2014;115:2255-2273.
231. Kouzarides, T. Chromatin Modifications and Their Function. *Cell* 2007;128:693-705.
232. Smerdon, M.J. DNA repair and the role of chromatin structure. *Curr. Opin. Cell. Biol.* 1991;3:422-428.
233. Soria, G., Polo, S.E., and Almouzni, G. Prime, Repair, Restore: The Active Role of Chromatin in the DNA Damage Response. *Mol. Cell* 2012;46:722-734.
234. Kamynina, E.A., Lachenauer, E.R., DiRisio, A.C., Liebenthal, R.P., Field, M.S., and Stover, P.J. Arsenic trioxide targets MTHFD1 and SUMO-dependent nuclear de novo thymidylate biosynthesis. *Proc. Natl. Acad. Sci. U S A* 2017;114:E2319-E2326.

235. Zhu, F., Zykova, T.A., Peng, C., Zhang, J., Cho, Y.Y., Zheng, D., Yao, K., Ma, W.Y., Lau, A.T.Y., Bode, A.M., and Dong, Z. Phosphorylation of H2AX at Ser139 and a new phosphorylation site Ser16 by RSK2 decreases H2AX ubiquitination and inhibits cell transformation. *Cancer Res.* 2011;71:393-403.
236. Howe, C.G., and Gamble, M.V. Influence of Arsenic on Global Levels of Histone Posttranslational Modifications: a Review of the Literature and Challenges in the Field. *Curr. Environ. Heal. reports* 2016;3:225-237.
237. Ren, X., Mchale, C.M., Skibola, C.F., Smith, A.H., Smith, M.T., and Zhang, L. An emerging role for epigenetic dysregulation in arsenic toxicity and carcinogenesis. *Environ. Health Perspect.* 2011;119:11-19.
238. Chervona, Y., Hall, M.N., Arita, A., Wu, F., Sun, H., Tseng, H.C., Ali, E., Uddin, M.N., Liu, X., Zoroddu, M.A., Gamble, M.V., and Costa, M. Associations between arsenic exposure and global posttranslational histone modifications among adults in Bangladesh. *Cancer Epidemiol. Biomarkers Prev.* 2012;21:2252-2260.
239. Zhou, X., Sun, H., Ellen, T.P., Chen, H., and Costa, M. Arsenite alters global histone H3 methylation. *Carcinogenesis* 2008;29:1831-1836.
240. Zhou, X., Li, Q., Arita, A., Sun, H., and Costa, M. Effects of Nickel, Chromate, and Arsenite on Histone 3 Lysine Methylation. *Toxicol. Appl. Pharmacol.* 2009;236:78-84.
241. Pournara, A., Kippler, M., Holmlund, T., Ceder, R., Grafstrom, R., Vahter, M., Broberg, K., and Wallberg, A.E. Arsenic alters global histone modifications in lymphocytes in vitro and in vivo. *Cell. Biol. Toxicol.* 2016;32:275-284.
242. Ray, P.D., Huang, B-W., and Tsuji, Y. Coordinated Regulation of Nrf2 and Histone H3 Serine 10 Phosphorylation in Arsenite-activated Transcription of the Human Heme Oxygenase-1 Gene. *Biochim. Biophys. Acta.* 2015;1849:1277-1288.
243. Li, J., Chen, P., Sinogeeva, N., Gorospe, M., Wersto, R.P., Chrest, F.J., Barnes, J., and Liu, Y. Arsenic trioxide promotes histone H3 phosphoacetylation at the chromatin of CASPASE-10 in acute promyelocytic leukemia cells. *J. Biol. Chem.* 2002;277:49504-49510.
244. Peterson, C.L., and Laniel, M.A. Histones and histone modifications. *Curr. Biol.* 2004;14:546-551.
245. Estève, P.O., Hang, G.C., and Pradhan, S. Molecular mechanisms of transactivation and doxorubicin-mediated repression of survivin gene in cancer cells. *J. Biol. Chem.* 2007;282:2615-2625.
246. McGarvey, K.M., Fahrner, J.A., Greene, E., Martens, J., Jenuwein, T., and Baylin, S.B. Silenced tumor suppressor genes reactivated by DNA demethylation do not return to a fully euchromatic chromatin state. *Cancer Res.* 2006;66:3541-3549.

247. Steffen, P.A., and Ringrose, L. What are memories made of? How polycomb and trithorax proteins mediate epigenetic memory. *Nat. Rev. Mol. Cell. Biol.* 2014;15:340-356.
248. Kim, H.G., Kim, D.J., Li, S., Lee, K.Y., Li, X., Bode, A.M., and Dong, Z. Polycomb (PcG) proteins, BMI1 and SUZ12, regulate arsenic-induced cell transformation. *J. Biol. Chem.* 2012;287:31920-31928.
249. Rubin, E., Wu, X., Zhu, T., Cheung, J.C.Y., Chen, H., Lorincz, A., Pandita, R.K., Sharma, G.G., Ha, H.C., Gasson, J., Hanakahi, L.A., Pandita, T.K., and Sukumar, S. A role for the HOXB7 homeodomain protein in DNA repair. *Cancer Res.* 2007;67:1527-1535.
250. Li, J., Poi, M.J., and Tsai, M-D. The Regulatory Mechanisms of Tumor Suppressor p16INK4 and Relevance to cancer. *Biochemistry* 2011;50:5566-5582.
251. Weber, H.O., Samuel, T., Rauch, P., and Funk, J.O. Human p14arf-mediated cell cycle arrest strictly depends on intact p53 signaling pathways. *Oncogene* 2002;21:3207-3212.
252. Fierz, B., Chatterjee, C., McGinty, R.K., Bar-dagan, M., Daniel, P., and Muir, T.W. Histone H2B ubiquitylation disrupts local and higher order chromatin compaction. *Nat. Chem. Bio.* 2011;7:113-119.
253. Shogren-Knaak, M., Ishii, H., Sun, J-M., Pazin, M.J., Davie, J.R., and Peterson, C.L. Histone H4-K16 Acetylation Controls Chromatin Structure and Protein Interactions. *Science* 2006;311:844-847.
254. Moyal, L., Lerenthal, Y., Gana-Weisz, M., Mass, G., So, S., Wang, S.Y., Eppink, B., Chung, Y.M., Shalev, G., Shema, E., Shkedy, D., Smorodinsky, N.I., van Vliet, N., Kuster, B., Mann, M., Ciechanover, A., Dahm-Daphi, J., Kanaar, R., Hu, M.C.T., Chen, D.J., Oren, M., and Shilon, Y. Requirement of ATM-Dependent Monoubiquitylation of Histone H2B for Timely Repair of DNA Double-Strand Breaks. *Mol. Cell* 2011;41:529-542.
255. Mailand, N., Bekker-Jensen, S., Fastrup, H., Melander, F., Bartek, J., Lukas, C., and Lukas, J. RNF8 Ubiquitylates Histones at DNA Double-Strand Breaks and Promotes Assembly of Repair Proteins. *Cell* 2007;131:887-900.
256. Zhang, R., Erler, J., and Langowski, J. Histone Acetylation Regulates Chromatin Accessibility: Role of H4K16 in Inter-nucleosome Interaction. *Biophys. J.* 2017;112:450-459.
257. Sapountzi, V., and Cote, J. MYST-family histone acetyltransferases: Beyond chromatin. *Cell. Mol. Life Sci.* 2011;68:1147-1156.
258. Tulin, A.V. *Poly (ADP-Ribose) Polymerase (Methods and Protocols)*. Second Edi. (Tulin, A.V, ed.). Humana Press, Totowa, NJ; 2017.



259. Ding, D., Zhang, Y., Wang, J., Zhang, X., Gao, Y., Yin, L., Li, Q., Li, J., and Chen, H. Induction and inhibition of the pan-nuclear gamma-H2AX response in resting human peripheral blood lymphocytes after X-ray irradiation. *Cell Death Discov.* 2016;2:16011.
260. Podhorecka, M., Skladanowski, A., and Bozko, P. H2AX Phosphorylation : Its Role in DNA Damage Response and Cancer Therapy. *J. Nucleic Acids* 2010;2010:920161.
261. Tiwari, M.K., and Rogers, F.A. XPD-dependent activation of apoptosis in response to triplex-induced DNA damage. *Nucleic Acids Res.* 2013;41:8979-8994.
262. Joe, Y.S., Jeong, J.H., Yang, S., Kang, H., Motoyama, N., Pandolfi, P.P., Chung, J.H., and Kim, M.K. ATR, PML, and CHK2 play a role in arsenic trioxide-induced apoptosis. *J. Biol. Chem.* 2006;281:28764-28771.
263. Watanabe, R., Unuma, K., Noritake, K., Funakoshi, T., Aki, T., and Uemura, K. Ataxia telangiectasia and rad3 related (ATR)-promyelocytic leukemia protein (PML) pathway of the DNA damage response in the brain of rats administered arsenic trioxide. *J. Toxicol. Pathol.* 2017;30:333-337.
264. Li, Y., Zhao, Y., Jiang, R., Xu, Y., Ling, M., Pang, Y., Shen, L., Zhou, Y., Zhang, J., Zhou, J., Wang, X., and Liu, Q. DNA-PKcs-mediated stabilization of p53 by JNK2 is involved in arsenite-induced DNA damage and apoptosis in human embryo lung fibroblast cells. *Toxicol. Lett.* 2012;210:302-310.
265. Zykova, T.A., Zhu, F., Lu, C., Higgins, L., Tatsumi, Y., Abe, Y., Bode, A.M., and Dong, Z. Lymphokine-activated killer T-cell-originated protein kinase phosphorylation of histone H2AX prevents arsenite-induced apoptosis in RPMI7951 melanoma cells. *Clin. Cancer Res.* 2006;12:6884-6893.
266. Li, J., Gorospe, M., Barnes, J., and Liu, Y. Tumor promoter arsenite stimulates histone H3 phosphoacetylation of proto-oncogenes c-fos and c-jun chromatin in human diploid fibroblasts. *J. Biol. Chem.* 2003;278:13183-13191.
267. Xanthoudakis, S., Miao, G., Wang, F., Pan, Y.C., and Curran, T. Redox activation of Fos-Jun DNA binding activity is mediated by a DNA repair enzyme. *EMBO J.* 1992;11:3323-3335.
268. Cavigelli, M., Li, W.W., Lin, A., Su, B., Yoshioka, K., and Karin, M. The tumor promoter arsenite stimulates AP-1 activity by inhibiting a JNK phosphatase. *EMBO J.* 1996;15:6269-6279.
269. Picco, V., and Pagès, G. Linking JNK Activity to the DNA Damage Response. *Genes and Cancer.* 2013;4:360-368.
270. Jjingjo, D., Conley, A.B., Yi, S.V., Lunyak, V.V., and King Jordan, I. On the presence and role of human gene-body DNA methylation. *Oncotarget* 2012;3:462-474.

271. Jones, P.A., and Gonzalzo, M.L. Altered DNA methylation and genome instability: A new pathway to cancer? *Proc. Natl. Acad. Sci. U S A.* 1997;94:2103-2105.
272. Reichard, J.F., Schnekenburger, M., and Puga, A. Long term low-dose arsenic exposure induces loss of DNA methylation. *Biochem. Biophys. Res. Commun.* 2007;352:188-192.
273. Cui, X., Wakai, T., Shirai, Y., Yokoyama, N., Hatakeyama, K., and Hirano, S. Arsenic trioxide inhibits DNA methyltransferase and restores methylation-silenced genes in human liver cancer cells. *Hum. Pathol.* 2006;37:298-311.
274. Ahlborn, G.J., Nelson, G.M., Ward, W.O., Knapp, G., Allen, J.W., Ouyang, M., Roop, B.C., Chen, Y., O'Brien, T., Kitchin, K.T., and Delker, D.A. Dose response evaluation of gene expression profiles in the skin of K6/ODC mice exposed to sodium arsenite. *Toxicol. Appl. Pharmacol.* 2008;227:400-416.
275. Rea, M., Eckstein, M., Eleazer, R., Smith, C., and Fondufe-mittendorf, Y.N. Genome-wide DNA methylation reprogramming in response to inorganic arsenic links inhibition of CTCF binding , DNMT expression and cellular transformation. *Sci. Rep.* 2017;7:41474.
276. Goering, P.L., Aposhian, H.V., Mass, M.J., Cebrián, M., Beck, B.D., and Waalkes, M.P. The enigma of arsenic carcinogenesis: Role of metabolism. *Toxicol. Sci.* 1999;49:5-14.
277. Coppin, J.F., Qu, W., and Waalkes, M.P. Interplay between cellular methyl metabolism and adaptive efflux during oncogenic transformation from chronic arsenic exposure in human cells. *J. Biol. Chem.* 2008;283:19342-19350.
278. Zhao, C.Q., Young, M.R., Diwan, B.A., Coogan, T.P., and Waalkes, M.P. Association of arsenic-induced malignant transformation with DNA hypomethylation and aberrant gene expression. *Proc. Natl. Acad. Sci. U S A.* 1997;94:10907-10912.
279. Pfeifer, G.P. Defining driver DNA methylation changes in human cancer. *Int. J. Mol. Sci.* 2018;19:1-13.
280. Hon, G.C., Hawkins, R.D., Caballero, O.L., Lo, C., Lister, R., Pelizzola, M., Valsesia, A., Ye, Z., Kuan, S., Edsall, L.E., Camargo, A.A., Steveson, B.J., Ecker, J.R., Bafna, V., Strausberg, R.L., Simpson, A.J., and Ren, B. Global DNA hypomethylation coupled to repressive chromatin domain formation and gene silencing in breast cancer. *Genome Res.* 2012;22:246-258.
281. Esteller, M., Fraga, M.F., Guo, M., Garcia-Foncillas, J., Hedenfalk, I., Godwin, A.K., Trojan, J., Vours-Barriere, C., Bignon, Y.J., Ramus, S., Benitez, J., Caldes, T., Akiyama, Y., Yuasa, Y., Launonen, V., Canal, M.J., Rodriguez, R., Capella, G., Peinado, M.A., Borg, A., Aaltonen, L.A., Ponder, B.A., Baylin, S.B., and Herman, J.G. DNA methylation patterns in hereditary human cancers mimic sporadic tumorigenesis. *Hum. Mol. Genet.* 2001;10:3001-3007.

282. Pilsner, J.R., Liu, X., Ahsan, H., Ilievski, V., Slavkovich, V., Levy, D., Factor-Litvak, P., Graziano, J.H., and Gamble, M.V. Folate deficiency, hyperhomocysteinemia, low urinary creatinine, and hypomethylation of leukocyte DNA are risk factors for arsenic-induced skin lesions. *Environ. Health Perspect.* 2009;117:254-260.
283. Williamson, L.M., and Lees-Miller, S.P. Estrogen receptor  $\alpha$ -mediated transcription induces cell cycle-dependent DNA double-strand breaks. *Carcinogenesis* 2011;32:279-285.
284. Caldon, C.E. Estrogen Signaling and the DNA Damage Response in Hormone Dependent Breast Cancers. *Front. Oncol.* 2014;4:1-9.
285. Hossain, M.B., Vahter, M., Concha, G., and Broberg, K. Environmental arsenic exposure and DNA methylation of the tumor suppressor gene p16 and the DNA repair gene MLH1: Effect of arsenic metabolism and genotype. *Metallomics* 2012;4:1167-1175.
286. Miao, Z., Wu, L., Lu, M., Meng, X., Gao, B., Qiao, X., Zhang, W., and Xue, D. Analysis of the transcriptional regulation of cancer-related genes by aberrant DNA methylation of the cis-regulation sites in the promoter region during hepatocyte carcinogenesis caused by arsenic. *Oncotarget* 2015;6:21493-21506.
287. Zhang, A., Li, H., Xiao, Y., Chen, L., Zhu, X., Li, J., Ma, L., Pan, X., Chen, W., and He, Z. Aberrant methylation of nucleotide excision repair genes is associated with chronic arsenic poisoning. *Biomarkers* 2017;22:429-438.
288. Bachman, M., Uribe-Lewis, S., Yang, X., Williams, M., Murrell, A., and Balasubramanian, S. 5-Hydroxymethylcytosine is a predominantly stable DNA modification. *Nat. Chem.* 2014;6:1049-1055.
289. Mellén, M., Ayata, P., Dewell, S., Kriaucionis, S., and Heintz, N. MeCP2 Binds to 5hmC Enriched within Active Genes and Accessible Chromatin in the Nervous System. *Cell* 2012;151:1417-1430.
290. Williams, K., Christensen, J., Pedersen, M.T., Johansen, J.V., Cloos, P.A.C., Rappaport, J., and Helin, K. TET1 and hydroxymethylcytosine in transcription and DNA methylation fidelity. *Nature* 2011;473:343-349.
291. Kafer, G.R., Li, X., Horii, T., Suetake, I., Tajima, S., Hatada, I., and Carlton, P.M. 5-Hydroxymethylcytosine Marks Sites of DNA Damage and Promotes Genome Stability. *Cell Rep.* 2016;14:1283-1292.
292. Kantidze, O.L., and Razin, S.V. 5-hydroxymethylcytosine in DNA repair: A new player or a red herring? *Cell Cycle* 2017;16:1499-1501.
293. Dickinson, B.C., and Chang, C.J. Chemistry and biology of reactive oxygen species in signaling or stress responses. *Nat. Chem. Biol.* 2011;7:504-511.

294. Lange, M., Ok, K., Shimberg, G.D., Bursac, B., Marko, L., Ivanovic-Burmazovic, I., Michel, S.L.J., and Filipovic, M.R. Direct Zinc Finger Protein Persulfidation by H<sub>2</sub>S Is Facilitated by Zn<sup>2+</sup>. *Angew. Chemie - Int. Ed.* 2019;58:7997-8001.
295. Lee, S.J., and Michel, S.L.J. Cysteine oxidation enhanced by iron in tristetraprolin, a zinc finger peptide. *Inorg. Chem.* 2010;49:1211-1219.
296. Kluska, K., Adamczyk, J., and Krężel, A. Metal binding properties, stability and reactivity of zinc fingers. *Coord. Chem. Rev.* 2018;367:18-64.
297. Zhou, X., Cooper, K.L., Sun, X., Liu, K.J., and Hudson, L.G. Selective sensitization of zinc finger protein oxidation by reactive oxygen species through arsenic binding. *J. Biol. Chem.* 2015;290:18361-18369.
298. Breydo, L., and Uversky, V.N. Role of metal ions in aggregation of intrinsically disordered proteins in neurodegenerative diseases. *Metallomics* 2011;3:1163-1180.
299. Alies, B., Hureau, C., and Faller, P.. The role of metal ions in amyloid formation: General principles from model peptides. *Metallomics* 2013;5:183-192.
300. De Santis, E., Minicozzi, V., Morante, S., Rossi, G.C., and Stellato, F. The role of metals in protein conformational disorders - The case of prion protein and A $\beta$  -peptide. *J. Phys. Conf. Ser.* 2016;689:012028.
301. Savelieff, M.G., Lee, S., Liu, Y., and Lim, M.H. Untangling amyloid- $\beta$ , tau, and metals in Alzheimer's disease. *ACS Chem. Biol.* 2013;8:856-865.
302. Greenough, M.A., Camakaris, J., and Bush, A.I. Metal dyshomeostasis and oxidative stress in Alzheimer's disease. *Neurochem. Int.* 2013;62:540-555.
303. Gong, G., and O'Bryant, S.E. The arsenic exposure hypothesis for Alzheimer disease. *Alzheimer Dis. Assoc. Disord.* 2010;24:311-316.
304. O'Bryant, S.E., Edwards, M., Menon, C.V., Gong, G., and Barber, R. Long-term low-level arsenic exposure is associated with poorer neuropsychological functioning: A project FRONTIER study. *Int. J. Environ. Res. Public Health* 2011;8:861-874.
305. Dodson, M., de la Vega, M.R., Harder, B., et al. Low-level arsenic causes proteotoxic stress and not oxidative stress. *Toxicol. Appl. Pharmacol.* 2018;341:106-113.
306. Balchin, D., Hayer-Hartl, M., and Hartl, F.U. In vivo aspects of protein folding and quality control. *Science* 2016;353:aac4354.
307. Sweeney, P., Park, H., Baumann, M., et al. Protein misfolding in neurodegenerative diseases: Implications and strategies. *Transl. Neurodegener.* 2017;6:1-13.
308. Choe, Y.J., Park, S.H., Hassemer, T., et al. Failure of RQC machinery causes protein aggregation and proteotoxic stress. *Nature* 2016;531:191-195.

309. DePristo, M.A., Weinreich, D.M., and Hartl, D.L. Missense meanderings in sequence space: A biophysical view of protein evolution. *Nat. Rev. Genet.* 2005;6:678-687.
310. Nagradova, N. Enzymes Catalyzing Protein Folding and Their Cellular Functions. *Curr. Protein Pept. Sci.* 2007;8:273-282.
311. Tzul, F.O., Vasilchuk, D., and Makhatadze, G.I. Evidence for the principle of minimal frustration in the evolution of protein folding landscapes. *Proc. Natl. Acad. Sci. U S A.* 2017;114:E1627-E16322.
312. Ramadan, D., Rancy, P.C., Nagarkar, R.P., Schneider, J.P., and Thorpe, C. Arsenic(III) species inhibit oxidative protein folding in Vitro. *Biochemistry* 2009;48:424-432.
313. Sharma, S.K., Goloubinoff, P., and Christen, P. Heavy metal ions are potent inhibitors of protein folding. *Biochem. Biophys. Res. Commun.* 2008;372:341-345.
314. Sharma, S.K., Goloubinoff, P., and Christen, P. Non-native Proteins as Newly-Identified Targets of Heavy Metals and Metalloids. In: *Cellular Effects of Heavy Metals*. Dordrecht: Springer Netherlands; 2011:263-274.
315. Klaips, C.L., Jayaraj, G.G., and Hartl, F.U. Pathways of cellular proteostasis in aging and disease. *J. Cell Biol.* 2018;217:51-63.
316. Pechmann, S., Willmund, F., and Frydman, J. The Ribosome as a Hub for Protein Quality Control. *Mol. Cell* 2013;49:411-421.
317. O'Brien, E.P., Vendruscolo, M., and Dobson, C.M. Prediction of variable translation rate effects on cotranslational protein folding. *Nat. Commun.* 2012;3:868.
318. Zhang, G., and Ignatova, Z. Folding at the birth of the nascent chain: Coordinating translation with co-translational folding. *Curr. Opin. Struct. Biol.* 2011;21:25-31.
319. Hebert, D.N., and Molinari, M. In and Out of the ER: Protein Folding, Quality Control, Degradation, and Related Human Diseases. *Physiol. Rev.* 2007;87:1377-1408.
320. Pawar, A.P., DuBay, K.F., Zurdo, J., Chiti, F., Vendruscolo, M., and Dobson, C.M. Prediction of "aggregation-prone" and "aggregation-susceptible" regions in proteins associated with neurodegenerative diseases. *J. Mol. Biol.* 2005;350:379-392.
321. Ford, A.E., Denicourt, C., and Morano, K.A. Thiol stress-dependent aggregation of the glycolytic enzyme triose phosphate isomerase in yeast and human cells. *Mol. Biol. Cell* 2019;30:554-565.
322. Farrer, B.T., McClure, C.P., Penner-Hahn, J.E., and Pecoraro, V.L. Arsenic(III) - Cysteine interactions stabilize three-helix bundles in aqueous solution. *Inorg. Chem.* 2000;39:5422-5423.

323. Zaher, H.S., and Green, R. Fidelity at the Molecular Level: Lessons from Protein Synthesis. *Cell* 2009;136:746-762.
324. LaRiviere, F.J., Cole, S.E., Ferullo, D.J., and Moore, M.J. A late-acting quality control process for mature eukaryotic rRNAs. *Mol. Cell* 2006;24:619-626.
325. Wolff, S., Weissman, J.S., and Dillin, A. Differential scales of protein quality control. *Cell* 2014;157:52-64.
326. Brandman, O., and Hegde, R.S. Ribosome-associated protein quality control. *Nat. Struct. Mol. Biol.* 2016;23:7-15.
327. Riba, A., Di Nanni, N., Mittal, N., Arhné, E., Schmidt, A., and Zavolan, M. Protein synthesis rates and ribosome occupancies reveal determinants of translation elongation rates. *Proc. Natl. Acad. Sci.* 2019;116:15023-15032.
328. Juszkievicz, S., and Hegde, R.S. Initiation of Quality Control during Poly(A) Translation Requires Site-Specific Ribosome Ubiquitination. *Mol. Cell* 2017;65:743-750.
329. Joazeiro, C.A.P. Ribosomal Stalling During Translation: Providing Substrates for Ribosome-Associated Protein Quality Control. *Annu. Rev. Cell. Dev. Biol.* 2017;33:343-368.
330. Sundaramoorthy, E., Leonard, M., Mak, R., Liao, J., Fulzele, A., and Bennett, E.J. ZNF598 and RACK1 Regulate Mammalian Ribosome-Associated Quality Control Function by Mediating Regulatory 40S Ribosomal Ubiquitylation. *Mol. Cell* 2017;65:751-760.
331. Ikeuchi, K., Izawa, T., and Inada, T. Recent progress on the molecular mechanism of quality controls induced by ribosome stalling. *Front. Genet.* 2019;10:1-7.
332. Defenouillère, Q., Namane, A., Mouaikel, J., Jacquier, A., and Fromont-Racine, M. The ribosome-bound quality control complex remains associated to aberrant peptides during their proteasomal targeting and interacts with Tom1 to limit protein aggregation. *Mol. Biol. Cell* 2017;28:1165-1176.
333. Brandman, O., Stewart-Ornstein, J., Wong, D., et al. A ribosome-bound quality control complex triggers degradation of nascent peptides and signals translation stress. *Cell* 2012;151:1042-1054.
334. Matsuo, Y., Ikeuchi, K., Saeki, Y., et al. Ubiquitination of stalled ribosome triggers ribosome-associated quality control. *Nat. Commun.* 2017;8:1-13.
335. Huang, B., Chiang, K.H., Yu, H.S., Chen, Y.L., You, H.L., and Liao, W.T. Arsenic modulates posttranslational s-nitrosylation and translational proteome in keratinocytes. *Sci. World J.* 2014;2014.

336. Tam, L.M., Jiang, J., Wang, P., and Wang, Y. Arsenite binds to ZNF598 to perturb regulatory ubiquitination of ribosomal proteins and induce proteostatic stress. *Chem. Res. Toxicol.* 2019. *Submitted.*
337. Shao, S., Brown, A., Santhanam, B., and Hegde, R.S. Structure and assembly pathway of the ribosome quality control complex. *Mol Cell.* 2015;57:433-444.
338. Dimitrova, L.N., Kuroha, K., Tatematsu, T., and Inada, T. Nascent peptide-dependent translation arrest leads to Not4p-mediated protein degradation by the proteasome. *J. Biol. Chem.* 2009;284:10343-10352.
339. Prieto-Dominguez, N., Parnell, C., and Teng, Y. Drugging the Small GTPase Pathways in Cancer Treatment: Promises and Challenges. *Cells.* 2019;8:255.
340. Haga, R.B., and Ridley, A.J. Rho GTPases: Regulation and roles in cancer cell biology. *Small GTPases* 2016;7:207-221.
341. Porter, A.P., Papaioannou, A., and Malliri, A. Deregulation of Rho GTPases in cancer. *Small GTPases* 2016;7:123-138.
342. Bousquet, E., Mazières, J., Privat, M., et al. Loss of RhoB expression promotes migration and invasion of human bronchial cells via activation of AKT1. *Cancer Res.* 2009;69:6092-6099.
343. Mazieres, J., Antonia, T., Daste, G., et al. Loss of RhoB Expression in Human Lung Cancer Progression. *Clin. Cancer Res.* 2004;10:2742-2750.
344. Bousquet, E., Calvayrac, O., Mazières, J., et al. RhoB loss induces Rac1-dependent mesenchymal cell invasion in lung cells through PP2A inhibition. *Oncogene* 2016;35:1760-1769.
345. van Drie, J.H. Protein folding, protein homeostasis, and cancer. *Chin. J. Cancer* 2011;30:124-137.
346. Korovila, I., Hugo, M., Castro, J.P., et al. Proteostasis, oxidative stress and aging. *Redox Biol.* 2017;13:550-567.
347. van den Boom, J., and Meyer, H. VCP/p97-Mediated Unfolding as a Principle in Protein Homeostasis and Signaling. *Mol. Cell* 2018;69:182-194.
348. Bassermann, F., Eichner, R., and Pagano, M. The ubiquitin proteasome system - Implications for cell cycle control and the targeted treatment of cancer. *Biochim. Biophys. Acta - Mol. Cell. Res.* 2014;1843:150-162.
349. Liebelt, F., and Vertegaal, A.C.O. Ubiquitin-dependent and independent roles of SUMO in proteostasis. *Am. J. Physiol. - Cell. Physiol.* 2016;311:C284-C296.

350. Voutsadakis, I.A. Proteasome expression and activity in cancer and cancer stem cells. *Tumor Biol.* 2017;39:1-17.
351. Yu, X., Ponce, R.A., and Faustman, E.M. Metals Induced Disruption of Ubiquitin Proteasome System, Activation of Stress Signaling and Apoptosis. In: *Cellular Effects of Heavy Metals*. Dordrecht: Springer Netherlands; 2011:291-311.
352. Chen, C.J., Chen, C.W., Wu, M.M., and Kuo, T.L. Cancer potential in liver, lung, bladder and kidney due to ingested inorganic arsenic in drinking water. *Br. J. Cancer* 1992;66:888-892.
353. Pi, J., He, Y., Bortner, C., et al. Low level, long-term inorganic arsenite exposure causes generalized resistance to apoptosis in cultured human keratinocytes: Potential role in skin co-carcinogenesis. *Int. J. Cancer* 2005;116:20-26.
354. Tillotson, J., Zerio, C.J., Harder, B., et al. Arsenic Compromises Both p97 and Proteasome Functions. *Chem. Res. Toxicol.* 2017;30:1508-1514.
355. Kors, S., Geijtenbeek, K., Reits, E., and Schipper-Krom, S. Regulation of Proteasome Activity by (Post-)transcriptional Mechanisms. *Front. Mol. Biosci.* 2019;6:48.
356. Nethe, M., and Hordijk, P.L. The role of ubiquitylation and degradation in RhoGTPase signalling. *J. Cell Sci.* 2010;123:4011-4018.



## **Chapter 2**

**Arsenite Binds to ZNF598 to Perturb**

**Regulatory Ubiquitination of Ribosomal Proteins and**

**Induce Proteotoxic Stress**

## Introduction

Arsenic is a metalloid prevalent in the environment, where it is naturally present in the Earth's crust and it is also anthropogenically introduced to the environment (e.g. through the use of arsenic-containing pesticides).<sup>1,2</sup> Arsenic exists in the environment in inorganic (trivalent arsenite or pentavalent arsenate) or organic forms, where inorganic trivalent arsenite is the most common arsenic species found in the environment and also imparts the highest relative potency in toxicity among the different chemical forms of arsenic.<sup>3</sup> Arsenic pollution, which influences more than 200 million people in over 70 countries, is viewed as one of the most serious public health problems worldwide.<sup>4</sup> Arsenic exposure has been found to contribute to the onset and/or progression of various human diseases, including neurodegenerative disorders, cancers, and type II diabetes.<sup>5-7</sup> Not surprisingly, arsenic has been ranked on the top of the Substance Priority List by the Agency for Toxic Substances and Disease Registry for many years. Hence, there is an urgent need for understanding the mechanisms through which arsenic exposure results in human diseases.

Approximately half of all human diseases are believed to emanate from protein misfolding.<sup>8</sup> Chronic exposure to low levels of arsenic in human populations is thought to be associated with arsenic-elicited proteostatic stress.<sup>9</sup> Additionally, arsenic was found to lower protein stability in cells; hence, arsenic exposure may perturb homeostasis of the proteome.<sup>9</sup> Examples of human diseases arising from arsenic-induced proteotoxic stress include neurodegenerative disorders, e.g. Alzheimer's disease and Huntington's disease.<sup>8</sup> Epidemiological and animal studies have documented the strong associations between arsenic exposure and cognitive impairment in humans and higher incidence of neurodegenerative diseases in rodents.<sup>10</sup> Thus, the arsenic-elicited onset and/or progression of neurodegenerative diseases could be potentially attributed to arsenic-induced proteotoxic stress.<sup>11</sup> Therefore, it is important to investigate the mechanisms through which arsenic exposure induces proteostatic stress.

In humans, there are several established mechanisms for maintaining the homeostasis of the proteome through prevention of protein aggregation and/or elimination of the misfolded proteins, i.e. molecular chaperones, ubiquitin-proteasome system (UPS) and co-translational ribosome-associated protein quality control (RQC).<sup>12,13</sup> Among them, RQC is energetically inexpensive, and it promptly eliminates aberrant mRNA and abnormal nascent polypeptides during translation, which constitutes the frontline defense against futile aberrant protein synthesis.<sup>14</sup> Only through RQC can abnormal, truncated polypeptides be rapidly degraded, thereby minimizing aberrant protein-protein interactions in the cytosol.<sup>13</sup> Poly-A sequences in coding regions of mRNA are among the stressors that result in ribosome stalling, thereby initiating the RQC pathway.<sup>15</sup> Regulatory ubiquitinations of RPS10 and RPS20, modulated by the ZNF598 E3 ubiquitin ligase, were demonstrated to be indispensable for the initiation of the RQC pathway.<sup>15,16</sup>

Arsenic is known to bind selectively to C<sub>3</sub>H- or C<sub>4</sub>-type zinc finger proteins.<sup>17</sup> Others and we demonstrated that arsenite targets the cysteine residues within the zinc finger motifs of proteins, which in turn diminishes their enzymatic activities for the post-translational modifications vital for cellular processes, including DNA repair and oxidative stress response.<sup>18-21</sup> Building upon these previous studies, we hypothesize that ZNF598's RING finger motif may be a molecular target of arsenic binding, which may impair proteostasis by compromising the RQC pathway.<sup>15,16</sup> To test this hypothesis, we examine the arsenite-induced perturbation in regulatory ubiquitinations of RPS10 and RPS20, investigate the interaction between ZNF598 and As<sup>3+</sup> in cells, and assess the impact of As<sup>3+</sup> exposure on RQC in human cells.

## **Experimental Procedures**

### **Cell culture**

HEK293T cells (ATCC) were cultured in Dulbecco's modified Eagle's medium (DMEM, Thermo Fisher Scientific). All culture media except those used for transfection were supplemented with 10% fetal bovine serum (FBS, Thermo Fisher Scientific) and 1% penicillin streptomycin solution (GE Healthcare). The cells were maintained in a humidified atmosphere with 5% CO<sub>2</sub> at 37 °C, with medium renewal in every 2-3 days depending on cell density. For plasmid transfection, the cells were cultured in the same media except that no penicillin streptomycin solution was added.

### **Plasmid and cell transfection**

The expression plasmid for ZNF598, pcDNA3.1-ZNF598-TEV-3×Flag, and the reporter cassettes, i.e. pmGFP-P2A-(K<sup>AAA</sup>)<sub>0</sub>-P2A-RFP and pmGFP-P2A-(K<sup>AAA</sup>)<sub>20</sub>-P2A-RFP, were obtained from Addgene. The expression plasmid for GFP-tagged ZNF598, i.e. pcDNA4/TO-GFP-ZNF598, was kindly provided by Dr. Simon Bekker-Jensen from the University of Copenhagen.<sup>22</sup> The plasmid was transfected into HEK293T cells using TransIT-2020 (Mirus Bio, Madison, WI) according to the manufacturer's protocol.

### **Streptavidin agarose affinity assay and Western blot**

The biotin-As probe was previously synthesized.<sup>21</sup> HEK293T cells were transfected with wild-type Flag-ZNF598. At 24 hr after the transfection, the cells were exposed with 5 μM biotin-As for 2 hr and lysed in CellLytic™ M lysis buffer supplemented with a protease inhibitor cocktail (Sigma-Aldrich). The cell lysates were subsequently incubated with high-capacity streptavidin agarose beads overnight. The streptavidin agarose beads were then washed with 1× PBS and resuspended in SDS-PAGE loading buffer.

After SDS-PAGE separation, proteins were transferred to a nitrocellulose membrane using a transfer buffer containing Tris (pH 8.3), methanol, glycine and water. The membranes were blocked

with 5% BSA in 1× PBS-T buffer, which contained PBS and 0.1% (v/v) Tween-20 (pH 7.5), for 1 hr, and then incubated with mouse anti-Flag antibody (1:5000 dilution, Santa Cruz Biotech) at room temperature for 2 hr. The membranes were washed with fresh PBS-T at room temperature for 6 times (5-10 min each). After washing, the membranes were incubated with mouse secondary antibody (1:10000 dilution, Santa Cruz Biotech) at room temperature for 1 hr. The membranes were then washed with PBS-T for 6 times. The protein bands were detected by using Amersham™ ECL™ Select Western blotting Detection Kit (GE Healthcare) and visualized with Hyblot CL autoradiography film (Denville Scientific, Inc., Metuchen, NJ). Similar experiments were also conducted by pre-treatment of cells with 10 μM ZnCl<sub>2</sub>, *p*-aminophenylarsine oxide (PAPAO) or NaAsO<sub>2</sub> for 1 hr prior to the biotin-As treatment.

#### **SILAC labeling, As<sup>3+</sup> exposure, immunoprecipitation, and LC-MS/MS analysis**

SILAC labeling of GM00637 cells in light or heavy RPMI 1640 medium, As<sup>3+</sup> exposure, immunoprecipitation of ubiquitin remnant peptides, and LC-MS/MS analysis of the enriched peptides were described previously.<sup>23</sup>

#### **Fluorescence Microscopy**

Wild-type pcDNA4/TO-GFP-ZNF598 plasmid (0.5 μg) was transfected into 1 × 10<sup>5</sup> HEK293T cells seeded on cover glasses placed in a 24-well plate. After 36 hr, the transfected cells were mock-treated or treated with 10 μM ZnCl<sub>2</sub>, NaAsO<sub>2</sub>, or PAPAO for 2 hr and then incubated with 5 μM ReAsH-EDT<sub>2</sub> (Invitrogen, Waltham, MA) in Opti-MEM medium at 37 °C for 1 hr. The cells were then washed with 1× BAL buffer for 3 times, fixed with 4% paraformaldehyde for 15 min, and stained with 4',6-diamidino-2-phenylindole (DAPI). The sample slides were subjected to imaging on a Zeiss 880 confocal microscope with Airyscan (Thornwood, NY) at the wavelengths of 355, 488, and 594 nm for DAPI, GFP, and ReAsH, respectively.

### **Dual fluorescence translation stalling assay**

Dual fluorescence reporter plasmids were transfected into cells using TransIT-2020 (Mirus Bio, Madison, WI) according to the manufacturer's guidelines. At 24 hr after the transfection, the cells were treated with 5.0  $\mu\text{M}$   $\text{NaAsO}_2$  (or mock treatment) for another 24 hr. The cells were then subjected to analysis on a MoFlo Astrios EQ Flow Cytometry system (Beckman Coulter, IN), where cellular GFP and ChFP fluorescence emissions were measured. Subsequent analysis of FACS data was conducted using FlowJo (v9.1).

### **Statistical Analysis**

Statistical analyses were performed by determining the mean and standard deviation of the values obtained from 3-4 independent experiments, except for the fluorescence microscopy data, where images from 30 cells in each group were analyzed, as detailed in the corresponding figure legends.

## **Results**

### **Arsenite exposure led to decreased regulatory ubiquitination of RPS10 and RPS20**

To test if arsenic could influence the level of ubiquitination of proteins which are important in the co-translational RQC pathway, we performed a di-glycine remnant pull-down experiment followed by LC-MS/MS analysis to identify proteins in GM00637 human skin fibroblasts exhibiting substantial changes in their ubiquitination levels after a 24-hr exposure to 5  $\mu\text{M}$   $\text{NaAsO}_2$ .<sup>23</sup> We found that the ubiquitination levels of lysines 138 and 139 (K138 and K139) in RPS10 and K8 in RPS20 were decreased to 60% and 52% relative to the levels observed in control cells, respectively (Fig. 2.1 and representative MS and MS/MS results for monitoring the ubiquitination of K8 in RPS20 are shown in Fig. 2.2). In this vein, these ubiquitination events on

RPS10 (i.e. K138, and K139) and RPS20 (K8) are known to play an important role in the initiation of ribosomal stalling and the onset of co-translational RQC pathway.<sup>15</sup>

**Arsenite binds to the cysteine residues in the RING finger domain of ZNF598 protein in cells**

To further elucidate how arsenite exposure diminishes the regulatory ubiquitination marks on ribosomal proteins RPS10 and RPS20, we focused our attention on the previously reported major E3 ubiquitin ligase of these ribosomal proteins, ZNF598.<sup>15,16</sup> In this vein, our previous quantitative proteomic experiments showed that a 24-hr treatment of GM00637 cells with 5.0  $\mu$ M arsenite did not give rise to any appreciable changes in the levels of expression of ZNF598, RPS10, or RPS20 protein, where the corresponding ratios of protein levels were  $0.98 \pm 0.07$ ,  $1.04 \pm 0.08$  and  $1.03 \pm 0.08$  in arsenite-treated over mock-treated cells.<sup>24</sup> Therefore, the arsenite-elicited decreases in the levels of ubiquitinated peptides of RPS10 and RPS20 are not due to diminished expression of these two proteins or ZNF598.

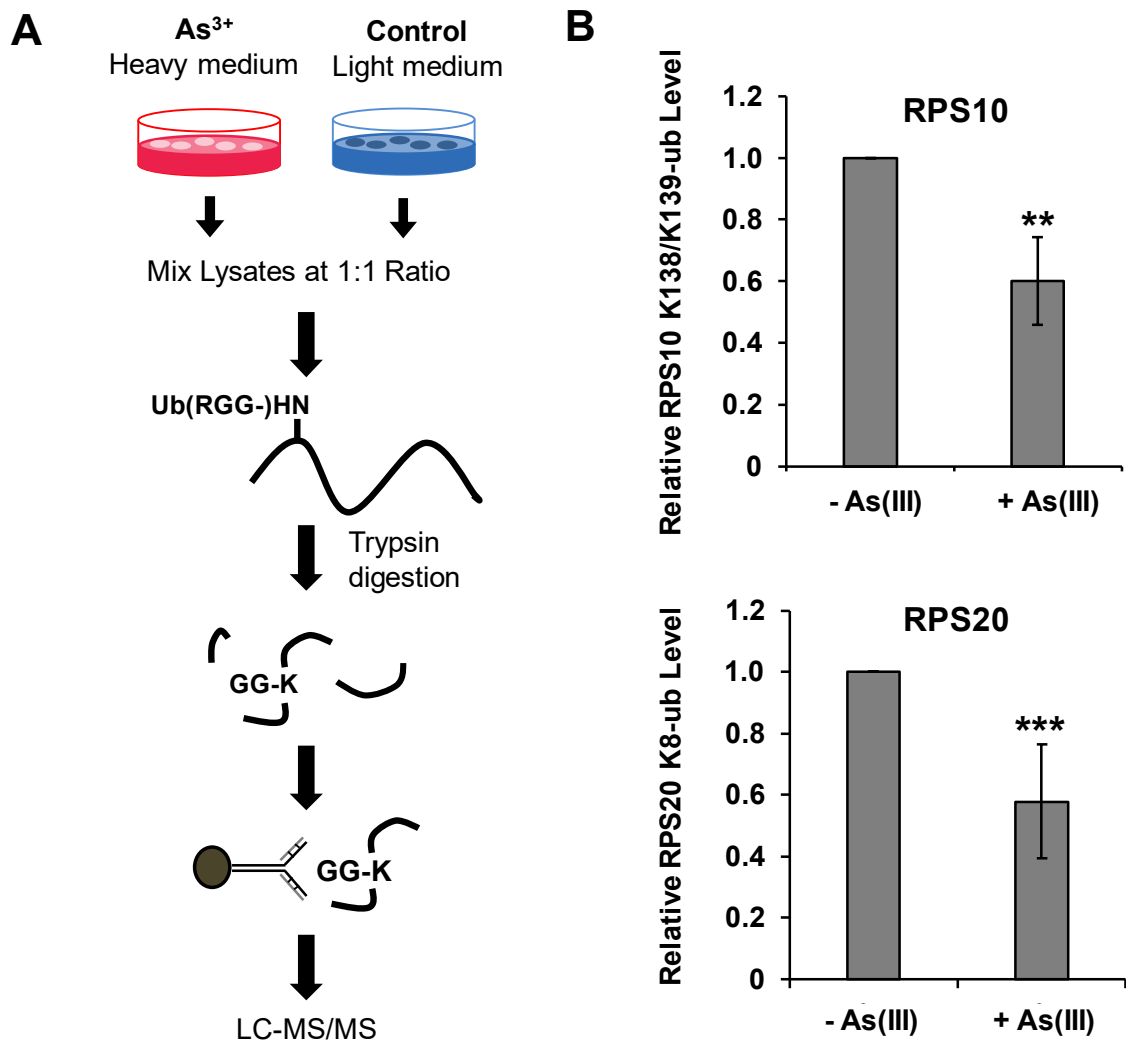


**Figure 2.1.** Arsenite diminishes the levels of site-specific ubiquitination in ribosomal proteins RPS10 and RPS20. (A) The workflow of SILAC and LC-MS/MS for studying the effect of a 24-hr exposure of human skin fibroblast GM00637 cells to 5  $\mu$ M NaAsO<sub>2</sub> on the global ubiquitinated proteome. (B) Quantification of the ubiquitination levels of K138/K139 in RPS10 and K8 in RPS20 upon a 24-hr exposure to 5  $\mu$ M NaAsO<sub>2</sub>. The data represents the mean  $\pm$  S.D. of results obtained from 4 biological replicates. The *p* values were calculated using an unpaired two-tailed Student's *t*-test (\*, 0.01  $\leq p < 0.05$ ; \*\*, 0.001  $\leq p < 0.01$ ; \*\*\*, *p* < 0.001).



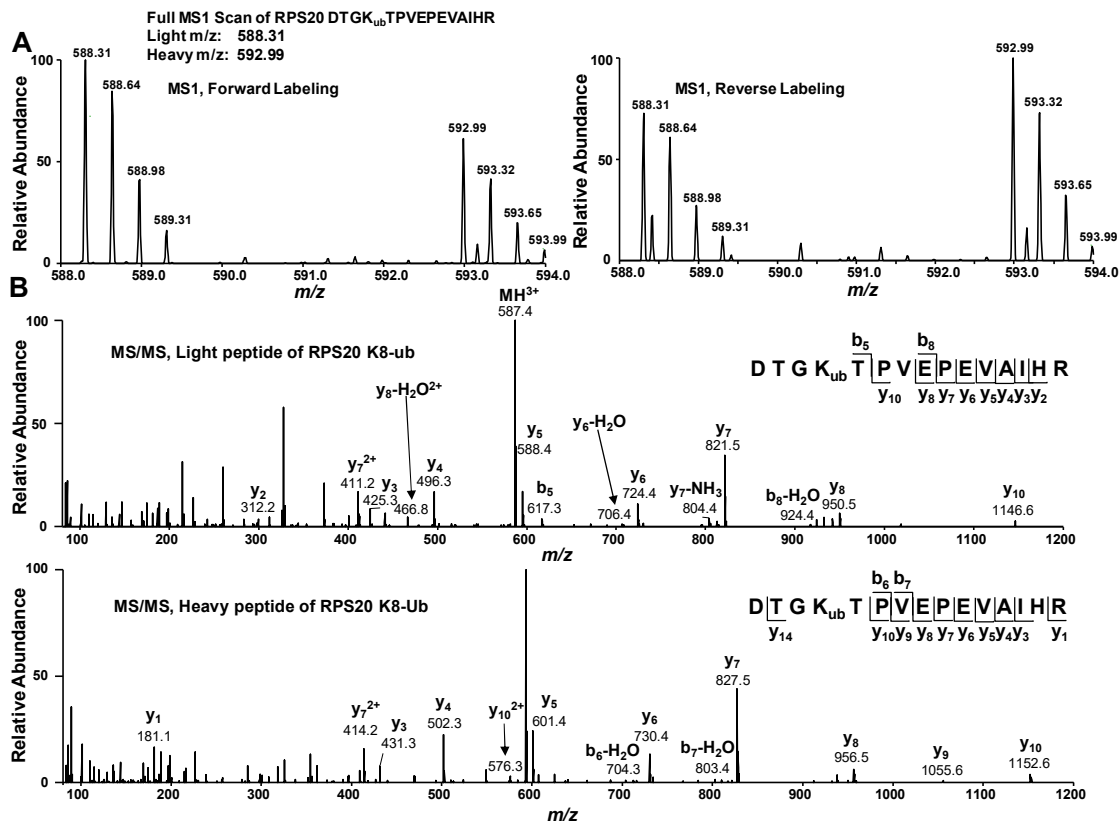


**Figure 2.2.** LC-MS and MS/MS results showing the arsenite-induced decreases in the relative abundance of K-ε-GG-containing tryptic peptide, DTG(K8-ε-GG)TPVEPEVAIHR, derived from RPS20. (A) Positive-ion ESI-MS showing the  $[M+3H]^{3+}$  ions of the peptide obtained from forward and reverse SILAC experiments, where the  $m/z$  values for the monoisotopic peaks for the light and heavy-labeled peptide are 588.31 and 592.99, respectively. (B) MS/MS for the light and heavy-labeled peptide, where the inset showing a scheme summarizing the observed  $b$  and  $y$  ions.

In light of the previous observations about the effects of As(III) binding on modulating the E3 ubiquitin ligase activities of other RING finger proteins,<sup>19,21,23</sup> we reason that the decrease in ubiquitination of RPS10 and RPS20 might be attributed to the interaction between As(III) and ZNF598 and the ensuing loss of its E3 ubiquitin ligase activity. To test this, we first examined the interaction between As(III) and ZNF598. We treated HEK293T cells with a *p*-aminophenylarsine oxide-conjugated biotin probe (Fig. 2.3.A) and assessed its interaction with ectopically expressed Flag-ZNF598 by a streptavidin agarose affinity assay.<sup>21</sup> The Western blot result revealed that the biotin-As probe facilitated the pull-down of the ectopically expressed Flag-ZNF598 protein from

human cells, where the control experiment without the addition of the biotin-As probe did not result in pull-down of the protein (Fig. 2.3.B). In addition, pre-treatment of Flag-ZNF598-expressing HEK293T cells with 10  $\mu$ M PAPA0 or NaAsO<sub>2</sub> could significantly attenuate the pull-down of Flag-ZNF598, though pre-treatment with ZnCl<sub>2</sub> did not lead to any significant decline in the pull-down of the protein (Fig. 2.3.C-D). This result suggests that As<sup>3+</sup> is capable of displacing the Zn<sup>2+</sup> ions bound with the RING finger motif of Flag-ZNF598.

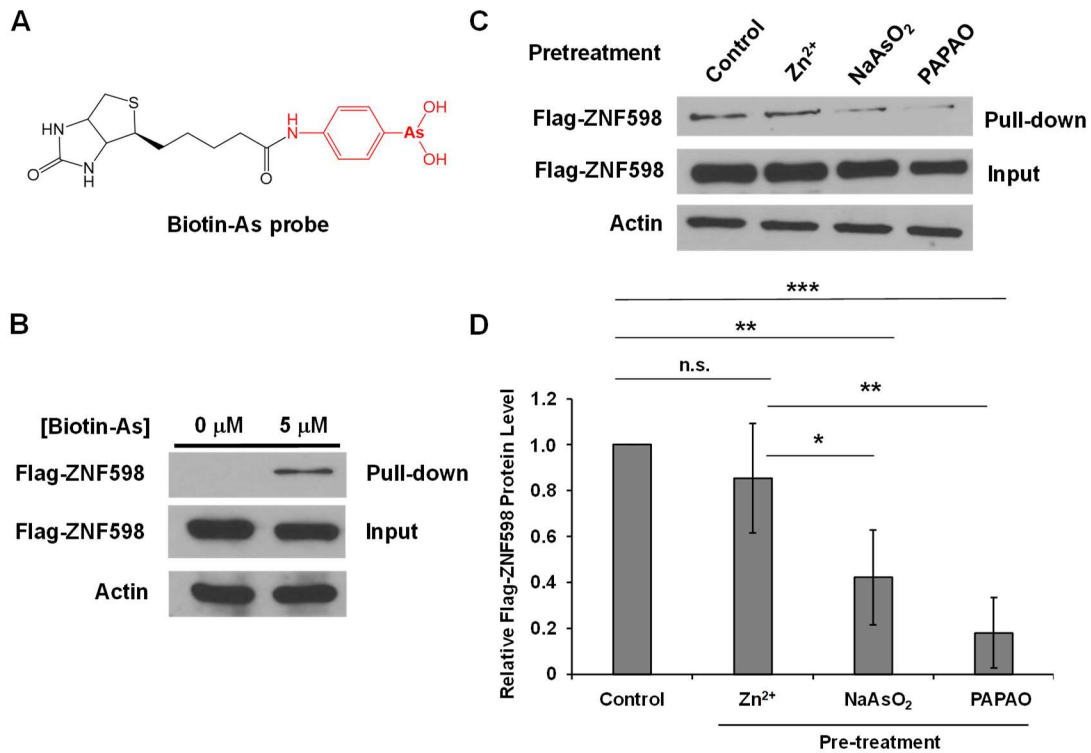


**Figure 2.3.** Arsenite binds to the ZNF598 protein in cells. (A) The chemical structure of the biotin-As probe. (B) Streptavidin agarose affinity pull-down assay showing the interaction between As<sup>3+</sup> and ZNF598 in cells. The biotin-As probe was used to pull down ectopically expressed Flag-ZNF598 in HEK293T cells. The Flag-ZNF598 signal was detected using the anti-Flag antibody, and the input Flag-ZNF598 and actin were also monitored. (C, D) The interaction between the biotin-As probe and ZNF598 was substantially diminished upon pre-treatment of HEK293T cells with 10  $\mu$ M NaAsO<sub>2</sub> and PAPA0, but not with 10  $\mu$ M Zn<sup>2+</sup>. The Western blot images are shown in (C), and the quantification results are displayed in (D). The data represents the mean  $\pm$  S.D. of results obtained from 4 biological replicates. The *p* values were calculated using an unpaired two-tailed Student's *t*-test (\*, 0.01  $\leq p < 0.05$ ; \*\*, 0.001  $\leq p < 0.01$ ; \*\*\*, *p* < 0.001, 'n.s.' stands for no significant difference).

We also explored the importance of cysteine residues, located in the RING finger motif of ZNF598, in binding with  $\text{As}^{3+}$  in cells by utilizing a GFP-tagged ZNF598 expression plasmid and a biarsenical labeling reagent ReAsH-EDT<sub>2</sub>, which contains two  $\text{As}^{3+}$  and displays red fluorescence when four nearby cysteine residues in proteins bind to its arsenic moieties.<sup>19</sup> We observed substantial co-localizations between the ectopically expressed GFP-ZNF598 and ReAsH, suggesting an interaction between  $\text{As}^{3+}$  and ZNF598 protein in cells (Fig. 2.4). This result also reveals that the tetracysteine motif within the RING finger motif of ZNF598 binds to the arsenic moieties in ReAsH.

To further examine if  $\text{As}^{3+}$  is capable of displacing  $\text{Zn}^{2+}$  coordinated by cysteine residues within the RING finger domain of ZNF598, we pre-treated GFP-ZNF598 expressing HEK293T cells with  $\text{Zn}^{2+}$ , PAPA0, or  $\text{NaAsO}_2$  prior to incubating cells with the ReAsH-EDT<sub>2</sub> dye. We observed a markedly attenuated co-localization between GFP-ZNF598 and ReAsH in cells upon pre-treatment with PAPA0 or  $\text{NaAsO}_2$ , but not  $\text{Zn}^{2+}$ , supporting the competitive binding of  $\text{As}^{3+}$  to cysteine residues in the RING finger domain of ZNF598 (Fig. 2.4).

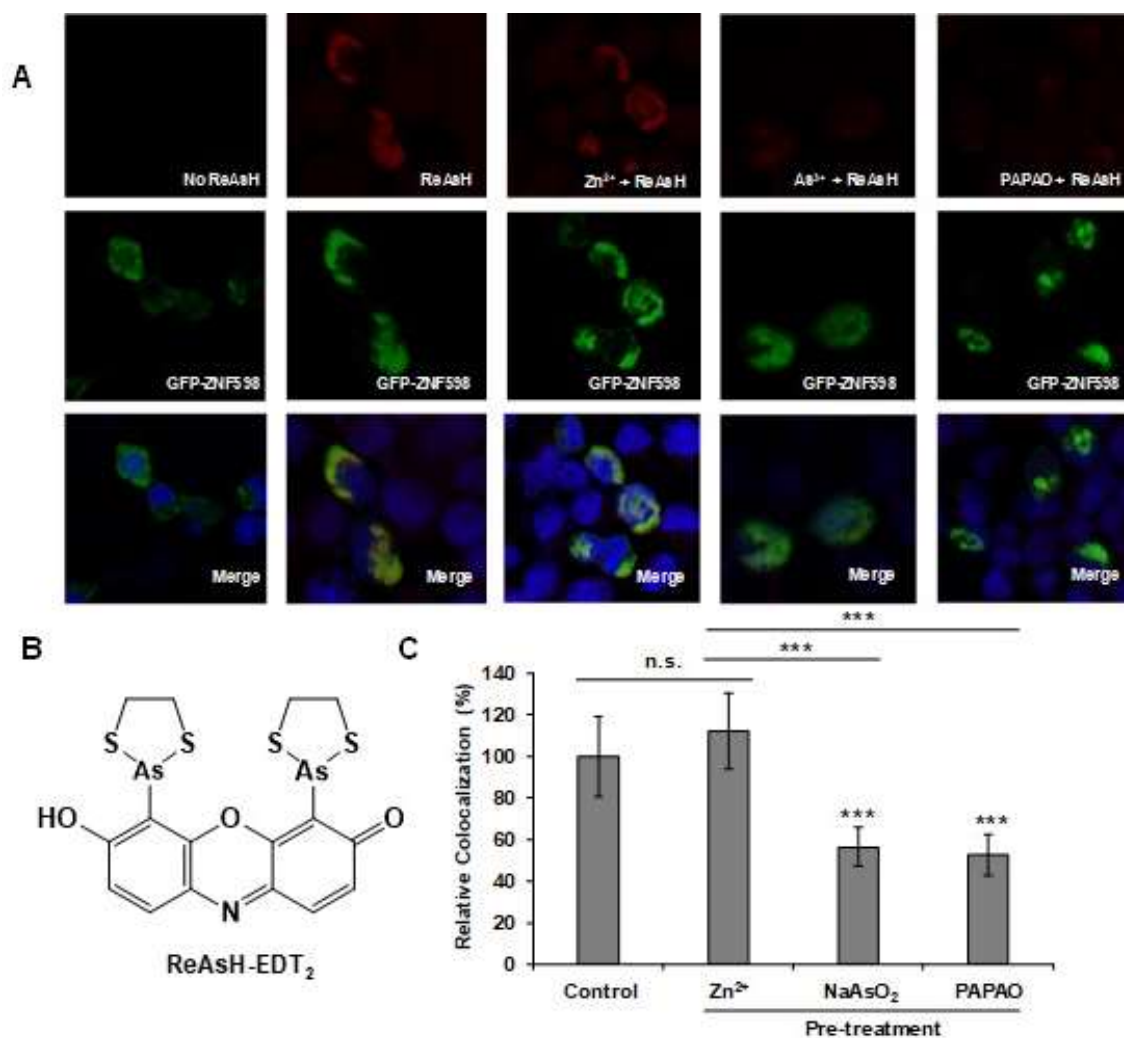


**Figure 2.4.** As<sup>3+</sup>-bearing biarsenical dye ReAsH co-localizes with GFP-ZNF598, and As<sup>3+</sup> competes with Zn<sup>2+</sup> for binding to the tetracysteine motif within the RING finger domain of ZNF598. (A) Fluorescence microscopy results revealed the co-localization between ReAsH and ectopically expressed GFP-ZNF598. The co-localization was significantly diminished in cells pre-treated with 10  $\mu$ M NaAsO<sub>2</sub> or PAPA0, but not Zn<sup>2+</sup>. (B) The chemical structure of ReAsH-EDT<sub>2</sub>. (C) Quantitative analysis of the frequencies of co-localization between ReAsH-EDT<sub>2</sub> and ZNF598. The data represents the mean  $\pm$  S.D. of results obtained from images of 30 different cells. The *p* values were calculated using an unpaired two-tailed Student's *t*-test (\*, 0.01  $\leq p <$  0.05; \*\*, 0.001  $\leq p <$  0.01; \*\*\*, *p* < 0.001, 'n.s.' represents no significant difference).

### **Arsenite increases the ribosomal read-through of the (K<sup>AAA</sup>)<sub>20</sub> mRNA sequence during translation**

We next explored to what degree the As<sup>3+</sup>-induced decreases in ubiquitination levels of RPS10 and RPS20 perturbs the co-translational RQC pathway. We adopted a previously reported flow cytometry-based assay to assess quantitatively ribosome stalling at poly-A sites in mammalian cells.<sup>15</sup> In particular, the reporter cassette contains N- and C-terminal GFP and ChFP markers flanked by a Flag-tagged stalling reporter (SR, Fig. 2.5A), as described previously.<sup>15</sup> Therefore, complete translation of the cassette yields three proteins (GFP, Flag-SR, and ChFP) in equi-molar quantities. By contrast, stalling during translation of Flag-SR would abolish translation prior to ChFP synthesis and lead to a sub-stoichiometric ChFP/GFP ratio.<sup>15</sup>

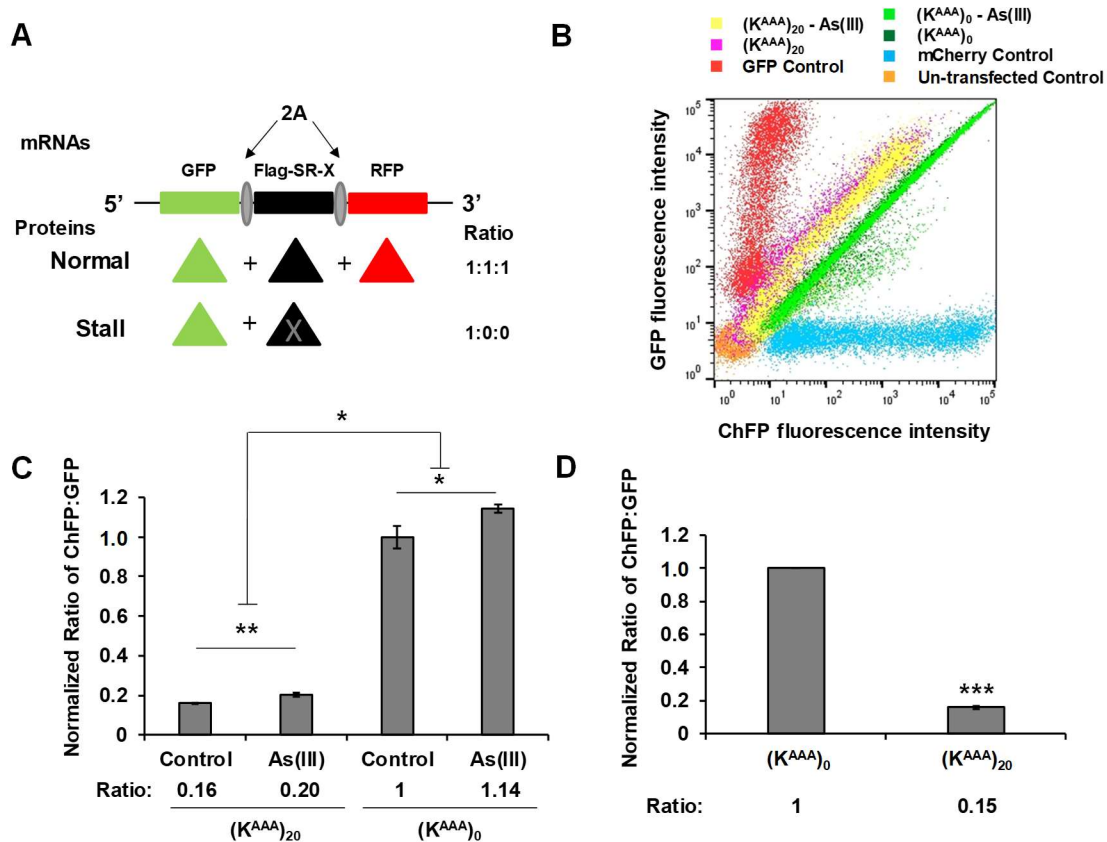


**Figure 2.5.** Arsenite inhibits the ribosomal stalling and augments the read-through of poly-A stalling sequences. (A) A schematic diagram showing the working principle of the dual fluorescence translation stall reporters. Plasmids expressing a reporter without a stall-inducing sequence or one containing 20 consecutive lysine codons (K<sup>AAA</sup>)<sub>20</sub> in the linker region were transfected into HEK293T cells. The diagram of the reporter cassette construct and expected protein products in the absence or presence of terminal stalling is modified from the work of Juskiewicz and Hedge.<sup>15</sup> (B) The resulting cellular GFP and ChFP levels are depicted in the scatter plot of individual cells. (C) Median ChFP:GFP ratio of 50,000 transfected HEK293T cells transiently expressing the reporter construct containing the indicated sequences. (D) Median ChFP:GFP ratio of 50,000 transfected cells transiently expressing the reporter plasmids containing either no stalling sequence or 20 consecutive lysine codons (K<sup>AAA</sup>)<sub>20</sub> in the linker region. In (C) and (D), the error bars represent S.E.M. for three separate transfections and flow cytometry measurements, and the *p* values were calculated using an unpaired two-tailed Student's *t*-test (\*, 0.01 ≤ *p* < 0.05; \*\*, 0.001 ≤ *p* < 0.01; \*\*\*, *p* < 0.001).

Previous findings revealed that tandem repeats of AAA lysine codons, i.e. (K<sup>AAA</sup>)<sub>n</sub>, are among the most potent trigger for ribosome stalling in mammalian cells and result in an appreciable decrease in the ChFP/EGFP ratio relative to the reporter lacking an insert between the GFP and

ChFP markers.<sup>15</sup> Flow cytometry analysis result revealed the expected correlation between GFP and ChFP levels across a wide expression range for  $(K^{AAA})_0$  but significantly reduced ChFP for  $(K^{AAA})_{20}$  (Fig. 2.5.D). To explore how arsenite exposure affects the ribosomal stalling of the  $(K^{AAA})_{20}$  sequence, we repeated the flow cytometry-based assay for the transfected cells after an 18-hr exposure to 5  $\mu$ M  $As^{3+}$ . These results show that arsenite exposure leads to an increased ratio of ChFP:GFP fluorescence intensities ( $1.32 \pm 0.05$ ) when compared to the untreated control (Fig. 2.5.C), suggesting that arsenite treatment could impede ribosomal stalling during the translation of mRNA sequence containing  $(K^{AAA})_{20}$ . The enhanced read-through of poly-A sequence  $(K^{AAA})_{20}$  are also reflected by the scatter plot shown in Fig. 2.5.B. In addition, we examined if the aforementioned effect arises from the  $As^{3+}$ -induced augmentation in overall translation elongation by including a negative control experiment with the use of the corresponding reporter without the poly-A stalling sequence, i.e.  $(K^{AAA})_0$ . The result showed that arsenite exposure increased the translation of ChFP relative to GFP using the  $(K^{AAA})_0$  sequence, i.e. ( $1.14 \pm 0.04$ ) when compared to the untreated control (Fig. 2.5.C). After normalization, we found that arsenite exposure augments the read-through of poly-A mRNA sequence  $(K^{AAA})_{20}$  by 16%.

## Discussion

### **$As^{3+}$ binds to RING finger motif of ZNF598 and induces proteostatic stress**

$As^{3+}$  is known to interact with zinc finger proteins,<sup>25</sup> especially with high affinity to the C<sub>3</sub>H- or C<sub>4</sub>- type zinc finger motifs,<sup>17</sup> and this interaction between arsenite and zinc finger proteins may play a pivotal role in human diseases arising from arsenic exposure, including protein misfolding-associated diseases, such as neurodegenerative disorders. Binding of  $As^{3+}$  to the zinc finger domains of TIP60 histone acetyltransferase and Tet ten-eleven translocation family proteins is known to disrupt the enzymatic activities of these proteins.<sup>18,26</sup> In addition, displacement of  $Zn^{2+}$

by  $\text{As}^{3+}$  in the RING finger domain of several E3 ubiquitin ligases was found to impair the ubiquitination of their substrate proteins.<sup>19,21,23</sup>

In the present study, we furnished two lines of evidence to support that arsenite can bind to the RING finger domain of ZNF598 by displacing its bound  $\text{Zn}^{2+}$  ions. In particular, our results from fluorescence microscopy experiment with the use of an  $\text{As}^{3+}$ -containing probe, i.e. ReAsH-EDT<sub>2</sub>, and biotin-As pull-down assay revealed the interaction between  $\text{As}^{3+}$  and ZNF598, which could be pronouncedly weakened by pre-treating cells with  $\text{NaAsO}_2$  and PAPA0, but not  $\text{Zn}^{2+}$  (Fig. 2.3.-2.4.).

ZNF598 is a major E3 ubiquitin ligase responsible for the site-specific regulatory ubiquitinations of ribosomal proteins RPS10 (at K138 and K139) and RPS20 (at K8).<sup>15,16</sup> The RING finger domain of ZNF598 is highly conserved and is essential for its E3 ubiquitin ligase activity, which is indispensable for efficient ribosome stalling at poly-A sequences in coding regions.<sup>27</sup> In line with these previous observations, we found that exposure of cultured human cells to  $\text{As}^{3+}$  and the ensuing interaction between  $\text{As}^{3+}$  and ZNF598 led to diminished ubiquitination of K138 and K139 in RPS10, and K8 in RPS20 (Fig. 2.1.-2.2.). These results, together with our observation of As(III)-induced augmented translational read-through of poly-A stalling sequence in template mRNA (Fig. 2.5.), substantiates that  $\text{As}^{3+}$  can displace  $\text{Zn}^{2+}$  from the RING finger domain of ZNF598, thereby inducing proteostatic stress through perturbing the RQC pathway.

### **Disturbance to protein quality control by arsenic exposure and human diseases**

Proteostasis is defined as the combined activity of cellular mechanisms regulating protein synthesis, folding, trafficking, degradation and clearance, and the failure to maintain proteostasis leads to proteotoxic stress.<sup>28</sup> Proteotoxic stress is implicated in many human diseases, including phenylketonuria, type II diabetes and neurodegenerative disorders, which arise largely from impaired cellular proteostasis.<sup>29,30</sup>



Ribosome-associated protein quality control constitutes one of the major mechanisms in maintaining proteostasis.<sup>13</sup> To achieve strict screening of translation errors, the RQC pathway is initiated by surveillance of defective mRNA, including premature polyadenylated mRNA, and degrades the aberrant truncated protein products generated by the stalled ribosomes.<sup>13</sup> RQC can be accomplished in three consecutive steps, i.e. splitting of a stalled ribosome into subunits, initiation of RQC assembly and nascent chain ubiquitination, and degradation of ubiquitinated nascent polypeptides.<sup>13</sup> Translation of poly-A sequence has been documented to stall the ribosome and trigger non-stop decay (NSD) as well as RQC, which are initiated by sensing of stalled ribosomes and are coupled with ribosomal rescue through dissociation of ribosomal subunits.<sup>31</sup> In this process, the site-specific regulatory ubiquitinations of RPS10 and RPS20 mediated by ZNF598 E3 ubiquitin ligase are required for the detection of ribosomal stalling and triggering the splitting of ribosomal subunits to initiate RQC.<sup>13,27,31</sup>

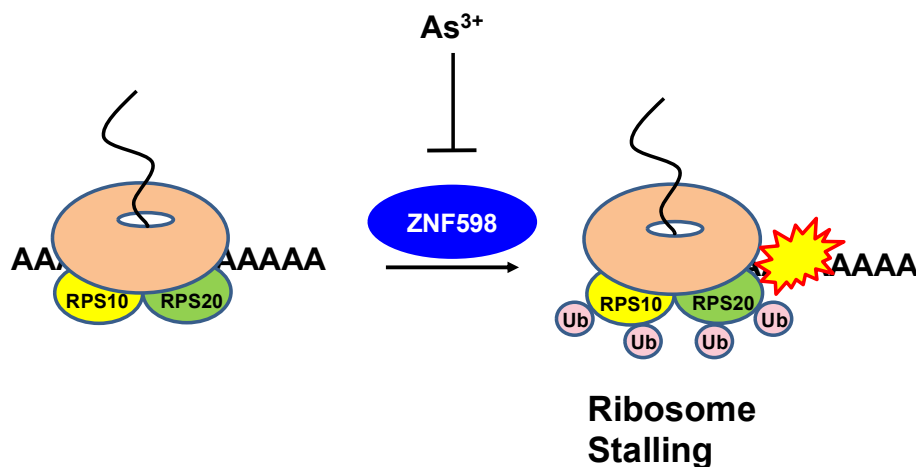


**Figure 2.6.**  $As^{3+}$  induces ribosome stalling through inhibiting ZNF598.  $As^{3+}$  binds to specific cysteine residues within zinc finger motif of ZNF598 E3 ubiquitin ligase, which subsequently inhibits its ubiquitination activity on specific lysine sites on RPS10 and RPS20, thereby diminishing the resolution of ribosome stalling.

Arsenic-induced malfunctioning of ribosomal stalling and its subsequent impairment of RQC can increase the quantity of defective non-stop mRNA and aberrant truncated nascent polypeptides that might have defective folding, function, and subcellular location (Fig. 2.6.).<sup>13,32</sup> Accumulation of the truncated mis-localized non-stop proteins can induce protein misfolding through energetically favorable oligomerization into non-native conformational states and ultimately result in proteinopathies including neurodegenerative disorders.<sup>8,12,28,33</sup> Arsenic was found to cause protein misfolding and aggregation in yeast and humans,<sup>2,11,34</sup> and arsenite is thought to affect the folding of nascent proteins during translation, though the exact underlying mechanisms were not known.<sup>11</sup> Our findings provided mechanistic insights into the arsenite-induced perturbation of proteostasis, i.e. through disruption of the ZNF598-mediated RQC pathway.

Apart from ZNF598, listerin E3 ubiquitin ligase, which is also involved in RQC through polyubiquitination of stalled truncated nascent polypeptides,<sup>13,30,32</sup> is also a RING finger protein. It can be envisaged that the listerin-mediated RQC pathway may also be impacted by the interaction between listerin and As<sup>3+</sup>. Hence, arsenic exposure may perturb the RQC pathway by not only disrupting the capability to properly stall the ribosomes while encountering poly-A sequences, but also compromising the degradation of the aberrant truncated nascent polypeptides. The latter is the subject of interest for future investigation.

### **Implications in mechanisms of toxicity of other metal ions**

In addition to arsenic, other metals and metalloids may also impair RING fingers by substituting Zn<sup>2+</sup> and disrupting the conformations of the RING finger proteins due to their high binding affinities with cysteine sulfhydryl groups. Metal ions (e.g. cadmium, mercury, chromium, manganese) and some metalloids (e.g. selenium) are known to favor sulfur as their ligands, which is also the preferred ligand for zinc in zinc finger proteins.<sup>11</sup> For example, cadmium and nickel are believed to interfere with estrogen receptor (ER) signaling by binding to ER which can bind to

DNA for transcriptional regulation via the N-terminal DNA-binding zinc finger regions.<sup>35,36</sup> Similarly, Cd<sup>2+</sup>, Ni<sup>2+</sup> and Pb<sup>2+</sup> were shown to displace Zn<sup>2+</sup> ions from the zinc finger domains in transcription factor IIIA by their higher binding affinities toward its zinc fingers.<sup>37,38</sup> Similar to arsenic, cadmium was found to confer protein misfolding and aggregation.<sup>39-41</sup> Therefore, due to the metal binding properties of zinc fingers, it can be envisaged that RING finger E3 ubiquitin ligases, including ZNF598, may also be susceptible to inhibition by a range of environmentally relevant metal ions; thus, exposure to these metal ions may also lead to proteostatic stress through a similar mechanism as As<sup>3+</sup>.

### **Implications in chronic arsenic exposure and risk assessment for arsenic-elicited human diseases**

Arsenic pollution, which impacts over 200 million people worldwide via contaminated drinking water and diet, is a serious global public health issue.<sup>4</sup> Chronic arsenic exposure has been associated with many human diseases, ranging from cancer, type II diabetes to neurodegenerative disorders, including Alzheimer's and Parkinson's diseases.<sup>2</sup> Most of these documented human diseases induced by arsenic exposure, especially neurodegenerative disorders, could be elicited by protein misfolding and aggregation.<sup>28,42</sup> Based on our understanding about adverse health consequences forged by arsenic-induced proteostatic stress, we should seriously assess and mitigate the risk of chronic arsenic exposure to safeguard public health. This can be achieved by stricter policy regulation on the environmental level of arsenic and improved worldwide public education to raise awareness for arsenic remediation of contaminated drinking water.<sup>43</sup>

## References:

1. Cholanians, A.B., Phan, A.V., Ditzel, E.J., Camenisch, T.D., Lau, S.S., and Monks, T.J. (2016) Arsenic induces accumulation of  $\alpha$ -synuclein: Implications for synucleinopathies and neurodegeneration. *Toxicol. Sci.* 153, 271-281.
2. Chin-Chan, M., Navarro-Yepes, J., and Quintanilla-Vega, B. (2015) Environmental pollutants as risk factors for neurodegenerative disorders: Alzheimer and Parkinson diseases. *Front. Cell. Neurosci.* 9, 1-22.
3. Chen, S.J., Zhou, G.B., Zhang, X.W., Mao, J.H., De Thé, H., and Chen, Z. (2011) From an old remedy to a magic bullet: Molecular mechanisms underlying the therapeutic effects of arsenic in fighting leukemia. *Blood* 117, 6425-6437.
4. Ravenscroft, P., Brammer, H., and Richards, K. *Arsenic Pollution: A Global Synthesis*. Wiley-Blackwell, UK; 2009.
5. Chen, P., Miah, M.R., and Aschner, M. (2016) Metals and Neurodegeneration. *F1000 Res.* 5, 366.
6. Rossman, T.G., Uddin, A.N., and Burns, F.J. (2004) Evidence that arsenite acts as a cocarcinogen in skin cancer. *Toxicol. Appl. Pharmacol.* 198, 394-404.
7. Islam, M.R., Khan, I., Hassan, S.M.N., McEvoy, M., D'Este, C., Attia, J., Peel, R., Sultana, M., Akter, S., and Milton, A.H. (2012) Association between type 2 diabetes and chronic arsenic exposure in drinking water: A cross sectional study in Bangladesh. *Environ. Heal.: A Glob Access Sci Source* 11, 38.
8. Chaudhuri, T.K., and Paul, S. (2006) Protein-misfolding diseases and chaperone-based therapeutic approaches. *FEBS J.* 273, 1331-1349.
9. Dodson, M., de la Vega, M.R., Harder, B., Castro-Portuguez, R., Rodrigues, S.D., Wong, P.K., Chapman, E., and Zhang, D.D. (2018) Low-level arsenic causes proteotoxic stress and not oxidative stress. *Toxicol. Appl. Pharmacol.* 341, 106-113.
10. Escudero-Lourdes, C. (2016) Toxicity mechanisms of arsenic that are shared with neurodegenerative diseases and cognitive impairment: Role of oxidative stress and inflammatory responses. *Neurotoxicology* 53, 223-235.
11. Tamás, M.J., Sharma, S.K., Ibstedt, S., Jacobson, T., and Christen, P. (2014) Heavy metals and metalloids as a cause for protein misfolding and aggregation. *Biomolecules* 4, 252-267.
12. Valastyan, J.S., and Lindquist, S. (2014) Mechanisms of protein-folding diseases at a glance. *Dis. Model Mech.* 7, 9-14.
13. Brandman, O., and Hegde, R.S. (2016) Ribosome-associated protein quality control. *Nat. Struct. Mol. Biol.* 23, 7-15.

14. Karamyshev, A.L., and Karamysheva, Z.N. (2018) Lost in translation: Ribosome-associated mRNA and protein quality controls. *Front. Genet.* *9*, 1-13.
15. Juszkievicz, S., and Hegde, R.S. (2017) Initiation of Quality Control during Poly(A) Translation Requires Site-Specific Ribosome Ubiquitination. *Mol. Cell* *65*, 743-750.
16. Sundaramoorthy, E., Leonard, M., Mak, R., Liao, J., Fulzele, A., and Bennett, E.J. (2017) ZNF598 and RACK1 Regulate Mammalian Ribosome-Associated Quality Control Function by Mediating Regulatory 40S Ribosomal Ubiquitylation. *Mol. Cell* *65*, 751-760.
17. Zhou, X., Sun, X., Cooper, K.L., Wang, F., Liu, K.J., and Hudson, L.G. (2011) Arsenite interacts selectively with zinc finger proteins containing C3H1 or C4 motifs. *J. Biol. Chem.* *286*, 22855-22863.
18. Tam, L.M., Jiang, J., Wang, P., Li L., Miao, W., Dong, X., and Wang, Y. (2017) Arsenite binds to the zinc finger motif of TIP60 histone acetyltransferase and induces its degradation via the 26S proteasome. *Chem. Res. Toxicol.* *30*, 1685-1693.
19. Jiang, J., Tam, L.M., Wang, P., and Wang, Y. (2018) Arsenite Targets the RING Finger Domain of Rbx1 E3 Ubiquitin Ligase to Inhibit Proteasome-mediated Degradation of Nrf2. *Chem. Res. Toxicol.* *31*, 380-387.
20. Zhang, X-W., Yan, X-J., Zhou, Z-R., Yang, F-F., Wu, Z-Y., Sun, H-B., Liang, W-X., Song, A-X., Lallemand-Breitenbach, V., Jeanne, M., Zhang, Q-Y., Yang, H-Y., Huang, Q-H., Zhou, G-B., Tong, J-H., Zhang, Y., Wu, J-H., Hu, H-Y., de The, H., Chen, S-J., and Chen, Z. (2010) Arsenic Trioxide Controls the Fate of the PML-RAR $\alpha$  Oncoprotein by Directly Binding PML. *Science* *328*, 240-243.
21. Zhang, F., Paramasivam, M., Cai, Q., Dai, X., Wang, P., Lin, K., Song, J., Seidman, M.M., and Wang, Y. (2014) Arsenite Binds to the RING Finger Domains of RNF20-RNF40 Histone E3 Ubiquitin Ligase and Inhibits DNA Double-Strand Break Repair. *J. Am. Chem. Soc.* *136*, 12884-12887.
22. Tollenaere, M.A.X., Tiedje, C., Rasmussen, S., Nielsen, J.C., Vind, A.C., Blasius, M., Bath, T.S., Mailand, N., Olsen, J.V., Gaestel, M., and Bekker-Jensen, S. (2019) GIGYF1/2-Driven Cooperation between ZNF598 and TTP in Posttranscriptional Regulation of Inflammatory Signaling. *Cell Rep.* *26*, 3511-3521.
23. Jiang, J., Bellani, M., Li, L., Wang, P., Seidman, M.M., and Wang, Y. (2017) Arsenite Binds to the RING Finger Domain of FANCL E3 Ubiquitin Ligase and Inhibits DNA Interstrand Cross-link Repair. *ACS Chem. Biol.* *12*, 1858-1866.
24. Zhang, F., Xiao, Y., and Wang, Y. (2017) SILAC-Based Quantitative Proteomic Analysis Unveils Arsenite-Induced Perturbation of Multiple Pathways in Human Skin Fibroblast Cells. *Chem. Res. Toxicol.* *30*, 1006-1014.

25. Shen, S., Li, X., Cullen, W.R., Weinfeld, M., and Le, X.C. (2013) Arsenic Binding to Proteins. *Chem. Rev.* 113, 1-48.
26. Liu, S., Jiang, J., Li, L., Amato, N.J., Wang, Z., and Wang, Y. (2015) Arsenite Targets the Zinc Finger Domains of Tet Proteins and Inhibits Tet-Mediated Oxidation of 5-Methylcytosine. *Environ. Sci. Technol.* 49, 11923-11931.
27. Garzia, A., Jafarnejad, S.M., Meyer, C., Chapat, C., Gogakos, T., Morozov, P., Amiri, M., Shapiro, M., Molina, H., Tuschl, T., and Sonenberg, N. (2017) The E3 ubiquitin ligase and RNA-binding protein ZNF598 orchestrates ribosome quality control of premature polyadenylated mRNAs. *Nat. Commun.* 8, 16056.
28. Sweeney, P., Park, H., Baumann, M., Dunlop, J., Frydman, J., Kopito, R., McCampbell, A., Leblanc, G., Venkateswaran, A., Nurmi, A., and Hodgson, R. (2017) Protein misfolding in neurodegenerative diseases: Implications and strategies. *Transl. Neurodegener.* 6, 6.
29. Welch, W.J. (2004) Role of quality control pathways in human diseases involving protein misfolding. *Semin. Cell. Dev. Biol.* 15, 31-38.
30. Samant, R.S., Livingston, C.M., Sontag, E.M., and Frydman, J. (2018) Distinct proteostasis circuits cooperate in nuclear and cytoplasmic protein quality control. *Nature* 563, 407-411.
31. Joazeiro, C.A.P. (2017) Ribosomal Stalling During Translation: Providing Substrates for Ribosome-Associated Protein Quality Control. *Annu. Rev. Cell. Dev. Biol.* 33, 111315-125249.
32. Bengtson, M.H., and Joazeiro, C.A.P. (2010) Role of a ribosome-associated E3 ubiquitin ligase in protein quality control. *Nature* 467, 470-473.
33. Kikis, E.A., Gidalevitz, T., and Morimoto, R.I. (2010) Protein homeostasis in models of aging and age-related conformational disease. *Adv. Exp. Med. Biol.* 694, 138-159.
34. Jacobson, T., Navarrete, C., Sharma, S.K., Sideri, T.C., Ibstedt, S., Priya, S., Grant, C.M., Christen, P., Goloubinoff, P., and Tamás, M.J. (2012) Arsenite interferes with protein folding and triggers formation of protein aggregates in yeast. *J. Cell Sci.* 125, 5073-5083.
35. Green, S., Kumar, V., Theulaz, I., Wahli, W., and Chambon, P. (1988) The N-terminal DNA-binding 'zinc finger' of the oestrogen and glucocorticoid receptors determines target gene specificity. *EMBO J.* 7, 3037-3044.
36. Aquino, N.B., Sevigny, M.B., Sabangan, J., and Louie, M.C. (2012) Role of Cadmium and Nickel in Estrogen Receptor Signaling and Breast Cancer: Metalloestrogens or Not? *J. Env. Sci. Heal. Env. Carcinog. Ecotoxicol. Rev.* 30, 189-224.
37. Petering, D.H., Huang, M., Moteki, S., and Shaw, III C.F. (2000) Cadmium and lead interactions with transcription factor IIIA from *Xenopus laevis*: a model for zinc finger protein reactions with toxic metal ions and metallothionein. *Mar. Environ. Res.* 50, 89-92.

38. Iuchi, S., and Kuldell, N. *Zinc Finger Proteins: From Atomic to Cellular Function*. New York: Kluwer Academic/Plenum Publishers; 2005.
39. Hartwig, A. (2001) Zinc Finger Proteins as Potential Targets for Toxic Metal Ions: Differential Effects on Structure and Function. *Antioxid. Redox Signal.* 3, 625-634.
40. Jacobson, T., Priya, S., Sharma, S.K., Andersson, S., Jakobsson, S., Tanghe, R., Ashouri, A., Rauch, S., Goloubinoff, P., Christen, P., and Tamás, M.J. (2017) Cadmium Causes Misfolding and Aggregation of Cytosolic Proteins in Yeast. *Mol. Cell. Biol.* 37, 1-15.
41. Tamás, M.J., Fauvet, B., Christen, P., and Goloubinoff, P. (2018) Misfolding and aggregation of nascent proteins: a novel mode of toxic cadmium action in vivo. *Curr. Genet.* 64, 177-181.
42. Kurtishi, A., Rosen, B., Patil, K.S., Alves, G.W., and Møller, S.G. (2019) Cellular Proteostasis in Neurodegeneration. *Mol. Neurobiol.* 56, 3676-3689.
43. Malik, A.H., Khan, Z.M., Mahmood, Q., Nasreen, S., and Bhatti, Z.A. (2009) Perspectives of low cost arsenic remediation of drinking water in Pakistan and other countries. *J. Hazard. Mater.* 168, 1-12.

## **Chapter 3**

# **Arsenite Binds to the Zinc Finger Motif of TIP60 Histone Acetyltransferase and Induces its Degradation via the 26S Proteasome**



## Introduction

Being the 20<sup>th</sup> most abundant element in the Earth's crust, arsenic exists in inorganic forms as arsenate and arsenite, as well as in organic forms.<sup>1</sup> Arsenite, the main inorganic form of arsenic present in the environment, especially in ground water, is generally more toxic to living organisms than the organic form. Due to various natural processes such as weathering and widespread industrial use, exposure to arsenic species has become a serious public health concern, as indicated by arsenic being on the top of the Priority List of Hazardous Substances in the Agency for Toxic Substances and Disease Registry.<sup>2</sup> In view of the tremendous environmental impact and toxic potential of arsenic, the World Health Organization and the US Environmental Protection Agency have recommended a threshold concentration for arsenic in drinking water as 10 ppb.<sup>3,4</sup> Nonetheless, approximately 150 million people in more than 70 countries are exposed to excessive amounts of arsenic species through contaminated drinking water and diet.<sup>5</sup>

Over the last few decades, numerous epidemiological, cellular, and animal studies have provided a large body of evidence to support that chronic exposure to arsenic in drinking water is strongly associated with the increased incidence of bladder, lung, liver, skin and kidney tumors.<sup>6,7</sup> Furthermore, arsenic is found to elicit other adverse human health effects including neurotoxicity, the endemic "blackfoot disease", cardiovascular disease and childhood neurodevelopmental defects.<sup>8</sup> However, the mechanisms through which arsenic exposure leads to carcinogenesis remain incompletely understood.

The binding between  $\text{As}^{3+}$  and protein cysteine sulfhydryl group is thought to play an important role in arsenic toxicity and carcinogenicity.<sup>2,9</sup> In this vein,  $\text{As}^{3+}$  was found to selectively bind to the C3H- and C4- types of zinc finger motifs.<sup>10</sup> In addition, our recently published data indicated that arsenite could bind to RNF20-RNF40 and FANCL E3 ubiquitin ligases as well as ten-eleven translocation (Tet) family proteins through their RING finger (C3HC4), RING-like PHD finger and

C3H-type zinc finger, respectively.<sup>11-13</sup> Along this line, apart from the carcinogenic effect, As<sup>3+</sup> in the form of arsenic trioxide has been approved by the Food and Drug Administration for the treatment of acute promyelocytic leukemia.<sup>14</sup> In this context, As<sup>3+</sup> was found to bind to the RING finger domain of PML in the oncogenic PML-RAR $\alpha$  fusion protein, which enhanced the proteasomal degradation of the fusion protein.<sup>15</sup>

Recently, it was argued that arsenic may induce carcinogenesis through perturbation of epigenetic pathways as global loss of acetylation and trimethylation of histone H4 is commonly found in human tumors associated with chemical exposure.<sup>7</sup> In this respect, acetylation of lysine 16 in histone H4 (H4K16Ac) is crucial for promoting the access of DNA repair enzymes to damaged DNA.<sup>16-18</sup> Although diminished H4K16Ac was observed in UTOsa human bladder epithelial cells upon chronic arsenite exposure, the molecular mechanism contributing to reduced H4K16 acetylation remains unclear.<sup>19,20</sup> Additionally, previous studies revealed that many crucial enzymes involved in the deposition of histone acetylation marks harbor a zinc finger motif that is essential for their enzymatic activities.<sup>21</sup> TIP60, a member of the MYST family histone acetyltransferases, which also contain zinc finger motifs, was found to play an important role in H4K16 acetylation.<sup>22</sup> On the basis of these previous findings, we reason that As<sup>3+</sup> may interact with the zinc finger motif of TIP60 histone acetyltransferase, thereby altering its conformation, stability and activity, and resulting in H4K16 hypoacetylation. To test the above hypothesis, we examined the interaction between As<sup>3+</sup> and the peptide derived from the zinc finger motif of human TIP60 protein *in vitro* and in human cells. We also demonstrated that arsenite exposure led to diminished levels of TIP60 protein via the ubiquitin-proteasome pathway. Finally, we found that the arsenite-induced decrease in H4K16Ac in cultured human cells depended, in part, on TIP60. Hence, the results from this study uncovered a novel molecular mechanism underlying the arsenic-induced

perturbation in epigenetic signaling, thereby broadening our understanding about the arsenic-induced carcinogenicity.

## **Experimental Procedures**

### **Cell Culture**

HEK293T cells (ATCC) were cultured in Dulbecco's modified Eagle's medium (DMEM, Thermo Fisher Scientific). All culture media except those used for transfection were supplemented with 10% fetal bovine serum (FBS, Thermo Fisher Scientific) and 1% penicillin streptomycin solution (Millipore). The cells were maintained in a humidified atmosphere with 5% CO<sub>2</sub> at 37°C, with medium renewal once in every 2 days depending on cell density. For plasmid transfection, cells were cultured in the same media as mentioned above except that no penicillin streptomycin solution was added.

### ***In vitro* arsenite binding assay**

The zinc finger peptide of TIP60 (with amino acid residues 261-286 a.a., i.e. LYLCEFLKYGRSLKCLQRHLTKCDL) was obtained from ChinaPeptides (Shanghai, China), purified by HPLC and used for *in vitro* binding assays. Arsenite binding to the zinc finger peptide was monitored by MALDI-TOF mass spectrometry in the linear, positive-ion mode on a Voyager DE STR instrument (Applied Biosystems, Framingham, MA). Peptides were dissolved at a concentration of 1 mg/ml in sterilized deionized water and diluted to a concentration of 100 μM in a buffer containing 20 mM Tris-HCl (pH 6.8) and 1 mM dithiothreitol. Aliquots of 100 μM peptides were incubated with 200 μM NaAsO<sub>2</sub> at room temperature for 1 hr. The resultant solution was diluted by 100 folds and mixed with an equal volume of 2,5-dihydroxybenzoic acid matrix solution before spotting onto a sample plate. The mass spectrometer was equipped with a pulsed nitrogen laser operating at 337 nm with a pulse duration of 3 ns. The acceleration voltage, grid voltage, and

delayed extraction time were set at 20 kV, 65%, and 190 ns, respectively. Each mass spectrum was acquired from an average of signal from 100 laser shots.

### **Plasmid construction**

The expression plasmids for TIP60 were pcDNA3.1-HA-TIP60 which is kindly provided from Dr. Yingli Sun<sup>23</sup> and pRK7-TIP60-3Flag. The expression plasmids of HA-TIP60 harboring the C263A, or C266A, or C283A mutation were obtained by site-directed mutagenesis, and the successful construction for the mutated plasmids was verified by sequencing analysis.

### **Streptavidin agarose affinity assay and Western blot**

Biotin-As was synthesized previously.<sup>11</sup> In general, HEK293T cells were transfected with wild-type or mutant form of HA-TIP60. At 24 h after the transfection, the cells were exposed with 5  $\mu$ M biotin-As for 2 h and lysed in CelLytic<sup>TM</sup> M lysis buffer supplemented with a protease inhibitor cocktail (Sigma Aldrich). The cell lysates were incubated with high-capacity streptavidin agarose beads for overnight. Streptavidin agarose beads were subsequently washed with 1 $\times$  PBST (0.1%), resuspended in SDS-PAGE loading buffer and separated by SDS-PAGE.

After SDS-PAGE separation, proteins were transferred to a nitrocellulose membrane using a transfer buffer containing Tris base, methanol, glycine and water. The membranes were blocked with 5% BSA in PBST buffer, which contained PBS and 0.1% (v/v) Tween-20 (pH 7.5), for 2 hrs and incubated with rabbit anti-HA antibody at 4°C overnight (1:10000 dilution, Sigma Aldrich). The membranes were washed with fresh PBST buffer at room temperature for 6 times (5-10 min each). After washing, the membranes were incubated with rabbit secondary antibody at room temperature for 1 h. The membranes were subsequently washed with PBST for 6 times. The secondary antibody was detected by using Amersham<sup>TM</sup> ECL<sup>TM</sup> Select Western blotting Detection Kit Reagent (GE Healthcare) and visualized with Hyblot CL autoradiography film (Denville Scientific, Inc., Metuchen, NJ). Similar experiments were also conducted by pretreatment of cells

with 10  $\mu\text{M}$   $\text{ZnCl}_2$ , PAPA0 or  $\text{NaAsO}_2$  for 1 h prior to the biotin-As treatment. Similarly, the pull-down experiments for mutant HA-TIP60 were conducted with the same biotin-As pull-down assay except that the cells were transfected with plasmids for expressing HA-TIP60 with specific Cys $\rightarrow$ Ala mutations.

For monitoring the effect of arsenite and/or MG132 on the protein level of HA-TIP60, HEK293T cells were transfected with HA-tagged TIP60 plasmids for 24 h, and exposed with several different concentrations of  $\text{NaAsO}_2$  (i.e. 0, 1, 2, and 5  $\mu\text{M}$ ) with or without co-treatment with 4  $\mu\text{M}$  MG132 (Sigma Aldrich) for another 24 h, followed by cell harvesting, protein extraction, and Western blot analysis for HA-TIP60, as described above.

#### **Histone acetyltransferase assay**

HEK293T cells were first transfected with FLAG-tagged TIP60 plasmid constructs for 24 h, followed by cell harvesting and protein extraction as described above. The FLAG-TIP60 protein was subsequently precipitated from protein lysates and quantified with Bradford assay. After that, 50  $\mu\text{g}$  protein lysate in 800  $\mu\text{l}$  lysis buffer including protease inhibitor was incubated overnight with anti-FLAG M2 affinity gel (Sigma Aldrich), followed by washing the beads with HAT buffer. Next, the beads with bound FLAG-TIP60 were suspended in a HAT reaction mixture which comprised of 0.5  $\mu\text{g}$  FLAG-TIP60, 3  $\mu\text{g}$  histone H4 and 100  $\mu\text{M}$  acetyl-coenzyme A in 60  $\mu\text{l}$  HAT buffer containing 50 mM Tris HCl, 0.1 mM EDTA, 1 mM DTT and 10% glycerol (pH 8.0), with or without 5  $\mu\text{M}$   $\text{NaAsO}_2$ . The HAT reaction was performed by incubating the reaction mixture at 37°C. After a 24-h incubation, the reaction mixture was analyzed by Western blot as described above, using rabbit anti-H4K16Ac (1:50000 dilution, Millipore) and rabbit anti-histone H4 antibodies (1:5000 dilution, Cell Signaling Technology).

## **Histone Extraction**

HEK293T cells were exposed to 0, 2 and 5  $\mu\text{M}$   $\text{NaAsO}_2$  for 24 h, and then harvested. The cell pellets were washed with  $1\times$  PBS, resuspended in Triton X-100 sucrose buffer containing 0.25 M sucrose, 0.01 M  $\text{MgCl}_2$ , 0.5 mM PMSF, 0.05 M Tris-HCl (pH 7.4) and 0.5% v/v Triton X-100. The resulting pellet was incubated overnight, with vortexing, in Triton X-100 sucrose buffer supplemented with protease inhibitor cocktail. The suspension was subsequently centrifuged, and the pellet was washed with the above-described sucrose buffer without Triton X-100. The histone proteins in the cell pellet were then extracted using 0.4 N sulfuric acid with vortexing at  $4^\circ\text{C}$  for 4 h. The supernatant was subsequently collected and mixed with 10 volumes of cold acetone to precipitate histone proteins from the mixture at  $-20^\circ\text{C}$  overnight. Finally, the pellet of the precipitate was washed with acetone, dried by Speedvac and redissolved in water for subsequent Western blot analysis, using rabbit anti-H4K16Ac and rabbit anti-histone H4 antibodies as described above. The same experiment was conducted using *TIP60*<sup>-/-</sup> HEK293T cells which were generated from CRISPR-Cas9 knockout technology, as described previously.<sup>24</sup>

## **Statistical Analysis**

The statistic of all the experiments are performed by using the average of the values from at least three independent experiments. The *p* values used for all data analysis were calculated using unpaired two-tailed student's *t*-test: \*,  $p < 0.05$ ; \*\*,  $p < 0.01$ ; \*\*\*,  $p < 0.001$ .

## **Results**

### **Arsenite exposure leads to diminished level of TIP60 protein, but not hMOF protein**

Jo *et al.*<sup>19</sup> showed that arsenite exposure could lead to H4K16 hypoacetylation in bladder epithelial cells. To explore the role of TIP60 in arsenite-induced alteration in H4K16Ac, we first asked whether arsenite exposure could alter the protein level of the histone acetyltransferase. In

this vein, it is worth noting that we attempted, but failed to detect endogenous TIP60 using Western blot analysis with TIP60 antibody from several commercial sources, which was also noted by others.<sup>25</sup> We were also not able to detect endogenous TIP60 by using a proteomic approach, where we fractionated the whole cell lysate of HEK293T cells using SDS-PAGE, cut the gel band from the region where TIP60 migrates, digested the proteins in-gel with trypsin, and subjected the digestion mixture to LC-MS/MS analysis on a Q Exactive Plus quadrupole-Orbitrap mass spectrometer. The failure in detecting endogenous TIP60 is likely attributed to the relatively low level of expression of this protein in HEK293T cells. Thus, we treated HEK293T cells, which express HA-tagged TIP60, with increasing concentrations (i.e., 0, 1, 2, and 5  $\mu\text{M}$ ) of  $\text{NaAsO}_2$  for 24 h and assessed the levels of HA-TIP60 by Western blot analysis. Our results revealed a dose-dependent decrease in the TIP60 protein level (Fig. 3.1A and 3.1B). In contrast, similar Western blot analysis of hMOF, the other member of MYST family of histone acetyltransferase, revealed no significant alteration in the level of this protein in cells upon treatment with  $\text{As}^{3+}$  (Fig. 3.1C and 3.1D).

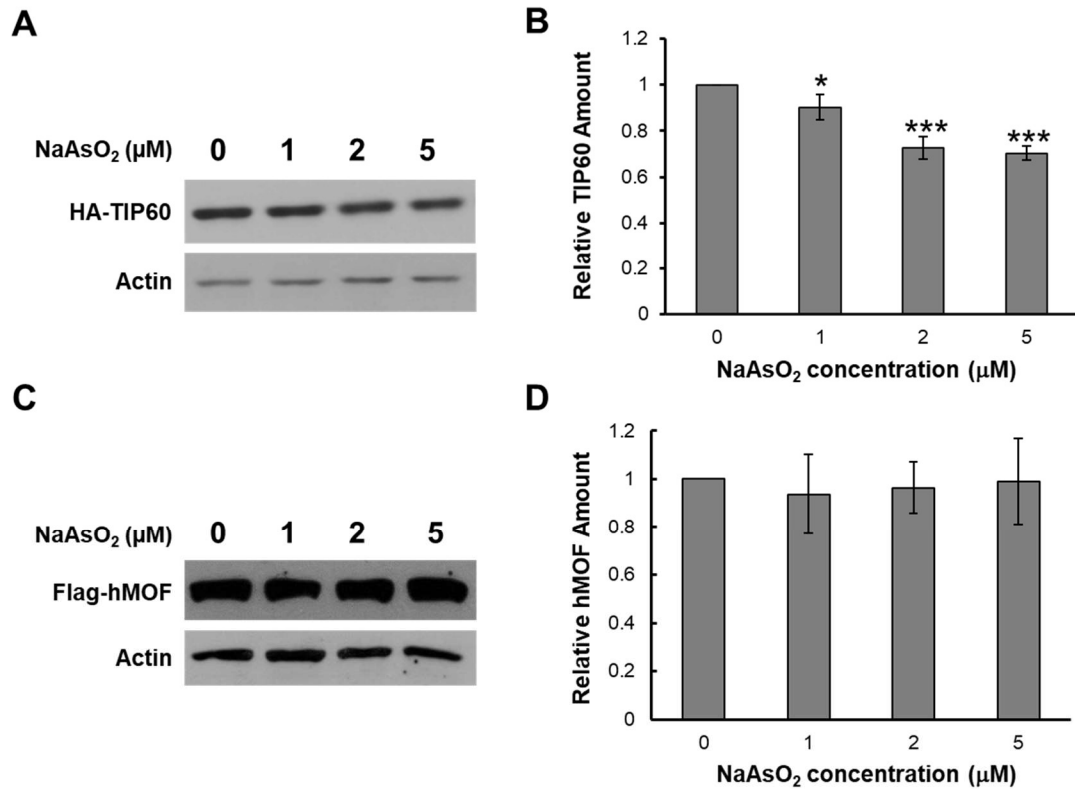


**Figure 3.1.** Arsenite treatment results in a dose-dependent decrease in TIP60, but not hMOF protein. Western blot images showing the effect of treatment with different doses of arsenite (0, 1, 2, and 5 μM) on the protein level of HA-TIP60 (A) and hMOF (C). The quantification results of the relative level of TIP60 (B) and hMOF (D) proteins following exposure to different doses of NaAsO<sub>2</sub> (n=3). Error bars represent standard deviations. The *p* values were calculated using unpaired two-tailed student's t-test, and the asterisks designate significant differences between arsenite-treated samples and untreated control (\*, *p* < 0.05; \*\*, *p* < 0.01; \*\*\*, *p* < 0.001).

**As<sup>3+</sup> binds to the cysteine residues in the zinc finger motif of TIP60 proteins *in vitro* and in cells**

To explore the mechanism through which As<sup>3+</sup> induces the decrease in TIP60 protein level, we examined whether NaAsO<sub>2</sub> could bind directly to the zinc finger motif of the protein by employing a mass spectrometry (MS)-based assay. We employed a synthetic peptide derived from the zinc finger motif of human TIP60, which carries a.a. 261-286. Positive-ion matrix-assisted laser



desorption ionization-time-of-flight mass spectrometry (MALDI-TOF MS) revealed the  $[M+H]^+$  ion of the apo-peptide at  $m/z$  3146.6 (Fig. 3.2A). Incubation of the apo-peptide with  $As^{3+}$  leads to a +72 Da mass shift (Fig. 3.2B), which emanates from the binding of the peptide with one  $As^{3+}$  after the release of three protons from the three Cys residues in the peptide. In accordance with previous findings about the interaction of  $As^{3+}$  with other C3H-type zinc finger proteins,<sup>10,13</sup> the MS result showed that arsenite could bind to the peptide derived from the  $Zn^{2+}$ -binding site of TIP60.

We also assessed how dithiothreitol (DTT) modulates the interaction between  $As^{3+}$  and the apo-peptide of TIP60 by conducting the MALDI-TOF MS experiments with the use of different molar ratios of  $As^{3+}/DTT$  (i.e., 1:1, 1:5 and 1:25). Our results showed that the presence of an equal concentration of DTT did not affect the binding between  $As^{3+}$  and zinc finger peptide (Fig. 3.S1A). Likewise, addition of five-fold excess of DTT ( $As^{3+}/DTT=1:5$ ) did not abolish the interaction, though the relative intensity of the peak for arsenite-bound peptide was weakened (Fig. 3.S1B). The presence of DTT in 25-fold excess, however, led to the loss of signal for the  $As^{3+}$ -bound peptide (Fig. 3.S1C). Thus,  $As^{3+}$  binds more strongly with the C3H-type zinc finger peptide than DTT, which is not surprising considering that these binding involve the formation of three and two As-S bonds, respectively.

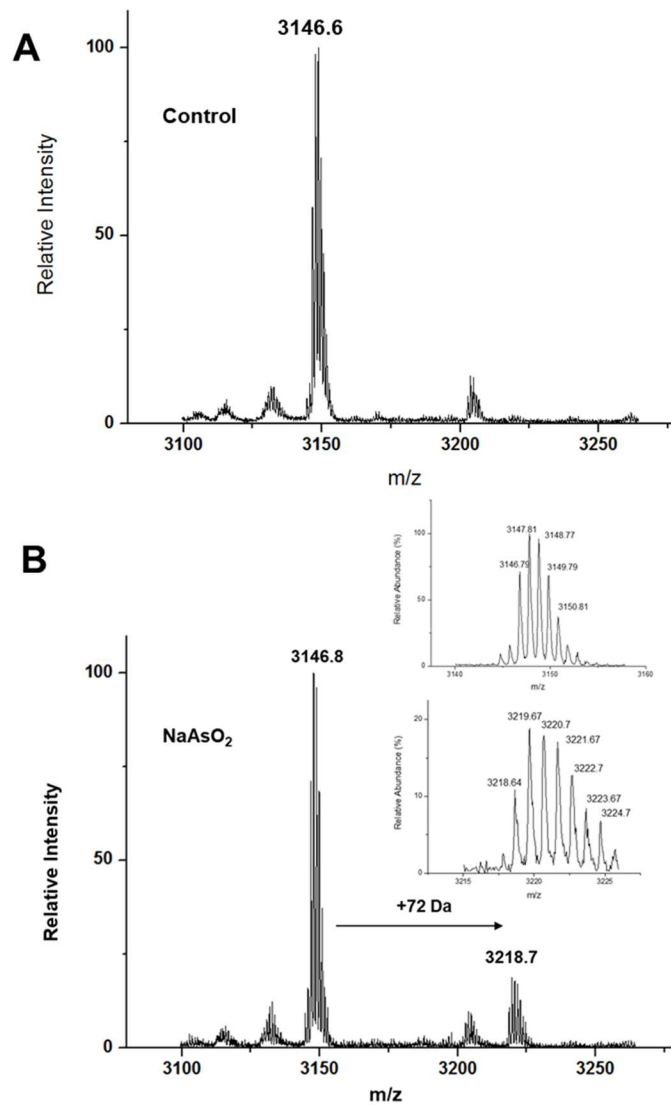


**Figure 3.2.** *In vitro* binding between arsenite and zinc finger peptide of TIP60. Shown is the MALDI-TOF MS results for monitoring the zinc finger peptide of TIP60 (A) and its interaction with As<sup>3+</sup> (B). The insets show the isotopic peaks of both apo-peptide of TIP60 and apo-peptide bound to arsenite.

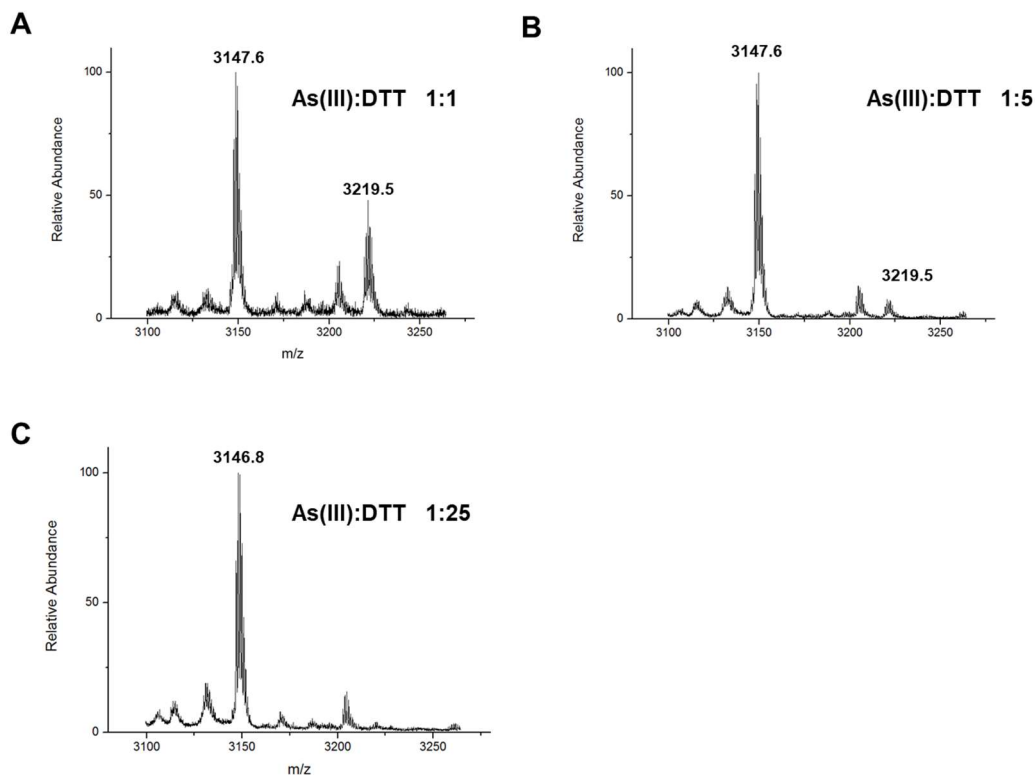


**Figure 3.S1.** The effects of DTT on the interaction between As<sup>3+</sup> and the zinc finger peptide of TIP60. Increasing concentration of DTT can affect the relative intensity of peak corresponding to As<sup>3+</sup>-bound peptide (at *m/z* 3219.5), as indicated in MALDI MS measurements when molar ratios of As<sup>3+</sup>/DTT were 1:1 (A), 1:5 (B) and 1:25 (C).

We next asked whether the binding of arsenite with TIP60 occurs in mammalian cells. To this end, we treated HEK293T cells with a *p*-aminophenylarsenoxide (PAPAO)-conjugated biotin probe (Fig. 3.3A), and assessed its interaction with ectopically expressed HA-TIP60 by streptavidin agarose affinity assay.<sup>11</sup> The Western blot result revealed that the biotin-As probe could facilitate the pull-down of HA-TIP60 protein in human cells, whereas we failed to pull down HA-TIP60 in the control experiment without the use of the biotin-As probe (Fig. 3.3B). This result suggested that As<sup>3+</sup> could bind to TIP60 in human cells. We next pretreated HA-TIP60-expressing HEK293T cells individually with 10  $\mu$ M ZnCl<sub>2</sub>, PAPAO and NaAsO<sub>2</sub>, and assessed the interaction between As<sup>3+</sup> and HA-TIP60 by conducting the same pull-down assay. The result showed that pre-treatment with

NaAsO<sub>2</sub> or PAPAO could suppress markedly the pull-down of HA-TIP60, though a slight decrease in pull-down was also observed for pretreatment with Zn<sup>2+</sup> (Fig. 3.3C,D). This result suggests that As<sup>3+</sup> can displace Zn<sup>2+</sup> bound to the zinc finger motifs. To further substantiate the involvement of zinc finger cysteine residues of TIP60 in its binding toward As<sup>3+</sup>, we performed site-directed mutagenesis to substitute individually the three Cys residues with Ala (i.e. C263A, C266A, and C283A) in the zinc finger motif of HA-TIP60, and conducted the same pull-down assays. Our results showed that all three mutant forms of HA-TIP60 exhibited significantly attenuated interaction with the biotin-As probe (Fig. 3.3E,F), indicating that the biotin-As probe interacts with the cysteine residues in the zinc finger motif of the TIP60.

It is worth noting that the use of the biotin-As probe may not fully recapitulate the interaction between arsenite and the zinc finger motif of TIP60 because As<sup>3+</sup> in the probe and arsenite can bind two and three cysteine residues, respectively. Hence, the binding affinity of biotin-As toward the zinc finger of TIP60 protein is expected to be weaker than that of arsenite. The observation that TIP60 can interact with the biotin-As probe in cells strongly suggests that the protein can also interact with arsenite in cells.

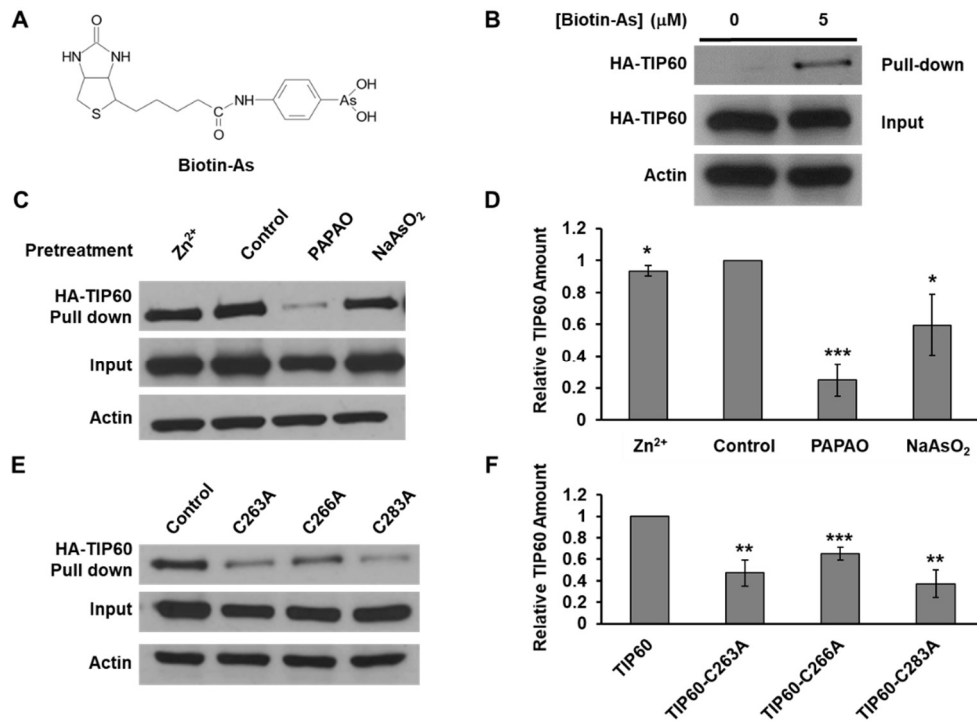


**Figure 3.3.** Streptavidin agarose affinity pull-down assay using biotin-As as a probe reveals the binding between  $\text{As}^{3+}$  and the C3H-type zinc finger domain of TIP60. (A) The structure of the biotin-As probe. (B) Treatment of HEK293T cells expressing HA-TIP60 with 5  $\mu\text{M}$  biotin-As probe could pull down HA-TIP60 by using streptavidin agarose. (C). Pre-treatment of cells with 10  $\mu\text{M}$   $\text{ZnCl}_2$ ,  $\text{NaAsO}_2$ , or PAPA0 (i.e. *p*-aminophenylarsenoxide) for 2 hrs attenuates the binding between biotin-As and TIP60. (D) Relative protein level of TIP60 pulled down by streptavidin agarose using biotin-As probe upon pretreatment with 10  $\mu\text{M}$   $\text{ZnCl}_2$  or  $\text{NaAsO}_2$  or PAPA0 when compared with untreated control ( $n=3$ ). The  $p$  values were calculated using unpaired two-tailed student's t-test, and the asterisks designate significant differences between different pretreatments and control without pretreatment (\*,  $p < 0.05$ ; \*\*,  $p < 0.01$ ; \*\*\*,  $p < 0.001$ ). (E) Mutations of cysteine residues (Cys  $\rightarrow$  Ala) in the zinc finger motif of TIP60 weakened the pull-down of TIP60 with the biotin-As probe. (F) Relative levels of different forms of TIP60 protein pulled down by streptavidin agarose using the biotin-As probe. Specific Cys  $\rightarrow$  Ala mutations within the zinc finger domains of TIP60 led to compromised interaction between TIP60 and biotin-As ( $n=3$ ). The  $p$  values were calculated using unpaired two-tailed student's t-test, and the asterisks designate significant differences between mutant forms of HA-TIP60 and the wild-type control (\*,  $p < 0.05$ ; \*\*,  $p < 0.01$ ; \*\*\*,  $p < 0.001$ ). Error bars in D and F indicate standard deviations.

### **Arsenite induces the degradation of TIP60 protein through the ubiquitin-proteasome pathway and inhibits TIP60-mediated H4K16 acetylation in mammalian cells**

We next investigated whether the ubiquitin-proteasome pathway contributes to the  $\text{As}^{3+}$ -induced decrease of HA-tagged TIP60 protein. We repeated the dose-dependent experiment by co-treating HA-TIP60-expressing HEK293T cells with 4  $\mu\text{M}$  MG132 (with DMSO as control) in conjunction with 0, 2, and 5  $\mu\text{M}$  of  $\text{NaAsO}_2$ , where MG132 acts as a proteasomal inhibitor. As displayed in Figure 3.4, we found that the addition of 4  $\mu\text{M}$  MG132 could augment the HA-TIP60 protein level in general when compared with the DMSO control group. Importantly, the arsenite-induced decrease in HA-TIP60 protein was abolished in cells co-treated with MG132 (Fig. 3.4B). Thus,  $\text{As}^{3+}$  induces decrease in HA-TIP60 protein by promoting its degradation via the ubiquitin-proteasome pathway.

Similar experiments with the aforementioned mutant forms of TIP60 protein (i.e. C263A, C266A and C283A) showed that the substitution of any of zinc finger cysteines to an alanine abrogated the arsenite-induced proteasomal degradation of the TIP60 protein (Fig. 3.S2). This result indicates that the arsenite-induced decrease in HA-TIP60 protein is due to the selective binding of arsenite to zinc-binding cysteine residues within the zinc finger motifs of TIP60.

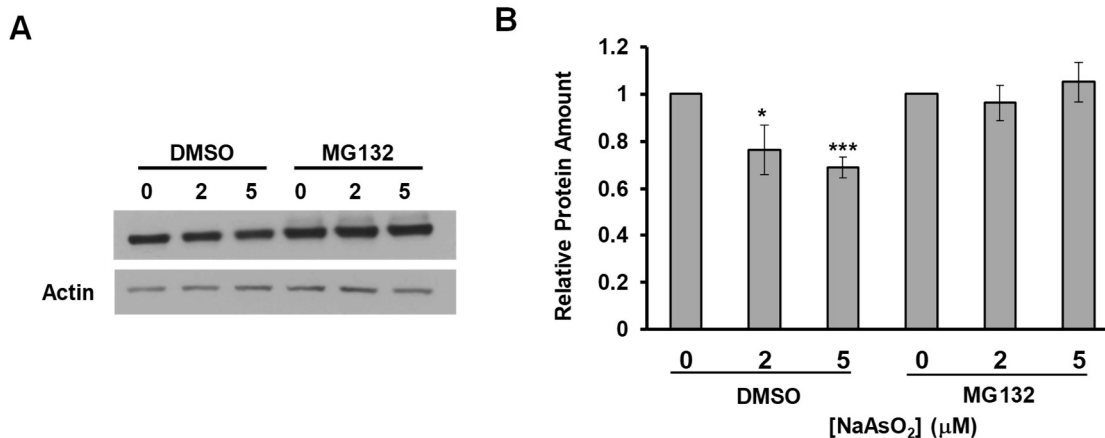


**Figure 3.4.** Exposure to arsenite induces proteasomal degradation of TIP60. (A) Co-treatment of HEK293T cells with 4 μM MG132 together with different doses of NaAsO<sub>2</sub> (0, 2, and 5 μM) could rescue the dose-dependent decrease of TIP60 protein induced by arsenite exposure. (B) Relative protein level of TIP60 upon treatment with different doses of NaAsO<sub>2</sub> together with MG132 or DMSO control (n=3). The *p* values were calculated using unpaired two-tailed student's *t*-test, and the asterisks designate significant differences between the arsenite-treated samples and untreated control (\*, *p* < 0.05; \*\*, *p* < 0.01; \*\*\*, *p* < 0.001). Error bars in panel B represent standard deviations.

Having demonstrated that As<sup>3+</sup> induces the degradation of TIP60 protein via the ubiquitin-proteasome pathway, we next investigated, by using histone acetyltransferase (HAT) assay, whether the As<sup>3+</sup>-induced hypoacetylation of H4K16 is attributed, in part, to the arsenite-induced decrease in enzymatic activity of HA-TIP60. After exposure to 5 μM arsenite for 24 h, we precipitated Flag-TIP60 from HEK293T cells using anti-FLAG M2 affinity gel and used the immunoprecipitated protein for HAT assay. Our result revealed that arsenite treatment did not result in any significant alteration in the HAT activity of TIP60 (Fig. 3.S3).

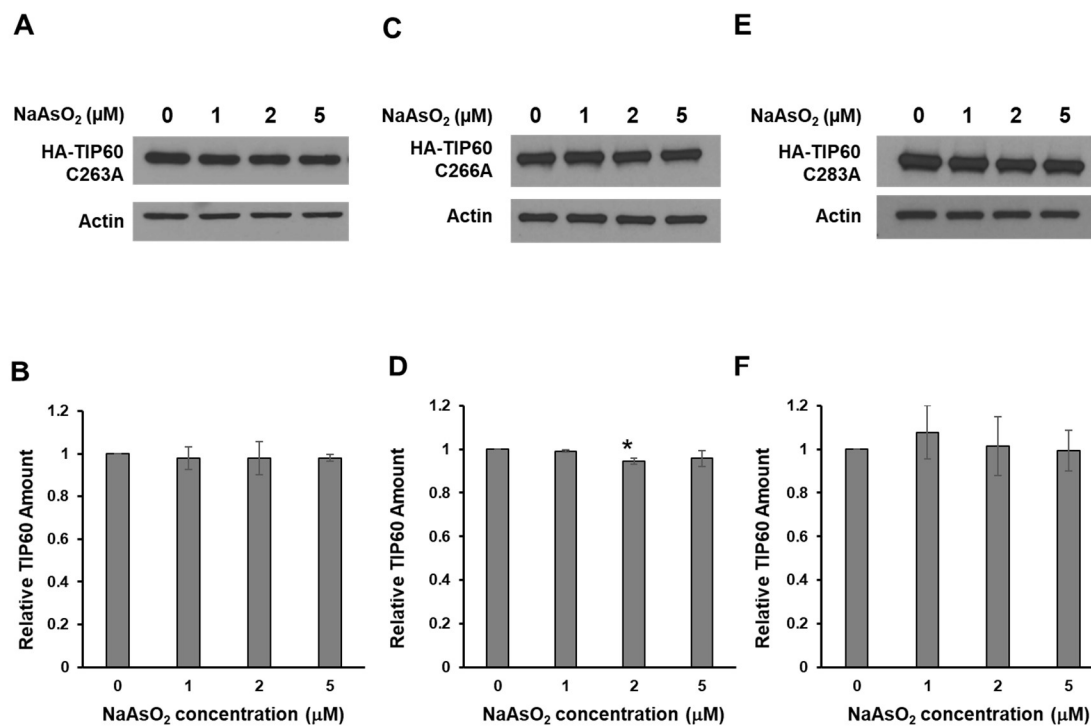


**Figure 3.S2.** Arsenite does not induce dose-dependent decrease in protein level of any three zinc finger mutants of TIP60, i.e. C263A, C266A and C283A. Western blot images showing the effect of mutations in critical cysteine residues of the C3H-type zinc finger of TIP60, i.e. C263A (A), C266A (C) and C283A (E). The quantification results of the relative level of TIP60 mutant proteins C263A (B), C266A (D) and C283A (F) following exposure to different concentrations of NaAsO<sub>2</sub> (n=3). Error bars represent standard deviations. The p values were calculated using unpaired two-tailed Student's t-test, and the asterisks designate significant differences between arsenite-treated samples and untreated control (\*, p < 0.05; \*\*, p < 0.01; \*\*\*, p < 0.001).



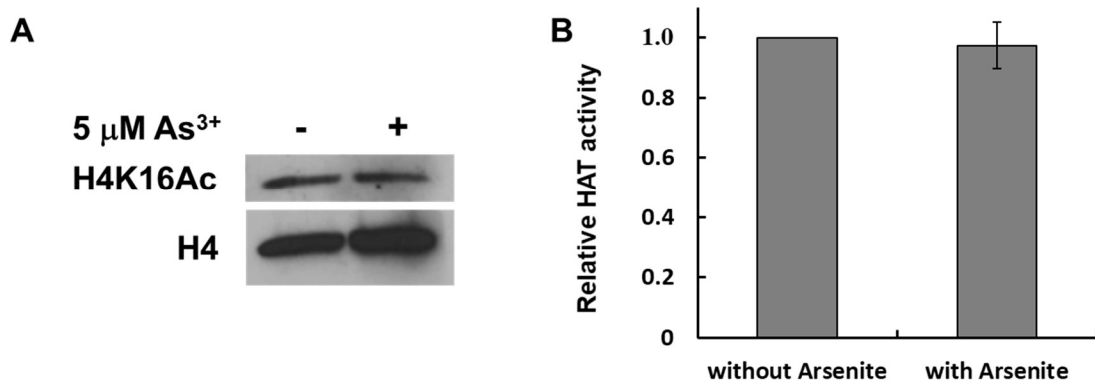


**Figure 3.S3.** Arsenite does not attenuate the histone acetyltransferase (HAT) activity of TIP60. (A) HAT assay indicating the effect of treatment of cells with 5  $\mu\text{M}$  of  $\text{NaAsO}_2$  on HAT activity of TIP60, as shown by the acetylation of H4K16 residue, with the untreated control. (B) Relative HAT activity of TIP60 with or without 5  $\mu\text{M}$  of  $\text{NaAsO}_2$ . The data represents the mean and standard deviation of results from three independent experiments.

Finally, we examined whether endogenous TIP60 plays a significant role in  $\text{As}^{3+}$ -induced decrease in H4K16Ac. Thus, we employed the CRISPR-Cas9 genome-editing method to generate *TIP60*<sup>-/-</sup> HEK293T cells<sup>24</sup>. Our Western blot result indicated that a 24-h treatment with 2 and 5  $\mu\text{M}$  of arsenite led to significantly decrease H4K16Ac level in both wild-type and *TIP60*<sup>-/-</sup> cells (Fig. 3.5A). However, the magnitude of decrease in the level of H4K16Ac in *TIP60*<sup>-/-</sup> cells was significantly lower than that in the HEK293T cells upon exposure with 5  $\mu\text{M}$   $\text{As}^{3+}$  (Fig. 3.5B), thereby demonstrating that  $\text{As}^{3+}$ -induced decrease in H4K16Ac level involves TIP60.

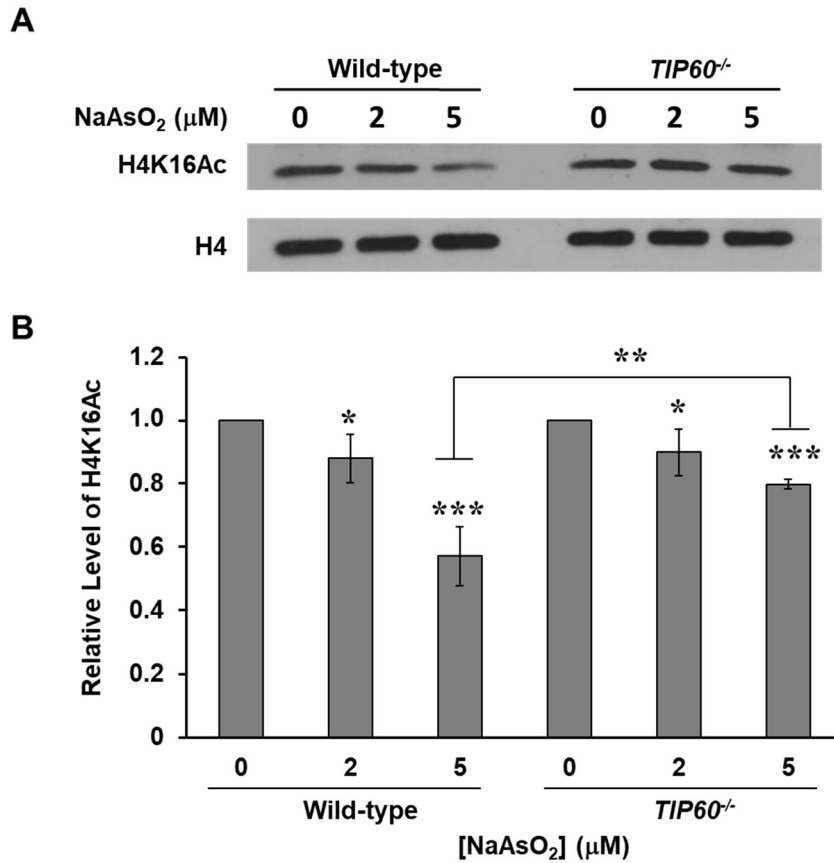


**Figure 3.5.** Arsenite exposure led to diminished H4K16Ac in both wild-type and *TIP60*<sup>-/-</sup> HEK293T cells, and a higher concentration of arsenite (i.e. 5 μM) gave rise to a more pronounced decrease in H4K16Ac level in wild-type cells than *TIP60*<sup>-/-</sup> cells. (A) Western blot image showing the effect of different concentrations (0, 2, and 5 μM) of NaAsO<sub>2</sub> on the level of H4K16Ac in wild-type and *TIP60*<sup>-/-</sup> HEK293T cells. (B) Relative levels of H4K16Ac in wild-type and *TIP60* knock-out cells upon treatment with different concentrations of arsenite (n=4). Error bars represent standard deviations. The *p* values were calculated using unpaired two-tailed student's t-test, and the asterisks designate significant differences between arsenite-treated cells and untreated control as well as the significant difference upon the same arsenite treatment between wild-type and *TIP60*<sup>-/-</sup> cell lines (\*, *p* < 0.05; \*\*, *p* < 0.01; \*\*\*, *p* < 0.001).

## Discussion

### Role of zinc fingers in the toxicity of arsenic and different mechanisms involving the MYST family of histone acetyltransferases

As<sup>3+</sup> can interact with zinc finger proteins,<sup>2,9</sup> particularly with the C3H- and C4-types of zinc finger motifs,<sup>10</sup> and the interaction between As<sup>3+</sup> and zinc finger domains of crucial DNA repair

enzymes is thought to contribute to arsenic toxicity and carcinogenicity.<sup>26</sup> In this vein, As<sup>3+</sup> is known to bind to, and inhibit the activities of several enzymes that function in DNA repair, including poly(ADP-ribose)polymerase-1 (PARP1), XPA and bacterial formamidopyrimidine-DNA glycosylase.<sup>10</sup> The results from our streptavidin agarose pull-down assay and MALDI-TOF-MS measurements demonstrated that the cysteine residues in the zinc-finger motif of TIP60 can bind directly with As<sup>3+</sup>. In addition, our Western blot results revealed that As<sup>3+</sup> binding could stimulate the degradation of TIP60 via the 26S proteasome, a finding that is reminiscent of the As<sup>3+</sup>-induced proteasomal degradation of the PML-RAR $\alpha$  oncoprotein.<sup>15</sup> Interestingly, Legube *et al.*<sup>25</sup> found that TIP60 protein undergoes ubiquitination-mediated degradation, where Mdm2 serves as the E3 ubiquitin ligase. Furthermore, arsenite was found to induce the overexpression of Mdm2 protein<sup>27</sup> without increasing its mRNA expression level,<sup>28</sup> though the mechanism underlying the arsenite-induced Mdm2 protein overexpression remains unknown.

Given that zinc finger motif within the catalytic MYST domain of TIP60 is indispensable for its acetyltransferase activity and protein-protein interaction,<sup>29</sup> the arsenic-induced structural alteration of TIP60 could modify the catalytic core of TIP60, thereby affecting its acetyltransferase activity and its interaction with regulatory proteins such as the aforementioned Mdm2. However, our *in vitro* HAT assay indicated that arsenic could not significantly diminish the histone acetyltransferase activity of TIP60, indicating that the catalytic core of TIP60 is not affected the potential conformational change conferred by As<sup>3+</sup> binding. Combining our result and the previous findings, two possible mechanisms for arsenic-induced proteasomal degradation of TIP60 can be deduced. In this respect, arsenite may elicit the overexpression of Mdm2 protein, which may stimulate the ubiquitination and proteasomal degradation of the TIP60 protein. Alternatively, As<sup>3+</sup> may displace the Zn<sup>2+</sup> ion in the zinc-finger domain of TIP60, thereby altering the the conformation

of the MYST domains of TIP60 and enhancing its proteasomal degradation. The relative contributions of these two mechanisms in arsenite-induced degradation of TIP60 remains unknown.

TIP60 and hMOF both regulate the level of H4K16Ac. Liu *et al.*<sup>30</sup> previously reported that arsenite induces global H4K16 hypoacetylation through binding directly to hMOF, another member of the MYST-family histone acetyltransferases. Different from our findings made for TIP60, Liu *et al.*<sup>30</sup> showed that arsenite does not cause significant dose-dependent change in the protein level of hMOF which is in keeping with our Western blot results. Therefore, arsenite targets hMOF and TIP60 by binding directly to zinc finger motifs. The arsenic-induced conformational change of catalytic MYST domains of these two HATs, however, elicits H4K16 hypoacetylation via distinct mechanisms, namely through enhanced protein degradation of TIP60 and diminished catalytic activities of hMOF. This observation unveiled the complexity in the mechanisms of MYST-family of histone acetyltransferase in arsenic epigenotoxicity.

#### **Implications in DNA repair from Arsenite-induced perturbations in epigenetic signaling**

Recently, epigenetic dysregulation is thought to play a central role in the mechanisms of arsenic carcinogenicity.<sup>31</sup> Previous research revealed the importance of TIP60-mediated acetylation in the sensing and repair of DNA double strand breaks (DSBs). In particular, the TIP60-catalyzed H4K16 acetylation is responsible for the decompaction of the 30 nm chromatin fibers,<sup>17</sup> where efficient DNA repair necessitates chromatin modification/remodeling to allow DNA repair machinery to access DNA damage sites in chromatin.<sup>32</sup> In addition, TIP60 functions in DNA damage response signaling by directly acetylating ATM.<sup>22</sup> We found that arsenite enhanced the proteasomal degradation of TIP60, thereby reducing the overall activities of TIP60. Thus, our work suggests that arsenite may trigger carcinogenesis by binding to TIP60 protein and triggering its degradation, thereby compromising DNA damage response signaling and DNA repair (Fig. 3.6.). In this context, it is worth noting that, owing to the lack of a suitable antibody for detecting endogenous TIP60

protein, most of our cellular experiments were conducted with the use of ectopically expressed TIP60. This may not fully reflect the interaction between  $As^{3+}$  and endogenous TIP60. Nevertheless, the finding that arsenite-induced decrease in H4K16Ac in TIP60-depleted cells is not as pronounced as in the isogenic wild-type cells (Fig. 3.5.) suggests that the findings made with the ectopically expressed TIP60 are relevant to what may occur with the endogenous protein upon arsenite exposure.

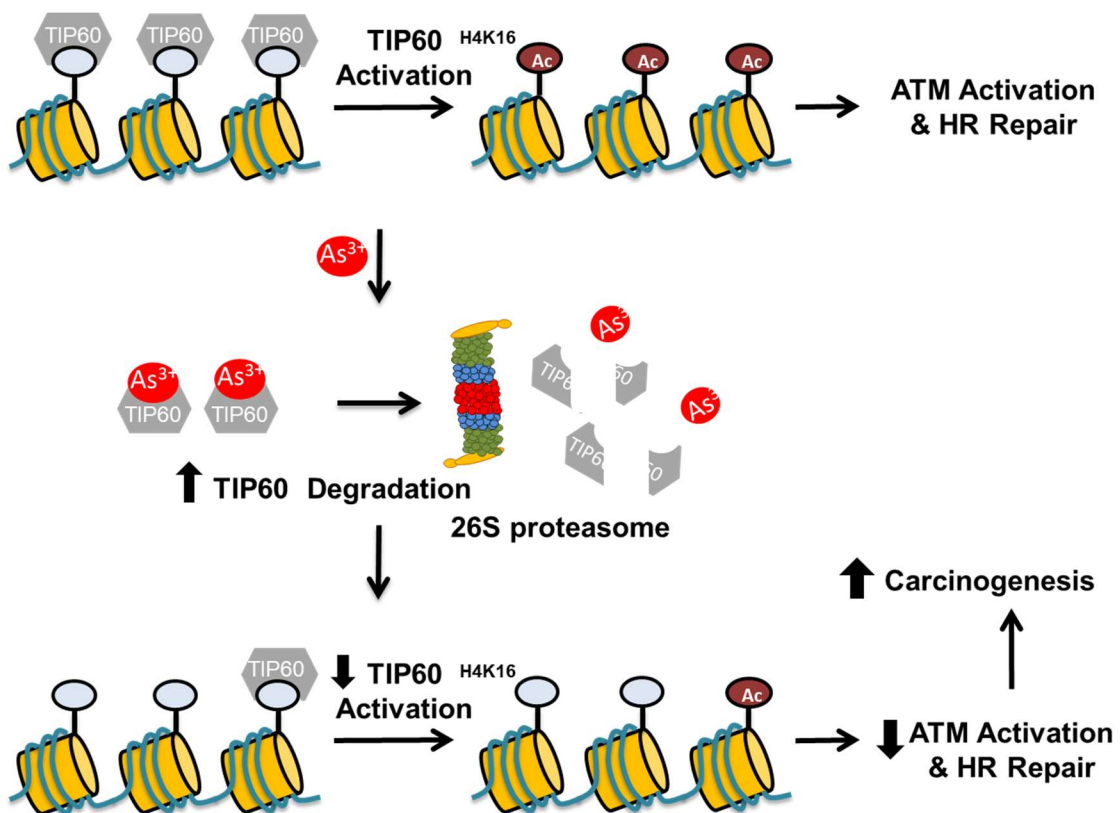


**Figure 3.6.** The proposed role of TIP60 in arsenic-induced carcinogenesis.  $As^{3+}$  interacts with cysteine residues in the zinc finger motifs of TIP60, promoting its degradation via the ubiquitin-proteasomal pathway. Diminished level of TIP60 protein results in lower level of H4K16Ac. This in turn generates a biochemically less accessible chromatin state, which may compromise DNA repair.

### **Implications in environmental exposure to arsenic**

There are about 150 million people living in the environment containing amounts of inorganic arsenic in drinking water that are much higher than the recommended standard of 10 ppb set by the World Health Organization and U.S. Environmental Protection Agency.<sup>5</sup> Early-life exposure to arsenic was found to confer elevated incidence and severity of cancer in childhood and adulthood as supported by a latency period that is decades long.<sup>33</sup> Arsenic-induced epigenetic dysregulation not only gives rise to DNA repair inhibition and cancer progression partly through disrupted gene imprinting, but also leads to the impairment in learning and memory as well as cognitive functions in children and adults after arsenic exposure.<sup>33,34</sup> Furthermore, histone acetylation was found to regulate cognitive gene expression by chromatin remodeling in neurons, similar to chromatin decompaction during DNA damage response.<sup>34</sup> Given that TIP60 is abundant in the learning and memory center in the *Drosophila* brain, and is necessary for mediating axonal outgrowth,<sup>34</sup> our work sets the stage for future studies on the roles of arsenic binding with TIP60 in perturbing the epigenetic patterns in cognitive impairment in human brains after chronic arsenic exposure. Combining all these profound implications together, we should protect the living environments of the populations especially infants and children to prevent chronic arsenic exposure via contaminated drinking water so as to alleviate the life-long risk of developing cancers and neurocognitive impairment.

**Abbreviations:** PAPAO, *p*-aminophenylarsenoxide; DTT, dithiothreitol; SILAC, stable isotope labeling with amino acids in cell culture; MALDI-TOF MS, matrix-assisted laser desorption ionization-time-of-flight mass spectrometry.

## References

1. Chen, S., Zhou, G., Zhang, X., Mao, J., de The, H., and Chen, Z. (2011) From an old remedy to a magic bullet: molecular mechanisms underlying the therapeutic effects of arsenic in fighting leukemia. *Blood* 117, 6425–6437.
2. Shen, S., Li, X. F., Cullen, W. R., Weinfeld, M., and Le, X. C. (2013) Arsenic binding to proteins. *Chem. Rev.* 113, 7769–7792.
3. Kumar, A., Adak, P., Gurian, P. L., and Lockwood, J. R. (2010) Arsenic exposure in US public and domestic drinking water supplies: a comparative risk assessment. *J. Exposure Sci. Environ. Epidemiol.* 20, 245–254.
4. Martinez, V.D., Vucic, E. A., Becker-Santos, D. D., Gil, L., and Lam, W. L. (2011) Arsenic exposure and the induction of human cancers. *J. Toxicol.* 2011, 431287.
5. Ravenscroft, P., Brammer, H., and Richards, K. (2009) in *Arsenic Pollution: A Global Synthesis*, Wiley-Blackwell, UK. DOI:10.1002/9781444308785.
6. Hartwig, A., Blessing, H., Schwerdtle, T., and Walter, I. (2003) Modulation of DNA repair processes by arsenic and selenium compounds. *Toxicology* 193, 161–169.
7. Arita, A., and Costa, M. (2009) Epigenetics in metal carcinogenesis: nickel, arsenic, chromium and cadmium. *Metallomics* 1, 222–228.
8. Chervona, Y., Hall, M. N., Arita, A., Wu, F., Sun, H., Tseng, H. C., Ali, E., Uddin, M. N., Liu, X., Zoroddu, M. A., Gamble, M. V., and Costa, M. (2012) Associations between arsenic exposure and global posttranslational histone modifications among adults in Bangladesh. *Cancer Epidemiol., Biomarkers Prev.* 21, 2252–2260.
9. Kitchin, K. T., and Wallace, K. (2008) The role of protein binding of trivalent arsenicals in arsenic carcinogenesis and toxicity. *J. Inorg. Biochem.* 102, 532–539.
10. Zhou, X., Sun, X., Cooper, K. L., Wang, F., Liu, K. J., and Hudson, L. G. (2011) Arsenite interacts selectively with zinc finger proteins containing C3H1 or C4 motifs. *J. Biol. Chem.* 286, 22855–22863.
11. Zhang, F., Paramasivam, M., Cai, Q., Dai, X., Wang, P., Lin, K., Song, J., Seidman, M. M., and Wang, Y. (2014) Arsenite binds to the RING finger domains of RNF20-RNF40 histone E3 ubiquitin ligase and inhibits DNA double-strand break repair. *J. Am. Chem. Soc.* 136, 12884–12887.
12. Jiang, J., Bellani, M., Li, L., Wang, P., Seidman, M. M., and Wang, Y. (2017) Arsenite binds to the RING finger domain of FANCL E3 ubiquitin ligase and inhibits DNA interstrand cross-link repair. *ACS Chem. Biol.* 12, 1858.

13. Liu, S., Jiang, J., Li, L., Amato, N. J., Wang, Z., and Wang, Y. (2015) Arsenite targets the zinc finger domains of Tet proteins and inhibits Tet-mediated oxidation of 5-methylcytosine. *Environ. Sci. Technol.* 49, 11923–11931.
14. Liu, J., Zhou, G., Chen, S., and Chen, Z. (2012) Arsenic compounds: revived ancient remedies in the fight against human malignancies. *Curr. Opin. Chem. Biol.* 16,92–98
15. Zhang, X. W., Yan, X. J., Zhou, Z. R., Yang, F. F., Wu, Z. Y., Sun, H. B., Liang, W. X., Song, A. X., Lallemand-Breitenbach, V., Jeanne, M., Zhang, Q. Y., Yang, H. Y., Huang, Q. H., Zhou, G. B., Tong, J. H., Zhang, Y., Wu, J. H., Hu, H. Y., de Thé, H., Chen, S. J., and Chen, Z. (2010) Arsenic trioxide controls the fate of the PML-RARalpha oncoprotein by directly binding PML. *Science* 328, 240–243.
16. Li, X., Corsa, C. A., Pan, P. W., Wu, L., Ferguson, D., Yu, X., Min, J., and Dou, Y. (2010) MOF and H4 K16 acetylation play important roles in DNA damage repair by modulating recruitment of DNA damage repair protein Mdc1. *Mol. Cell. Biol.* 30, 5335–5347.
17. Shogren-Knaak, M., Ishii, H., Sun, J. M., Pazin, M. J., Davie, J. R., and Peterson, C. L. (2006) Histone H4-K16 acetylation controls chromatin structure and protein interactions. *Science* 311, 844–847.
18. Zhong, J., Li, X., Cai, W., Wang, Y., Dong, S., Yang, J., Zhang, J., Wu, N., Li, Y., Mao, F., Zeng, C., Wu, J., Xu, X., and Sun, Z. S. (2017) TET1 modulates H4K16 acetylation by controlling auto-acetylation of hMOF to affect gene regulation and DNA repair function. *Nucleic Acids Res.* 45, 672–684.
19. Jo, W. J., Ren, X., Chu, F., Aleshin, M., Wintz, H., Burlingame, A., Smith, M. T., Vulpe, C. D., and Zhang, L. (2009) Acetylated H4K16 by MYST1 protects UROtsa cells from arsenic toxicity and is decreased following chronic arsenic exposure. *Toxicol. Appl. Pharmacol.* 241, 294–302.
20. Chu, F., Ren, X., Chasse, A., Hickman, T., Zhang, L., Yuh, J., Smith, M. T., and Burlingame, A. L. (2011) Quantitative mass spectrometry reveals the epigenome as a target of arsenic. *Chem. -Biol. Interact.* 192, 113–117.
21. Takechi, S., and Nakayama, T. (1999) Sas3 is a histone acetyltransferase and requires a zinc finger motif. *Biochem. Biophys. Res. Commun.* 266, 405–410.
22. Sapountzi, V., and Cote, J. (2011) MYST-family histone acetyltransferases: beyond chromatin. *Cell. Mol. Life Sci.* 68, 1147–1156.
23. Sun, Y., Jiang, X., Xu, Y., Ayrapetov, M. K., Moreau, L. A., Whetstine, J. R., and Price, B. D. (2009) Histone H3 methylation links DNA damage detection to activation of the tumour suppressor Tip60. *Nat. Cell Biol.* 11, 1376–1382.
24. Li, L., and Wang, Y. (2017) Crosstalk between the H3K36me3 and H4K16ac histone epigenetic marks in DNA double-strand break repair. *J. Biol. Chem.* 292, 11951–11959.



25. Legube, G., Linares, L. K., Lemerrier, C., Scheffner, M., Khochbin, S., and Trouche, D. (2002) Tip60 is targeted to proteasome-mediated degradation by Mdm2 and accumulates after UV irradiation. *EMBO J.* 21, 1704–1712.
26. Walter, I., Schwerdtle, T., Thuy, C., Parsons, J. L., Dianov, G. L., and Hartwig, A. (2007) Impact of arsenite and its methylated metabolites on PARP-1 activity, PARP-1 gene expression and poly(ADP-ribosyl)ation in cultured human cells. *DNA Repair* 6,61– 70.
27. Hamadeh, H. K., Vargas, M., Lee, E., and Menzel, D. B. (1999) Arsenic disrupts cellular levels of p53 and mdm2: a potential mechanism of carcinogenesis. *Biochem. Biophys. Res. Commun.* 263, 446–449.
28. Tokumoto, M., Lee, J. Y., Fujiwara, Y., Uchiyama, M., and Satoh, M. (2013) Inorganic arsenic induces apoptosis through down- regulation of Ube2d genes and p53 accumulation in rat proximal tubular cells. *J. Toxicol. Sci.* 38, 815–820.
29. Sapountzi, V., Logan, I. R., and Robson, C. N. (2006) Cellular functions of TIP60. *Int. J. Biochem. Cell Biol.* 38, 1496–1509.
30. Liu, D., Wu, D., Zhao, L., Yang, Y., Ding, J., Dong, L., Hu, L., Wang, F., Zhao, X., Cai, Y., and Jin, J. (2015) Arsenic trioxide reduces global histone H4 acetylation at lysine 16 through direct binding to histone acetyltransferase hMOF in human cells. *PLoS One* 10, e0141014.
31. Ren, X., McHale, C. M., Skibola, C. F., Smith, A. H., Smith, M. T., and Zhang, L. (2010) An emerging role for epigenetic dysregulation in arsenic toxicity and carcinogenesis. *Environ. Health Perspect.* 119,11–19.
32. Murr, R., Loizou, J. I., Yang, Y. G., Cuenin, C., Li, H., Wang, Z. Q., and Herceg, Z. (2006) Histone acetylation by Trrap-Tip60 modulates loading of repair proteins and repair of DNA double-strand breaks. *Nat. Cell Biol.* 8,91–99.
33. Naujokas, M. F., Anderson, B., Ahsan, H., Aposhian, H. V., Graziano, J. H., Thompson, C., and Suk, W. A. (2013) The broad scope of health effects from chronic arsenic exposure: update on a worldwide public health problem. *Environ. Health Perspect.* 121, 295– 302.
34. Xu, S., and Elefant, F. (2015) Tip off the HAT- Epigenetic control of learning and memory by Drosophila Tip60. *Fly* 9,22–28.

## **Chapter 4**

# **Targeted Quantitative Proteomics Revealed Arsenite-induced Proteasomal Degradation of RhoB in Fibroblast Cells**

## **Introduction**

Arsenic, a naturally occurring element in the Earth's crust, has been recognized as the most detrimental metalloid existing prevalently in the environment, and arsenic exposure constitutes a major public health concern.<sup>1,2</sup> It was estimated that at least 150 million people in over 70 countries are exposed to excessive amount of arsenic species via contaminated drinking water and diet.<sup>3</sup> Arsenic has received substantial attention from the scientific community and it is ranked on the top of the Priority List of Hazardous Substances in the Agency for Toxic Substances and Disease Registry (ATSDR).<sup>4</sup> Due to the tremendous public health burden from arsenic exposure through drinking water, the World Health Organization and the US Environmental Protection Agency (EPA) have set the maximum contamination level of arsenic in drinking water to be 10 ppb.<sup>5,6</sup> In addition, arsenic has been classified as a class I human carcinogen by the International Agency for Research on Cancer (IARC).

Chronic exposure to arsenic in drinking water was found to be associated with elevated incidences of various human diseases including bladder, lung, liver, skin and kidney cancers.<sup>7,8</sup> Arsenic exists in both inorganic and organic forms.<sup>9</sup> However, arsenite, one of the major inorganic form of arsenic commonly detected in drinking water from the environment,<sup>10</sup> is found to show more potent toxicity towards humans than organic arsenic species.<sup>11</sup> Hence, it is critical and urgent to understand fully the molecular mechanisms underlying arsenite-induced carcinogenesis so as to develop suitable therapeutic and chemopreventive approaches.

Over the past few decades, small GTPases of the Ras superfamily have been widely studied and shown to be implicated in human cancers.<sup>12,13</sup> By shuffling between their GTP-bound active and GDP-bound inactive forms, small GTPases can serve as molecular switches in regulating a wide range of cellular processes including signal transduction, cell division and cell motility.<sup>14</sup> Among them, Rho GTPases play important roles in controlling cell motility and cytoskeleton

rearrangements, thereby regulating the architecture of stress fibers, focal adhesion and membrane ruffles.<sup>14</sup> Additionally, a large number of studies demonstrated that Rho GTPases play regulatory roles in cancer cell migration and metastasis,<sup>13</sup> and act as tumor suppressors or proto-oncogenes.<sup>15</sup> Furthermore, small Rho GTPases Rac1 and Cdc42 were previously found to be affected by arsenite exposure in rat nervous system.<sup>16</sup> We reason that a systematic study about how arsenite exposure modulates small GTPase signaling may provide new insights into the molecular mechanisms of arsenic toxicity and carcinogenicity.

Over the past two decades, mass spectrometry-based quantitative proteomics have become widely utilized to probe systematically the changes in protein expression and to study the signaling pathways involved in various human diseases.<sup>17,18</sup> Recently, several quantitative proteomic approaches have been developed and applied to study small GTPase proteins.<sup>19–21</sup>

In this study, we utilized our recently reported targeted quantitative proteomic method<sup>21</sup> for assessing the altered expression of small GTPases in cultured IMR90 human lung fibroblast cells upon arsenite treatment. We were able to quantify 87 small GTPases, among which RhoB exhibited the most pronounced down-regulation upon arsenite treatment. We also confirmed by Western blot analysis that exposure to arsenite led to a dose-dependent decrease in the levels of both endogenous and ectopically-expressed RhoB protein in cultured human cells, and that the decreased protein levels of RhoB involves the 26S proteasome.

## **Experimental Procedures**

### **Cell culture**

HEK293T human embryonic kidney epithelial cells (ATCC), HeLa human cervical cancer cells, and GM00637 human skin fibroblast cells were cultured in Dulbecco's modified Eagle's medium (DMEM, Thermo Fisher Scientific). IMR90 human lung fibroblast cells were cultured in

Corning™ Eagle's Minimum Essential Medium (EMEM, Thermo Fisher Scientific). All culture media except those used for transfection were supplemented with 10% fetal bovine serum (FBS, Thermo Fisher Scientific) and 1% penicillin streptomycin solution (PS, GE Healthcare). The cells were maintained at 37°C in a humidified atmosphere with 5% CO<sub>2</sub>, with medium renewal in every 2-3 days depending on cell density. For plasmid transfection, the cells were cultured in the same media as described above except that no penicillin streptomycin solution was added.

### **Plasmid and cell transfection**

The expression plasmid for RhoB (pCMV3-HA-RhoB) was kindly provided by Dr. George Prendergast and Dr. Lisa Laury-Kleintop (Lankenau Institute for Medical Research).<sup>22,23</sup> The plasmid was transfected into GM00637, HEK293T, HeLa, and IMR90 cells using TransIT-2020 (Mirus Bio, Madison, WI) according to the manufacturer's recommended protocol.

### **Western blot analysis**

IMR90, HEK293T, HeLa and GM00637 cells were transfected with wild-type HA-RhoB. At 24 h after the transfection, the cells were exposed to different concentrations (i.e. 0, 1, 2, 5 μM) of NaAsO<sub>2</sub> for another 24 h and lysed in CellLytic™ M lysis buffer supplemented with a protease inhibitor cocktail (Sigma Aldrich). For monitoring the expression of endogenous RhoB protein, untransfected IMR90 cells were exposed to the above-mentioned concentrations of NaAsO<sub>2</sub> for 24 h and lysed in the same way. After SDS-PAGE separation, proteins were transferred to a nitrocellulose membrane using a transfer buffer containing Tris base (25 mM, pH 8.1-8.5), methanol, glycine and water. The membranes were blocked with 5% BSA in PBS-T buffer, which contained PBS and 0.1% (v/v) Tween-20 (pH 7.5), for 1.5 h and incubated with rabbit anti-RhoB antibody (1:5000 dilution, Cell Signaling Technology) at room temperature for 2 h. The membranes were rinsed with fresh PBS-T at room temperature for 6 times (5-10 min each). After washing, the membranes were incubated with rabbit secondary antibody at room temperature for 1 h. The

membranes were subsequently washed with PBS-T for 6 times. The protein bands were detected using Amersham™ ECL™ Select Western blotting Detection Kit (GE Healthcare) and visualized with Hyblot CL autoradiography film (Denville Scientific, Inc., Metuchen, NJ).

To assess the effect of arsenite and/or MG132, a 26S proteasomal inhibitor, on the protein level of RhoB, HEK293T cells were transfected with HA-tagged RhoB plasmid for 24 h, and exposed with several different concentrations of NaAsO<sub>2</sub> (i.e. 0, 1, 2, and 5 μM) in the presence or absence of 4 μM MG132 (Sigma Aldrich) for another 24 h, followed by cell harvesting, protein extraction, and Western blot analysis, as described above.

#### **Sample preparation and LC-MRM analysis**

For SILAC-based quantitative proteomics experiments, ‘heavy’ and ‘light’ SILAC DMEM media were freshly prepared by adding 0.146 g/L [<sup>13</sup>C<sub>6</sub>,<sup>15</sup>N<sub>2</sub>]-L-lysine (Lys-8) and 0.84 g/L [<sup>13</sup>C<sub>6</sub>]-L-arginine (Arg-6) (Cambridge Isotopes Inc.) or the corresponding un-labeled lysine (Lys-0) and arginine (Arg-0) to DMEM depleted of L-lysine and L-arginine (Thermo Scientific™ Pierce). The media were also supplemented with 10% dialyzed FBS (Corning) and 1% PS. IMR90 cells were cultured in the heavy-DMEM medium for at least 10 days or six cell doublings to enable complete heavy-isotope incorporation.

To assess the differential expression of small GTPases upon arsenite exposure, we conducted one forward and one reverse SILAC labeling experiment, where lysates of mock-treated light-labeled and arsenite (5 μM)-treated heavy-labeled IMR90 human lung fibroblast cells were combined at a 1:1 ratio (by mass) in the forward labeling experiment (Fig. 4.1A). The reverse labeling experiment was conducted in the opposite way. The combined cell lysate (100 μg in total) was mixed with 4× Laemmli sample buffer (Bio-Rad) with 10% (v/v) 2-mercaptoethanol, boiled at 95°C for 5 min, and then loaded and separated on a 10% SDS-PAGE gel at 120 V and at room temperature for 40 min. The gel band corresponding to the molecular weight range of 15–37 kDa

was excised, and proteins in the gel slices were then reduced with 20 mM dithiothreitol, alkylated with 55 mM iodoacetamide, and digested in-gel with trypsin at an enzyme/protein ratio of 1:100 in 50 mM ammonium bicarbonate (pH 7.8) at 37 °C overnight. After tryptic digestion, the peptide mixtures were desalted and subjected to LC-MRM analyses.

All LC-MRM experiments were performed on a TSQ Vantage triple-quadrupole mass spectrometer (Thermo Scientific). The mass spectrometer was coupled with an EASY-nLC II system (Thermo Scientific), and the samples were automatically loaded onto a 4 cm trapping column (150  $\mu\text{m}$  i.d.) packed with ReproSil-Pur 120 C18-AQ resin (5  $\mu\text{m}$  in particle size and 120 Å in pore size, Dr. Maisch GmbH HPLC) at 3  $\mu\text{L}/\text{min}$ . The trapping column was coupled to a 15-cm fused silica analytical column (75  $\mu\text{m}$  i.d.) packed in-house with ReproSil-Pur 120 C18-AQ resin (3  $\mu\text{m}$  in particle size and 120 Å in pore size, Dr. Maisch GmbH HPLC). The peptide mixtures were separated with a 157-min linear gradient of 2–35% acetonitrile in 0.1% formic acid and at a flow rate of 230 nL/min. The spray voltage was 1.8 kV, Q1 and Q3 resolutions were 0.7 Da, and the cycle time was 5 s. The optimal collisional energy (CE) for each targeted peptide was calculated using a linear equation specific to the TSQ Vantage instrument and the precursor mass-to-charge ratio ( $m/z$ ) according to the default setting in Skyline. A total of 432 peptides representing 113 non-redundant or 131 isoform-specific small GTPases were included in the library. The corresponding precursor and fragment ions of peptides harboring the light and heavy forms of lysine and/or arginine were monitored in two scheduled LC-MRM runs.

### **Statistical Analysis**

The statistical analyses of all the Western blot experiments were performed by using the average of the values obtained from 3-4 independent experiments. The  $p$  values used for all data analysis were calculated using unpaired two-tailed Student's  $t$ -test, indicating the significant difference

between the treated samples and the control with the asterisks as indicated (\*,  $0.01 \leq p < 0.05$ ; \*\*,  $0.001 \leq p < 0.01$ ; \*\*\*,  $p < 0.001$ ).

## Results

### Targeted Quantitative Profiling of Differential Expression of Small GTPases upon Arsenite Exposure in Lung Fibroblasts.

Lung constitutes a major target organ for arsenic-related carcinogenesis.<sup>24</sup> Given the crucial roles of small GTPases in cell signaling and trafficking related to various aspects of tumorigenesis and cancer progression,<sup>25</sup> we sought to investigate systematically the differential protein expression of small GTPases upon acute arsenite exposure in IMR90 human lung fibroblast cells. To this end, we employed a previously established targeted quantitative proteomics workflow, which involves SILAC, SDS-PAGE fractionation, and scheduled multiple-reaction monitoring (MRM) analysis (Fig. 4.1A).<sup>21</sup>

To obtain reliable quantification results, we carried out the SILAC experiments in one set of forward labeling (Fig. 4.1A) and one set of reverse labeling. In this vein, by adopting the scheduled MRM analysis, where the mass spectrometer is set up to monitor targeted transitions in a defined retention time window, high-throughput detection of peptides from small GTPases can be achieved. The entire library of small GTPase tryptic peptides could be monitored in two LC-MRM runs with retention time scheduling by using the iRT algorithm.<sup>26</sup>

The scheduled MRM analyses facilitated reproducible quantification of 87 small GTPases in both forward and reverse SILAC labeling experiments (Table 4.S1 and Fig. 4.S1). By contrast, analysis of the same samples by LC-MS/MS in the data-dependent acquisition (DDA) mode only led to the identification of 36 and 39 small GTPases in the forward and reverse SILAC samples, respectively (Fig. 4.1B). Moreover, MRM exhibited better sensitivity than the shotgun proteomic



approach, as reflected by the substantially increased coverage of the small GTPase proteome in two one-dimensional LC-MRM runs (Fig. 4.1B). We also examined the inter-replicate reproducibility of the MRM-based quantification. As illustrated in Fig. 4.1C, the  $\text{Log}_2$ -transformed SILAC ratios for all the quantified small GTPases obtained from forward and reverse SILAC labeling experiments are consistent, with a reasonably good linear fit ( $R^2 = 0.824$ ). Taken together, the above results demonstrated that scheduled MRM analysis facilitates highly sensitive and reproducible quantitative profiling of perturbed expression of small GTPases in IMR90 cells upon acute arsenite exposure (5  $\mu\text{M}$ , 12 h).

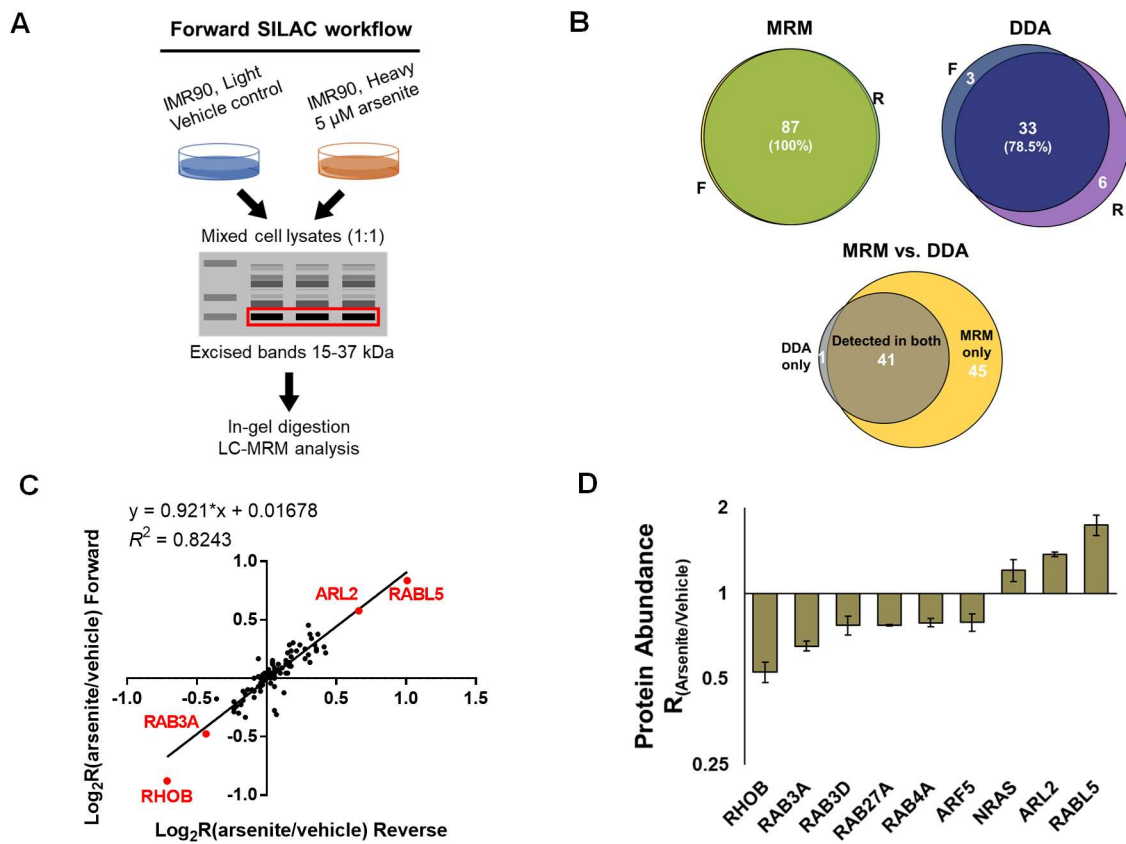


**Figure 4.1. A targeted proteomic strategy for high-throughput quantitative profiling of small GTPases upon arsenite exposure in IMR90 human lung fibroblast cells.** (A) A schematic illustration of the targeted quantitative proteomic workflow, relying on forward SILAC labeling, SDS-PAGE fractionation, and scheduled LC-MRM analysis; (B) Venn diagrams displaying the overlap between quantified small GTPases in the forward and reverse SILAC experiments obtained from the MRM and DDA analyses, respectively, and the comparison between the performances of the two methods; (C) Correlation between the  $\text{Log}_2$ -transformed SILAC ratios ( $\text{Log}_2R$ ) obtained from one forward and one reverse SILAC labeling experiments with a relatively high linear correlation coefficient ( $R^2 = 0.8243$ ); (D) A bar chart showing significantly up- and down-regulated ( $> 1.5$ -fold) small GTPases quantified from two LC-MRM experiments.

**Table 4.S1** Quantification data of LC-MRM analysis results.

Protein IPI	Full name	Gene name	Peptide sequence	Ratio (arsenite/vehicle)		
				F1	1/R	Average
PI000215914	ADP-ribosylation factor 1	ARF1	NIFTVWDVGGQDK	0.97	0.92	0.95
PI000215917	ADP-ribosylation factor 3	ARF3	LGLHSLR	1.08	1.07	1.07
PI000215918	ADP-ribosylation factor 4	ARF4	IQEVADELQK	1.12	1.14	1.13
PI000215918	ADP-ribosylation factor 4	ARF4	DAVLLLFANK	0.92	0.91	0.92
PI000215918	ADP-ribosylation factor 4	ARF4	LGLOSLR	1.14	1.17	1.15
PI000215919	ADP-ribosylation factor 5	ARF5	NICTVWDVGGQDK	0.83	0.83	0.83
PI000215919	ADP-ribosylation factor 5	ARF5	VOESADELQK	0.88	0.84	0.86
PI000215919	ADP-ribosylation factor 5	ARF5	LGLOHLR	0.89	0.83	0.86
PI000215920	ADP-ribosylation factor 6	ARF6	ILMLGLDAAGK	1.18	1.18	1.18
PI000215920	ADP-ribosylation factor 6	ARF6	FNWWDVGGQDK	1.02	0.89	0.95
PI000015178	ADP-ribosylation factor related protein 1	ARFRP1	TFLEQSK	1.07	1.05	1.06
PI000015178	ADP-ribosylation factor related protein 1	ARFRP1	TAFSDCTSK	1.03	1.02	1.03
PI000015178	ADP-ribosylation factor related protein 1	ARFRP1	DCLTQACSALTGK	1.05	1.00	1.03
PI000219518	ADP-ribosylation factor-like 1	ARL1	ILILGLDGAGK	0.75	0.85	0.80
PI000219518	ADP-ribosylation factor-like 1	ARL1	AILVVFANK	0.78	0.91	0.85
PI00005163	ADP-ribosylation factor-like 15	ARL15	ELGGADNIR	0.97	0.91	0.94
PI00003326	ADP-ribosylation factor-like 2	ARL2	EGOSLVEER	1.35	1.39	1.37
PI00003327	ADP-ribosylation factor-like 3	ARL3	ILLGLDNAGK	0.89	0.90	0.90
PI00003327	ADP-ribosylation factor-like 3	ARL3	QLASEDISHITPQGFIK	0.93	0.93	0.93
PI00001923	ADP-ribosylation factor-like 5A	ARL5A	AGLLIFANK	0.89	0.91	0.90
PI00102036	ADP-ribosylation factor-like 5B	ARL5B	AAVLIFANK	1.11	1.26	1.19
PI00060031	ADP-ribosylation factor-like 8A	ARL8A	LWDIGGQPR	0.82	0.97	0.90
PI00060031	ADP-ribosylation factor-like 8A	ARL8A	DLPGALDEKELIEK	1.12	1.21	1.16
PI00018871	ADP-ribosylation factor-like 8B	ARL8B	DLPNALDEK	0.94	0.92	0.93
PI00007189	cell division cycle 42 (GTP binding protein, 25kDa); cell division cycle 42 pseudogene 2	CDC42	TCLLUSYTTNK	0.96	0.99	0.98
PI000002919	DIRAS family, GTP-binding RAS-like 1	DIRAS1	VVVFAGGVGK	0.88	1.03	0.95
PI000002919	DIRAS family, GTP-binding RAS-like 1	DIRAS1	EAQAVAEWK	0.74	0.82	0.78
PI000000005	neuroblastoma RAS viral (v-ras) oncogene homolog	NRAS	SFADINLYR	1.28	1.13	1.21
PI00410705	NFKB inhibitor interacting Ras-like 1	NKIRAS1	QVDAEVAQQWAK	0.96	0.81	0.89
PI00410705	NFKB inhibitor interacting Ras-like 1	NKIRAS1	TLIEPFTLLASK	0.76	0.95	0.86
PI00021124	NFKB inhibitor interacting Ras-like 2	NKIRAS2	VVVGQAASVQK	0.88	0.88	0.88
PI00002644	RAB, member of RAS oncogene family-like 2A	RABL2A	IICLGDSAVGK	1.01	0.97	0.99
PI00087292	RAB, member of RAS oncogene family-like 4	RABL4	CILAGDPAVGK	0.96	0.94	0.95
PI000009700	RAB, member RAS oncogene family-like 5	RABL5	FESCWPALMK	1.64	1.84	1.74
PI00016513	RAB10, member RAS oncogene family	RAB10	TYDLFLK	0.90	0.82	0.86
PI00016513	RAB10, member RAS oncogene family	RAB10	FHTITTSYYR	0.93	0.98	0.96
PI00016513	RAB10, member RAS oncogene family	RAB10	NIDEHANEVVER	1.00	1.15	1.07

Protein IPI	Full name	Gene name	Peptide sequence	Ratio (arsenite/vehicle)		
				F1	1/R	Average
IP00020436	RAB11B, member RAS oncogene family	RAB11B	NILTEYR	0.99	0.96	0.98
IP000419932	RAB12, member RAS oncogene family	RAB12	AGGGGLGAGSPALSGGGGR	0.86	0.85	0.86
IP000419932	RAB12, member RAS oncogene family	RAB12	LQV//IGSR	0.87	0.85	0.86
IP00016373	RAB13, member RAS oncogene family; similar to hCG24991	RAB13	LQVWDTAGQER	0.96	0.96	0.96
IP000291928	RAB14, member RAS oncogene family	RAB14	YIIIGDMGVGK	1.38	0.86	1.12
IP000291928	RAB14, member RAS oncogene family	RAB14	STYNHLSSWLTDR	0.98	0.88	0.93
IP000291928	RAB14, member RAS oncogene family	RAB14	TGENVEDAFLEAAK	0.83	0.98	0.90
IP00007866	RAB17, member RAS oncogene family	RAB17	SILPTVGCFFTK	0.90	0.97	0.94
IP00014577	RAB18, member RAS oncogene family	RAB18	ILIGESGVGK	1.03	0.85	0.94
IP00014577	RAB18, member RAS oncogene family	RAB18	LAIWDTAGQER	1.04	1.08	1.06
IP00014577	RAB18, member RAS oncogene family	RAB18	TLTPSYR	1.02	1.05	1.04
IP000478209	RAB19, member RAS oncogene family	RAB19	ILIGDSNVGK	0.75	0.86	0.80
IP00005719	RAB1A, member RAS oncogene family	RAB1A	NATNVEQSFMTMAAEIK	0.96	1.21	1.09
IP00005719	RAB1A, member RAS oncogene family	RAB1A	MGPATAGGAEK	0.97	1.14	1.06
IP00008964	RAB1B, member RAS oncogene family	RAB1B	NATNVEQAFMTMAAEIK	1.06	1.08	1.07
IP00007755	RAB21, member RAS oncogene family	RAB21	VLLGEGCVGK	0.88	0.93	0.90
IP00007755	RAB21, member RAS oncogene family	RAB21	VNLAIWDTAGQER	0.85	0.97	0.91
IP00007755	RAB21, member RAS oncogene family	RAB21	HVSIQEAESYAESVGA	0.85	0.91	0.88
IP00007756	RAB22A, member RAS oncogene family	RAB22A	TVYQNELHK	0.78	0.85	0.82
IP00007756	RAB22A, member RAS oncogene family	RAB22A	EETFSTLK	0.91	0.87	0.89
IP00007756	RAB22A, member RAS oncogene family	RAB22A	DYADSIHAIFVETSAK	0.90	0.80	0.85
IP00008034	RAB23, member RAS oncogene family	RAB23	QIQVNDVDV	0.83	0.84	0.83
IP00056496	RAB24, member RAS oncogene family	RAB24	AQLFETSSK	0.92	1.09	1.00
IP00016381	RAB27A, member RAS oncogene family	RAB27A	FLALGDSGVGK	0.75	0.68	0.72
IP00016381	RAB27A, member RAS oncogene family	RAB27A	TSVLYQYTDGK	0.69	0.77	0.73
IP00016381	RAB27A, member RAS oncogene family	RAB27A	SWIPEGVVR	0.77	0.70	0.74
IP00016377	RAB28, member RAS oncogene family	RAB28	IVVLGDGASGK	0.99	0.90	0.94
IP00016377	RAB28, member RAS oncogene family	RAB28	VAAEILGIK	0.96	0.83	0.90
IP00016377	RAB28, member RAS oncogene family	RAB28	IVVLGDGASGK	0.87	0.91	0.89
IP00031169	RAB2A, member RAS oncogene family	RAB2A	MITIDGK	0.94	0.90	0.92
IP00031169	RAB2A, member RAS oncogene family	RAB2A	KEEGEAFAR	0.82	1.00	0.91
IP00031169	RAB2A, member RAS oncogene family	RAB2A	TASNVEEAFINTAK	0.86	0.90	0.88
IP00031169	RAB2A, member RAS oncogene family	RAB2A	IQEGVFDINNEANGIK	0.79	1.00	0.89
IP00064352	RAB2B, member RAS oncogene family	RAB2B	TACNVEEAFINTAK	0.99	0.95	0.97
IP000302030	RAB30, member RAS oncogene family	RAB30	IVLIGNAGVVK	1.04	0.89	0.97
IP00014376	RAB31, member RAS oncogene family	RAB31	QDSFYTLK	0.96	0.97	0.97
IP00014377	RAB32, member RAS oncogene family	RAB32	DNINIEAAR	1.04	0.99	1.02



Protein IPI	Full name	Gene name	Peptide sequence	Ratio (arsenite/vehicle)		
				F1	I/R	Average
IP100021475	RAB33B, member RAS oncogene family	RAB33B	IIVIGDSNVGK	0.72	1.12	0.92
IP100021475	RAB33B, member RAS oncogene family	RAB33B	AVEIDGER	0.82	0.79	0.80
IP100021475	RAB33B, member RAS oncogene family	RAB33B	SAIQVPTDLAQK	0.90	0.82	0.86
IP100001618	RAB39, member RAS oncogene family	RAB39	IKLQLWDTAGGER	1.00	1.00	1.00
IP100060801	RAB39B, member RAS oncogene family	RAB39B	YIETSAR	0.97	0.97	0.97
IP100023504	RAB3A, member RAS oncogene family	RAB3A	TYSWDNAQVLLVGNK	0.63	0.67	0.65
IP100032808	RAB3D, member RAS oncogene family	RAB3D	LLLIGNSSVVGK	0.81	0.73	0.77
IP100329441	RAB43, member RAS oncogene family, hypothetical	RAB43	YAGSNIVQLLIGNK	0.93	0.79	0.86
IP100329441	LOC100131426					
IP100329441	RAB43, member RAS oncogene family, hypothetical	RAB43	DSSNVEEAFLR	0.88	0.76	0.82
IP100329441	LOC100131426					
IP100480056	RAB4A, member RAS oncogene family	RAB4A	FLVIGNAGTGK	0.85	0.77	0.81
IP100480056	RAB4A, member RAS oncogene family	RAB4A	IESGELDPER	0.73	0.71	0.72
IP100480056	RAB4A, member RAS oncogene family	RAB4A	MSSGIQYGDAALR	0.69	0.76	0.73
IP100187143	RAB4B, member RAS oncogene family	RAB4B	FLVIGSAGTGK	1.10	1.07	1.08
IP100023510	RAB5A, member RAS oncogene family	RAB5A	QASPNIVIALSGNK	1.16	1.18	1.17
IP100023510	RAB5A, member RAS oncogene family	RAB5A	NEPQNPANSAR	0.84	1.67	1.26
IP100023510	RAB5A, member RAS oncogene family	RAB5A	GVDLTEPTQPTR	0.79	1.49	1.14
IP100017344	RAB5B, member RAS oncogene family	RAB5B	QASPSVIALAGNK	0.79	0.93	0.86
IP100017344	RAB5B, member RAS oncogene family	RAB5B	SEPNLGGAAAGR	0.90	1.19	1.04
IP100017344	RAB5B, member RAS oncogene family	RAB5B	GVDLHEGSQQNK	0.92	1.07	0.99
IP100016339	RAB5C, member RAS oncogene family	RAB5C	QASPNIVIALAGNK	0.62	0.69	0.66
IP100016339	RAB5C, member RAS oncogene family	RAB5C	NEPQNTGAPGR	0.68	1.35	1.01
IP100016339	RAB5C, member RAS oncogene family	RAB5C	GVDLQENNPASR	0.57	1.28	0.92
IP100016891	RAB6B, member RAS oncogene family	RAB6B	QITIEEGEQR	0.98	0.99	0.99
IP100030304	RAB6C, member RAS oncogene family, RAB6A, member RAS oncogene family, hypothetical	RAB6C	TDLADKR	0.97	0.97	0.97
IP100024775	RAB7, member RAS oncogene family-like 1	RAB7	VLQWSDYEIVR	1.11	1.10	1.11
IP100016342	RAB7A, member RAS oncogene family	RAB7A	FQSLGVAFYR	0.87	1.05	0.96
IP100016342	RAB7A, member RAS oncogene family	RAB7A	NNIPYFETSAK	0.76	1.21	0.99
IP100016342	RAB7A, member RAS oncogene family	RAB7A	EAINVEQAFQTIAR	0.89	0.97	0.93
IP100028481	RAB8A, member RAS oncogene family	RAB8A	NIEEHASADVEK	0.99	0.98	0.99
IP100028481	RAB8A, member RAS oncogene family	RAB8A	LALDYGIK	0.84	0.90	0.87
IP100028481	RAB8A, member RAS oncogene family	RAB8A	LEGNSPQGSNQGK	0.90	0.97	0.94
IP100024282	RAB8B, member RAS oncogene family	RAB8B	NIEEHASDVEK	0.94	0.95	0.95
IP100016372	RAB9A, member RAS oncogene family	RAB9A	QVSTEEAAQWCR	0.79	1.00	0.90
IP100016372	RAB9A, member RAS oncogene family	RAB9A	DATNVAAAFEEAVR	0.95	0.88	0.91

Ratio (arsenite/vehicle)					
Protein IPI	Full name	Gene name	Peptide sequence	Average ratios	
			F1	1/R	
IP100014603	RAB9B, member RAS oncogene family	RAB9B	VILGGGVGK	0.89	0.87
IP100014603	RAB9B, member RAS oncogene family	RAB9B	EFYIYADVK	0.87	0.84
IP100643041	RAN, member RAS oncogene family	RAN	FNVWDTAGQEK	0.92	0.88
IP100643041	RAN, member RAS oncogene family	RAN	VCEINIPVLCGNK	0.81	1.09
IP100643041	RAN, member RAS oncogene family	RAN	NLQYDIDSAK	0.90	0.91
IP100019345	RAP1A, member of RAS oncogene family	RAP1A	QWCNCAFLESSAK	0.93	0.94
IP100015148	RAP1B, member of RAS oncogene family	RAP1B	QWNCAFLESSAK	1.02	1.04
IP100019346	RAP2A, member of RAS oncogene family	RAP2A	VPVILVGNK	0.77	1.12
IP100019346	RAP2A, member of RAS oncogene family	RAP2A	ALAEWGPCPFMETSAK	0.78	1.39
IP100019346	RAP2A, member of RAS oncogene family	RAP2A	TMVDELFAEIVR	0.78	1.18
IP100018364	RAP2B, member of RAS oncogene family	RAP2B	ASVDELFAEIVR	1.15	1.23
IP100009607	RAP2C, member of RAS oncogene family	RAP2C	VPVILVGNK	0.93	0.94
IP100016669	Ras homolog enriched in brain	RHEB	ALAESWNAAFLESSAK	0.72	1.13
IP100016669	Ras homolog enriched in brain	RHEB	ENQTAVDVFR	0.77	1.14
IP100478231	ras homolog gene family, member A	RHOA	QEPV/KPEEGR	0.83	1.14
IP100478231	ras homolog gene family, member A	RHOA	IGAFGYM[+16.0]ECSAK	0.83	0.97
IP100478231	ras homolog gene family, member A	RHOA	IGAFGYMECSAK	0.84	0.89
IP100000041	ras homolog gene family, member B	RHOB	LVVVGDGACGK	0.63	0.53
IP100000041	ras homolog gene family, member B	RHOB	IQAYDYLECSAK	0.51	0.48
IP100000041	ras homolog gene family, member B	RHOB	EVFETATR	0.51	0.48
IP100027434	ras homolog gene family, member C	RHOC	ISAFGYLECSAK	0.95	1.24
IP100017342	ras homolog gene family, member G (rho G)	RHOG	TVNINLWDTAGQEEYDR	0.93	0.97
IP100017342	ras homolog gene family, member G (rho G)	RHOG	YLECSALQDQGVK	0.88	0.97
IP100010271	ras-related C3 botulinum toxin substrate 1 (rho family, Rac3) small GTP binding protein Rac1	RAC3	LTPITYPQGLAMAK	1.02	1.01
IP100010317	Ras-related GTP binding B	RRAGB	SIIFANYIAR	0.97	0.97
IP100012512	related RAS viral (r-ras) oncogene homolog 2; similar to related RAS viral (r-ras) oncogene homolog 2	RRAS2	LVVVGGGGVVK	0.80	1.22
IP100012512	related RAS viral (r-ras) oncogene homolog 2; similar to related RAS viral (r-ras) oncogene homolog 2	RRAS2	TGEGFLVFSVTDR	0.78	1.06
IP100012512	related RAS viral (r-ras) oncogene homolog 2; similar to related RAS viral (r-ras) oncogene homolog 2	RRAS2	QVTOEEGQQLAR	0.99	1.19
IP10001437	Rho family GTPase 3	RND3	IVVGDSCGK	1.10	1.06
IP100001437	Rho family GTPase 3	RND3	TALLHFAK	1.18	1.00
IP100015954	SAR1 homolog A (S. cerevisiae)	SAR1A	TDaiseek	0.89	0.89
IP100015954	SAR1 homolog A (S. cerevisiae)	SAR1A	EIFGLYQQTGK	0.77	0.92



Protein IPI	Full name	Gene name	Peptide sequence	Ratio (arsenite/vehicle)		
				F1	1/R	Average
IP100002149	SAR1 homolog B ( <i>S. cerevisiae</i> )	SAR1B	EMFGLYGGTTGK	0.90	0.92	0.91
IP100295098	signal recognition particle receptor, B subunit	SRPRB	AVLLVGLCDGSK	0.78	0.89	0.84
IP100295098	signal recognition particle receptor, B subunit	SRPRB	DTQTSITDSCAVYR	0.81	0.88	0.85
IP100295098	signal recognition particle receptor, B subunit	SRPRB	LIQQQLEK	0.91	0.79	0.85
IP100300096	similar to hCG1778032; RAB35, member RAS oncogene family	RAB35	TITSTYYR	0.90	0.96	0.93
IP100300096	similar to hCG1778032; RAB35, member RAS oncogene family	RAB35	WVETEDAYK	0.73	0.84	0.78
IP100300096	similar to hCG1778032; RAB35, member RAS oncogene family	RAB35	QQQQQQNDVVK	1.12	0.74	0.93
IP100003328	tripartite motif-containing 23	TRIM23	DALLIFANK	1.18	1.15	1.16
IP100000006	v-Ha-ras Harvey rat sarcoma viral oncogene homolog	HRAS	TGEGFLC/FAINNTK	1.03	1.00	1.02
IP100423568	v-Ki-ras2 Kirsten rat sarcoma viral oncogene homolog	KRAS4A	DSEDVPMV/LVGNK	1.18	1.20	1.19
IP100423570	v-Ki-ras2 Kirsten rat sarcoma viral oncogene homolog	KRAS4B	QGVDDAFYTLVR	1.18	1.22	1.20
IP100217519	v-ral simian leukemia viral oncogene homolog A (ras related)	RALA	GQNSLALHK	0.99	0.89	0.94
IP100217519	v-ral simian leukemia viral oncogene homolog A (ras related)	RALA	QVSVEEAK	0.80	1.08	0.94
IP100217519	v-ral simian leukemia viral oncogene homolog A (ras related)	RALA	AEQWNVVYVETSAK	0.75	1.04	0.90
IP100004397	v-ral simian leukemia viral oncogene homolog B (ras related; GTP binding protein)	RALB	GQSSLALHK	0.81	0.91	0.86
IP100004397	v-ral simian leukemia viral oncogene homolog B (ras related; GTP binding protein)	RALB	QV/PVEEAR	0.89	1.05	0.97
IP100004397	v-ral simian leukemia viral oncogene homolog B (ras related; GTP binding protein)	RALB	AEEWGVQYVETSAK	1.10	0.99	1.04
						0.96

**Western blot analysis validated differential expression of small GTPases in IMR90 cells upon arsenite exposure.**

Among the 87 quantified small GTPases, RhoB exhibited the most pronounced attenuation at the protein level after arsenite exposure (Fig. 4.1D). Hence, we decided to choose this protein for further study. We first conducted Western blot analyses of several small GTPases to confirm the relative protein expression levels of small GTPases in arsenite-treated over control cells observed from the targeted proteomic analysis. Our results showed that the protein expression levels of endogenous RhoB and ectopically expressed HA-RhoB were diminished substantially in IMR90 cells upon a 24 h exposure to 5  $\mu$ M NaAsO<sub>2</sub>, which is in line with the proteomic data (Fig. 4.2B). Moreover, we examined the protein expression levels of two other small GTPases, Rab31 and Rab32, under the same exposure conditions. The Western blot analysis again confirmed the findings made from the proteomics experiment, where the protein expression levels of Rab31 and Rab32 remain unchanged upon arsenite exposure (Fig. 4.S1).



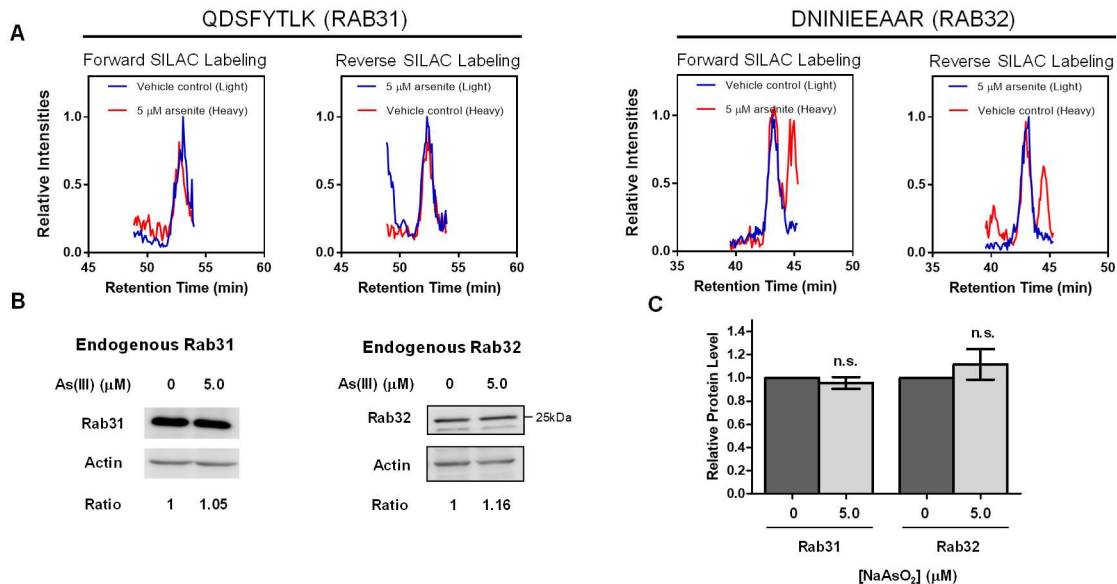


**Figure 4.S1. LC-MRM and Western blots revealed no appreciable change in levels of expression of Rab31 and Rab32 upon a 12 h exposure to 5  $\mu$ M NaAsO<sub>2</sub> in IMR90 cells.** (A) Extracted MRM traces for three transitions ( $y_6$ ,  $y_4$ , and  $y_3$ ) monitored for the  $[M+2H]^{2+}$  ( $m/z$  501.25) of a unique tryptic peptide from RAB31, i.e. QDSFYTLK, and for three transitions ( $y_7$ ,  $y_6$ , and  $y_4$ ) monitored for the  $[M+2H]^{2+}$  ( $m/z$  572.78) ion of a unique tryptic peptide from RAB32, i.e. DNINIEEAAR, with blue and red traces denoting MRM transitions for the light- and heavy-isotope labeled peptides respectively. (B) Western blot analysis confirmed the lack of change in the expression of endogenous Rab31 and Rab32 proteins upon a 24 h exposure to 5  $\mu$ M of NaAsO<sub>2</sub> in IMR90 lung fibroblast cells. (C) The quantification results of the relative expression of endogenous Rab31 and Rab32 proteins following exposure to 5  $\mu$ M NaAsO<sub>2</sub> ( $n=3$ ). Error bars represent standard deviations. The  $p$  values were calculated using unpaired two-tailed student's  $t$ -test, and the asterisks designate significant differences between arsenite-treated samples and untreated control (\*,  $0.01 \leq p < 0.05$ ; \*\*,  $0.001 \leq p < 0.01$ ; \*\*\*,  $p < 0.001$ ). n.s. represents no significant difference between arsenite-treated samples and untreated control.

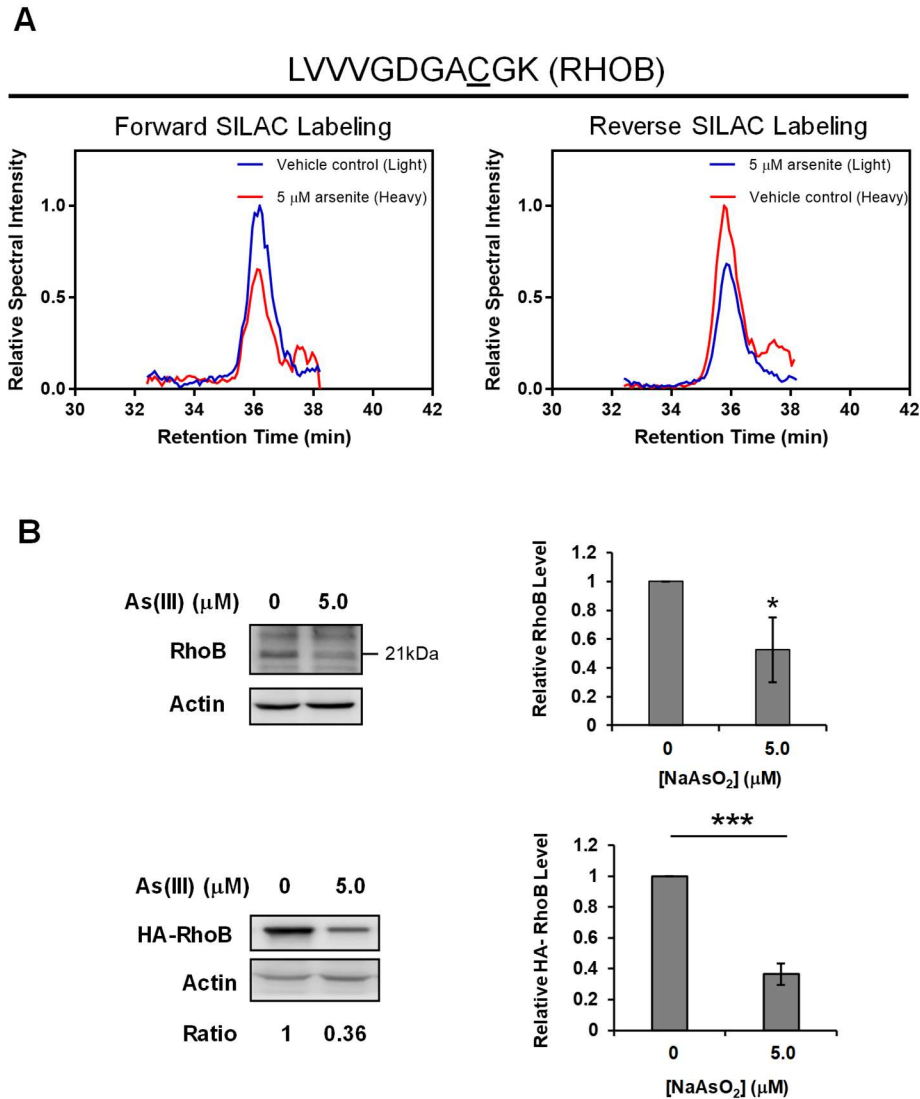


**Figure 4.2. LC-MRM and Western blot analyses revealed consistently lower levels of expression of RhoB upon a 12 h exposure to 5 μM NaAsO<sub>2</sub> in IMR90 cells.** (A) Extracted MRM traces for three transitions ( $y_9$ ,  $y_8$ , and  $y_7$ ) monitored for the  $[M+2H]^{2+}$  ion ( $m/z$  537.78) of a tryptic peptide from RhoB, i.e. LVVVGDGACGK (underlined ‘C’ designates carbamidomethylated Cys), with blue and red traces representing MRM transitions for the light- and heavy-isotope labeled forms of the peptide, respectively; (B) Western blot analysis confirmed the diminished expression of both endogenous and ectopically-expressed RhoB in IMR90 cells upon exposure to 5 μM of NaAsO<sub>2</sub> for 24 h. Shown are the quantification results for the relative levels of RhoB protein following exposure to 5 μM of NaAsO<sub>2</sub> obtained from Western blot analysis. Error bars represent standard deviations ( $n = 3$ ). The  $p$  values were calculated using unpaired two-tailed student’s  $t$ -test, and the asterisks designate significant differences between arsenite-treated samples and untreated control (\*,  $0.01 \leq p < 0.05$ ; \*\*,  $0.001 \leq p < 0.01$ ; \*\*\*,  $p < 0.001$ ).

**Arsenite exposure led to a dose-dependent decrease in the expression level of RhoB in IMR90, HEK293T, HeLa and GM00637 cells**

We next examined whether arsenite could induce a dose-dependent change in the expression level of RhoB. To this end, we exposed IMR90 cells with increasing concentrations (i.e. 0, 1, 2 and 5  $\mu\text{M}$ ) of  $\text{NaAsO}_2$  for 24 h, and assessed the levels of endogenous RhoB by Western blot analysis. The Western blot result showed a dose-dependent decrease in the endogenous RhoB protein (Fig. 4.3).

We also asked if this dose-dependent decrease in protein expression level of RhoB can be observed in other cell lines. Therefore, we exposed HEK293T cells, which were transfected with a plasmid for the ectopic expression of HA-RhoB, with increasing concentrations (i.e. 0, 1, 2 and 5  $\mu\text{M}$ ) of  $\text{NaAsO}_2$  for 24 h, and assessed the levels of HA-RhoB by Western blot analysis. Our results revealed a dose-dependent decrease in the level of RhoB protein (Fig. 4.3). Similar findings were also made for HeLa human cervical cancer cells and GM00637 human skin fibroblast cells (Fig. 4.3).

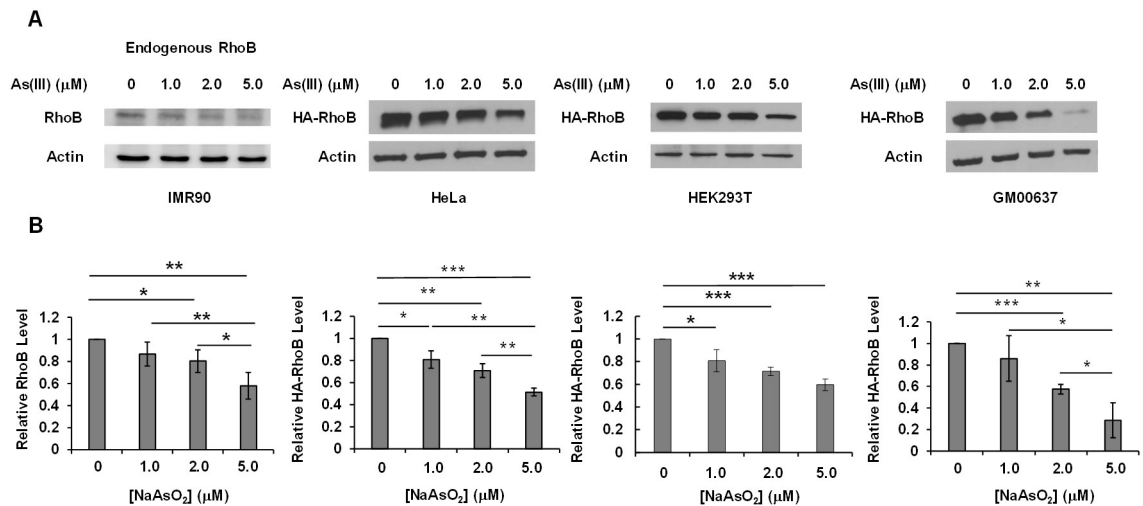


**Figure 4.3. Arsenite treatment results in a dose-dependent decrease in both endogenous and ectopically expressed RhoB proteins.** (A) Western blot images showing the effect of 24 h treatment with different doses of arsenite (0, 1, 2, and 5 μM) on expression level of endogenous RhoB protein in IMR90 cells and ectopically-expressed RhoB protein in HeLa, HEK293T and GM00637 cells. (B) The quantification results of the relative levels of endogenous and ectopically-expressed RhoB protein in the four cell lines as shown in (A) following exposure to different doses of NaAsO<sub>2</sub>. Error bars represent standard deviations (n = 3). The *p* values were calculated using unpaired two-tailed student's *t*-test, and the asterisks designate significant differences between arsenite-treated samples and untreated control (\*, 0.01 ≤ *p* < 0.05; \*\*, 0.001 ≤ *p* < 0.01; \*\*\*, *p* < 0.001).

### Proteasomal degradation is involved in the arsenite-induced decline in the protein level of RhoB

We also explored the mechanism through which arsenite induces the decrease in RhoB protein level by asking whether the ubiquitin-proteasome pathway is involved. To this end, we treated HA-RhoB-overexpressing HEK293T cells with 0, 2, or 5 μM of NaAsO<sub>2</sub> together with 4 μM MG132. As depicted in Fig. 4.4, we found that MG132 treatment could augment the HA-RhoB protein level significantly when compared with the untreated control group. Importantly, the arsenite-induced decrease in HA-RhoB protein was abolished in cells co-treated with MG132 (Fig. 4.4). Thus, arsenite induces the decrease in HA-RhoB protein through promoting its degradation via the ubiquitin-proteasome pathway (Fig. 4.5).

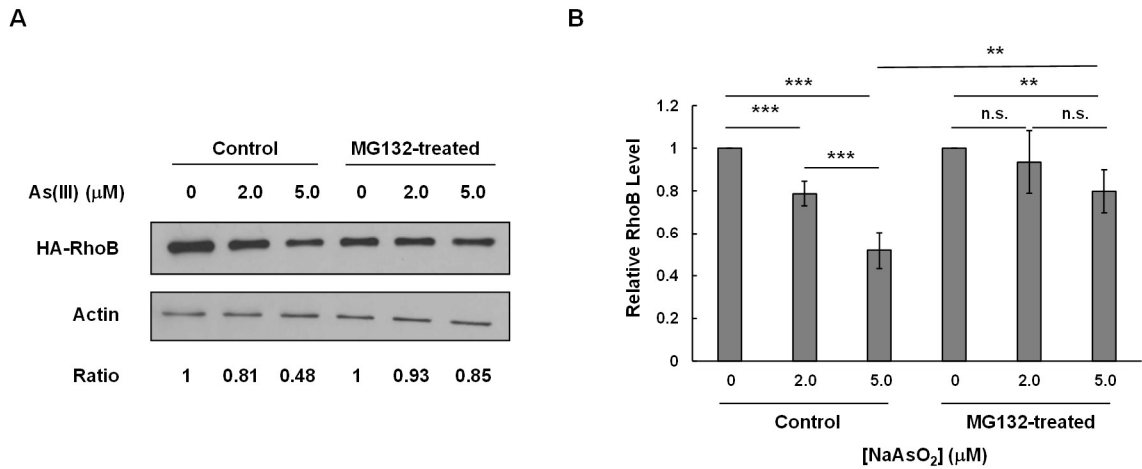


**Figure 4.4. Exposure to arsenite induces proteasomal degradation of RhoB.** (A) Co-treatment of HEK293T cells with 4  $\mu\text{M}$  MG132 together with different doses of NaAsO<sub>2</sub> (0, 2, and 5  $\mu\text{M}$ ) for 24 h could abolish the dose-dependent decrease of RhoB protein induced by arsenite exposure. (B) Relative protein level of HA-RhoB upon treatment with different doses of NaAsO<sub>2</sub> together with MG132 or DMSO control (n = 3). The *p* values were calculated using unpaired two-tailed student's *t*-test, and the asterisks designate significant differences between the arsenite-treated samples and untreated control (\*, 0.01  $\leq p < 0.05$ ; \*\*, 0.001  $\leq p < 0.01$ ; \*\*\*,  $p < 0.001$ ). n.s. represents no significant difference between arsenite-treated samples and untreated control.

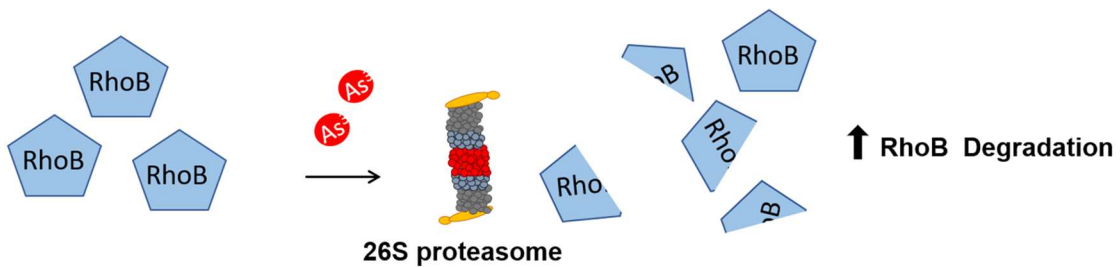


**Figure 4.5. Arsenite exposure diminishes the protein expression level of RhoB through enhancing its proteasomal degradation.**

## Discussion

### Targeted quantitative measurement of small GTPases in arsenite-treated lung fibroblast cells

Increasing body of evidence from cellular, animal and epidemiological studies support that small GTPases, particularly Rho GTPases, play critical roles in the initiation, progression and

metastatic transformation of human cancer.<sup>12,13,27,28</sup> Rho GTPases can serve as key molecular “switches” regulating cell motility, migration, invasion and proliferation.<sup>27,29</sup> Moreover, arsenic is well known for its carcinogenic effect.<sup>6</sup> Hence, we sought to investigate systematically the differential expression of small GTPases upon arsenite exposure, with the goal of gaining a mechanistic understanding about how arsenite exposure influences small GTPase signaling.

Our LC-MRM-based targeted quantitative proteomics method consistently detected the majority of small GTPases and revealed substantially changed expression of a number of small GTPases in IMR90 cells upon exposure to arsenite. Together with metabolic labeling by SILAC and fractionation by SDS-PAGE, the method facilitated unbiased and reproducible quantification of 87 small GTPases in arsenite-/vehicle-treated IMR90 cells. Compared to conventional DDA analysis, the MRM-based approach exhibits greater reproducibility, higher sensitivity and increased throughput for the detection of small GTPases. We envision that this high-throughput and highly reliable method can be generally applicable for detecting and studying the protein expressions of small GTPases that are changed upon exposure to other environmental agents.

#### **Potential Roles of RhoB and Rab15 in arsenite-induced initiation of malignant transformation in lung fibroblast cells**

Our targeted quantitative proteomics results showed that several small GTPases, including RhoB and Rab15, have altered protein expression levels in IMR-90 cells upon arsenite treatment. We further validated, by using Western blot analysis, that arsenite can induce the decrease in the levels of endogenous RhoB protein in IMR90 cells and ectopically expressed RhoB protein in IMR90, HEK293T, HeLa, and GM00637 cells (Fig. 4.2 and 4.3). We also found that the arsenite-stimulated decrease of RhoB protein expression in HEK293T cells involves the 26S proteasome.

During the early stage (i.e. initiation) of the arsenite-induced malignant transformation, cells begin to exhibit several hallmarks of cancer, including enhanced cell proliferation and autonomous

cell growth.<sup>30,31</sup> In addition, arsenic was found to perturb an array of signaling pathways including the PI3K/AKT pathway, which involves proteins that enhance cell growth, metabolism, survival and proliferation.<sup>24</sup> Down-regulation of RhoB is known to promote the migration and invasion of human bronchial epithelial cells through activation of AKT1 and involvement of Rac1,<sup>32</sup> and also can induce Rac1-dependent epithelial-mesenchymal transition in lung cells through inhibition of PP2A.<sup>33</sup> Hence, our quantitative proteomics data, together with previous findings, support the notion that arsenic may promote tumor progression, in part, by suppressing the RhoB-AKT-Rac1 pathway. Additionally, PI3K/AKT/mTOR pathway is commonly activated in non-small-cell lung cancer that constitutes more than 80% of worldwide lung cancer incidents.<sup>34,35</sup> Furthermore, RhoB is known to regulate negatively the migration and invasion of lung tissues through the AKT pathway.<sup>36</sup> However, the upstream target through which arsenic exposure induces the activation of PI3K/AKT/mTOR pathway remains unclear. Hence, our discovery of arsenic-induced proteasomal degradation of RhoB might shed light on understanding how low-dose arsenic exposure could activate the PI3K/AKT/mTOR pathway, which is critical for lung oncogenesis.

It is worth noting that our quantitative proteomic experiment also led to observation of a markedly augmented expression of Rab15 protein in IMR90 cells upon arsenite exposure (Fig. 4.1D). Rab15 protein was previously shown to be a component of the IFT-B complex responsible for anterograde ciliary protein trafficking inside primary cilium.<sup>37,38</sup> Primary cilia function to sense diverse extracellular signals through a network of surface receptors on the ciliary membrane and play important roles in interpreting extracellular signals and regulating cell homeostasis by modulating different intracellular signaling pathways,<sup>37,39</sup> including the Hedgehog signaling pathway in vertebrates.<sup>38,39</sup> Exposure to environmental arsenic could activate Hedgehog signaling, whose dysregulation may contribute to arsenic-induced tumorigenesis.<sup>40</sup> It will be important to

investigate whether and how the arsenite-elicited up-regulation of Rab15 protein contributes to arsenic toxicity and carcinogenicity.

### **Implications in environmental exposure to arsenic**

It was estimated that more than 150 million people in the world are exposed to inorganic arsenic in groundwater, in the concentration range of < 1 ppb (mostly) to 5300 ppb (in certain regions).<sup>3,41</sup> In addition, multiple lines of evidence support that chronic exposure to low dose of arsenic species is strongly associated with malignancies including lung and skin cancers.<sup>7,8,42-45</sup> Therefore, it is imperative for us to understand comprehensively how long-term exposure to low levels of arsenite increases cell proliferation and hence augment the likelihood of the onset of malignant transformation. On the basis of the findings made from the present study, we propose that the onset of malignant transformation elicited by chronic, low-dose exposure to arsenic could be partly attributed to persistent induction of signaling pathways controlling cell cycle progression including the RhoB-Rac1 axis in PI3K/AKT signaling. In this context, it is worth noting that the present study was conducted under conditions of acute exposure of cultured human cells to a relatively high concentration of arsenite (5  $\mu$ M). It will be important to examine, in the future, whether the findings made in the present study can be extended to chronic exposure to low doses of arsenic species. Last but not the least, growing body of literature supports the linkage between chronic arsenite exposure around the threshold concentration and the increased rates of arsenite-induced carcinogenesis in the exposed populations.<sup>46</sup> Therefore, US EPA should improve the current regulatory standard of arsenite in drinking water (10 ppb which is equivalent to 77 nM) to safeguard the public health.



## References:

1. Argos, M., Ahsan, H., and Graziano, J.H. (2012). Arsenic and human health: epidemiologic progress and public health implications. *Rev. Environ. Health*. 27:191-195.
2. Naujokas, M.F., Anderson, B., Ahsan, H., Aposhian, H.V., Graziano, J.H., Thompson, C., and Suk, W.A. (2013). The broad scope of health effects from chronic arsenic exposure: Update on a worldwide public health problem. *Environ. Health Perspect*. 121:295-302.
3. Chen, S.J., Zhou, G.B., Zhang, X.W., Mao, J.H., De Thé, H., and Chen, Z. (2011). From an old remedy to a magic bullet: Molecular mechanisms underlying the therapeutic effects of arsenic in fighting leukemia. *Blood* 117:6425-6437.
4. Bissen, M., and Frimmel, F.H. (2003). Arsenic – A Review. Part I: Occurrence, Toxicity, Speciation, Mobility. *Acta. Hydrochim. Hydrobiol*. 31:9-18.
5. Hughes, M.F. (2002). Arsenic toxicity and potential mechanisms of action. *Toxicol. Lett*. 133:1-16.
6. Ravenscroft, P., Brammer, H., and Richards, K. (2009). Arsenic Pollution: A Global Synthesis. Wiley-Blackwell, UK.
7. Shen, S., Li, X., Cullen, W.R., Weinfeld, M., and Le, X.C. (2013). Arsenic Binding to Proteins. *Chem. Rev*. 113:1-48.
8. Kumar, A., Adak, P., Gurian, P.L., and Lockwood, J.R. (2010). Arsenic exposure in US public and domestic drinking water supplies: A comparative risk assessment. *J. Expo. Sci. Environ. Epidemiol*. 20:245-254.
9. Martinez, V.D., Vucic, E.A., Becker-Santos, D.D., Gil, L., and Lam, W.L. (2011). Arsenic exposure and the induction of human cancers. *J. Toxicol*. 2011:431287.
10. Hartwig, A., Blessing, H., Schwerdtle, T., and Walter, I. (2003). Modulation of DNA repair processes by arsenic and selenium compounds. *Toxicol*. 193:161-167.
11. Arita, A., and Costa, M. (2009). Epigenetics in metal carcinogenesis: Nickel, Arsenic, Chromium and Cadmium. *Metallomics* 1:222-228.
12. Porter, A.P., Papaioannou, A., and Malliri, A. (2016). Deregulation of Rho GTPases in cancer. *Small GTPases* 7:123-138.
13. Alan, J.K., and Lundquist, E.A. (2013). Mutationally activated Rho GTPases in cancer. *Small GTPases* 4:159-163.
14. Delprato, A. (2012). Topological and Functional Properties of the Small GTPases Protein Interaction Network. *PLoS One* 7:e44882.

15. Zandvakili, I., Lin, Y., Morris, J.C., and Zheng, Y. (2017). Rho GTPases: Anti- or Pro-neoplastic Targets? *Oncogene* 36:3213-3222.
16. Heck, A.J., and Krijgsveld, J. (2004). Mass spectrometry-based quantitative proteomics. *Expert Rev. Proteomics* 1:317-326.
17. Aebersold, R., and Mann, M. (2003). Mass spectrometry-based proteomics. *Nature* 537:347-355.
18. Zhang, C.C., Li, R., Jiang, H., Lin, S., Rogalski, J.C., Liu, K., and Kast, J. (2015). Development and application of a quantitative multiplexed small GTPase activity assay using targeted proteomics. *J. Proteome Res.* 14:967-976.
19. Marelli, M., Smith, J.J., Jung, S., Yi, E., Nesvizhskii, A.I., Christmas, R.H., Saleem, R.A., Tam, Y.Y.C., Fagarasanu, A., Goodlett, D.R., Aebersold, R., Rachubinski, R.A., and Aitchison, J.D. (2004). Quantitative mass spectrometry reveals a role for the GTPase Rho 1 p in actin organization on the peroxisome membrane. *J. Cell Biol.* 167:1099-1112.
20. Huang, M., Qi, T.F., Li, L., Zhang, G., and Wang, Y. (2018). A targeted quantitative proteomic approach assesses the reprogramming of small GTPases during melanoma metastasis. *Cancer Res.* 78:5431-5445.
21. Lebowitz, P., Davide, J., and Prendergast, G.C. (1995). Evidence that farnesyltransferase inhibitors suppress Ras transformation by interfering with Rho activity. *Mol. Cell Biol.* 15:6613-6622.
22. Mandik-Nayak, L., DuHadaway, J.B., Mulgrew, J., Pigott, E., Manley, K., Sedano, S., Prendergast, G.C. and Laury-Kleintop, L.D. (2017). RhoB blockade selectively inhibits autoantibody production in autoimmune models of rheumatoid arthritis and lupus. *Dis. Model Mech.* 10:1313-1322.
23. An, Y., Liu, T., Liu, X., Zhao, L., and Wang, J. (2016). Rac1 and Cdc42 Play Important Roles in Arsenic Neurotoxicity in Primary Cultured Rat Cerebellar Astrocytes. *Biol. Trace Elem. Res.* 170:173-82.
24. Hubaux, R., Becker-Santos, D. D., Enfield, K. S., Rowbotham, D., Lam, S., Lam, W. L., Martinez, V. D. (2013). Molecular features in arsenic-induced lung tumors. *Mol. Cancer* 12:20.
25. Prieto-Dominguez, N., Parnell, C., and Teng, Y. (2019). Drugging the Small GTPase Pathways in Cancer Treatment: Promises and Challenges. *Cells* 8:255.
26. Escher, C., Reiter, L., MacLean, B., Ossola, R., Herzog, F., Chilton, J., MacCoss, M. J., and Rinner, O. (2012). Using iRT, a normalized retention time for more targeted measurement of peptides. *Proteomics* 12:1111-1121.
27. Haga, R.B., and Ridley, A.J. (2016). Rho GTPases: Regulation and roles in cancer cell biology. *Small GTPases.* 7:207-221.

28. Kazanietz, M.G., and Caloca, M.J. (2017). The Rac GTPase in cancer: From old concepts to new paradigms. *Cancer Res.* 77:5445-5451.
29. Cardama, G.A., Gonzalez, N., Maggio, J., Lorenzano Menna, P., and Gomez, D.E. (2017). Rho GTPases as therapeutic targets in cancer. *Int. J. Oncol.* 51:1025-1034.
30. Hanahan, D., and Weinberg, R.A. (2000). The hallmarks of cancer. *Cell* 100:57-70.
31. Cooper, G.M. (2000). *The Cell: A Molecular Approach*. 2nd Edition. Sunderland (MA): Sinauer Associates; 2000.
32. Bousquet, E., Mazières, J., Privat, M., Rizzati, V., Casanova, A., Ledoux, A., Mery, E., Coudere, B., Gavre, G., and Pradines, A. (2009). Loss of RhoB expression promotes migration and invasion of human bronchial cells via activation of AKT1. *Cancer Res.* 69:6092-6099.
33. Bousquet, E., Calvayrac, O., Mazières, J., Lajoie-Mazenc, I., Boubekeur, N., Favre, G., and Pradines, A. (2016). RhoB loss induces Rac1-dependent mesenchymal cell invasion in lung cells through PP2A inhibition. *Oncogene* 35:1760-1769.
34. Cheng, H., Shcherba, M., Pendurti, G., Liang, Y., Piperdi, B., and Perez-Soler, R. (2014). Targeting the PI3K/AKT/mTOR pathway: potential for lung cancer treatment. *Lung Cancer Manag.* 3:67-75.
35. Pérez-Ramírez, C., Cañadas-Garre, M., Molina, M.Á., Faus-Dáder, M.J. and Calleja-Hernández, M.Á. (2015). PTEN and PI3K/AKT in non-small-cell lung cancer. *Pharmacogenomics* 16:1843-1862.
36. Jiang, K., Sun, J., Cheng, J., Djeu, J.Y., Wei, S., and Sebt, S. (2004). Akt mediates Ras downregulation of RhoB, a suppressor of transformation, invasion, and metastasis. *Mol. Cell Biol.* 24:5565-5576.
37. Yuan, X., Serra, R.A., and Yang, S. (2015). Function and regulation of primary cilia and intraflagellar transport proteins in the skeleton. *Ann. N. Y. Acad. Sci.* 1335:78-99.
38. Lechtreck, K.F. (2015). IFT-cargo interactions and protein transport in cilia. *Trends Biochem. Sci.* 40:765-778.
39. Wang, L., and Dynlacht, B.D. (2018). The regulation of cilium assembly and disassembly in development and disease. *Development* 145:dev151407.
40. Fei, D.L., Li, H., Kozul, C.D., Black, K.E., Singh, S., Gosse, J.A., DiRenzo, J., Martin, K.A., Wang, B., Hamilton, J.W., Karagas, M.R., and Robbins, D.J. (2010). Activation of Hedgehog signaling by the environmental toxicant arsenic may contribute to the etiology of arsenic induced tumors. *Cancer Res.* 70:1981-1988.

41. Smedley, P.L., and Kinniburgh, D.G. (2000). Source and behaviour of arsenic in natural waters. *Br. Geol. Surv.* 2000:61.
42. Person, R.J., Ngalame, N.N.O., Makia, N.L., Bell, M.W., Waalkes, M.P., and Tokar, E.J. (2015). Chronic inorganic arsenic exposure in vitro induces a cancer cell phenotype in human peripheral lung epithelial cells. *Toxicol. Appl. Pharmacol.* 286:36-43.
43. Stueckle, T.A., Lu, Y., Davis, M.E., Wang, L., Jiang, B., Holaskova, I., Schafer, R., Barnette, J.B., and Rojanasakui, Y. (2012). Chronic occupational exposure to arsenic induces carcinogenic gene signaling networks and neoplastic transformation in human lung epithelial cells. *Toxicol. Appl. Pharmacol.* 261:204-216.
44. Yoshida, T., Yamauchi, H., and Sun, G.F. (2004). Chronic health effects in people exposed to arsenic via the drinking water: Dose-response relationships in review. *Toxicol. Appl. Pharmacol.* 198:243-252.
45. Reichard, J.F., Schnekenburger, M., and Puga, A. (2007). Long term low-dose arsenic exposure induces loss of DNA methylation. *Biochem. Biophys. Res. Commun.* 352:188-192.
46. Schmidt, C.W. (2014). Low-dose arsenic in search of a risk threshold. *Environ. Health Perspect.* 122:130-134.

## Chapter 5

### Conclusions and Future Directions

Inorganic arsenic is a metalloid widely distributed in the environment partly due to the natural occurrence from arsenic-containing minerals. The concern about arsenic toxicity has increased because arsenic pollution influences more than 200 million people in over 70 countries worldwide through contaminated drinking water. In particular, the unprecedented large-scale arsenic pollution in Bangladesh involving at least 65 million people makes arsenic-contaminated drinking water a leading global public health issue.<sup>1</sup> Due to high hydrophilicity, inorganic arsenite from both natural and anthropogenic sources can concentrate in the hydrosphere including the groundwater mostly used for drinking. Given that an average daily water intake of 1.6 L/day in the US and an average arsenic level of 2.5 µg/L in water, those individuals who are chronically exposed to arsenic through contaminated drinking water have significantly higher lifetime risk of suffering from the onset of cancer and other age-associated human diseases later in their life.<sup>2</sup>

As inorganic arsenic is considered as a universal toxicant, it is thought to induce a series of human diseases by interfering with a plethora of important signal transduction pathways.<sup>3,4</sup> Arsenic exposure may accelerate the natural processes of aging, with two potential mechanisms being through inhibiting DNA repair machinery and via perturbing various arms of the proteostasis network. Every step of genetic information flow from replicating correct genetic codes in DNA to ensuring translation fidelity for the correct three-dimensional protein folding is heavily and strictly regulated to prevent stochastic error.<sup>5-8</sup> If these vital processes are dysregulated or disrupted, numerous gene mutations and erroneous translation products can be generated, which can promote aging and age-associated protein misfolding disorders, including neurodegenerative diseases and cancers.<sup>9-12</sup> Therefore, researchers identify DNA repair and protein quality control particularly

important for understanding the environmental influence on the proteostasis network and its consequent induction of age-related human diseases.

The proteostasis network, which mainly consists of ribosome quality control (RQC), ubiquitin-proteasome system (UPS) and autophagy, involves a plethora of cross-talks among various components of protein quality control pathways, ranging from sensing stress during protein synthesis, labeling misfolded proteins, degrading aberrant mRNA templates, to eliminating misfolded proteins.<sup>10,13,14</sup> Therefore, numerous regulatory proteins and post-translational modifications are necessary to coordinate the quality control of DNA replication and protein synthesis, especially the involvement of essential mineral zinc and zinc-binding proteomes. Genes encoding zinc-binding proteins, including zinc finger-containing enzymes, constitute approximately 10% of the human genome, indicating the necessity of the zinc proteome in various critical cellular processes.<sup>15-18</sup> However, exposure to arsenic was proposed to inhibit zinc finger proteins through binding to the zinc finger motifs critical for their structures and functions.<sup>18-20</sup> As a result, it is urgent and necessary to understand how exposure to arsenic impairs DNA repair and proteostasis through disrupting the PTMs mediated by zinc finger proteins, which is the focus of my PhD work.

The primary goals of this dissertation were to characterize the toxicity of inorganic arsenite *in vitro* and in human cells, and to elucidate the molecular mechanisms underlying the potential induction of age-associated proteinopathies, particularly cancer and neurological diseases. Specifically, the objectives were four-fold: 1. To characterize the molecular interaction between  $\text{As}^{3+}$  and  $\text{Zn}^{2+}$ -binding cysteine residues of zinc finger proteins; 2. To evaluate the effect of  $\text{As}^{3+}$ -cysteine interaction in zinc finger proteins on their corresponding enzymatic activities as reflected by post-translational modifications of their substrates; 3. To investigate the cellular toxicity of  $\text{As}^{3+}$  through disruption of important PTMs in human cells; 4. To examine the potential pathogenesis of

proteinopathies induced by As<sup>3+</sup>-elicited disruption of proteostasis. These studies were all performed in cultured human cells, i.e. HEK293T, HeLa, GM00637 and IMR90 cell lines.

Arsenic has been proposed to induce protein misfolding, and also facilitate the onset of age-associated proteinopathies, such as neurodegenerative disorders.<sup>21,22</sup> In order to examine the effect of arsenite exposure on proteostasis, the effect of arsenite on the E3 ubiquitin ligase ZNF598, which is central in the RQC pathway, was investigated. As<sup>3+</sup> was shown, based on biotin-As pull-down and ReAsH fluorescent labeling experiments, to interact with critical cysteine residues in the RING finger motif of ZNF598. We demonstrated, by using LC-MS/MS analysis, that As<sup>3+</sup> exposure conferred diminutions in site-specific ubiquitinations of regulatory ribosomal protein subunits RPS10 and RPS20. By studying how As<sup>3+</sup> alters the resolution of ribosomal stalling, the arsenic-induced decrease in ubiquitination activity of ZNF598 was shown to enhance the readthrough of poly-(A) mRNA stall sequence, thus lowering the efficiency of ribosomal stalling and of RQC pathway to eliminate default mRNAs and aberrant polypeptide chains. Therefore, the work in Chapter 2 supports that arsenic may result in translation infidelity through impairing RQC machinery in the proteostasis network, which might help explain the observed protein misfolding upon As<sup>3+</sup> exposure.<sup>21</sup>

In addition to arsenic-induced proteotoxicity, the epigenotoxicity of arsenite on TIP60 histone acetyltransferase was examined. We found that arsenite could bind to critical cysteine residues responsible for zinc coordination within the zinc finger motif of TIP60 (i.e. C263, C266, C283), based on the site-directed mutagenesis and biotin-As pull-down experiment. Hence, arsenite was shown to diminish, in a dose-dependent manner, the protein level of TIP60 by proteasomal degradation while it does not attenuate the histone acetyltransferase activity of TIP60. Finally, the experiment utilizing *TIP60* knockout HEK293T cells showed that TIP60 is partly responsible for arsenite-elicited dose-dependent diminution of H4K16Ac, which offers a plausible mechanism

through which arsenite exposure induces chromatin compaction, thereby prohibiting the access of DNA damage sites by DNA repair enzymes. Therefore, Chapter 3 suggests a molecular mechanism underlying arsenic-elicited carcinogenesis, i.e. through disruption of H4K16Ac by As<sup>3+</sup> binding to TIP60, aside from binding to hMOF.<sup>23</sup>

Apart from zinc finger proteins involved in proteostasis and DNA repair, small GTPases are crucial in regulating signaling cascades, especially in cellular protein transport and dynamics. We utilized a targeted quantitative proteomic method to investigate whether acute As<sup>3+</sup> exposure influences the protein expression levels of small GTPases. The proteomic results showed that exposure to 5  $\mu$ M As<sup>3+</sup> led to a  $\sim$  40% decrease in RhoB protein level, which was later validated by Western blot in several human cell lines. This As<sup>3+</sup>-induced decrease in RhoB protein level was due to enhanced proteasomal degradation of RhoB, implying the influence of As<sup>3+</sup> on UPS of the proteostasis network. The findings made from Chapter 4 are in accordance with the recent observation that As<sup>3+</sup> impairs segregase p97 and proteasome in the UPS.<sup>24</sup>

These studies were the first to show the As<sup>3+</sup>-elicited impairment of degradation capacity of the proteostasis network by decreasing the efficiency of RQC and UPS, and to show the epigenotoxicity of As<sup>3+</sup> by diminishing the histone acetyltransferase activity of TIP60. However, the studies were conducted under the conditions of acute As<sup>3+</sup> exposure (i.e. 24-hr), which do not recapitulate the real-life environmental exposure to As<sup>3+</sup>. Therefore, future studies should focus on the sub-chronic and chronic exposure (i.e. months to 1 year) to environmentally relevant concentrations of As<sup>3+</sup> (ideally lower than 1  $\mu$ M) to better assess the chronic arsenite toxicity in most contaminated regions in the world.



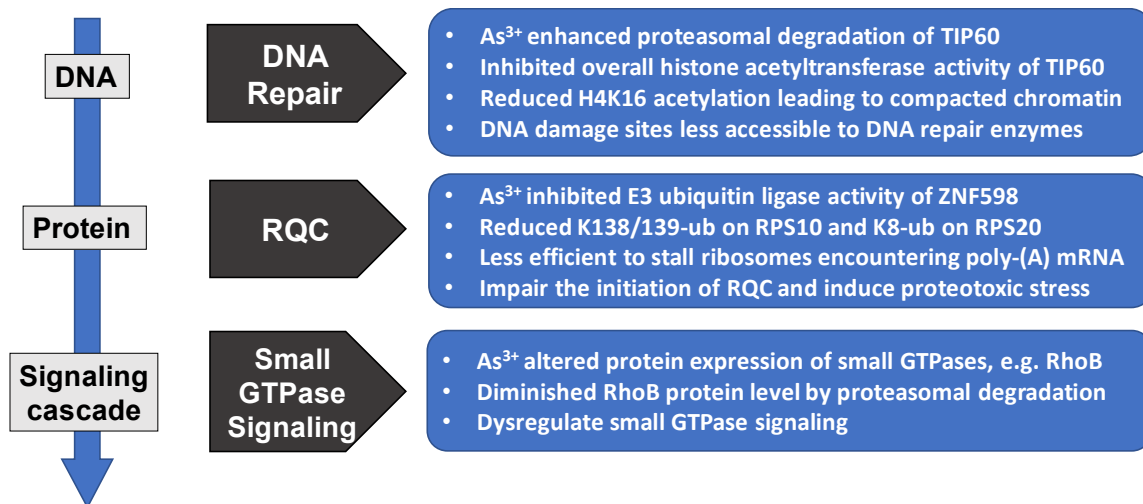


**Figure 5.1.** Summary of the conclusions from Chapters 2-4.

In summary, we found that arsenite exposure could lead to dose-dependent disruptions of DNA repair and proteostasis in cultured human cells (Fig. 5.1.). These results suggest the importance in identifying the major targets in the proteostasis network upon arsenite exposure and understanding how this leads to  $As^{3+}$ -induced protein misfolding. Oxidative stress has been proposed as the major mechanism underlying the toxicity of arsenic exposure.<sup>25-28</sup> However, a recent study suggested that chronic low-level arsenite exposure primarily induces proteotoxic stress instead of oxidative stress.<sup>29</sup> Additionally, most aging-associated human diseases are attributed to a progressive decline in degradation capacity of the proteostasis network,<sup>30</sup> which might explain the gradual deterioration of cellular defense against oxidative stress over the lifetime of humans.<sup>31</sup> In RQC of the proteostasis network, listerin, TRIP4 and Not4 are also C3H- or C4- type zinc finger proteins which can be targeted by arsenite binding. The questions about whether these three proteins can be inhibited by chronic low-level exposure to inorganic arsenic remain to be resolved for understanding how iAs exposure facilitates the generation of misfolded proteins. In particular, listerin which are responsible for the proteolytic polyubiquitination of defective nascent translation products.<sup>32</sup> Due

to the prevalence of arsenic contamination worldwide, it is urgent and important to explore whether arsenic exposure accelerates the natural processes of ageing. After this hypothesis is validated, we next need to focus on potential targets and mechanisms for iAs-accelerated aging process. For example, given the observation of premature aging in patients deficient of certain DNA repair genes (e.g. that of WRN RecQ helicase in Werner syndrome),<sup>33</sup> it raises the possibility that exposure to iAs accelerates aging through inducing genomic instability. Apart from zinc finger proteins and small GTPase signaling, kinase signaling (i.e. ATP-binding proteins) is also one of important protein targets that can be impaired by iAs exposure. Tyrosine phosphorylation system is extremely important in modulating DNA repair<sup>34</sup> and proteostasis;<sup>35-37</sup> therefore, future research should be conducted to unveil the potential targets of iAs in kinases signaling cascade.

Apart from arsenic, further studies are needed to consider the role of environmental exposure to carcinogenic metals, as well as daily diet, in modulating proteostasis. This is particularly critical in determining whether the environmental risk factors can accelerate the aging process and protein misfolding, which is believed to account for the etiology of approximately 50% of human diseases.<sup>38</sup> Finally, there is an increasing body of literature supporting the combined roles of aging and diminished proteostasis in the pathogenesis of aging-related human diseases. Therefore, understanding the molecular mechanisms of arsenic toxicity revealed from research presented in this dissertation will inform future work in environmental gerontology.

## References:

1. Hossain, M.F. Arsenic contamination in Bangladesh - An overview. *Agric. Ecosyst. Environ.* 2006;113:1-16.
2. Smith, A.H., Hopenhayn-Rich, C., Bates, M.N., et al. Cancer risks from arsenic in drinking water. *Environ. Health Perspect.* 1992;97:259-267.
3. Stueckle, T.A., Lu, Y., Davis, M.E., et al. Chronic occupational exposure to arsenic induces carcinogenic gene signaling networks and neoplastic transformation in human lung epithelial cells. *Toxicol. Appl. Pharmacol.* 2012;261:204-216.
4. Martinez, V.D., Vucic, E.A., Becker-Santos, D.D., Gil, L., and Lam, W.L. Arsenic exposure and the induction of human cancers. *J. Toxicol.* 2011;2011.
5. Simms, C.L., and Zaher, H.S. Quality control of chemically damaged RNA. *Cell. Mol. Life Sci.* 2016;73:3639-3653.
6. Cochella, L., and Green, R. Fidelity in protein synthesis. *Curr. Biol.* 2005;15:536-540.
7. Ogle, J.M., and Ramakrishnan, V. Structural Insights Into Translational Fidelity. *Annu. Rev. Biochem.* 2005;74:129-177.
8. Zaher, H.S., and Green, R. Fidelity at the Molecular Level: Lessons from Protein Synthesis. *Cell* 2009;136:746-762.
9. van Drie, J.H. Protein folding, protein homeostasis, and cancer. *Chin. J. Cancer* 2011;30:124-137.
10. Klaips, C.L., Jayaraj, G.G., and Hartl, F.U. Pathways of cellular proteostasis in aging and disease. *J. Cell. Biol.* 2018;217:51-63.
11. Sweeney, P., Park, H., Baumann, M., et al. Protein misfolding in neurodegenerative diseases: Implications and strategies. *Transl Neurodegener.* 2017;6:1-13.
12. Dubnikov, T., Ben-Gedalya, T., and Cohen, E. Protein quality control in health and disease. *Cold Spring Harb. Perspect. Biol.* 2017;9: a023523.
13. Sontag, E.M., Samant, R.S., and Frydman, J. Mechanisms and Functions of Spatial Protein Quality Control. *Annu. Rev. Biochem.* 2017;86:97-122.
14. Balchin, D., Hayer-Hartl, M., and Hartl, F.U. In vivo aspects of protein folding and quality control. *Science* 2016;353: aac4354.
15. Element, K. Zinc Biochemistry : From a Single Zinc Enzyme to a key element of life. *Adv. Nutr.* 2013;4:82-91.

16. Andreini, C., Banci, L., Bertini, I., and Rosato, A. Counting the zinc-proteins encoded in the human genome. *J. Proteome Res.* 2006;5:196-201.
17. Andreini, C., Banci, L., Bertini, I., and Rosato, A. Zinc through the three domains of life. *J. Proteome Res.* 2006;5:3173-3178.
18. Laity, J.H., Lee, B.M., and Wright, P.E. Zinc finger proteins: new insights into structural and functional diversity. *Curr. Opin. Struct. Biol.* 2001;11:39-46.
19. Hartwig, A. Zinc Finger Proteins as Potential Targets for Toxic Metal Ions: Differential Effects on Structure and Function. *Antioxid. Redox Signal.* 2001;3:625-634.
20. Shen, S., Li, X., Cullen, W.R., Weinfeld, M., and Le, X.C. Arsenic Binding to Proteins. *Chem. Rev.* 2013;113:1-48.
21. Jacobson, T., Navarrete, C., Sharma, S.K., et al. Arsenite interferes with protein folding and triggers formation of protein aggregates in yeast. *J. Cell Sci.* 2012;125:5073-5083.
22. O'Bryant, S.E., Edwards, M., Menon, C.V., Gong, G., and Barber, R. Long-term low-level arsenic exposure is associated with poorer neuropsychological functioning: A project FRONTIER study. *Int. J. Environ. Res. Public Health* 2011;8:861-874.
23. Liu, D., Wu, D., Zhao, L., et al. Arsenic trioxide reduces global histone H4 acetylation at lysine 16 through direct binding to histone acetyltransferase hMOF in human cells. *PLoS One* 2015;10:1-16.
24. Tillotson, J., Zerio, C.J., Harder, B., et al. Arsenic Compromises Both p97 and Proteasome Functions. *Chem. Res. Toxicol.* 2017;30:1508-1514.
25. Flora, S.J.S. Arsenic-induced oxidative stress and its reversibility. *Free Radic. Biol. Med.* 2011;51:257-281.
26. Jomova, K., Jenisova, Z., Feszterova, M., et al. Arsenic: Toxicity, oxidative stress and human disease. *J. Appl. Toxicol.* 2011;31:95-107.
27. Hughes, M.F. Arsenic methylation, oxidative stress and cancer-is there a link? *J. Natl. Cancer Inst.* 2009;101:1660-1661.
28. Kitchin, K.T., and Ahmad, S. Oxidative stress as a possible mode of action for arsenic carcinogenesis. *Toxicol. Lett.* 2003;137:3-13.
29. Dodson, M., de la Vega, M.R., Harder, B., et al. Low-level arsenic causes proteotoxic stress and not oxidative stress. *Toxicol. Appl. Pharmacol.* 2018;341:106-113.
30. Cuanalo-Contreras, K., Mukherjee, A., and Soto, C. Role of protein misfolding and proteostasis deficiency in protein misfolding diseases and aging. *Int. J. Cell. Biol.* 2013;2013:638083.

31. Korovila, I., Hugo, M., Castro, J.P., et al. Proteostasis, oxidative stress and aging. *Redox Biol.* 2017;13:550-567.
32. Bengtson, M.H., and Joazeiro, C.A.P. Role of a ribosome-associated E3 ubiquitin ligase in protein quality control. *Nature* 2010;467:470-473.
33. Shamanna, R.A., Croteau, D.L., Lee, J-H., and Bohr, V.A. Recent advances in understanding Werner Syndrome. *F1000 Fac. Rev.* 2017;6:1779.
34. Mahajan, K., and Mahajan, N.P. Cross talk of tyrosine kinases with the DNA damage signaling pathways. *Nucleic Acids Res.* 2015;43:10588-10601.
35. Centonze, F.G., Reiterer, V., Nalbach, K., et al. LTK is an ER-resident receptor tyrosine kinase that regulates secretion. *J. Cell Biol.* 2019;218:2470-2480.
36. Lavoie, C., Chevet, E., Roy, L., et al. Tyrosine phosphorylation of p97 regulates transitional endoplasmic reticulum assembly in vitro. *Proc. Natl. Acad. Sci. U. S. A.* 2000;97:13637-13642.
37. Xu, W., Mollapour, M., Prodromou, C., et al. Dynamic Tyrosine Phosphorylation Modulates Cycling of the HSP90-P50CDC37-AHA1 Chaperone Machine. *Mol. Cell* 2012;47:434-443.
38. Bradbury, J. Chaperones: keeping a close eye on protein folding. *Lancet* 2003;361:1194-1195.